Report UAG - 87

WORLD DATA CENTER A
for
Solar-Terrestrial Physics

CHANGES IN THE GLOBAL ELECTRIC FIELDS AND CURRENTS FOR MARCH 17-19, 1978 FROM SIX IMS MERIDIAN CHAINS OF MAGNETOMETERS

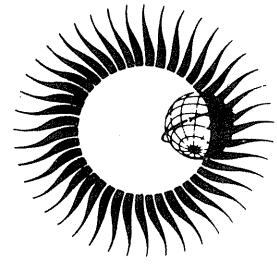

November 1982

WORLD DATA CENTER A
National Academy of Sciences
2101 Constitution Avenue, NW
Washington, D.C. 20418 USA

World Data Center A consists of the Coordination Office and the following eight Subcenters:

COORDINATION OFFICE
World Data Center A
National Academy of Sciences
2101 Constitution Avenue, NW
Washington, D.C. 20418 USA
[Telephone: (202) 334-3359]

GLACIOLOGY (Snow and Ice)
World Data Center A: Glaciology
(Snow and Ice)
Cooperative Inst. for Research in
Environmental Sciences
University of Colorado
Boulder, Colorado 80309 USA
[Telephone: (303) 492-5171]

MARINE GEOLOGY AND GEOPHYSICS
(Gravity, Magnetics, Bathymetry,
Seismic Profiles, Marine Sediment
and Rock Analyses):

World Data Center A for Marine
Geology and Geophysics
NOAA, D64
325 Broadway
Boulder, Colorado 80303 USA
[Telephone: (303) 497-6487]

METEOROLOGY (and Nuclear Radiation)
World Data Center A: Meteorology
National Climatic Center
Federal Building
Asheville, North Carolina 28801 USA
[Telephone: (704) 258-2850, ext. 381]

OCEANOGRAPHY
World Data Center A: Oceanography
National Oceanic and Atmospheric
Administration
2001 Wisconsin Avenue, NW
Page Bldg. 1, Rm. 414
Washington, D.C. 20235 USA
[Telephone: (202) 634-7249]

ROCKETS AND SATELLITES
World Data Center A: Rockets and
Satellites
Goddard Space Flight Center
Code 601
Greenbelt, Maryland 20771 USA
[Telephone: (301) 344-6695]

ROTATION OF THE EARTH
World Data Center A: Rotation
of the Earth
U.S. Naval Observatory
Washington, D.C. 20390 USA
[Telephone: (202) 254-4547]

SOLAR-TERRESTRIAL PHYSICS (Solar and
Interplanetary Phenomena, Inospheric
Phenomena, Flare-Associated Events,
Geomagnetic Variations, Aurora,
Cosmic Rays, Airglow):

World Data Center A
for Solar-Terrestrial Physics
NOAA, D63
325 Broadway
Boulder, Colorado 80303 USA
[Telephone: (303) 497-6323]

SOLID-EARTH GEOPHYSICS (Seismology,
Tsunamis, Gravimetry, Earth Tides,
Recent Movements of the Earth's
Crust, Magnetic Measurements,
Paleomagnetism and Archeomagnetism
Volcanology, Geothermics):

World Data Center A
for Solid-Earth Geophysics
NOAA, D62
325 Broadway
Boulder, Colorado 80303 USA
[Telephone: (303) 497-6521]

World Data Centers conduct international exchange of geophysical observations in accordance with the principles set forth by the International Council of Scientific Unions. WDC-A is established in the United States under the auspices of the National Academy of Sciences. Communications regarding data interchange matters in general and World Data Center A as a whole should be addressed to World Data Center A, Coordination Office (see address above). Inquiries and communications concerning data in specific disciplines should be addressed to the appropriate sub center listed above.

WORLD DATA CENTER A
for
Solar-Terrestrial Physics

Report UAG - 87

CHANGES IN THE GLOBAL ELECTRIC FIELDS AND CURRENTS FOR MARCH 17-19, 1978 FROM SIX IMS MERIDIAN CHAINS OF MAGNETOMETERS

by

Y. Kamide, H.W. Kroehl, A.D. Richmond, B.-H. Ahn, S.-I. Akasofu,
W. Baumjohann, E. Friis-Christensen, S. Matsushita, H. Maurer,
G. Rostoker, R.W. Spiro, J.K. Walker and A.N. Zaitzev

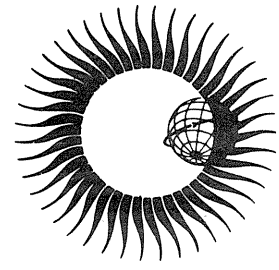

November 1982

U.S. DEPARTMENT OF COMMERCE
NATIONAL OCEANIC AND ATMOSPHERIC ADMINISTRATION
ENVIRONMENTAL DATA AND INFORMATION SERVICE
Boulder, Colorado, USA 80303

TABLE OF CONTENTS

CHANGES IN THE GLOBAL ELECTRIC FIELDS AND CURRENTS FOR MARCH 17-19, 1978

FROM SIX IMS MERIDIAN CHAINS OF MAGNETOMETERS

by

Y. Kamide[1,2], H. W. Kroehl[3], A. D. Richmond[1], B.-H. Ahn[4], S.-I. Akasofu[4], W. Baumjohann[5], E. Friis-Christensen[6], S. Matsushita[7], H. Maurer[8], G. Rostoker[9], R. W. Spiro[10], J. K. Walker[11], and A. N. Zaitzev[12]

PART 1

I. INTRODUCTION

In the first half of this century the pioneering work of K. Birkeland, soon followed by S. Chapman and H. Alfvén, attempted to infer the electric current system responsible for ground magnetic disturbances. Studies of ground-based magnetic records have been widely used to examine processes ocurring in the magnetosphere and ionosphere in terms of the growth and decay of the three-dimensional current system in the polar region which consists of ionospheric currents and field-aligned currents. In the past, however, because the magnetometer shows the complicated superimposed effect of various types of currents, it was not possible to determine ionospheric currents and field-aligned currents, separately. Studies on this subject were primarily based on the so-called equivalent ionospheric current system. The equivalent current system can be determined by assuming that all overhead currents contributing to ground-based magnetic perturbations flow in a spherical shell (i.e., the ionosphere) concentric with the earth. During the last two decades there have been a number of new techniques to measure the field-aligned current-density, electric fields, etc., in and near the ionosphere. However, although these 'direct' measurements are most valuable, it is still not possible to construct the distribution of the three-dimensional currents without a number of assumptions. Furthermore, it is not practical to construct instantaneous three-dimensional current distributions from polar orbiting satellite measurements of particles, fields and/or currents. Therefore, it has become a compelling task for us to develop methods which could determine the current and field distribution on the basis of ground magnetometer data.

Owing to the significant improvement of the ground magnetic networks, as well as various numerical techniques developed during the last decade, it has now become possible to estimate the three-dimensional current system over the polar region during individual magnetospheric substorms with a relatively high time resolution. It has taken more than half a century to quantify the pioneering concepts of Birkeland, Chapman and Alfvén, although improved accuracy of the estimation procedures is still a desirable goal.

In 1973, the International Association of Geomagnetism and Aeronomy (IAGA) established a working group on the Geomagnetic Meridian Project to evaluate the need for improved magnetometer networks at high latitudes. The working group stressed the importance of coordinated observations of magnetic fields in the polar region, particularly along meridian lines to be compared with simultaneous satellite, rocket and radar observations. Then, during the International Magnetospheric Study (IMS), a joint effort was made to set up magnetometer chains along several magnetic meridians. As a result, seven meridian chains were operating in 1978 and 1979: the Alaska chain, the Alberta chain, the Fort Churchill chain, the Greenland chain, the Scandinavia chain, the IZMIRAN chain, and the SibIZMIR chain. In addition to the projects conducted by individual meridian chain groups, the IMS meridian chain group has as a whole agreed to study jointly the growth and decay of ionospheric currents and field-aligned currents for magnetospheric substorm events.

The purpose of this report is to present some of our products: calculated ionospheric electric poten-

[1] Space Environment Laboratory, NOAA, Boulder, Colorado 80303
[2] On leave of absence from Kyoto Sangyo University, Kyoto 603, Japan
[3] National Geophysical Data Center, NOAA, Boulder, Colorado 80303
[4] Geophysical Institute, University of Alaska, Fairbanks, Alaska 99701
[5] Institut für Geophysik der Westfälischen Wilhelms-Universität, Corrensstr. 24, D-4400 Münster, Federal Republic of Germany
[6] Meteorological Institute, Division of Geophysics, DK-2100, Copenhagen, Denmark
[7] High Altitude Observatory, National Center for Atmospheric Research, Boulder, Colorado 80307 (which is sponsored by the National Science Foundation)
[8] Institut für Geophysik und Meteorologie, TU Braunschweig, D-3300 Braunschweig, Federal Republic of Germany
[9] Institute of Earth and Planetary Physics and Department of Physics, University of Alberta, Edmonton, Canada T6G 2J1
[10] Department of Space Physics and Astronomy, Rice University, Houston, Texas 77251
[11] Earth Physics Branch, Department of Energy, Mines and Resources, Ottawa, Ontario, Canada K1A 0Y3 (Contribution 1028 from Earth Physics Branch)
[12] Polar Geomagnetic Research Laboratory, IZMIRAN, Troitsk, Moscow Region 142092, U.S.S.R.

tials, ionospheric and field-aligned currents, and Joule heating rates by the ionospheric currents. Also included are the measured ground magnetic perturbations on March 17, 18 and 19, 1978: from seventy-one stations. Part 1 contains brief comments on the method used in the estimation of these quantities. Part 2 displays common-scale magnetograms in the X_m (geomagnetic north) and Y_m (east) components from all the 71 stations. In Part 3 are plots at hourly intervals of the global distribution of these parameters. It is hoped that these data sets provide the scientific community with new information to improve our understanding of magnetospheric and ionospheric processes.

II. OUTLINE OF THE PROJECT

Three consecutive days, March 17, 18 and 19, 1978, were selected initially since the largest number of magnetic stations of the six meridian chains were operating. (Unfortunately, the SibIZMIR chain was not operating in the spring of 1978, leaving a longitudinal gap in the East-Siberia sector.) The geomagnetic index ΣKp on those days was 31_-, 30_- and 23_0, respectively. This joint effort emphasizes particularly the global scale features, since small-scale features can be studied in more detail by individual chains. The University of Alaska group took the responsibility of assembling, digitizing and formating the necessary data set (5-minute average values) and also of modifying the original computer codes for this particular project. For three days in March 1982, the first workshop was conducted at the National Geophysical Data Center in Boulder, Colo., which was attended by representatives from the IMS meridian chains. A summary of the workshop as well as the agreements reached at the Boulder workshop is described in the Appendices A and B. An initial result emphasizing an intense substorm on March 19, 1978, has been published by Kamide et al. (1982).

Table 1

List of the magnetic stations whose data are used.

	Station Name	Geographic Lat.	Geographic Long.	Eccentric Dipole Lat.	Eccentric Dipole Long.
	Alaska Chain				
0.	Eureka	80.0	274.3	89.0	325.3
1.	Isachsen	78.8	256.0	86.0	268.4
2.	Mould Bay	76.2	240.6	81.7	262.5
3.	Johnson Point	72.5	241.7	78.7	276.1
4.	Sachs Harbor	72.0	234.7	77.3	268.0
5.	Cape Parry	70.2	235.3	75.7	272.2
6.	Inuvik	68.3	226.7	72.7	264.8
7.	Arctic Village	68.1	214.4	70.5	251.6
8.	Fort Yukon	66.6	214.7	69.2	253.8
9.	College	64.7	211.9	66.9	252.9
10.	Anchorage	61.2	210.1	63.3	254.0
	Alberta Chain				
11.	Resolute Bay	74.7	265.1	83.3	311.5
12.	Cambridge Bay	69.1	255.0	77.1	301.7
13.	Yellowknife	62.5	245.5	69.6	294.1
14.	Fort Providence	61.4	242.6	68.2	291.1
15.	Hay River	60.8	244.2	67.8	293.5
16.	Fort Smith	60.0	248.0	67.4	298.9
17.	Uranium City	59.6	251.5	67.4	303.6
18.	Fort Chipewyan	58.8	248.0	66.2	299.5
19.	Fort McMurray	56.7	248.8	64.2	301.4
20.	Meanook	54.6	246.7	61.9	299.6
21.	Leduc	53.3	246.6	60.6	300.0
	Fort Churchill Chain				
22.	Pelly Bay	68.5	270.5	77.4	327.4
23.	Baker Lake	64.3	264.0	72.9	318.7
24.	Rankin Inlet	62.8	267.7	71.6	324.6
25.	Eskimo Point	61.1	265.9	69.8	322.5
26.	Fort Churchill	58.8	265.9	67.5	323.0
27.	Back	57.7	265.7	66.4	322.9
28.	Thompson	55.0	263.0	63.6	320.0
29.	Island Lake	53.9	265.3	62.6	323.1
30.	Whiteshell	49.8	264.8	58.6	323.1
	Greenland Chain				
31.	Thule	77.5	290.8	85.5	22.7
32.	Upernavik	72.8	303.8	79.8	28.0
33.	Umanak	70.7	307.8	77.4	29.5
34.	Godhavn	69.3	306.5	76.2	25.5
35.	Godthab	64.2	308.3	71.2	22.5
36.	Frederickshab	62.0	310.3	68.9	23.3
37.	Narssarssuaq	61.0	314.6	67.4	27.9
	Scandinavia chain				
38.	Nord	81.6	343.3	80.2	101.6
39.	Ny Alesund	78.9	12.0	74.8	107.3
40.	Bjornoya	74.5	19.2	70.2	104.1
41.	Skarsvag	71.1	25.8	66.3	105.1
42.	Kunes	70.4	26.5	65.6	104.9
43.	Kevo	69.8	27.0	64.9	104.8
44.	Martti	67.5	28.3	62.6	104.0
45.	Kuusamo	65.9	29.1	61.0	103.6
46.	Borok	58.0	38.3	52.2	107.2
	IZMIRAN chain				
47.	Heiss Island	80.6	58.0	72.3	135.3
48.	Karmakuly	72.3	52.5	64.7	125.1
49.	Dixon Island	73.5	80.6	64.3	144.6
50.	Belyy Island	73.0	71.1	64.1	138.5
51.	Kharasavey	71.5	67.5	62.8	135.1
52.	Tambei	71.5	71.9	62.6	138.2
53.	Amderma	69.7	61.6	61.4	130.2
54.	Kamennyi	68.4	73.5	59.4	138.4
	Other stations				
55.	St. John's	47.6	307.3	55.4	14.0
56.	Leirvogur	64.2	338.3	67.0	56.9
57.	Kap Tobin	70.4	338.0	72.7	64.1
58.	Hartland	51.0	355.5	52.0	65.9
59.	Danmarkshavn	76.8	341.4	77.4	81.3
60.	Niemegk	52.1	12.7	50.3	82.4
61.	Abisko	68.4	18.8	64.7	97.2
62.	Cape Chelyuskin	77.7	104.3	68.4	159.8
63.	Tixie Bay	71.6	129.0	63.1	177.9
64.	Yakutsk	62.0	129.7	53.3	181.5
65.	Cape Wellen	66.2	190.2	64.8	230.3
66.	Barrow	71.3	203.2	71.7	236.0
67.	Sitka	57.1	224.7	61.6	272.6
68.	Victoria	48.5	236.6	54.7	289.9
69.	Great Whale River	55.3	282.2	64.3	344.8
70.	Ottawa	45.5	284.5	54.6	347.1

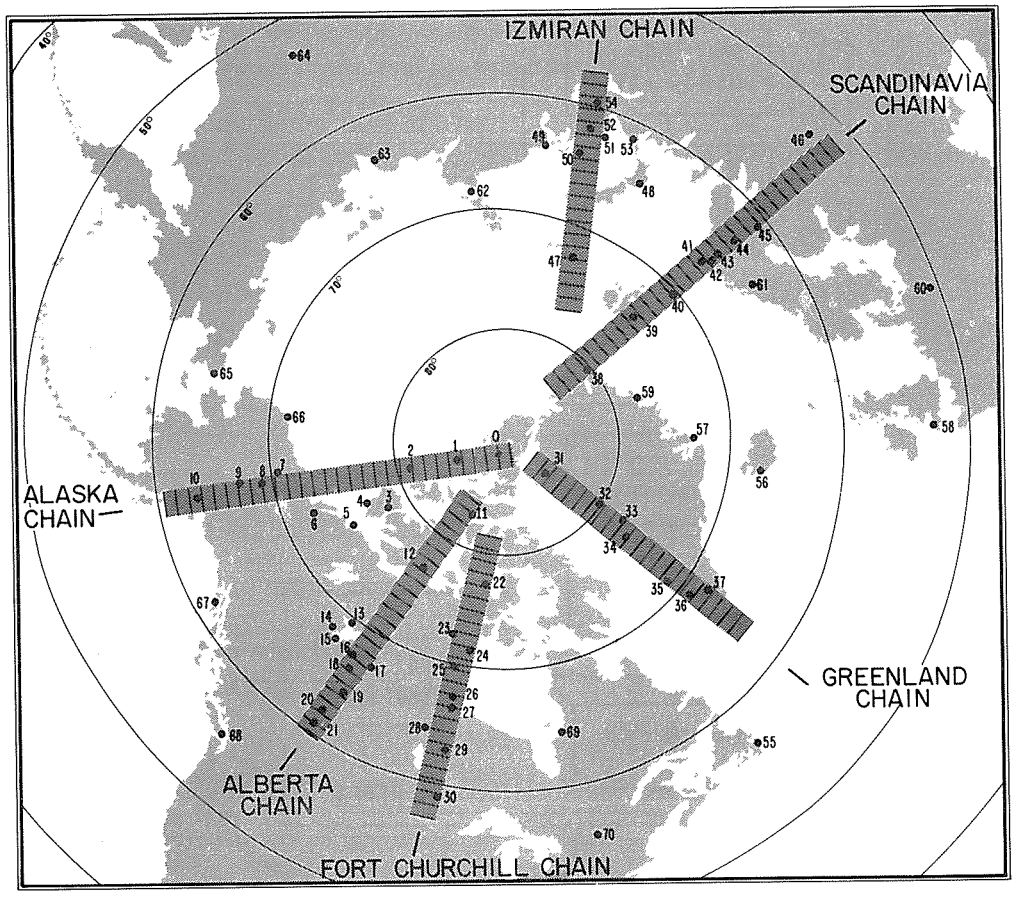

Fig. 1 Map (in eccentric dipole coordinates) of the six IMS meridian chains of magnetometer stations and of standard observatories, whose data are used in the present modeling. For identification of station names, see Table 1.

Magnetic records from a total of seventy-one stations above 50° in geomagnetic latitude are used in this study, and those stations are listed in Table 1. After the paper by Kamide et al. (1982) went to press, data from Eureka, closest to the eccentric dipole pole, became available, thus the designation of 0 for this station. The station distribution in eccentric dipole coordinates (Cole, 1963) is shown in Figure 1. Note that several subauroral stations were added for better accuracy of the determination of the auroral electrojet location. Data used in this paper represent horizontal magnetic perturbations relative to the average magnetic field level on March 12, 1978, which the quietest day in March 1978.

III. METHOD

A summary diagram outlining steps from digitization through final production of a motion picture film is given in Figure 2. The practical procedures for each time step are as follows:

(1) Digitization of the H and D (or X and Y) components from magnetograms from each station. Approximately 25% of all the stations used digital recorders, so that only a formating process was necessary for these stations. However, errors are generated during the digitization process for most of the other stations. We have attempted to minimize this problem and consider timing of all digital values to be within 2.5 minutes of their actual time.

(2) Subtraction of a base line (the average level of March 12, 1978) for each station and transformation into geomagnetic north, X_m, and geomagnetic east, Y_m, components. In this report, the X_m and Y_m components refer to the northward and eastward components in eccentric dipole coordinates.

(3) Calculation of geomagnetic activity indices (derived from 71 sets of X_m values). In view of the fact that this data set is one of the most comprehensive assembled to date from high-latitude magnetometers, we have constructed two auroral electrojet activity indices: AE(71) and the total westward electrojet index F_m. Substorm activity described by these indices for the three-day interval is presented in Section IV.

(4) Computation of the equivalent current function. This process involves fitting a magnetic potential function to the observed data and estimating the portion of this potential associated with overhead currents.

(5) Computation of the electric potential in the ionosphere at each grid point, every 1° in colatitude and 15° (1 hr.) in longitude (local time). This process involves the most extensive computer calculation to solve numerically the second-order differential equation in two dimensions. A suitable model of the ionosphere conductivity is to be assumed.

(6) Calculation of the ionospheric current vector at each grid point.

(7) Derivation of the field-aligned current, which is the divergence of the ionospheric current.

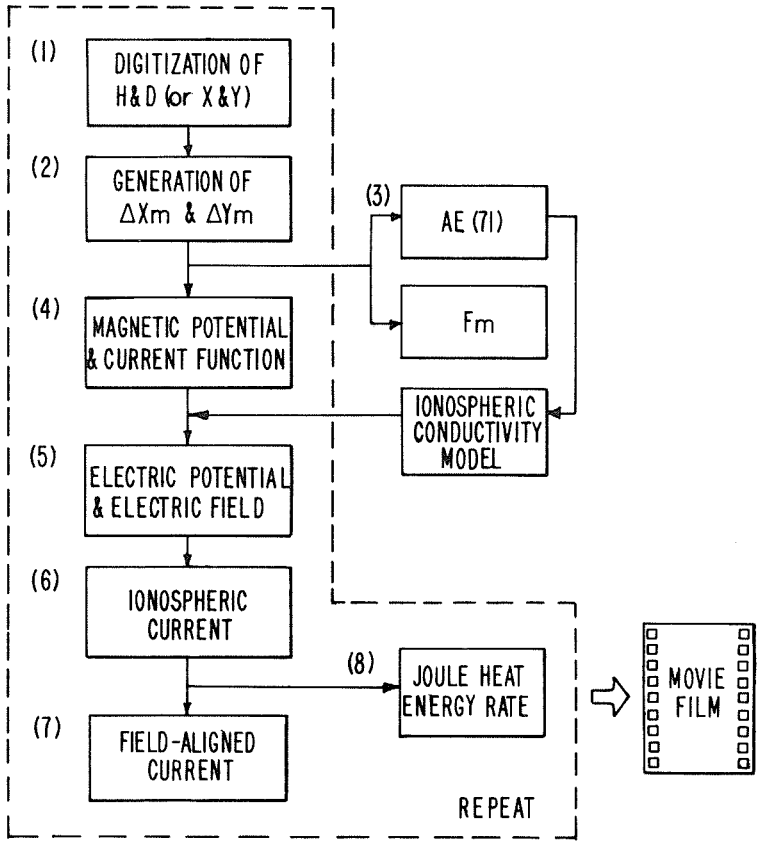

Fig. 2 Flow chart describing the important steps in the present project.

(8) Estimation of Joule heating rate, which is the scalar product of the ionospheric current and electric field vectors.

(9) Repetition of these steps for each time in the entire period and preparation of a master 35-mm film to be printed on 16-mm films.

Additional details of the computations in steps (4) through (8) are described briefly in the following:

Current Function

The observed magnetic data from the 71 stations were fitted to a magnetic potential function V which is represented by a spherical harmonic series with longitudinal wave numbers m from 0 to 6 and order n=m to 56, as expressed by the standard form:

$$V(\theta,\lambda)= \sum_{m=0}^{6} \sum_{n=m}^{56} (a_n^m \cos m\lambda + b_n^m \sin m\lambda) P_n^m(\cos\theta) \quad (1)$$

where θ and λ are colatitude and east longitude (measured from midnight), respectively, in the eccentric dipole coordinate system. All terms involving associated Legendre polynomials P_n^m with even (n-m) are omitted from the series, except the n=m term, as the odd terms alone are basically sufficient to represent the northern hemispheric potential. The X_m and Y_m components at each station are expressed by:

$$X_m= - \sum_m \sum_n (a_n^m \cos m\lambda + b_n^m \sin m\lambda) \frac{dP_n^m}{d\theta} \quad (2)$$

$$Y_m= - \sum_m \sum_n m (a_n^m \sin m\lambda - b_n^m \cos m\lambda) \frac{P_n^m}{\sin\theta} \quad (3)$$

The choice of these maximum n and m values is based on trial and error tests with a variety of values. There are in total 358 coefficients, a_n^m and b_n^m, to be determined in the harmonic series (1).

In seeking an appropriate potential function V, it is required here that the potential vary smoothly in space between stations. We started with the algorithm of Richmond et al. (1979), which performs a least-squares fit of the negative horizontal gradient of V to the observed magnetic variations, with additional constraints to provide smooth interpolations between stations. We found that the results obtained from this algorithm could be improved by making several ad hoc modifications to the smoothing constraints, primarily by increasing the smoothing in longitude with respect to smoothing in latitude. This permitted a reduction in the maximum m value and an increase in the maximum n value without increasing the total number of coefficients. The root-mean-square difference between computed and observed magnetic perturbations is typically 15%. However, at certain times the discrepancy rises above 20%.

It is then assumed that there is a relatively small internal contribution to the magnetic potential caused by a perfectly conducting layer 300 km below the earth's surface. The remaining external potential $V^{(e)}$ is extrapolated to 110 km altitude and converted to an equivalent ionospheric current function ψ by the standard procedure:

$$\psi_n = \frac{1}{\mu_o} \frac{2n+1}{n+1} \left(\frac{a}{R_E}\right)^n V_n^{(e)} \qquad (4)$$

where

$$\psi = \sum_n \psi_n(\theta,\lambda)$$

$$a = R_E + 110 \text{ km}$$

$$\mu_o = 4\pi \times 10^{-7} \text{ H/m}$$

Ionospheric Conductivity

At present there is no way to monitor continuously the global distribution of the ionospheric conductivity. Recently, several conductivity models have been developed based on radar and satellite measurements of precipitating electrons (e.g., Vanyan and Osypova, 1976; Wallis and Budzinski, 1981; Vickrey et al., 1981; Spiro et al., 1982). In this report it is assumed that the conductance, that is, the height-integrated ionospheric conductivity, has two components: one is a background conductance of solar ultraviolet origin and the other simulates an enhancement presumably due to substorm-associated particle bombardment. We may call the former the quiet time conductance and the latter auroral enhancement conductance.

For the background conductance, we follow the quiet time distribution for equinoctial months, as described in equations (19) and (20) of Kamide and Matsushita (1979). For the auroral enhancement, we use an empirical model based on the work of Spiro et al. (1982) with updated improvements. This is because the height-integrated Hall and Pedersen conductivities (Σ_H and Σ_P) in this model are tabulated at every 1-2° (in latitude) and 1 hour (in MLT) for each level of auroral electrojet activity measured by the AE index. Spiro et al. (1982) used data of precipitating particle energy flux and average electron energy obtained from the Atmosphere Explorer satellites (AE-C and AE-D) along with the dependence of the height-integrated conductivities on the characteristic energy of precipitating electrons obtained by Vickrey et al. (1981).

It should be noted that at two instants with the same value of the AE index, the auroral distribution and the conductivity distribution, as well as the current patterns in the polar region, may be significantly different. Thus, although the ionospheric current patterns are only weakly dependent on the choice of the conductivity (e.g., Kamide and Richmond, 1982), the following adjustment is employed in the use of the conductivity model: by assuming that the latitude of the maximum equivalent current strength coincides with the latitude of the highest Hall conductivity, a latitudinal shift is made for the entire conductivity distribution whenever a difference between the two latitudes of the maxima is found.

Electric Potential

During the last several years, different techniques have been developed to analyze global magnetometer data in order to infer the three-dimensional distribution of electric currents around the earth (e.g., Kisabeth, 1979; Mishin et al., 1980; Kamide et al., 1981). These methods take the distribution of magnetic perturbation vectors observed on the earth's surface as the input and try to estimate the distribution of ionospheric and field-aligned currents and other related quantities as outputs for a given model of ionospheric conductivities. Akasofu et al. (1981) compared the algorithms of Kisabeth (1979) and of Kamide et al. (1981) using daily average data from the Alaska meridian chain as input. They found that the gross distribution patterns of both ionospheric and field-aligned currents computed from these techniques agree satisfactorily, lending credence to the reliability of such methods in inferring the actual electric currents from the data. In this report, we employ an improved version of the computer algorithm developed by Kamide et al. (1981).

The height-integrated ionospheric current can be considered to consist of two elements. The toroidal (solenoidal) current $\underline{J}_T$ is related to the equivalent current function ψ as

$$J_{T\theta} = -\frac{\partial\psi}{a\sin\theta\partial\lambda}$$

$$J_{T\lambda} = \frac{\partial\psi}{a\partial\theta} \qquad (5)$$

The other part, the poloidal current $\underline{J}_P$ can be considered as a closing current for field-aligned currents $j_{||}$. (Note that $j_{||} = \text{div } \underline{J}_P$ and div $\underline{J}_T = 0$ by definition and that $j_{||}$ and $\underline{J}_P$ together produce no ground magnetic variation under the assumption of magnetic field lines penetrate vertically into the horizontal ionosphere). The associated electric field $\underline{E}$ is derivable from an electrostatic potential Φ. A partial differential equation for Φ in terms of ψ can then be written as

$$A\frac{\partial^2\Phi}{\partial\theta^2} + B\frac{\partial\Phi}{\partial\theta} + C\frac{\partial^2\Phi}{\partial\lambda^2} + D\frac{\partial\Phi}{\partial\lambda} = F(\psi,\theta,\lambda) \qquad (6)$$

where

$$A = \sin\theta \cdot \Sigma_H$$

$$B = \frac{\partial}{\partial\theta}(\sin\theta \cdot \Sigma_H) + \frac{\partial}{\partial\lambda}\Sigma_P$$

$$C = \Sigma_H/\sin\theta \qquad (7)$$

$$D = -\frac{\partial}{\partial\lambda}(\Sigma_H/\sin\theta) - \frac{\partial}{\partial\theta}\Sigma_P$$

$$F = \frac{\partial}{\partial\theta}\left(\sin\theta\frac{\partial\psi}{\partial\theta}\right) + \frac{1}{\sin\theta}\frac{\partial^2\psi}{\partial\lambda^2}$$

The above differential equation (6) is to be numerically solved with approximate boundary conditions:

$$\Phi(0,\lambda) = 0 \qquad \text{at the pole}$$

$$\frac{\partial\Phi(\pi/2,\lambda)}{\partial\theta} = 0 \qquad \text{at the equator} \qquad (8)$$

Once the electrostatic potential is obtained, the electric field $\underline{E}$ is derivable from the potential Φ as

$$\underline{E} = -\text{grad } \Phi \,. \qquad (9)$$

Practically, we solve (6) numerically by a finite difference scheme over a network of grid points spaced 1° in θ and 15° in λ. As discussed by Kamide et al. (1981), it was assumed in deriving (6) that the magnetic contributions of the magnetospheric ring currents and tail currents to ψ can be neglected and geomagnetic field lines are effectively radial. The breakdown of these assumptions at lower latitudes probably invalidates the calculated potential values at low latitudes.

Ionospheric Currents and Field-Aligned Currents

Once the electric field is determined, it is possible to derive the ionospheric current vector $\underline{J}$ from

$$\underline{J} = \Sigma_P \underline{E} + \Sigma_H \underline{E} \times \underline{n}_r \qquad (10)$$

where $\underline{n}_r$ is a unit radial vector. From the requirement that the three-dimensional current be divergence free, the field-aligned current density $j_{\parallel}$ (positive downwards) can be calculated as

$$j_{\parallel} = \text{div } \underline{J} = \text{div } \underline{J}_P \qquad (11)$$

Joule Heating Rate

The height-integrated Joule heating rate is defined by

$$u_J = \underline{J} \cdot \underline{E} = \Sigma_P E^2 \qquad (12)$$

The Joule heating rate in the entire northern hemisphere ionosphere U_J can then be obtained by integrating u_J as

$$U_J = \iint u_J \, a^2 \sin\theta \, d\theta d\lambda \qquad (13)$$

IV. MAGNETIC ACTIVITY ON MARCH 17-19, 1978

Figure 3 shows the combined X_m component traces from all the 71 stations for March 17, 18 and 19, 1978. The upper and lower envelopes provide the AU and AL indices, respectively, and the distance between the two envelopes gives the AE index. Note that, from this definition, these activity indices are supposed to register the peak current density, rather than an integrated total electrojet current.

During the three-day interval, there occurred a number of intense substorms which are identified by enhancements in the auroral electrojet activity. The successive substorms at auroral latitudes have divergent characteristics ranging from an isolated substorm to continuous substorm activity, and from small substorms to large substorms.

V. EXAMPLES OF THE OUTPUTS

In Figures 4a-j, we show some of the outputs from the extensive calculation for, as an example, 1200 UT on March 19, 1978, which is the maximum epoch of an intense substorm.

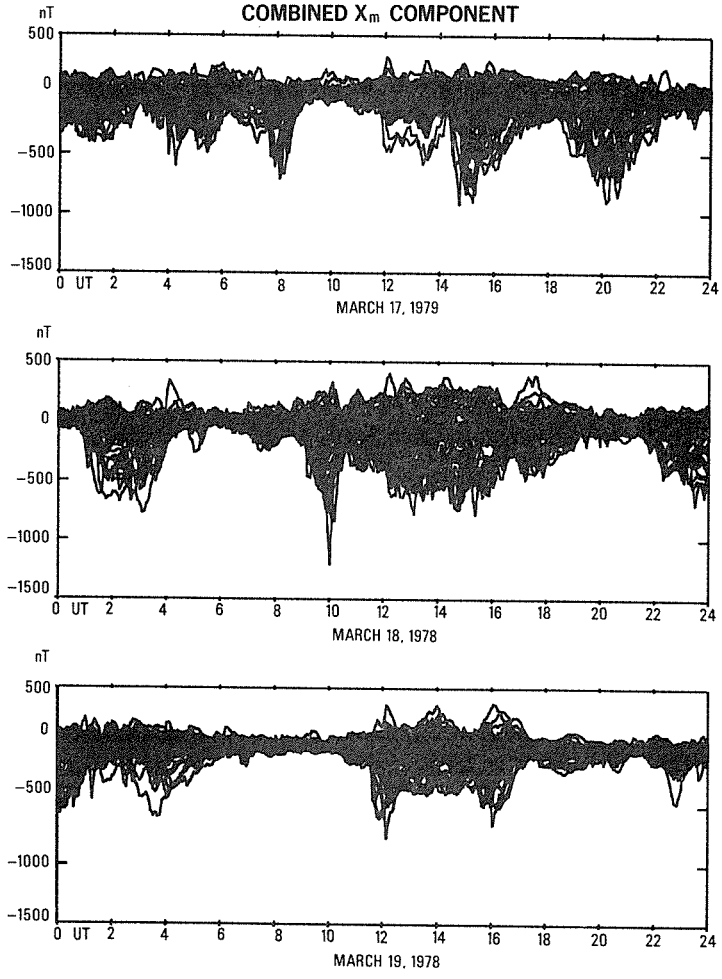

Fig. 3 The combined Xm component from 71 high-latitude stations for March 17, 18 and 19, 1978. The upper and lower envelopes give the AU (71) and AL (71) indices, respectively.

Figure 4a shows the distribution of the equivalent ionospheric current vectors which are the observed magnetic perturbation vectors clockwise by 90°. One can see that the nightside westward electrojet flows in a wide local time span, from the late morning nightside sector to the evening sector, and maximizes in the midnight sector. In Figures 4b and 4c, we show the distribution of isointensity contours of calculated external current function (the so-called equivalent ionospheric current system) and of the associated equivalent current vectors, respectively. The current vectors are plotted at our grid points every 1° (in latitude) and 1 hour (in local time). Comparing Figures 4a and 4c, one must be cautious in interpreting the derived equivalent currents in regions where there is an absence of measurements. In particular, the large gap in the distribution of surface magnetometers over the Arctic Ocean and eastern Siberia can produce significant uncertainties.

Isocontours of the assumed height-integrated Pedersen and Hall conductivities are displayed in Figure 4d. Note the different contour intervals used for the two conductivities. Figure 4e shows isocontours of the electric potential calculated for the combined set of the current function (Fig. 4b) and the conductivity model (Fig. 4d), and Figure 4f shows the corresponding electric field computed at our grid points. The potential pattern consists essentially of twin vortices in high latitudes with the highest and lowest potentials existing in the early morning and early afternoon sectors, respectively. However, there can exist many local deformations. It is important to point out that in many earlier works, the pattern of the electric potential has been assumed to be identical to that of the equivalent current system. By comparing Figures 4e and 4b, it is noticeable that the potential pattern is significantly different from the equivalent current system at and near auroral latitudes. Such a difference is caused simply by the nonuniform distribution of the ionospheric conductance.

Figure 4g shows the distribution of the calculated ionospheric current vectors. One can notice by comparing the equivalent and 'true' ionospheric currents, that although the gross distributions of the two currents are similar, there are significant differences both in the current direction and strength. For example, the equivalent currents flow nearly in the pure east-west direction, but the 'true' ionospheric currents have a considerable north-south component. In Figure 4h, we compare the Pedersen and Hall currents, separately. It is evident that the Hall currents are remarkably similar to the equivalent currents. However, a significant difference can be found in the polar cap, indicating that the main source of the polar cap magnetic perturbations is field-aligned currents, at least, during substorms.

Figure 4i shows isocontours of the calculated field-aligned currents. There is a great variability in the field-aligned current distribution in comparison with the statistical pattern obtained by averaging a number of satellite measuarements.

Finally in Figure 4j, we show the distribution of the Joule heat production rate associated with the auroral electrojets. In the left-bottom corner, the total Joule heating integrated over the entire polar ionosphere (from the north pole to 50° latitude) is indicated in the unit of watts.

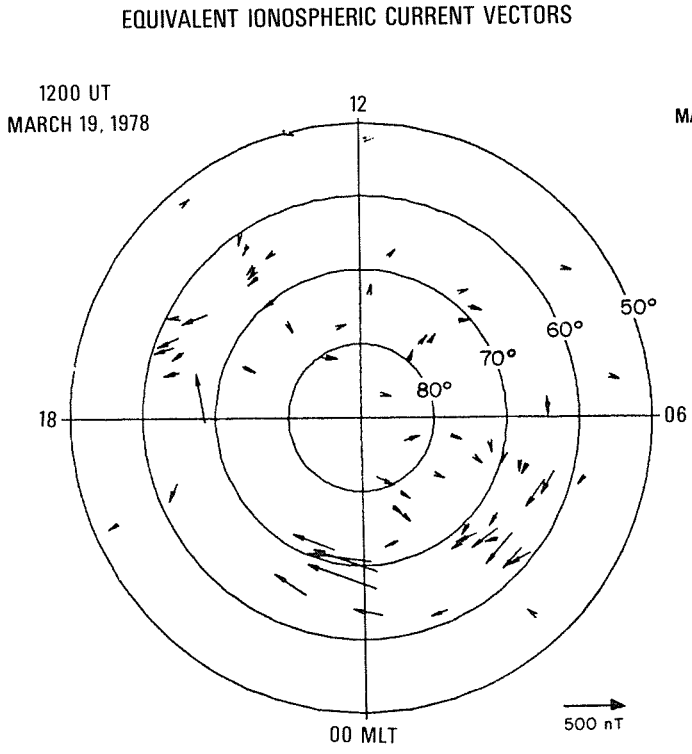

Fig. 4a Examples of the outputs from the calculation. Equivalent current vectors deduced from observed magnetic perturbations.

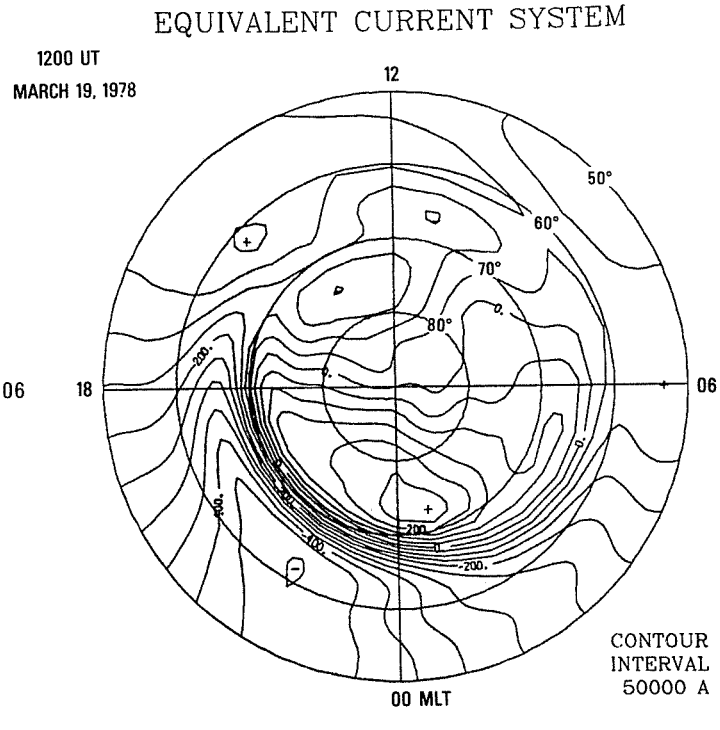

Fig. 4b Calculated equivalent current functions.

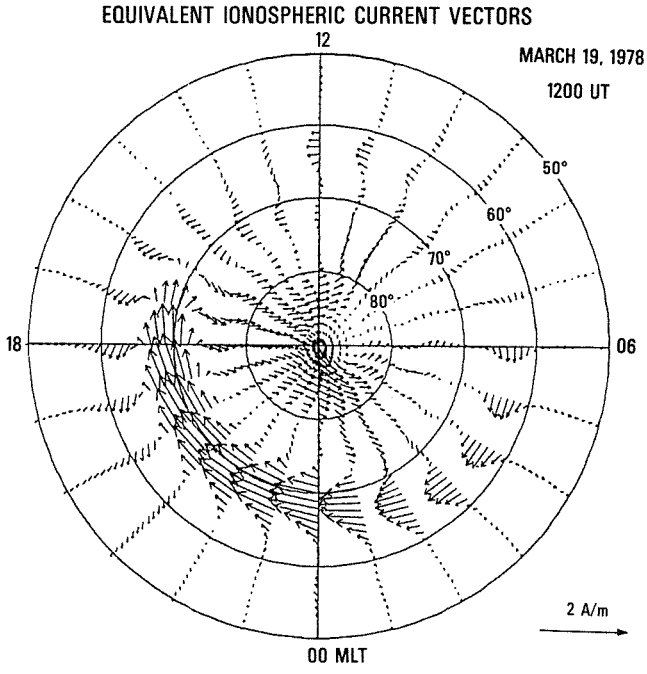

Fig. 4c Equivalent current vectors calculated at the grid points.

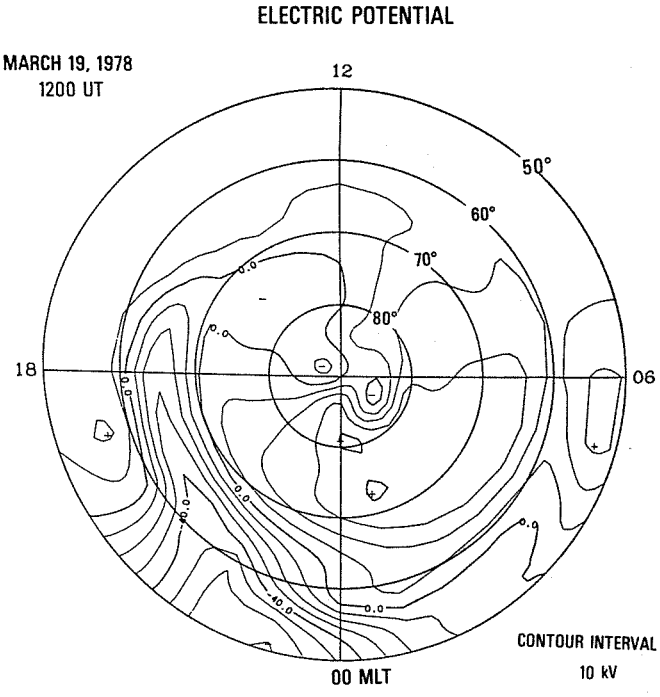

Fig. 4e Electric potential contours.

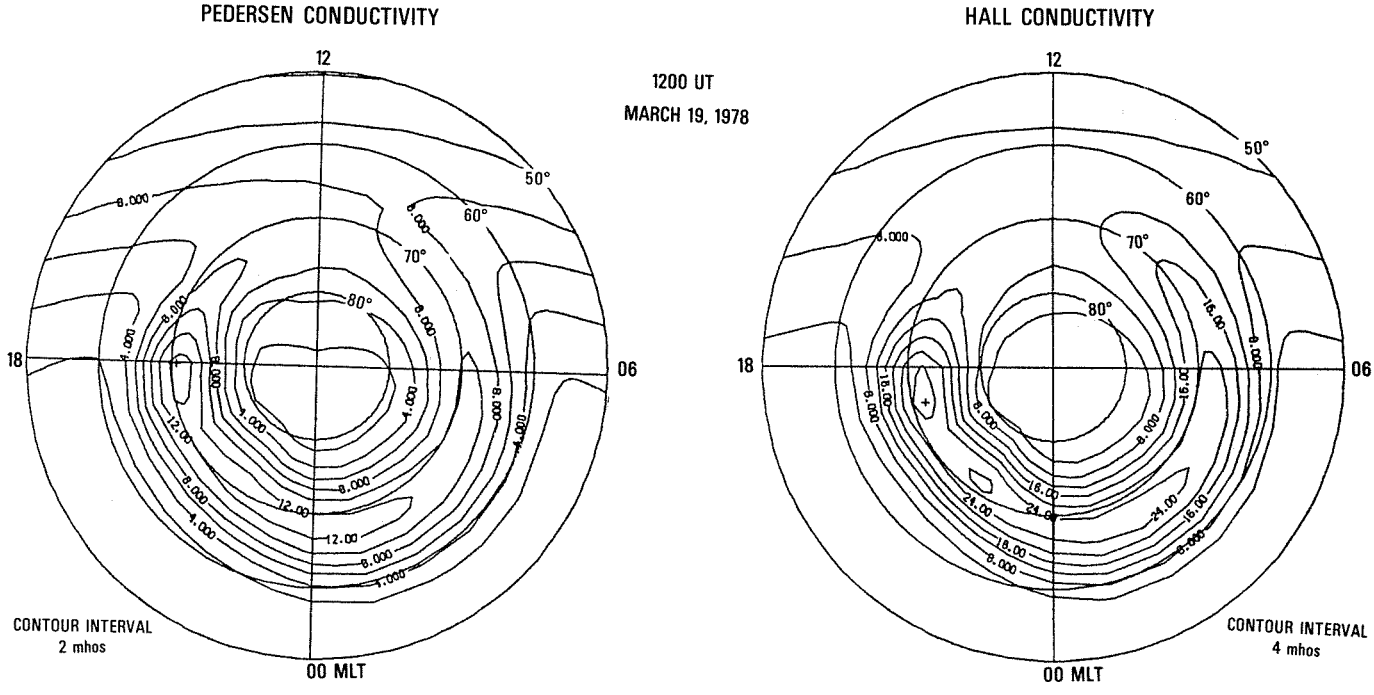

Fig. 4d Assumed height-integrated Pedersen and Hall conductivities.

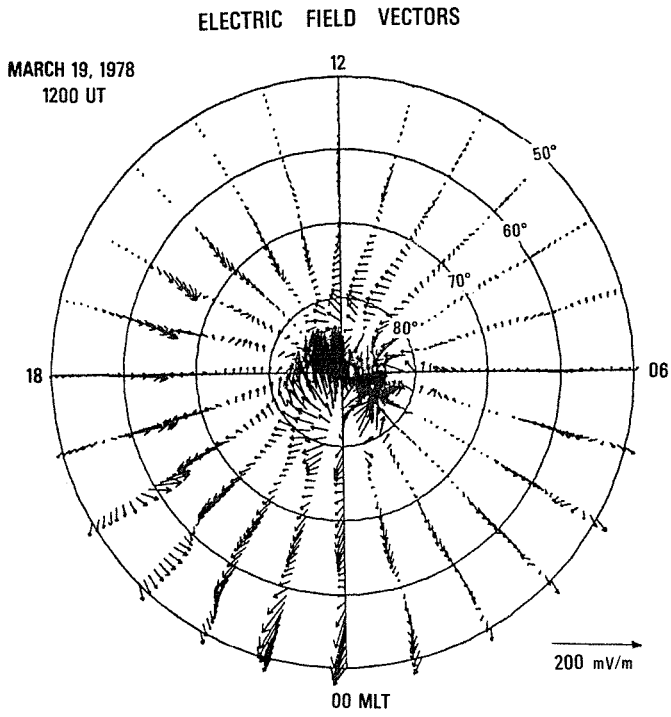

Fig. 4f Electric field vectors.

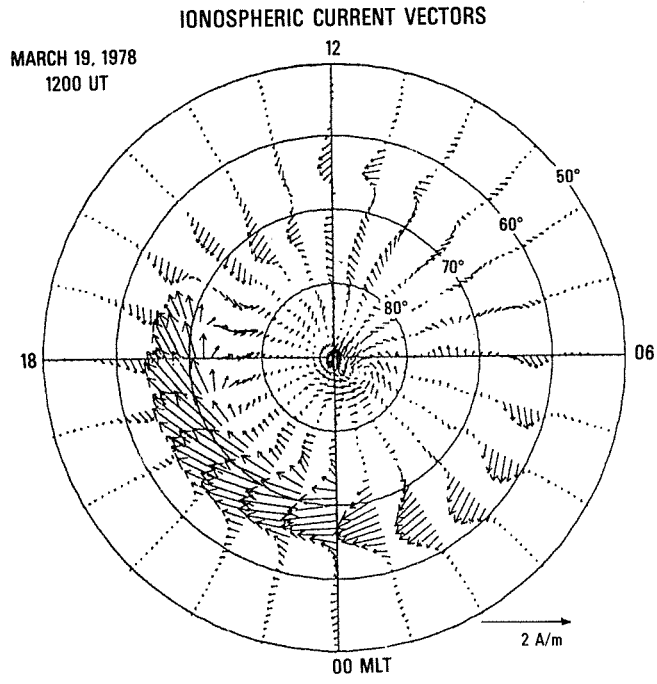

Fig. 4g Ionospheric current vectors.

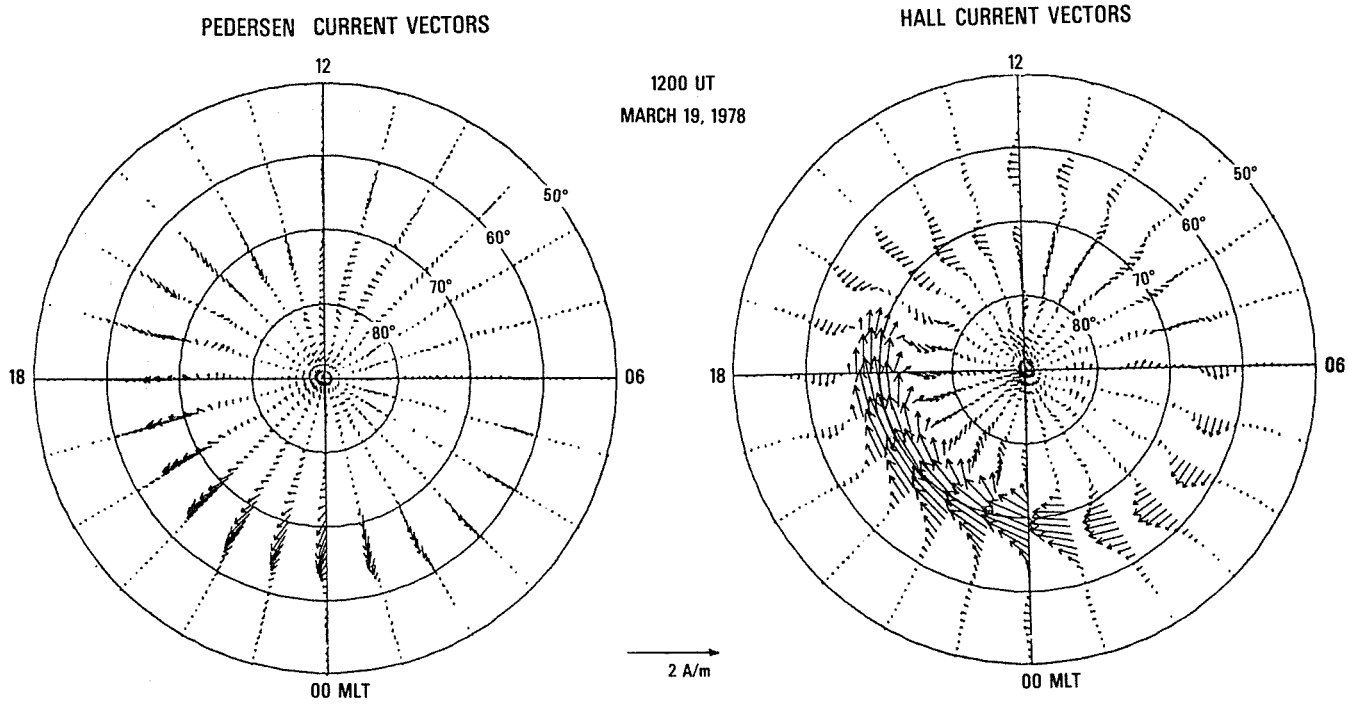

Fig. 4h Pedersen and Hall current vectors.

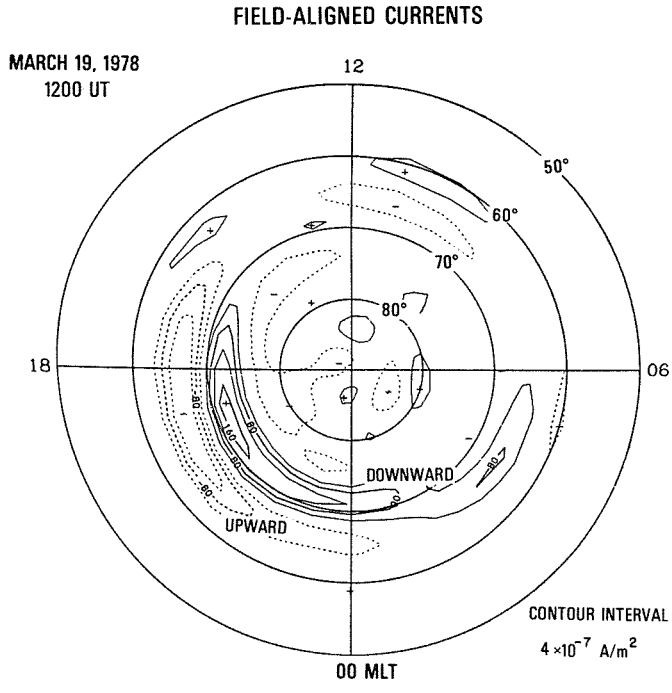

Fig. 4i Field-aligned current distribution.

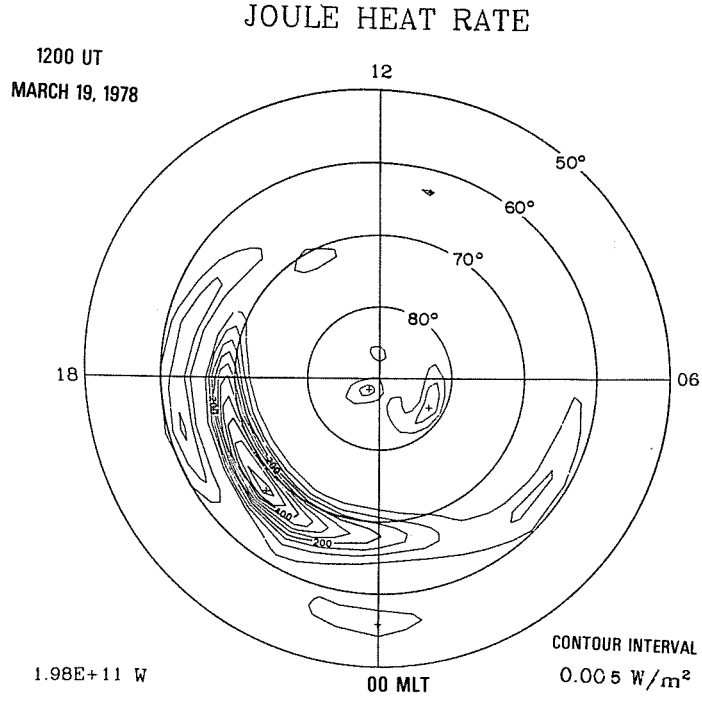

Fig. 4j Joule heating rate and total Joule heat rate integrated over the northern hemisphere.

VI. AVAILABILITY OF DETAILED DATA PRODUCTS

The complete data set is available in a form of a 16mm cine color film, which consists of four segments: (1) equivalent current system, (2) electric potential contours and ionospheric currents, (3) field-aligned currents, and (4) contours of Joule heating rate. Each frame of the film is repeated five times, allowing the viewer to follow the progression of changes in these quantities. This creates a movie which lasts 13 minutes. Film copies may be obtained from NOAA National Geophysical Data Center, Boulder, Colorado, 80303 USA at a cost of $150 per film. Magnetic tape copies containing the 5-min original magnetometer data from the 71 stations are also available from World Data Center A for Solar-Terrestrial Physics at the same address for a cost of $110.

Acknowledgments

The present work would have been impossible without the help of numerous persons and institutions in obtaining the original magnetometer data. We wish to thank Rick Guritz of the University of Alaska for his skillful computer work in handling the large amount of data. It would also have been impossible without the financial support of funding agencies in many different countries: We would like to thank the National Science Foundation which supported both the operation of the Alaska meridian chain and the major part of the data analysis reported in this paper (ATM-81-08994). Y. K. was supported in part by the Ministry of Education, Science and Culture of Japan under a Grant-in-Aid for Scientific Research Project #00554105. The research reported in this paper was accomplished while Y. K. held a Senior Resident Research Associateship of U.S. National Research Council at NOAA Space Environment Laboratory. W. B. and H. M. wish to thank the Deutsche Forschungsgemeinschaft for financial support . G. R. acknowledges support from the Natural Sciences and Engineering Research Council of Canada.

The workshop exemplifies the leadership, direction and foresightedness of the previous Director of NGDC, Alan H. Shapley. Larry D. Schultz was the leader tasked with carrying forward the concept, establishing the hardware and software requirements and providing software support. Bonnie A. Hausman provided outstanding programming support in developing all the new products prepared before, during and after the workshop. Essential programming assistance was provided by Peter Wilcoxen, Peter Sloss, and Maurine Hobbs. The typing headaches fell upon Carol Weathers as four drafts of the joint paper were prepared during the workshop. Additional support was provided by Kathy Joniak, Terri Fryar, Ron Buhmann, Joe Salazar, Carl Abstron, John Kinsfather, and Chuck Shanks. Essential managerial support, and useful comments on this paper were provided by Joe H. Allen, Director of WDC-A for STP.

APPENDIX A

IMS Meridian Chain Workshop

On March 9-11, 1982, a workshop on this particular project, sponsored by National Geophysical Data Center (NGDC), was conducted in Boulder, Colorado. This workshop was jointly organized by Y. Kamide and H. W. Kroehl, and was attended both by representatives of the IMS meridian chains and by scientists who provided computer algorithms to model the current distribution. The objective of the workshop was to discuss the dynamics of magnetic perturbations recorded during the March 17-19, 1978, period, to discuss some of the results as well as future works using that data base, and to estimate the global distribution of electric fields and currents, on an interactive basis through computer terminals located in the workshop room. The terminals were connected to a CDC CYBER-750 which is the main computer system in the NOAA Boulder Laboratories. In particular, this was perhaps the first attempt to provide each workshop participant with the ability to change the input parameters and assumptions and to see the effects of the changes on the output from a numerical modeling.

The procedure used is outlined as follows: The distribution of the magnetic perturbations in the geomagnetic north-south and east-west components relative to the average level of March 12, 1978 (the quietest day in March 1978) was used to calculate the equivalent current function in the ionosphere using a computer method developed by A. D. Richmond of the NOAA Space Environment Laboratory. From the current function and each of several different ionospheric conductivity models (e.g., the model compiled by R. W. Spiro of Rice University), the electric potential, the ionospheric and field-aligned currents, and Joule heat energy were then determined using the algorithm developed by Y. Kamide.

The workshop was conducted alternating between brief presentations by the participants and interactions with the data set through the computer terminals. G. Rostoker of the University of Alberta, Canada, pointed out the need to adjust the fitting program for the equivalent current function in order to account for the continuity of the auroral electrojets through regions of sparse data. He also argued the importance of the Z component for locating the electrojets, something not included in our original data base. B.-H. Ahn and S.-I. Akasofu, both of the University of Alaska, showed the possibility of estimating a better result for the global electric potential by using more realistic conductivities including local enhancements associated with local geomagnetic perturbations. As one of the outcomes of the joint study and the workshop, a paper describing the data set and some of the initial results has been accepted for publication (Kamide et al., 1982).

An important agreement was reached at the workshop to transfer all the collected and rearranged data on magnetic tape to WDC-A for STP for further distribution to the scientific community. The data base includes three days of 5-minute magnetometer data in the geomagnetic X_m and Y_m components from stations of six IMS meridian chains plus some standard observatories, a total of 71 stations above 50° in geomagnetic latitude in the Northern Hemisphere. The Z component data are available in a digital or analog form (depending on stations) on request to the representative of each meridian chain or from WDC-A.

APPENDIX B

THE DATA UTILIZATION WORKSHOP CONCEPT

The IMS Meridian Chain Workshop at NGDC was the first Data Utilization Workshop (DUW), an effort to bring the research community and the data center closer together and improve the access to high-quality data collections and analytical programs and facilities. Simply stated, the core functions of a data center are to collect, archive, disseminate, publish and analyze data. The analysis function is essential in addressing questions of data quality assessment, data usability, development of future programs and plans to meet new data needs of the scientific community. NGDC's analysis capabilities were developed over several years by resident staff professionals and visiting guestworkers, who developed programs and data products in pursuit of their scientific interests. Building on this foundation, the DUW's concept is to expand the data center's historical functions to include the collection, preparation and evaluation of a very good data base and to improve our understanding of an environmental phenomenon through the interactive analysis of these data and programs by many scientists. Some of the advantages to the scientists of holding this type of focused workshop at the data center are the human and computer resources in residence there and the availability of complementary data to answer questions that arise. Advantages to the data center include the expansion of their software library, improved quality assessment of the workshop data, increased utility of the data, and improved user relations. Each participant expressed his opinion that this workshop was extremely successful scientifically and encouraged the data center to expand the DUW concept in this and other fields.

REFERENCES

AKASOFU, S.-I., Y. KAMIDE, and J. L. KISABETH — 1981 — Comparison of two modeling methods for three dimensional current systems, J. Geophys. Res., 86, 3389.

COLE, K. D. — 1963 — Eccentric dipole coordinates, Australian J. Phys., 16, 423.

KAMIDE, Y., and S. MATSUSHITA — 1979 — Simulation studies of ionospheric electric fields and currents in relation to field-aligned currents, 1. Quiet periods, J. Geophys. Res., 84, 4083.

KAMIDE, Y., and A. D. RICHMOND — 1982 — Ionospheric conductivity dependence of electric fields and currents estimated from ground magnetic observations, J. Geophys. Res., 87, 8331.

KAMIDE, Y., A. D. RICHMOND, and S. MATSUSHITA — 1981 — Estimation of ionospheric electric fields, ionospheric currents and field-aligned currents from ground magnetic records, J. Geophys. Res., 86, 801.

KAMIDE, Y., B.-H. AHN, S.-I. AKASOFU, W. BAUMJOHANN, E. FRIIS-CHRISTENSEN, H. W. KROEHL, H. MAURER, A. D. RICHMOND, G. ROSTOKER, R. W. SPIRO, J. K. WALKER, and A. N. ZAITZEV — 1982 — Global distribution of ionospheric and field-aligned currents during substorms as determined from six IMS meridian chains of magnetometers. Initial results, J. Geophys. Res., 87, 8228.

KISABETH, J. L. — 1979 — On calculating magnetic and vector potential fields due to large-scale magnetospheric current systems and induced currents in an infinitely conducting earth, in Quantitative Modeling of Magnetospheric Processes, ed. by W. P. Olson, Amer. Geophys. Union, pp. 473-498.

MISHIN, V. M., A. D. BAZARZHAPOV, and G. V. SHPYNEV — 1980 — Electric fields and currents in the earth's magnetosphere, in Dynamics of the Magnetosphere, ed. by S.-I. Akasofu, D. Reidel, pp. 249-268.

RICHMOND, A. D. H. W. KROEHL, M. A. HENNING, and Y. KAMIDE — 1979 — Magnetic potential plots over the northern hemisphere for 26-28 March 1976, WDC-A Report UAG-71.

SPIRO, R. W., P. H. REIFF, and L. G. MAHER, JR. — 1979 — Precipitating electron energy flux and auroral zone conductances—An empirical model, J. Geophys. Res., 87, 8215.

VANYAN, L. L., and I. L. OSYPOVA — 1976 — The electrical conductivity of the polar ionosphere, Geomag. Aeronomy, 15, 847.

VICKREY, J. F., R. R. VONDRAK, and S. J. MATTHEWS — 1981 — The diurnal and latitudinal variation of auroral zone ionospheric conductivity, J. Geophys. Res., 86, 65.

WALLIS, D. D., and E. E. BUDZINSKI — 1981 — Empirical models of height integrated conductivities, J. Geophys. Res., 86, 125.

PART 2

Common-Scale Magnetograms from the 71 Stations

In Part 2, we show X_m and Y_m component traces for all the 71 stations for March 17, 18 and 19, 1978. The scale value is marked at the right-bottom corner of each figure.

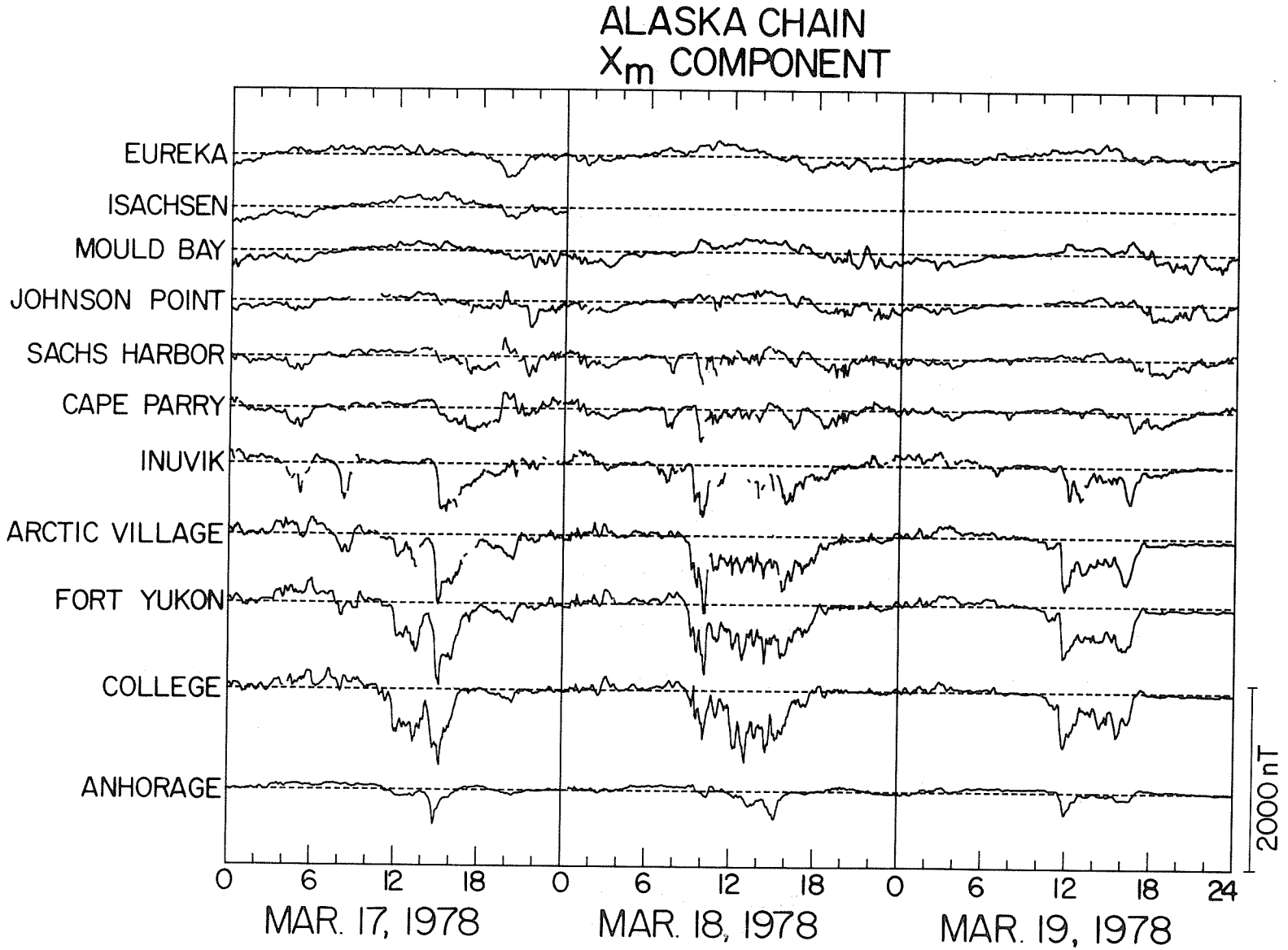
ALASKA CHAIN
X_m COMPONENT
EUREKA
ISACHSEN
MOULD BAY
JOHNSON POINT
SACHS HARBOR
CAPE PARRY
INUVIK
ARCTIC VILLAGE
FORT YUKON
COLLEGE
ANHORAGE
2000 nT
0 6 12 18 0 6 12 18 0 6 12 18 24
MAR. 17, 1978
MAR. 18, 1978
MAR. 19, 1978

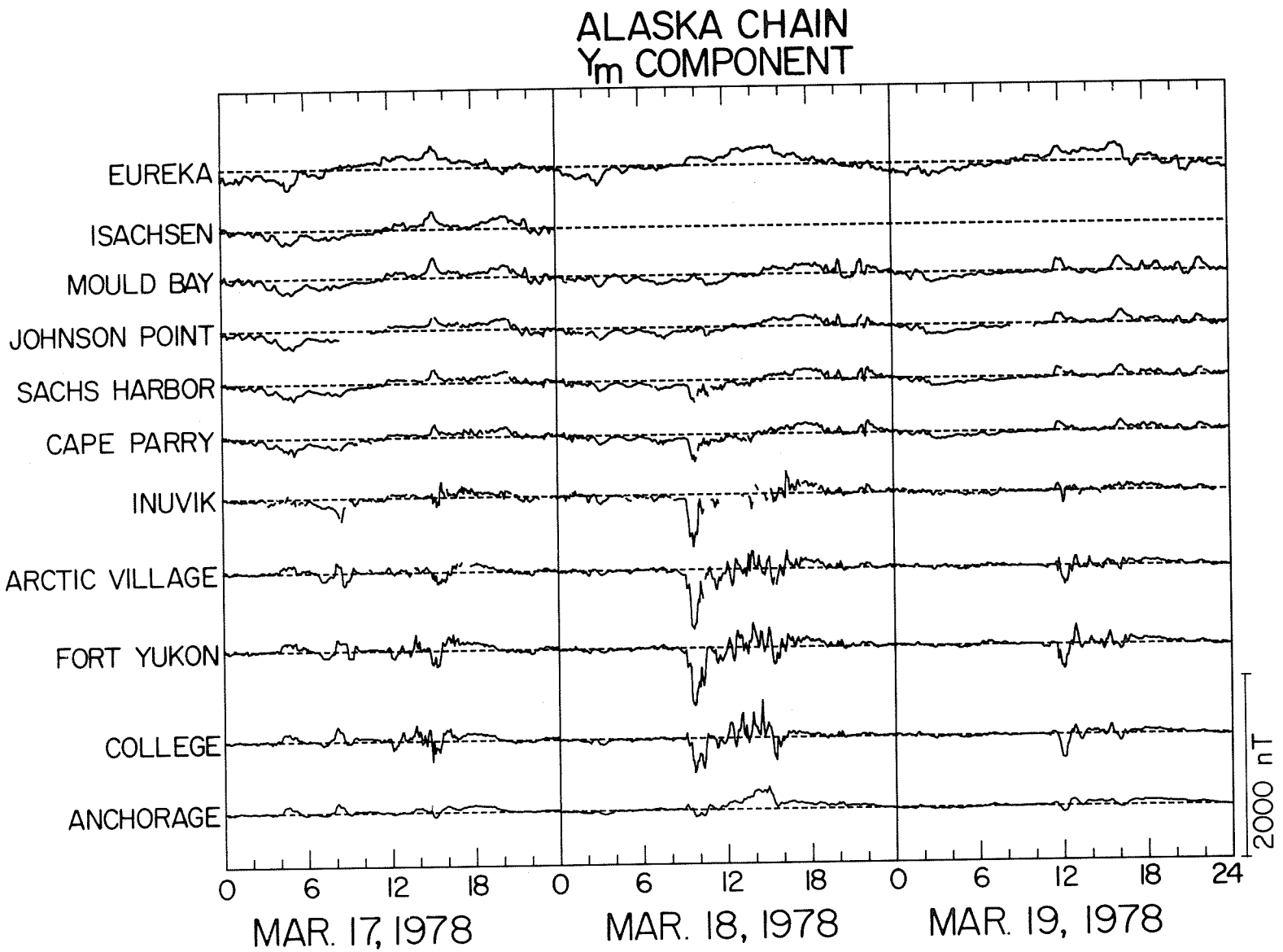
ALASKA CHAIN
Ym COMPONENT
EUREKA
ISACHSEN
MOULD BAY
JOHNSON POINT
SACHS HARBOR
CAPE PARRY
INUVIK
ARCTIC VILLAGE
FORT YUKON
COLLEGE
ANCHORAGE
2000 nT
0 6 12 18 0 6 12 18 0 6 12 18 24
MAR. 17, 1978
MAR. 18, 1978
MAR. 19, 1978

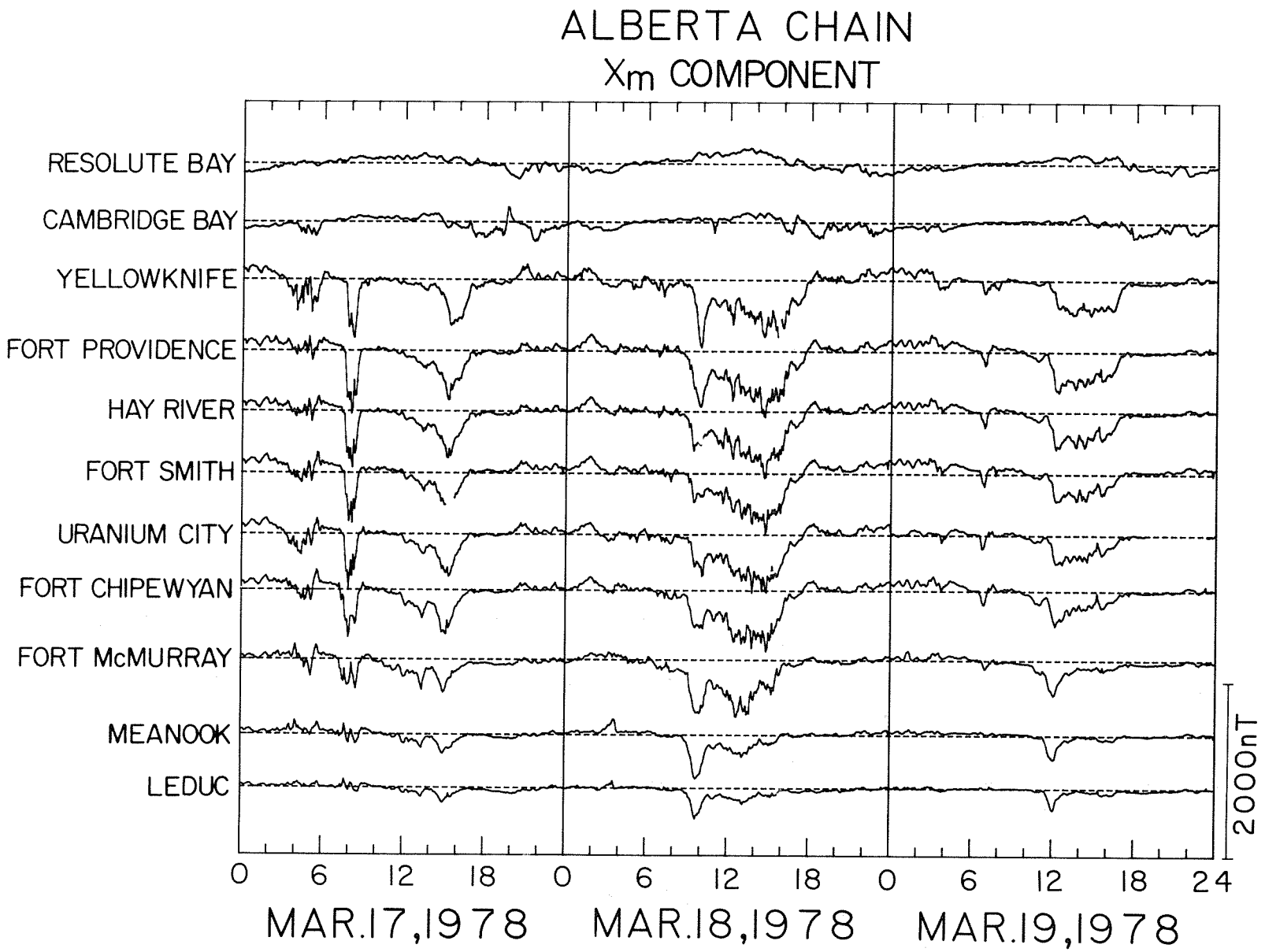
ALBERTA CHAIN
Xm COMPONENT
RESOLUTE BAY
CAMBRIDGE BAY
YELLOWKNIFE
FORT PROVIDENCE
HAY RIVER
FORT SMITH
URANIUM CITY
FORT CHIPEWYAN
FORT McMURRAY
MEANOOK
LEDUC
2000nT
0 6 12 18 0 6 12 18 0 6 12 18 24
MAR.17,1978
MAR.18,1978
MAR.19,1978

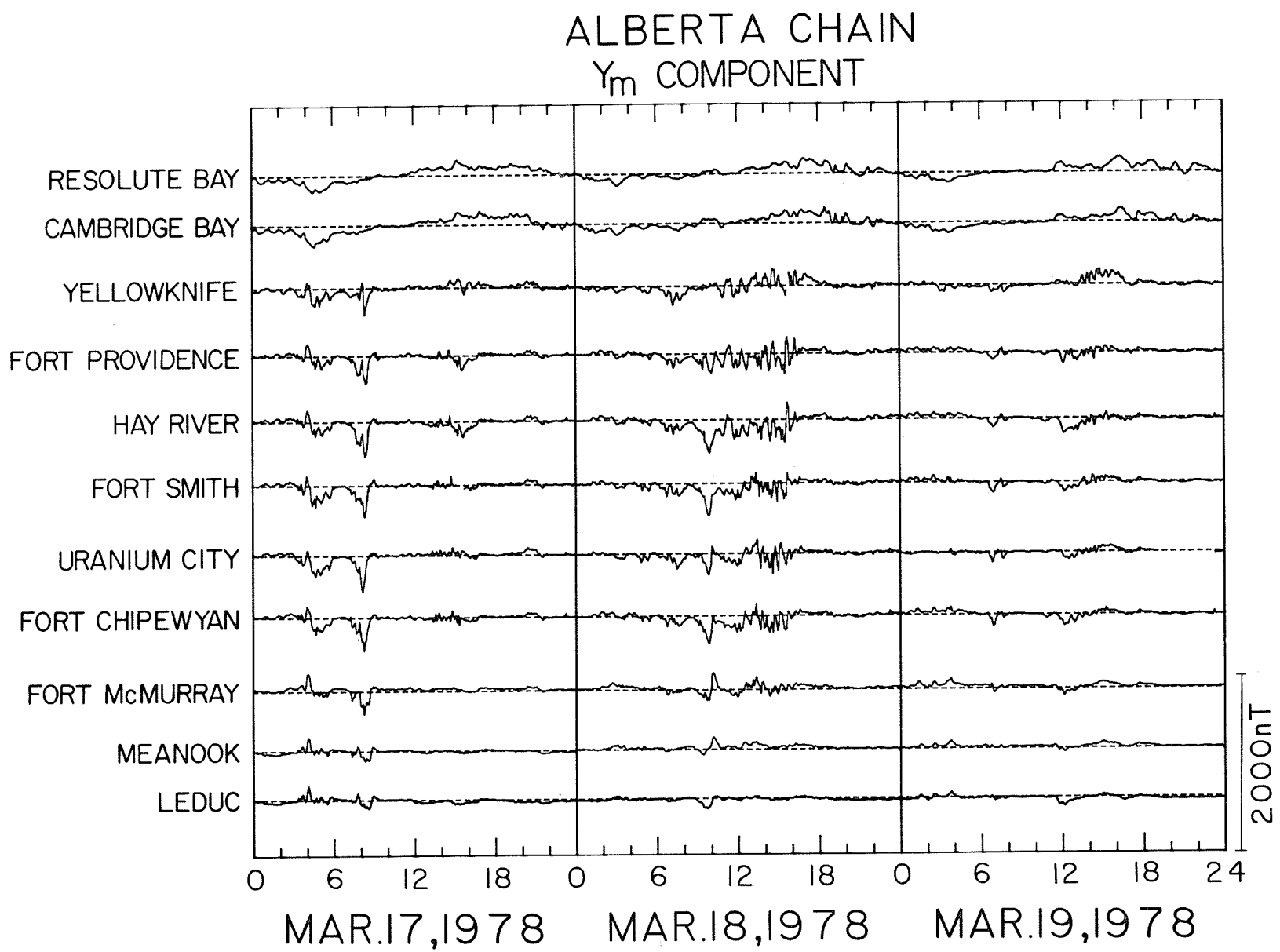
ALBERTA CHAIN
Ym COMPONENT
RESOLUTE BAY
CAMBRIDGE BAY
YELLOWKNIFE
FORT PROVIDENCE
HAY RIVER
FORT SMITH
URANIUM CITY
FORT CHIPEWYAN
FORT McMURRAY
MEANOOK
LEDUC
2000nT
0 6 12 18 0 6 12 18 0 6 12 18 24
MAR.17,1978
MAR.18,1978
MAR.19,1978

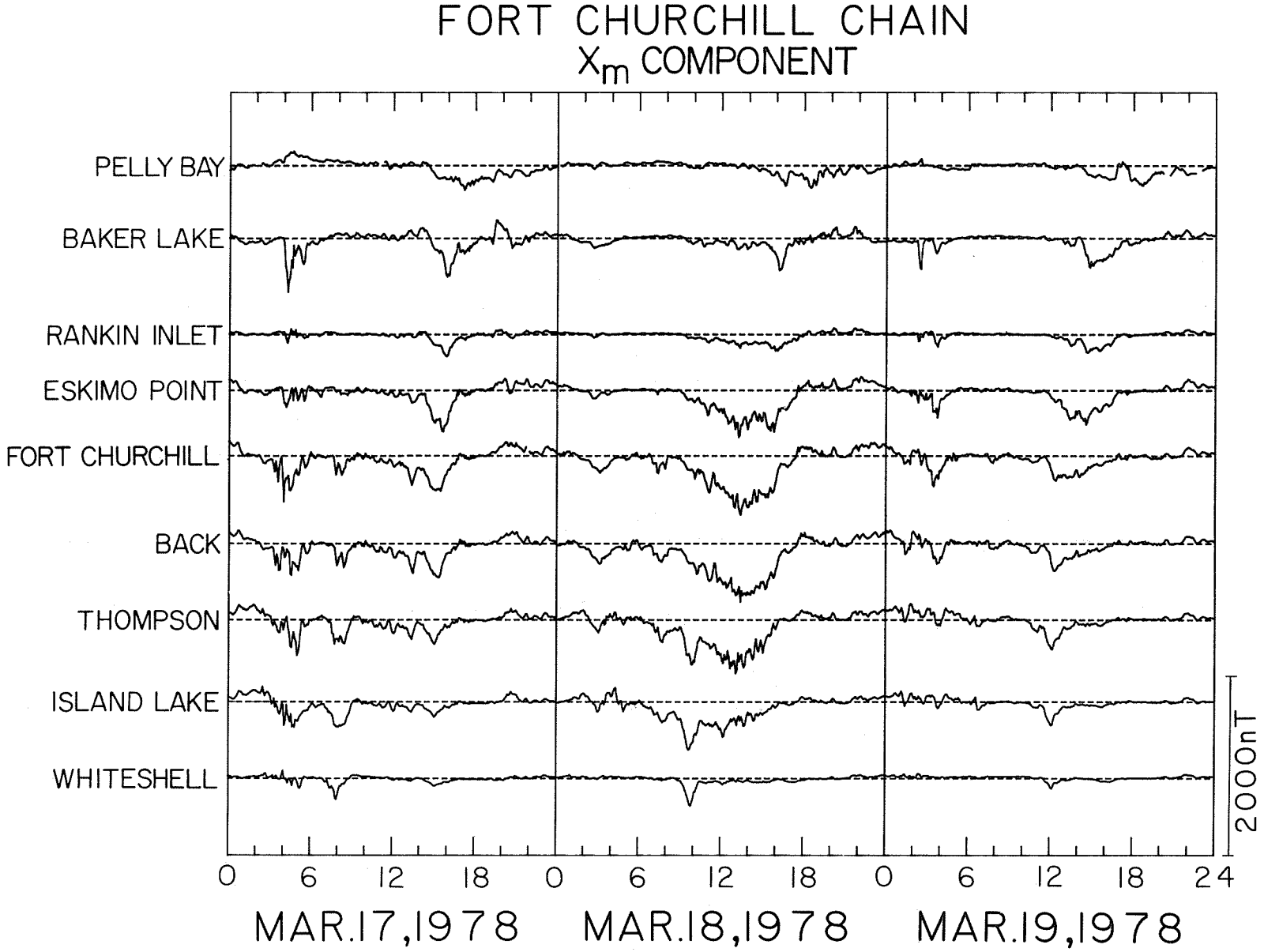
FORT CHURCHILL CHAIN
X_m COMPONENT
PELLY BAY
BAKER LAKE
RANKIN INLET
ESKIMO POINT
FORT CHURCHILL
BACK
THOMPSON
ISLAND LAKE
WHITESHELL
2000nT
0 6 12 18 0 6 12 18 0 6 12 18 24
MAR.17,1978 MAR.18,1978 MAR.19,1978

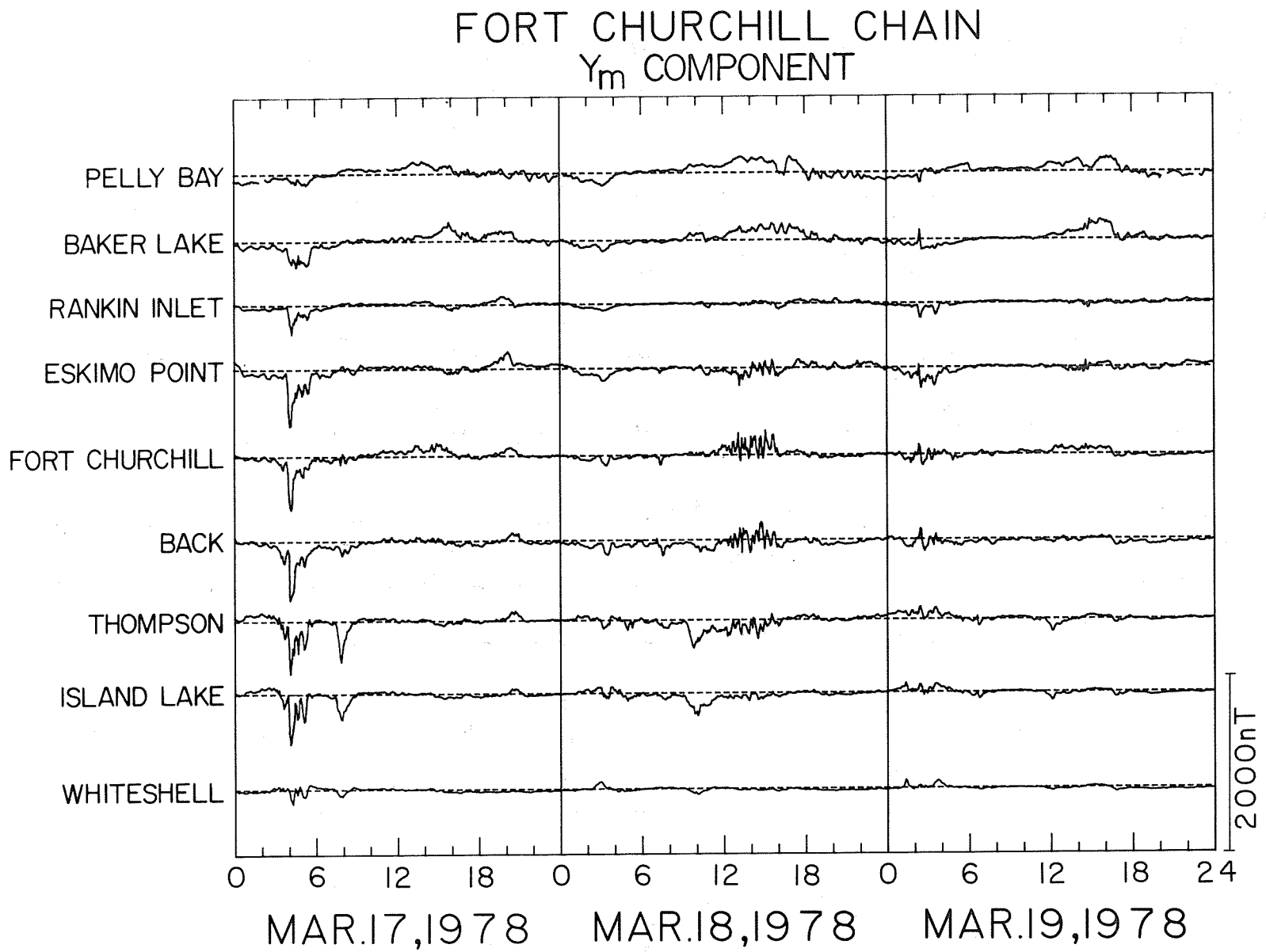
FORT CHURCHILL CHAIN
Ym COMPONENT
PELLY BAY
BAKER LAKE
RANKIN INLET
ESKIMO POINT
FORT CHURCHILL
BACK
THOMPSON
ISLAND LAKE
WHITESHELL
2000nT
0 6 12 18 0 6 12 18 0 6 12 18 24
MAR.17,1978 MAR.18,1978 MAR.19,1978

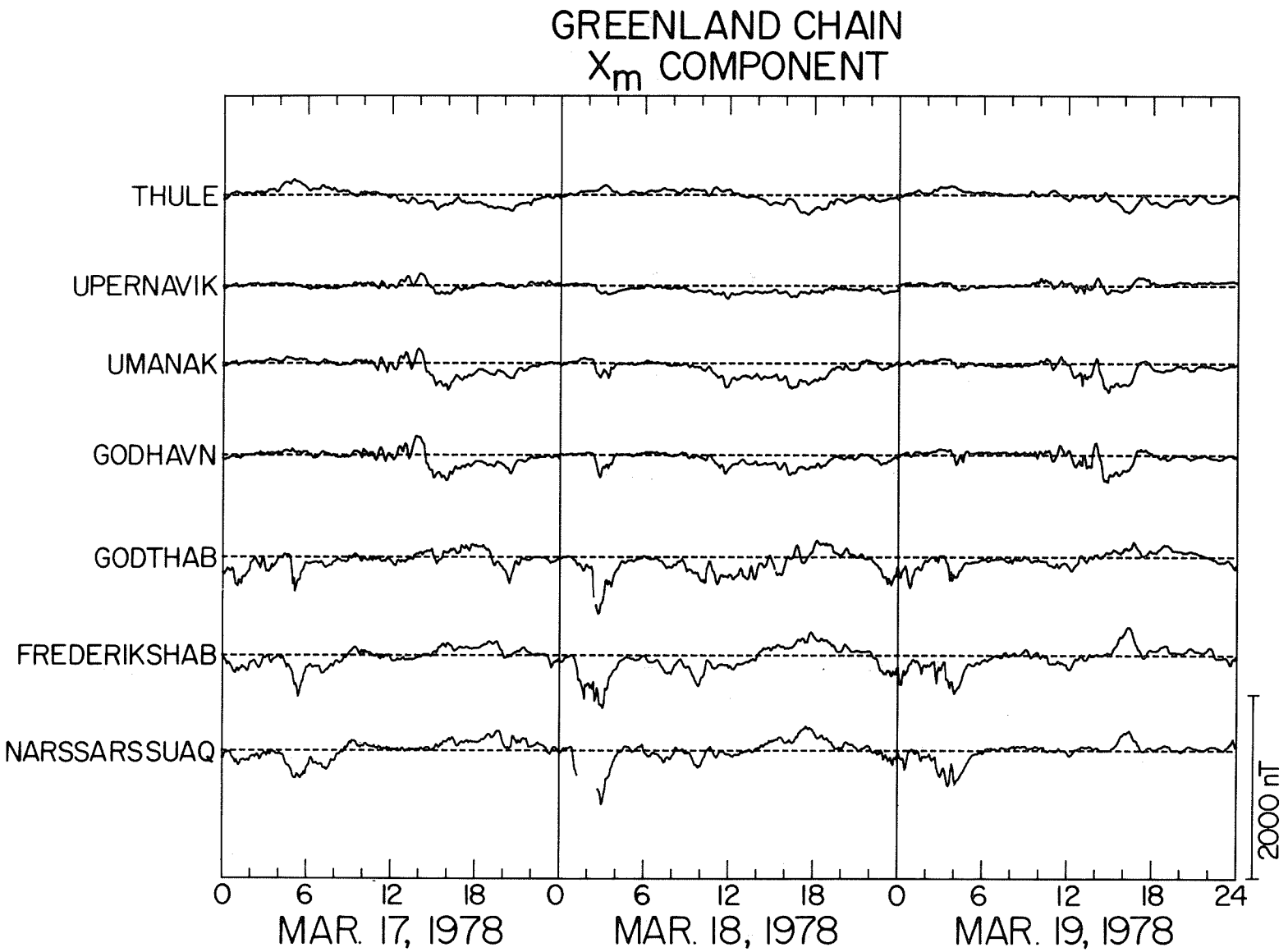
GREENLAND CHAIN
X_m COMPONENT
THULE
UPERNAVIK
UMANAK
GODHAVN
GODTHAB
FREDERIKSHAB
NARSSARSSUAQ
2000 nT
0 6 12 18 0 6 12 18 0 6 12 18 24
MAR. 17, 1978
MAR. 18, 1978
MAR. 19, 1978

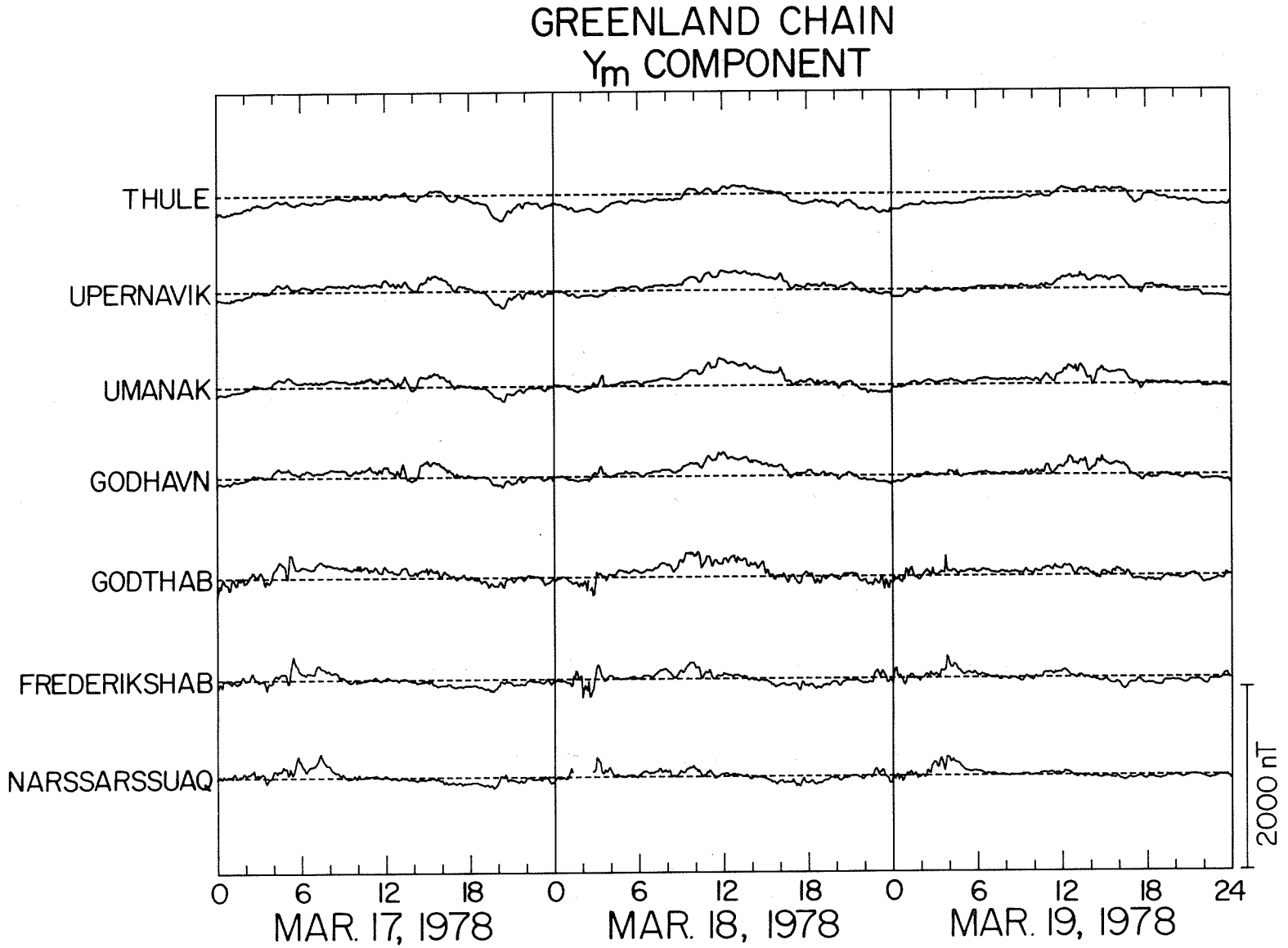
GREENLAND CHAIN
Ym COMPONENT
THULE
UPERNAVIK
UMANAK
GODHAVN
GODTHAB
FREDERIKSHAB
NARSSARSSUAQ
2000 nT
0
6
12
18
0
6
12
18
0
6
12
18
24
MAR. 17, 1978
MAR. 18, 1978
MAR. 19, 1978

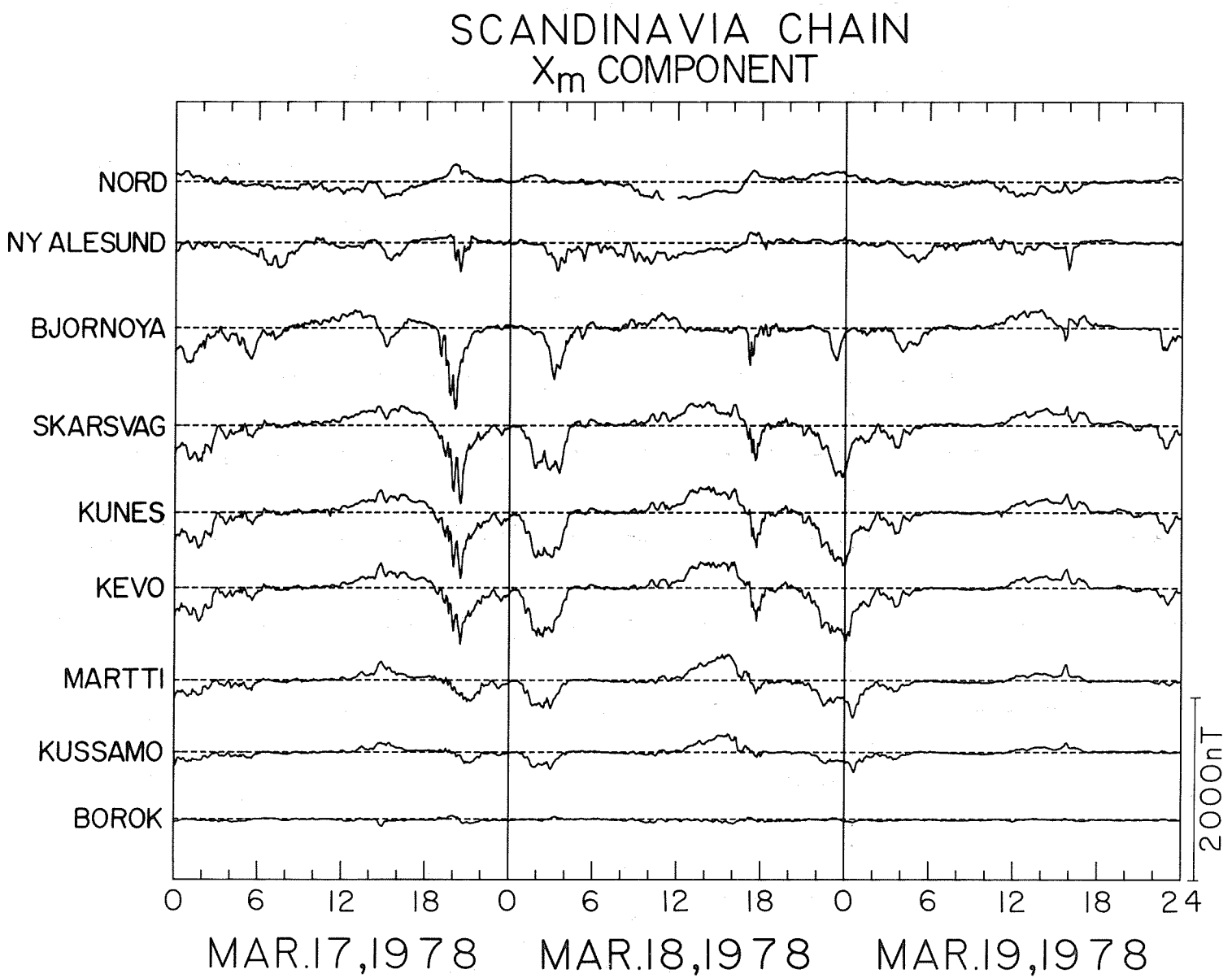
SCANDINAVIA CHAIN
X_m COMPONENT
NORD
NY ALESUND
BJORNOYA
SKARSVAG
KUNES
KEVO
MARTTI
KUSSAMO
BOROK
2000nT
0 6 12 18 0 6 12 18 0 6 12 18 24
MAR.17,1978 MAR.18,1978 MAR.19,1978

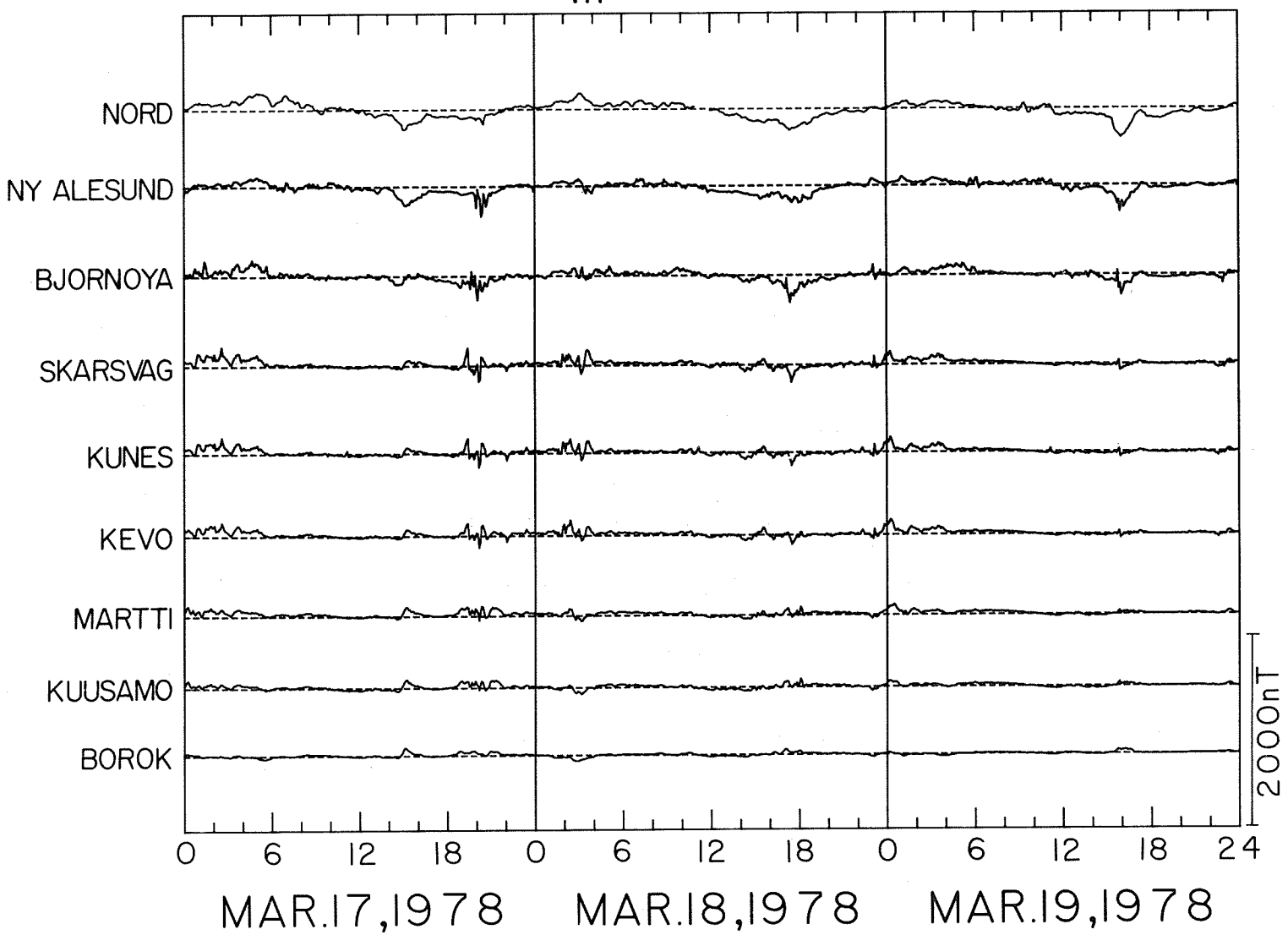
SCANDINAVIA CHAIN
Y_m COMPONENT
NORD
NY ALESUND
BJORNOYA
SKARSVAG
KUNES
KEVO
MARTTI
KUUSAMO
BOROK
2000nT
0 6 12 18 0 6 12 18 0 6 12 18 24
MAR.17,1978 MAR.18,1978 MAR.19,1978

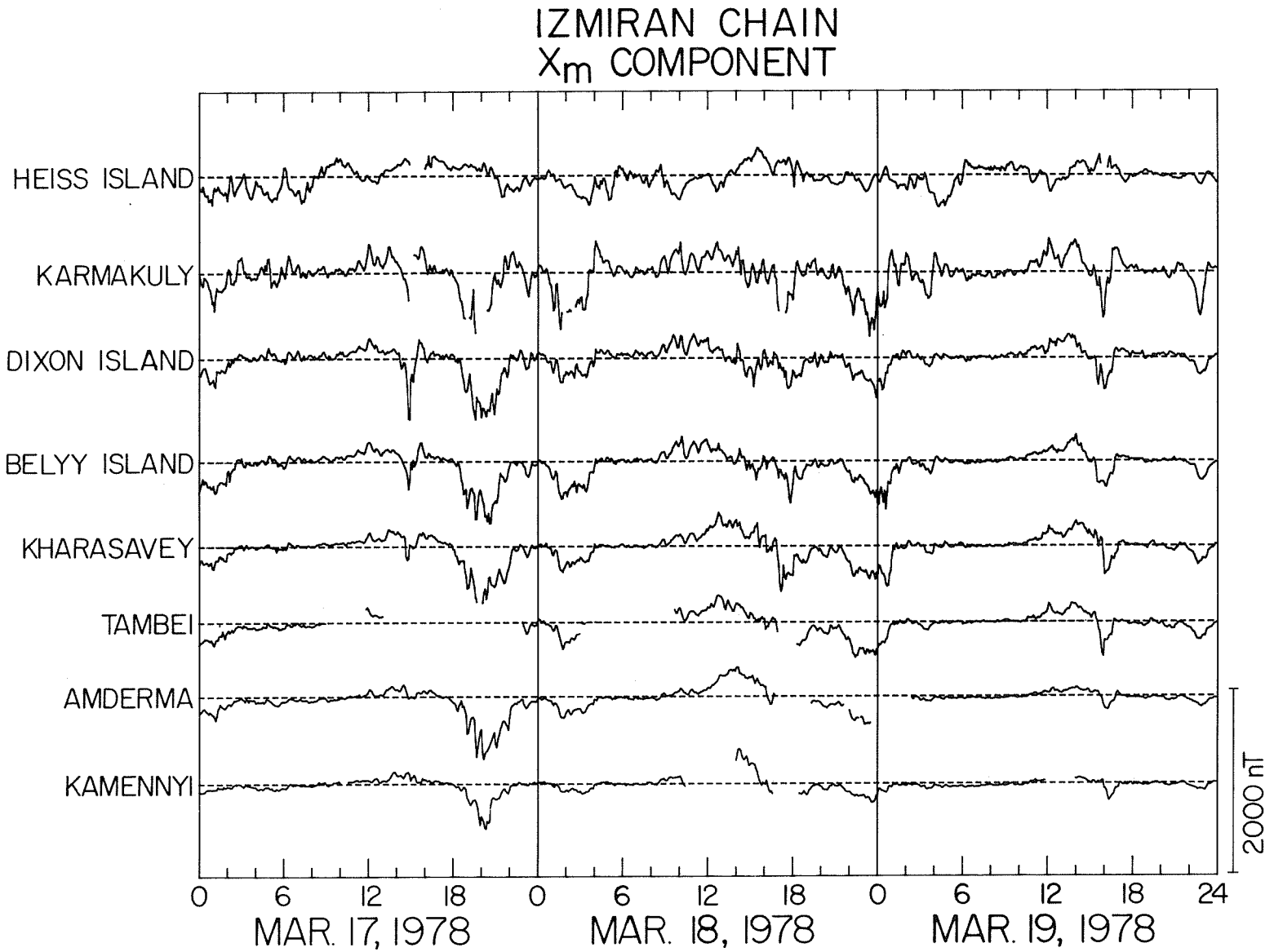
IZMIRAN CHAIN
Xm COMPONENT
HEISS ISLAND
KARMAKULY
DIXON ISLAND
BELYY ISLAND
KHARASAVEY
TAMBEI
AMDERMA
KAMENNYI
2000 nT
0 6 12 18 0 6 12 18 0 6 12 18 24
MAR. 17, 1978
MAR. 18, 1978
MAR. 19, 1978

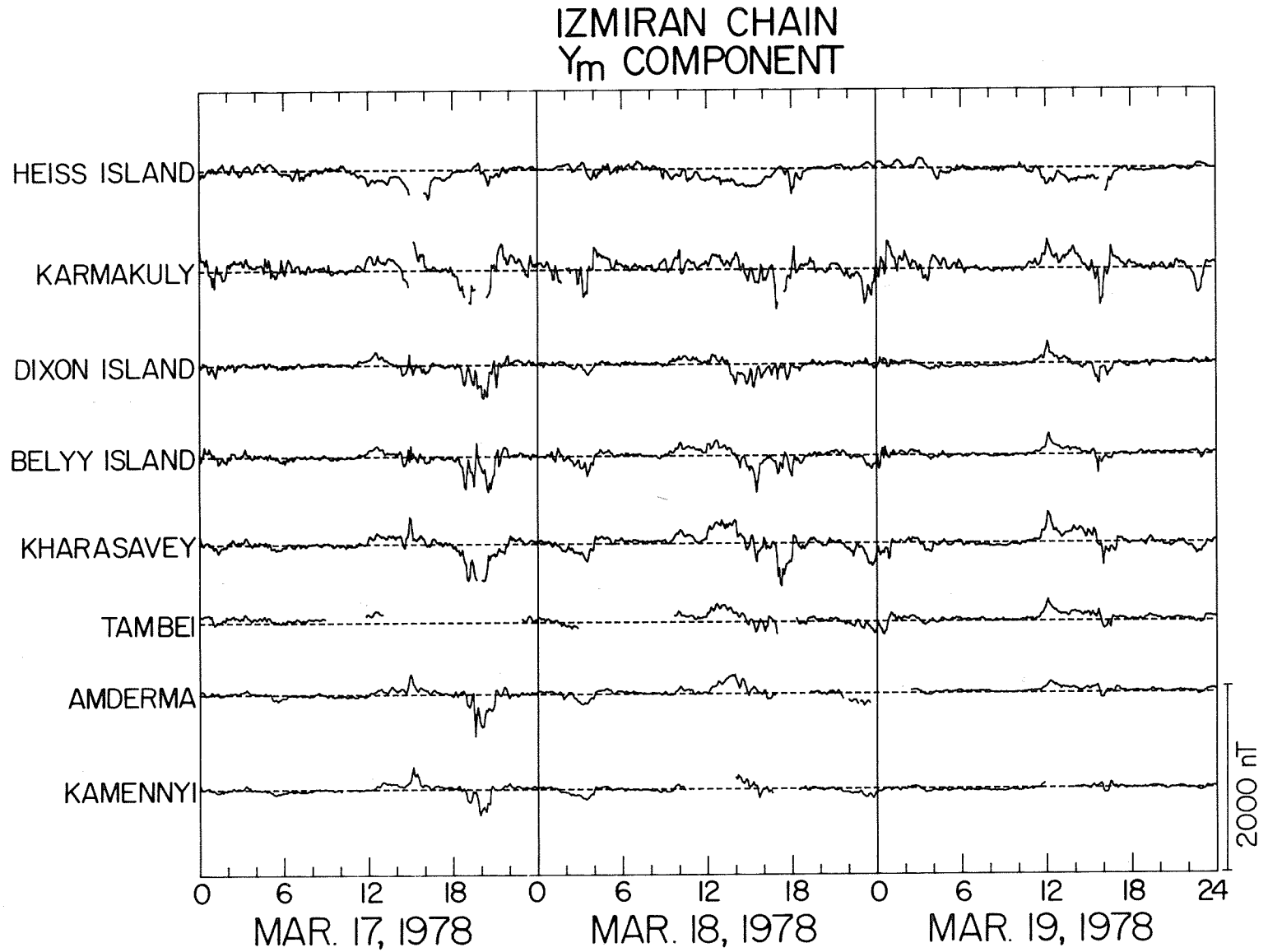
IZMIRAN CHAIN
Ym COMPONENT
HEISS ISLAND
KARMAKULY
DIXON ISLAND
BELYY ISLAND
KHARASAVEY
TAMBEI
AMDERMA
KAMENNYI
2000 nT
0 6 12 18 0 6 12 18 0 6 12 18 24
MAR. 17, 1978
MAR. 18, 1978
MAR. 19, 1978

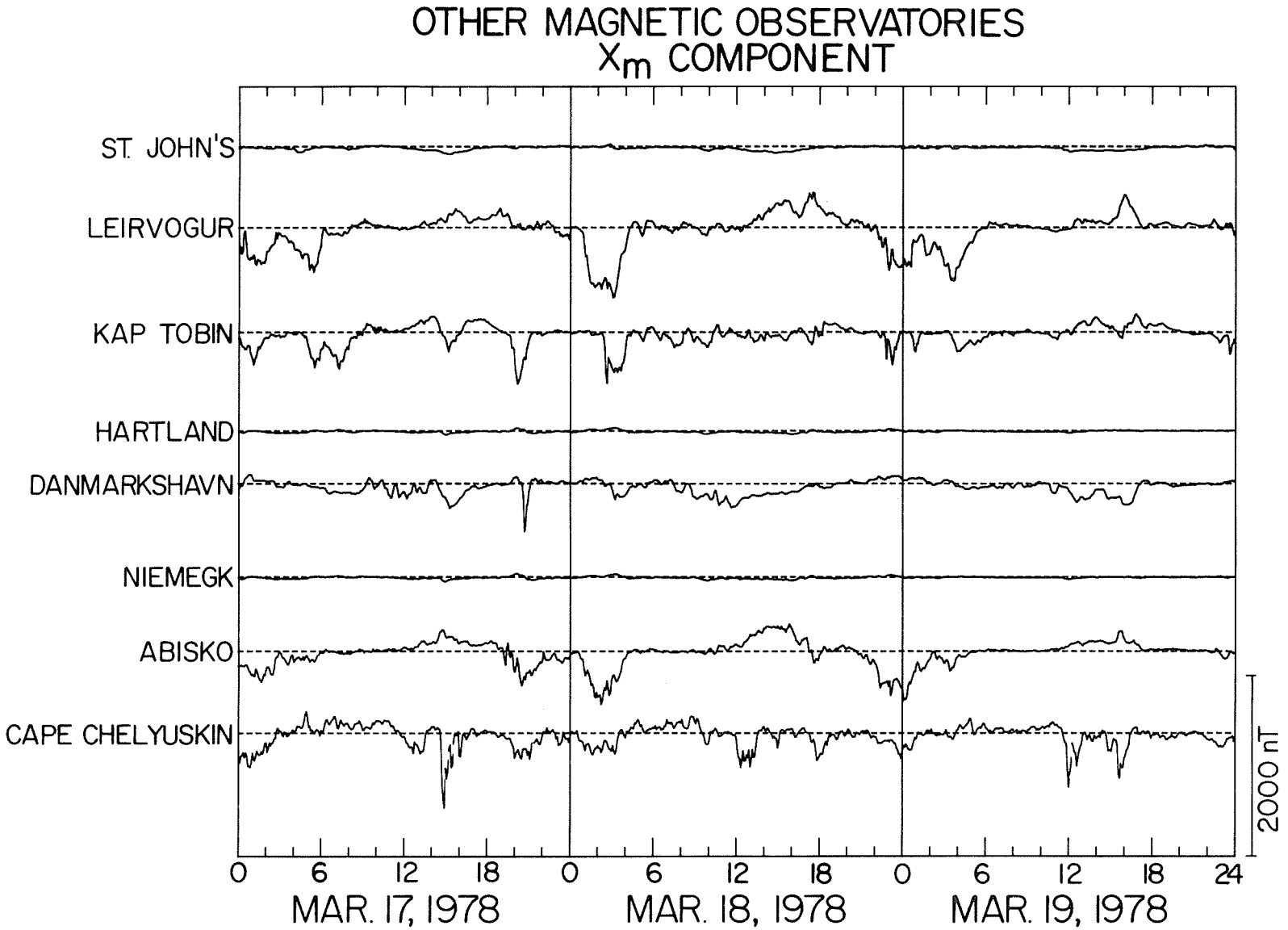
OTHER MAGNETIC OBSERVATORIES
X_m COMPONENT
ST. JOHN'S
LEIRVOGUR
KAP TOBIN
HARTLAND
DANMARKSHAVN
NIEMEGK
ABISKO
CAPE CHELYUSKIN
2000 nT
0
6
12
18
0
6
12
18
0
6
12
18
24
MAR. 17, 1978
MAR. 18, 1978
MAR. 19, 1978

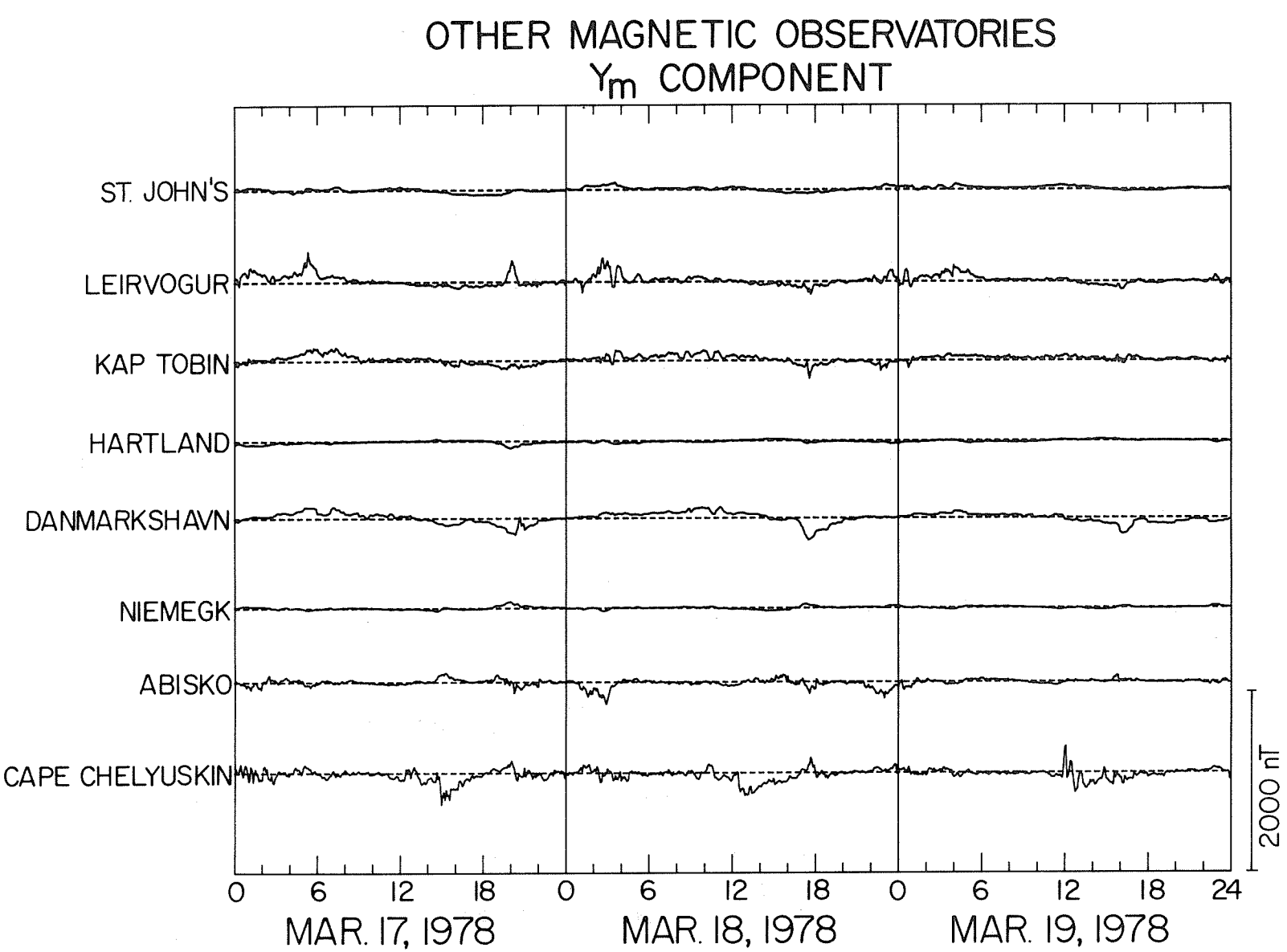
OTHER MAGNETIC OBSERVATORIES
Y_m COMPONENT
ST. JOHN'S
LEIRVOGUR
KAP TOBIN
HARTLAND
DANMARKSHAVN
NIEMEGK
ABISKO
CAPE CHELYUSKIN
2000 nT
0 6 12 18 0 6 12 18 0 6 12 18 24
MAR. 17, 1978
MAR. 18, 1978
MAR. 19, 1978

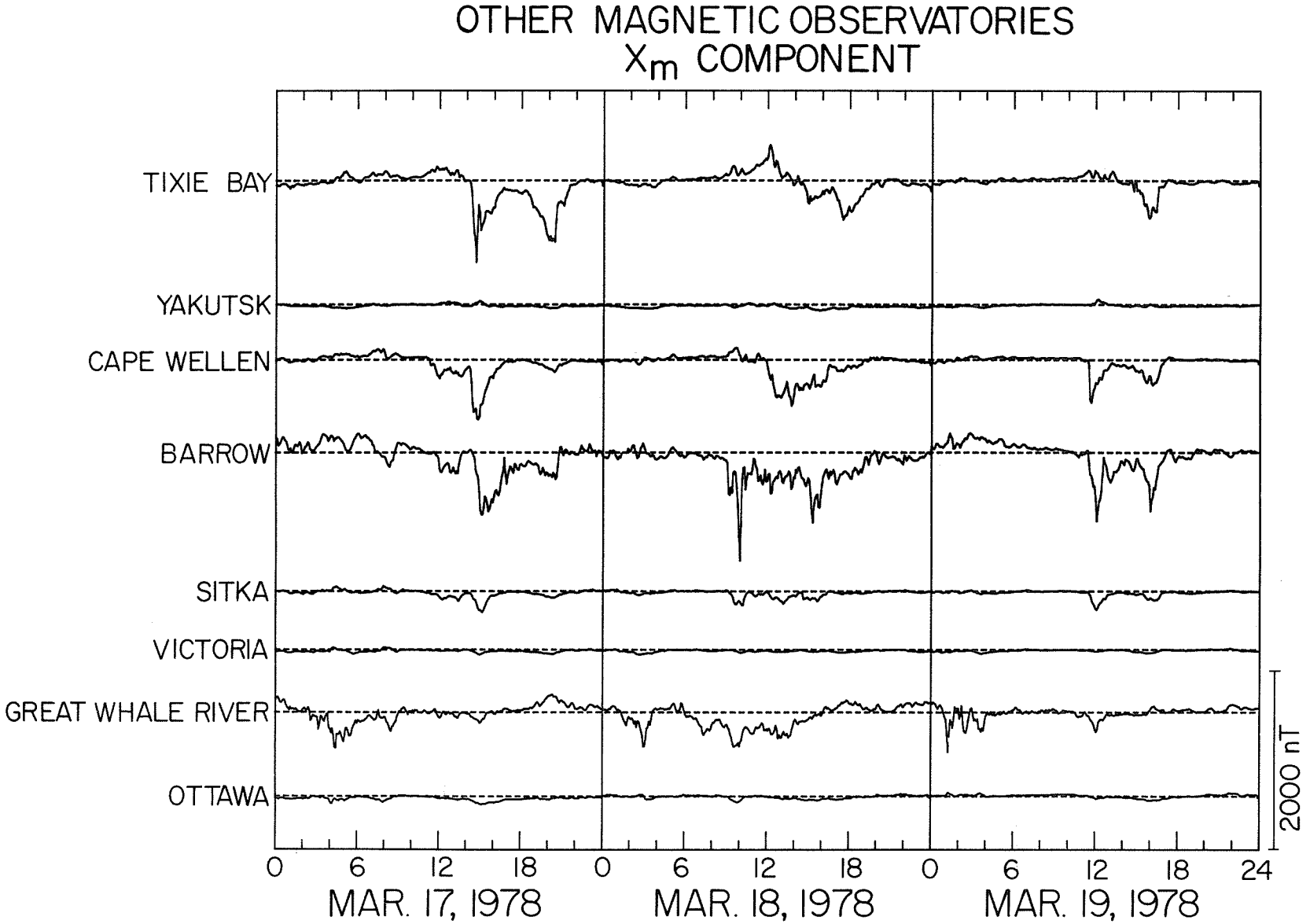
OTHER MAGNETIC OBSERVATORIES
X_m COMPONENT
TIXIE BAY
YAKUTSK
CAPE WELLEN
BARROW
SITKA
VICTORIA
GREAT WHALE RIVER
OTTAWA
2000 nT
0 6 12 18 0 6 12 18 0 6 12 18 24
MAR. 17, 1978
MAR. 18, 1978
MAR. 19, 1978

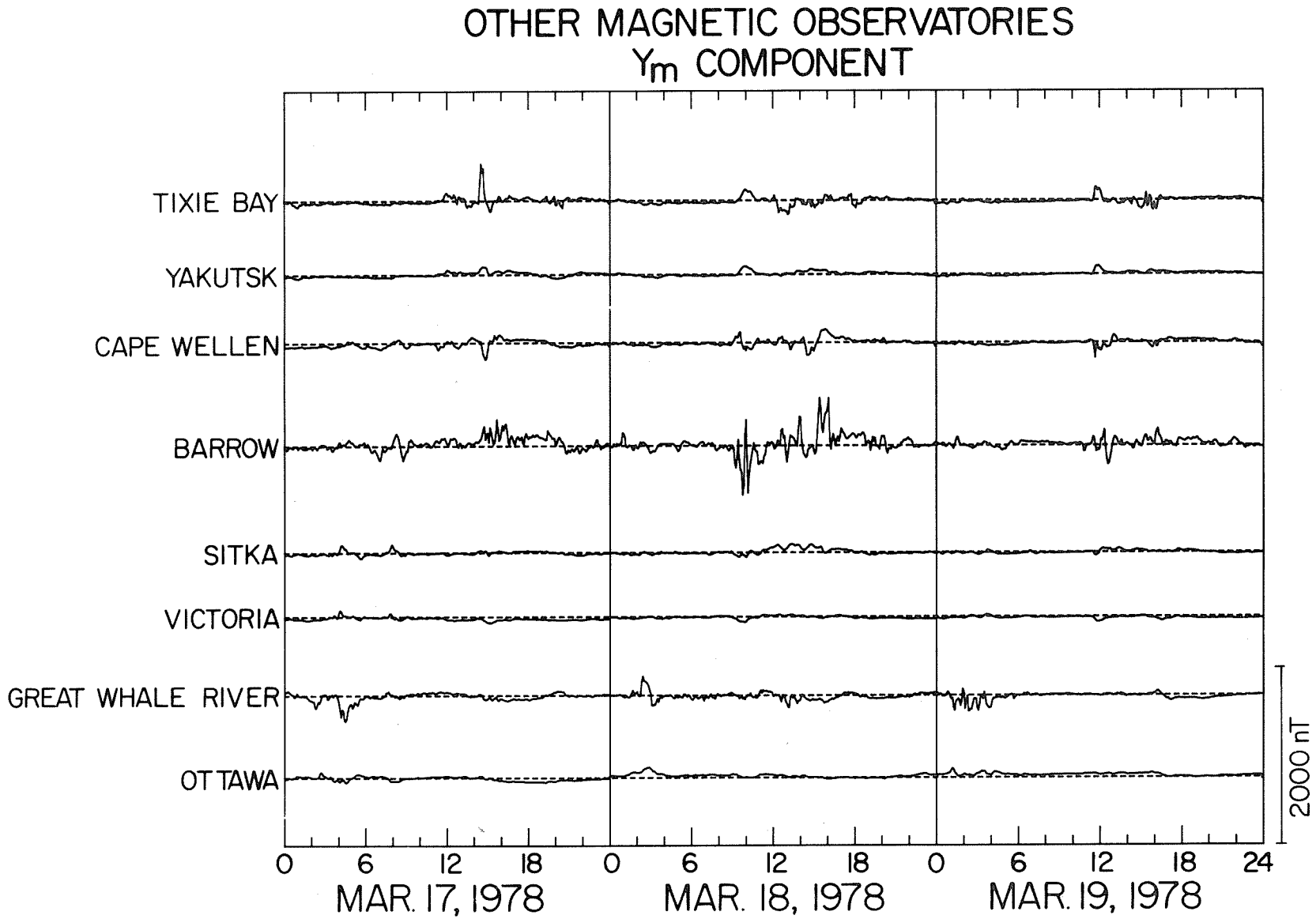
OTHER MAGNETIC OBSERVATORIES
Ym COMPONENT
TIXIE BAY
YAKUTSK
CAPE WELLEN
BARROW
SITKA
VICTORIA
GREAT WHALE RIVER
OTTAWA
2000 nT
0 6 12 18 0 6 12 18 0 6 12 18 24
MAR. 17, 1978
MAR. 18, 1978
MAR. 19, 1978

PART 3

The Hourly Plots of Observed Magnetic Perturbation Vectors, Equivalent Ionospheric Current Systems, Estimated Ionospheric Vectors, Joule Heating Rates, and Field-Aligned Currents

Out of the various outputs shown in Figures 4a-j, five plots (equivalent ionospheric current system, electric potential, ionospheric current vectors, Joule heating rate, and field-aligned current density) as well as the distribution of observed magnetic perturbations (in the form of their equivalent currents) are displayed every 1 hour for the 3-day interval. The outermost circle represents 50^{o} N in eccentric dipole latitude, with the other other circles every 10^{o}. Date and Universal Time are marked for each diagram: 76 = March 17, 77 = March 18, and 78 = March 19, 1978.

EQUIVALENT CURRENT

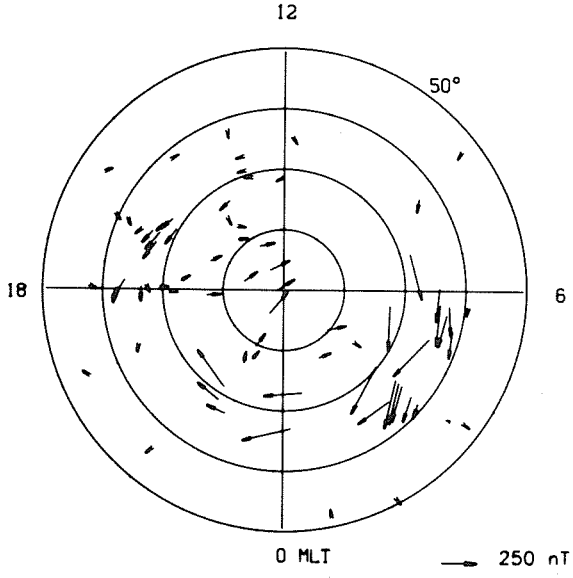

EQUIVALENT CURRENT SYSTEM

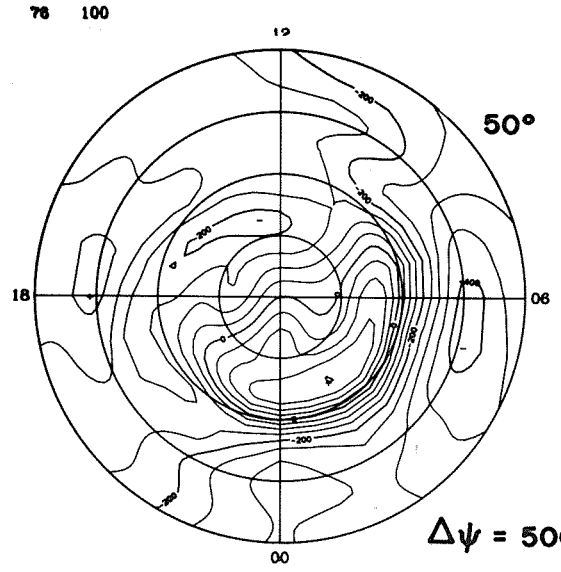

ELECTRIC POTENTIAL

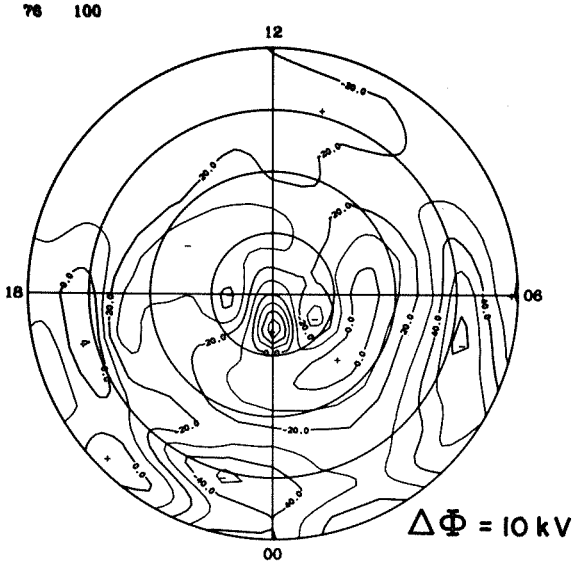

IONOSPHERIC CURRENT

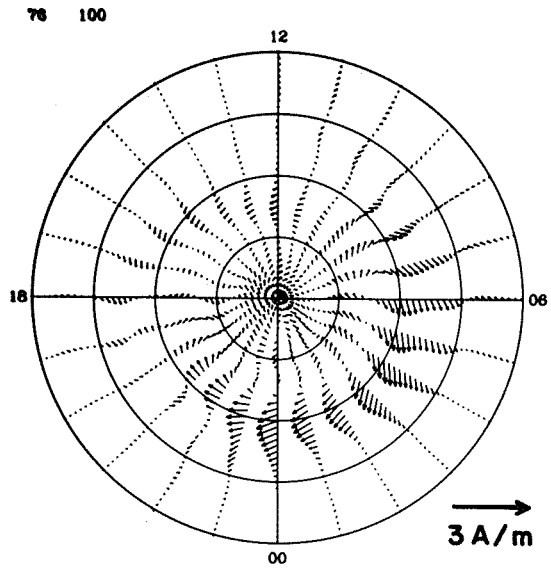

JOULE HEATING

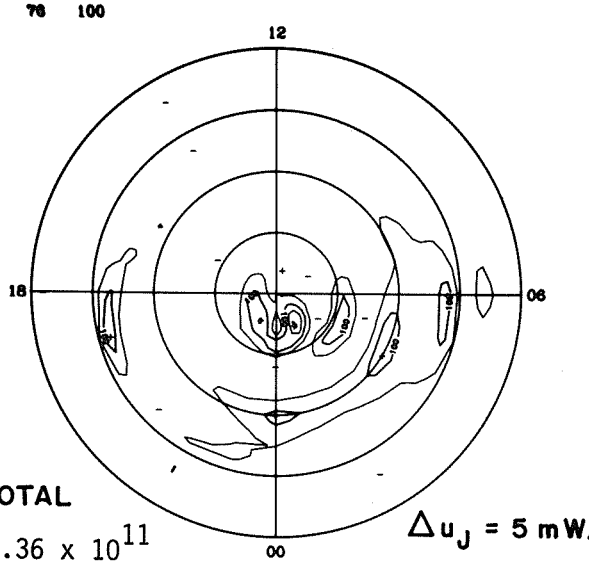

TOTAL

1.36×10^{11}

FIELD-ALIGNED CURRENT

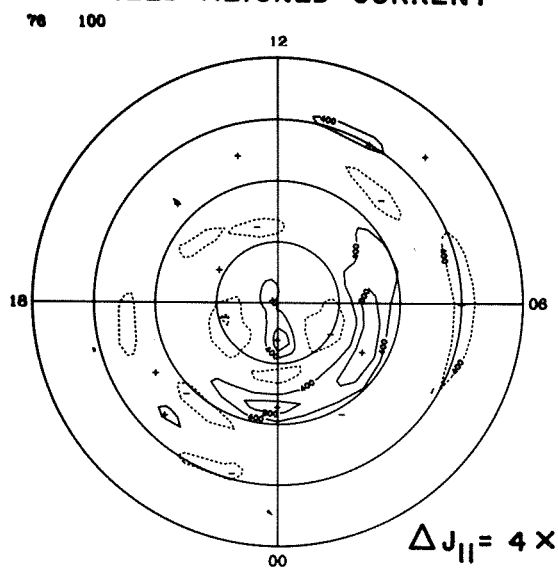

EQUIVALENT CURRENT

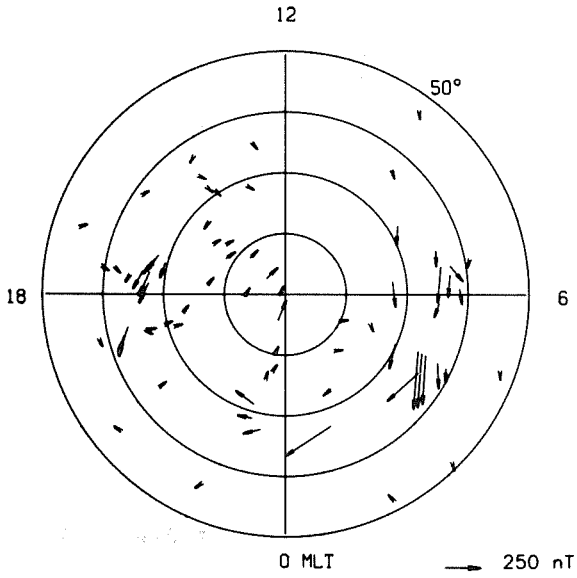

EQUIVALENT CURRENT SYSTEM

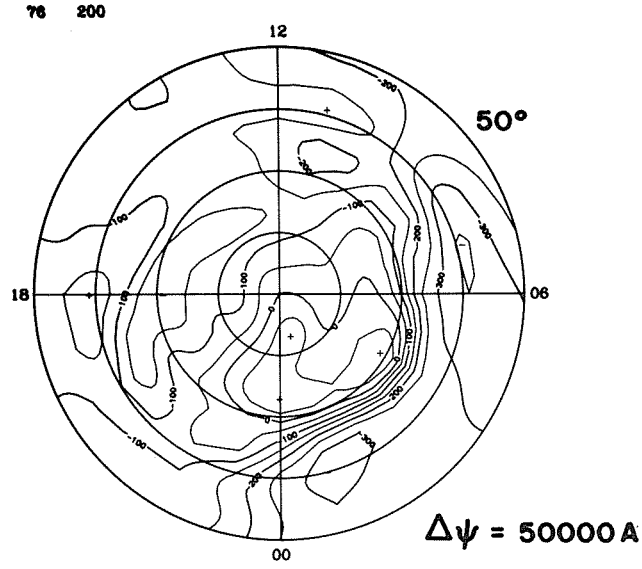

ELECTRIC POTENTIAL

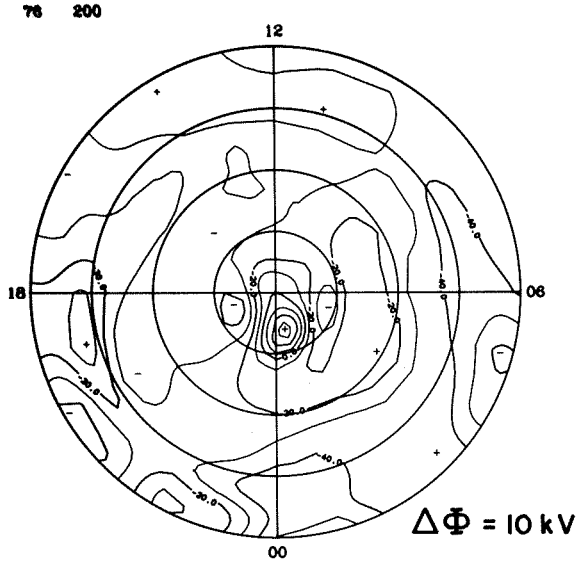

IONOSPHERIC CURRENT

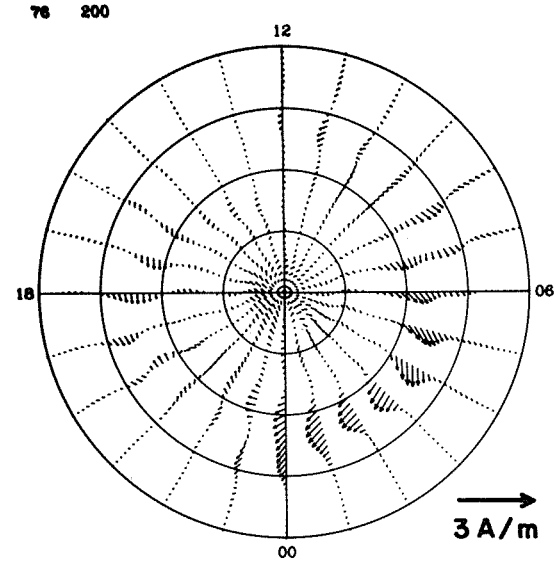

JOULE HEATING

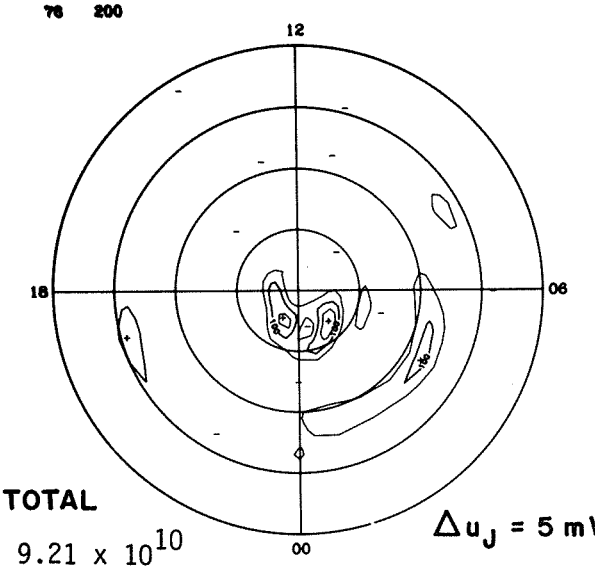

TOTAL

9.21×10^{10}

FIELD-ALIGNED CURRENT

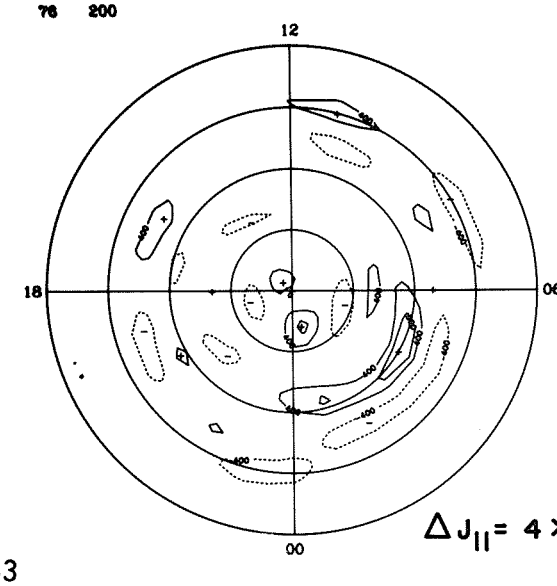

EQUIVALENT CURRENT

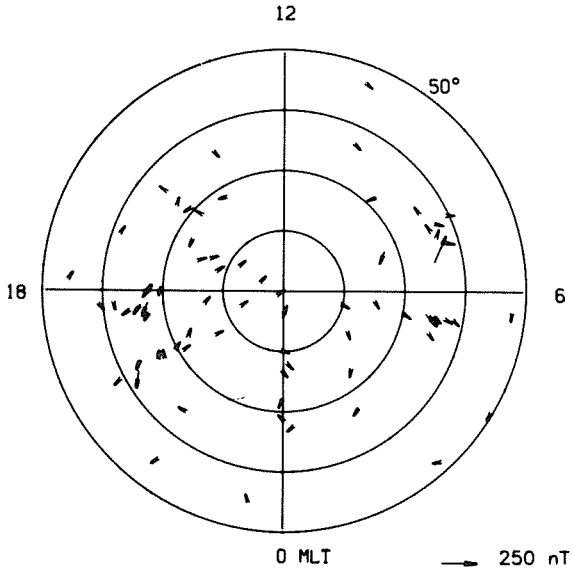

EQUIVALENT CURRENT SYSTEM

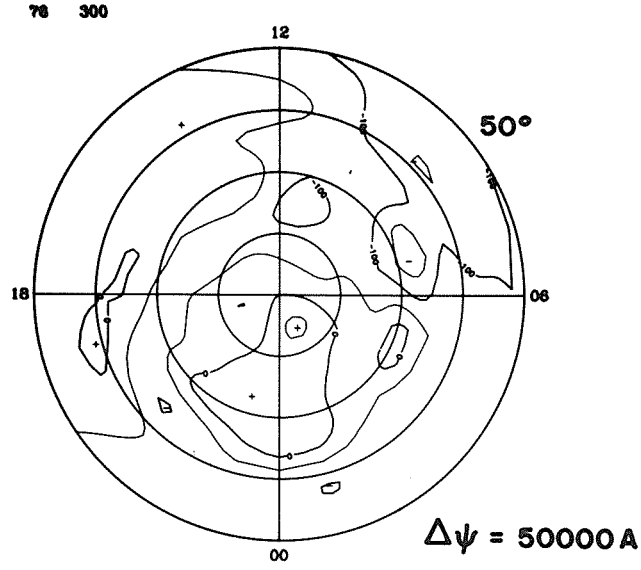

ELECTRIC POTENTIAL

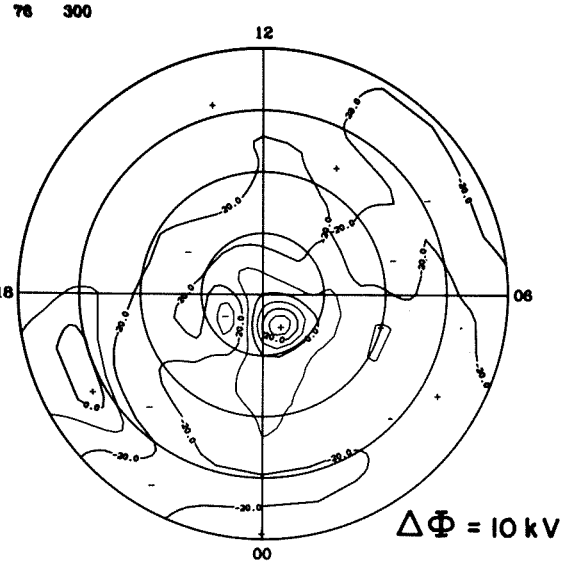

IONOSPHERIC CURRENT

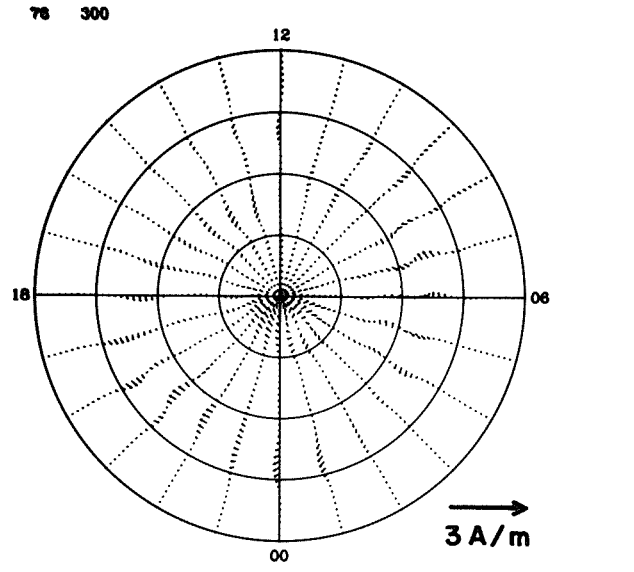

JOULE HEATING

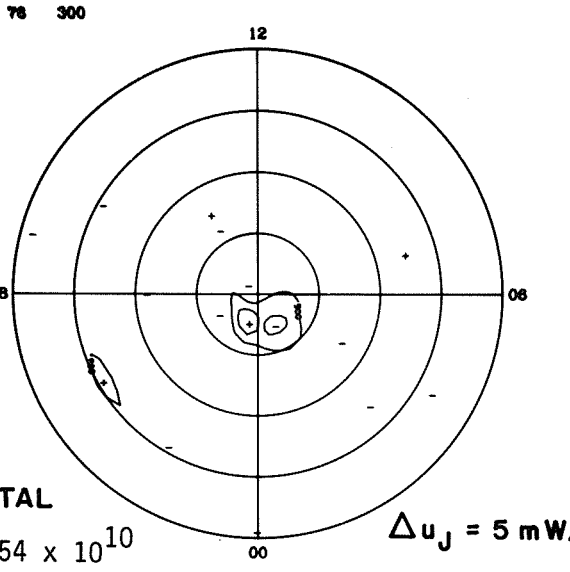

TOTAL

4.54 x 10^{10}

FIELD-ALIGNED CURRENT

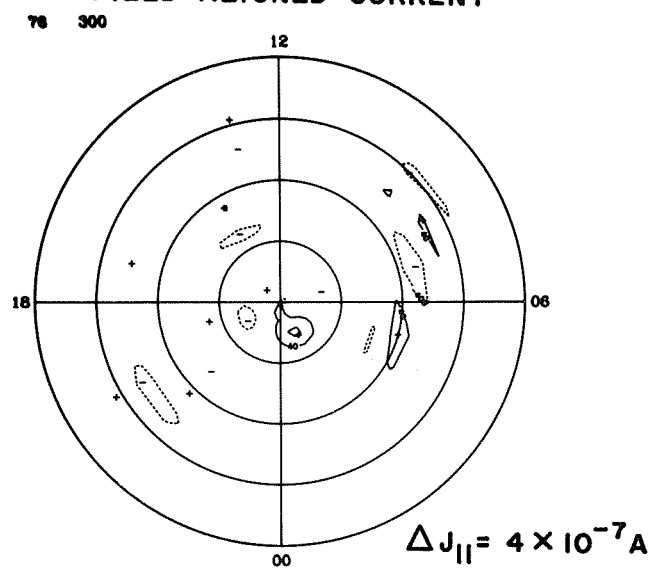

EQUIVALENT CURRENT

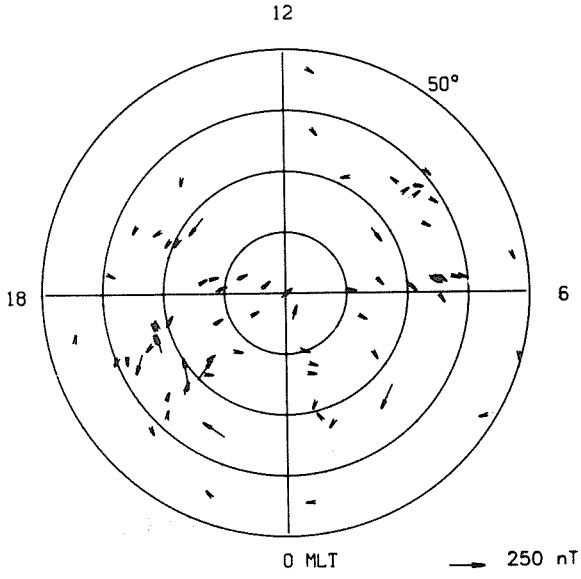

EQUIVALENT CURRENT SYSTEM

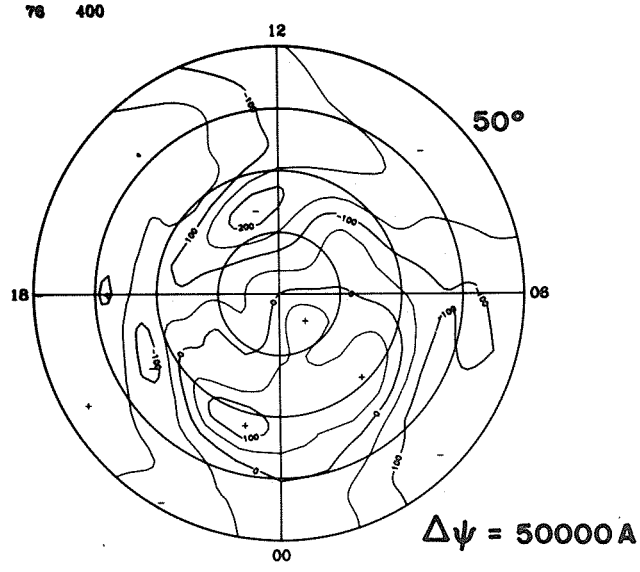

ELECTRIC POTENTIAL

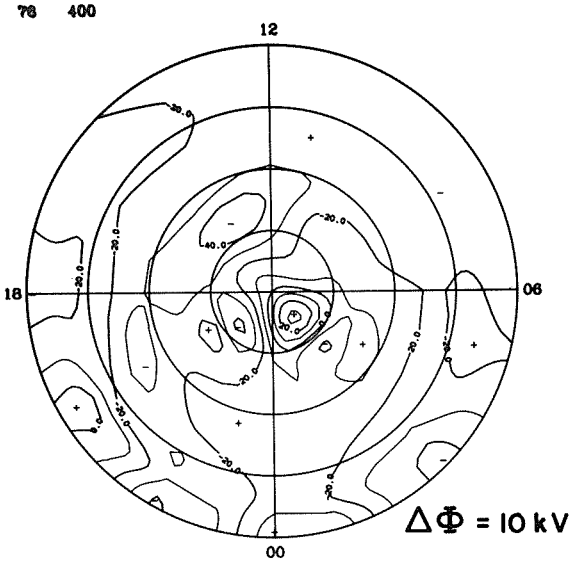

IONOSPHERIC CURRENT

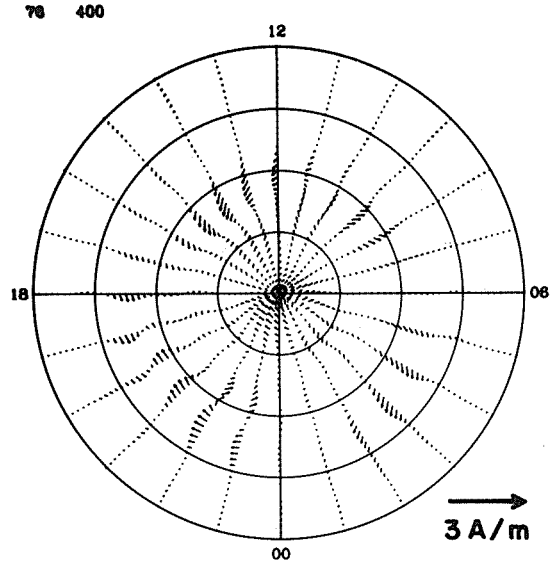

JOULE HEATING

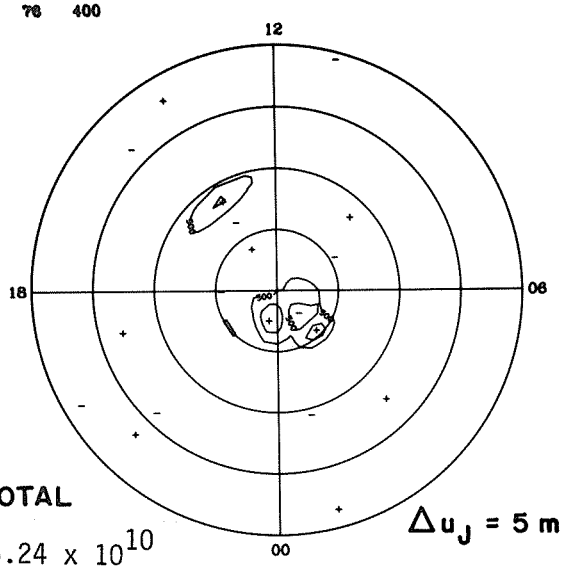

FIELD-ALIGNED CURRENT

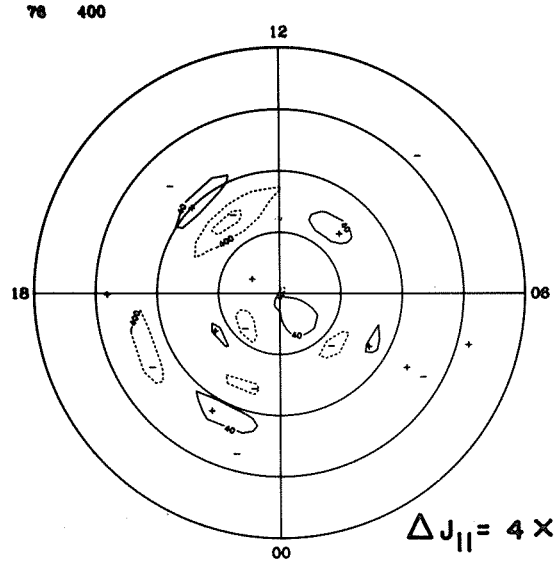

EQUIVALENT CURRENT

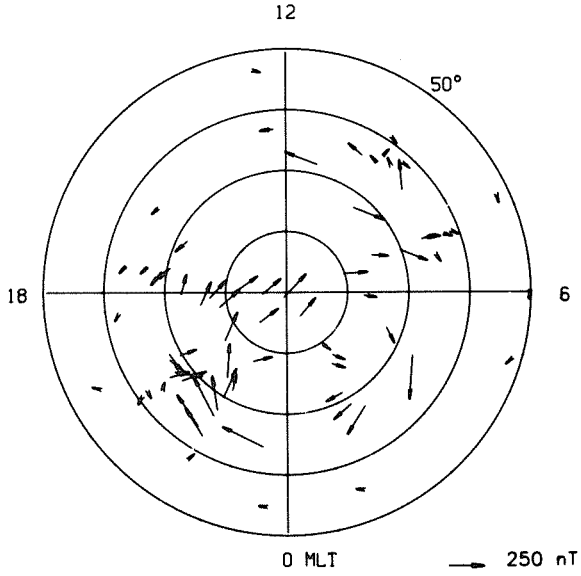

EQUIVALENT CURRENT SYSTEM

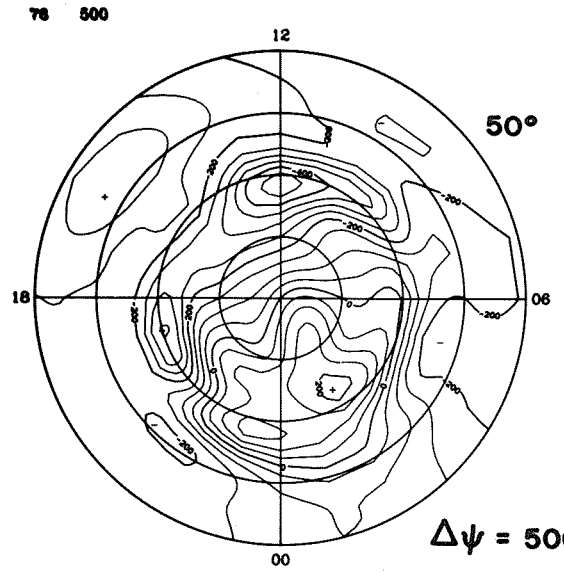

ELECTRIC POTENTIAL

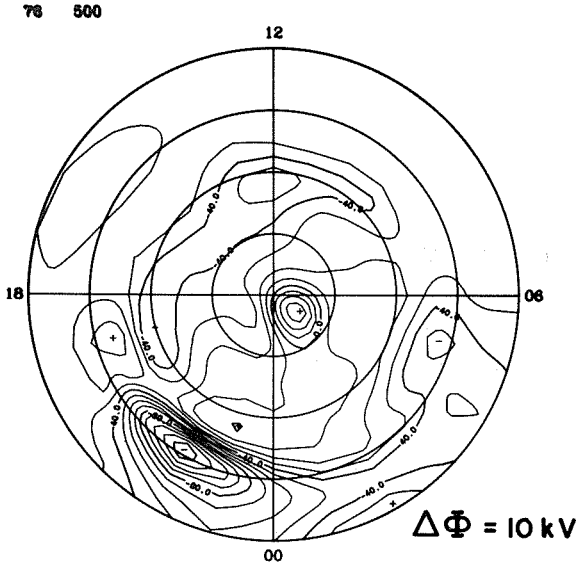

IONOSPHERIC CURRENT

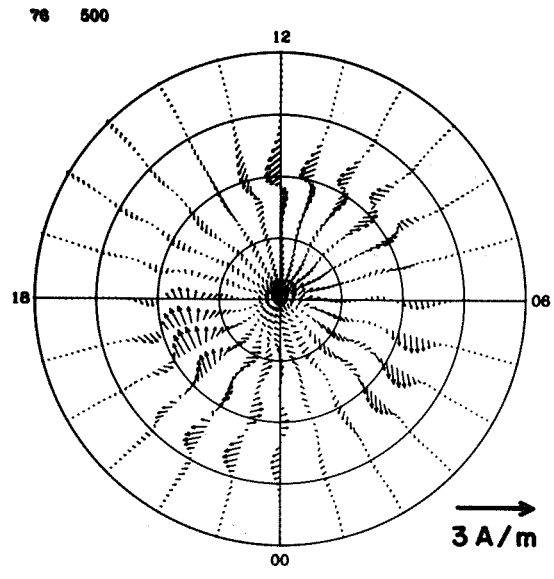

JOULE HEATING

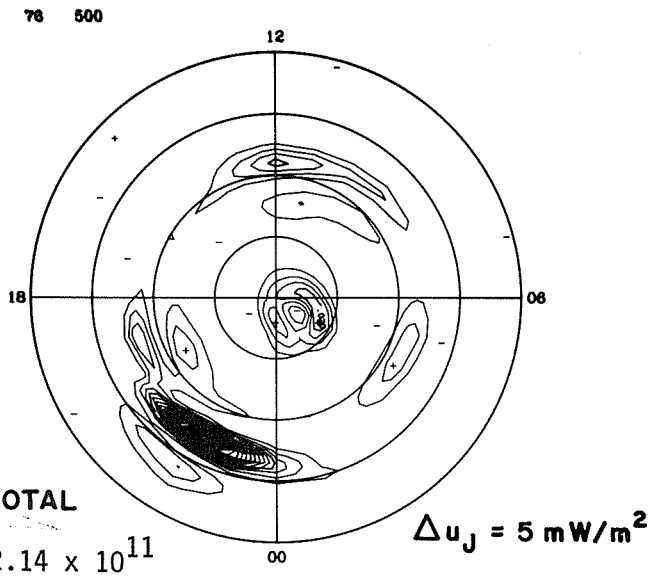

FIELD-ALIGNED CURRENT

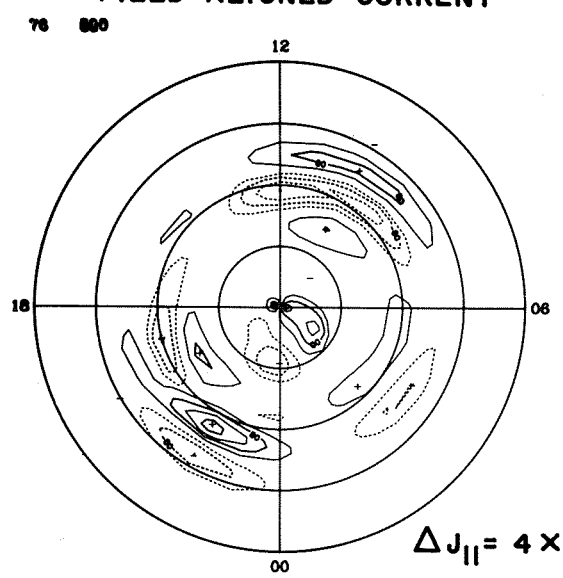

EQUIVALENT CURRENT

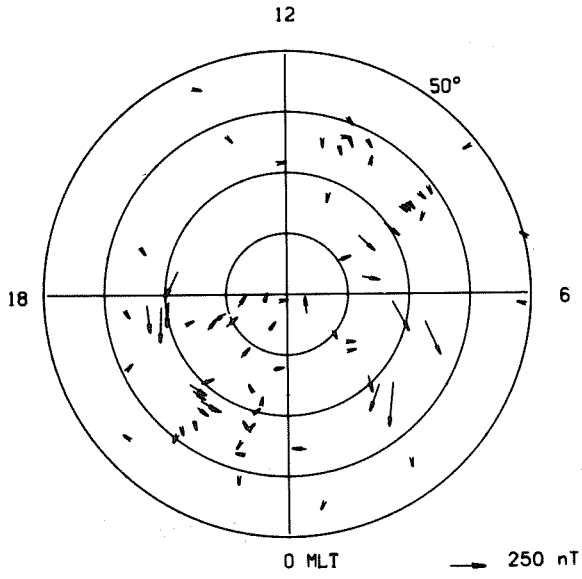

EQUIVALENT CURRENT SYSTEM

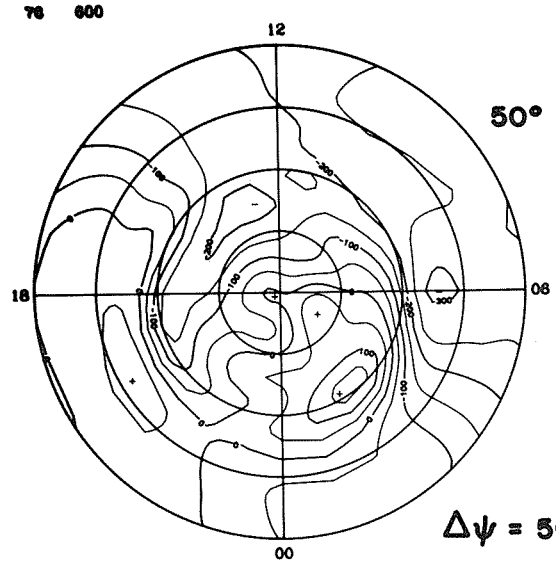

ELECTRIC POTENTIAL

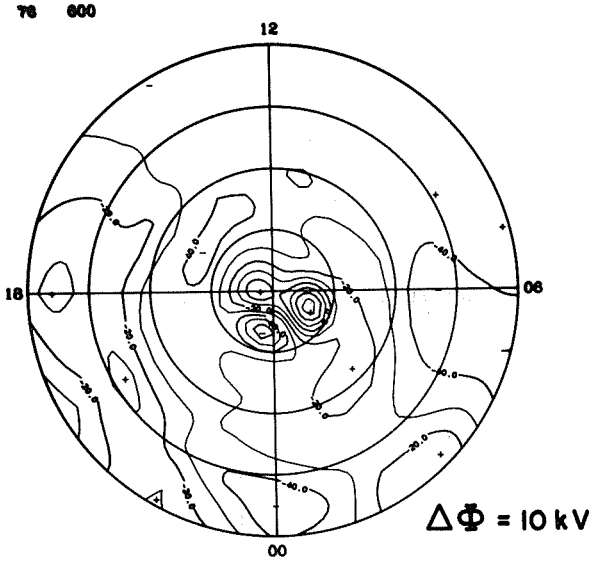

IONOSPHERIC CURRENT

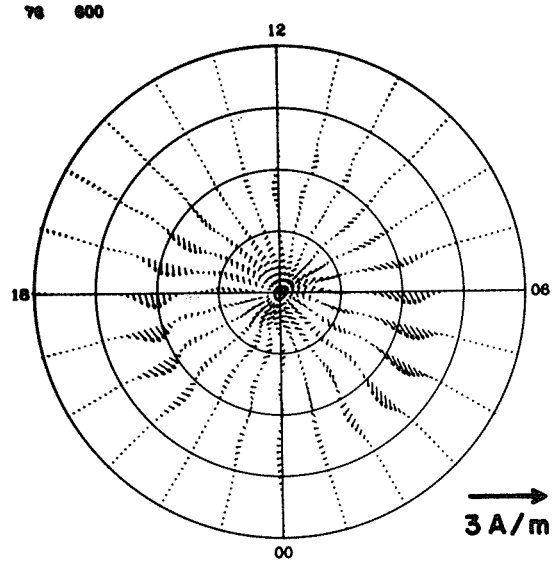

JOULE HEATING

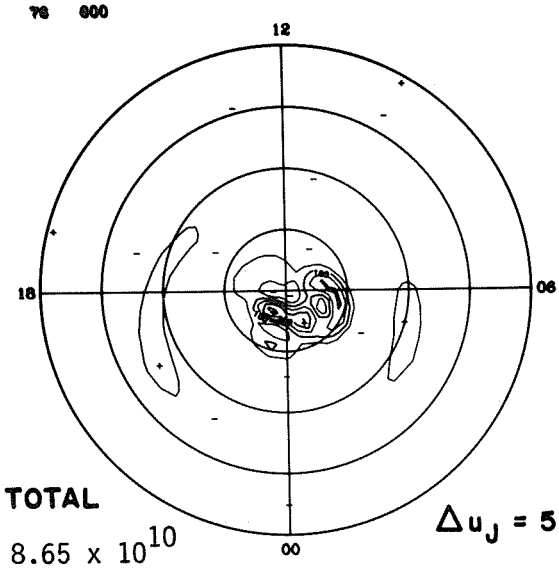

FIELD-ALIGNED CURRENT

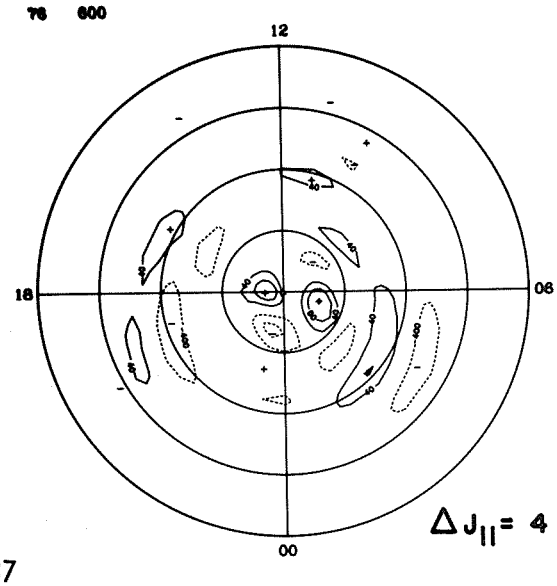

EQUIVALENT CURRENT

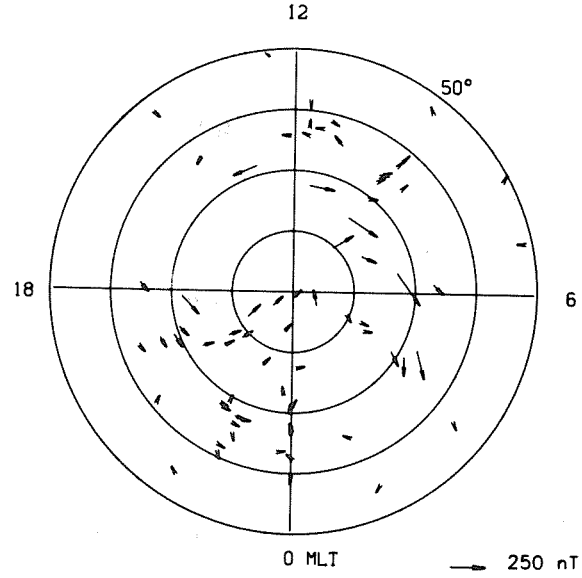

EQUIVALENT CURRENT SYSTEM

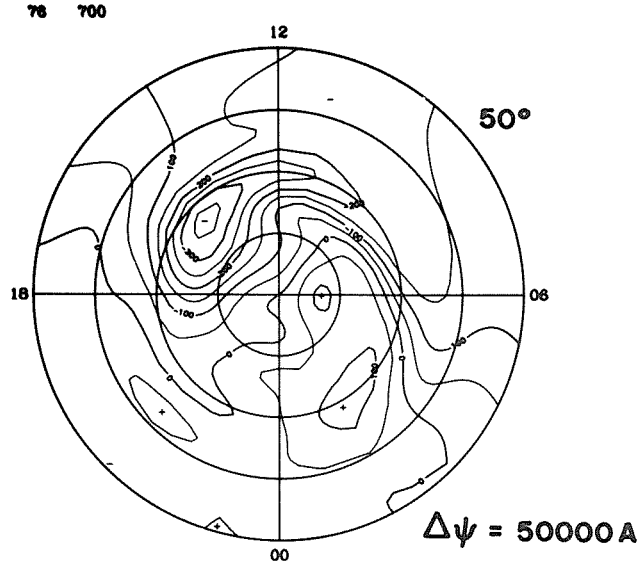

ELECTRIC POTENTIAL

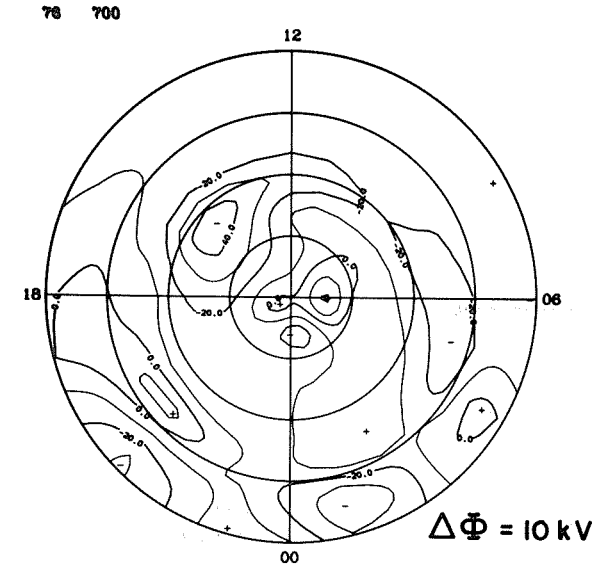

IONOSPHERIC CURRENT

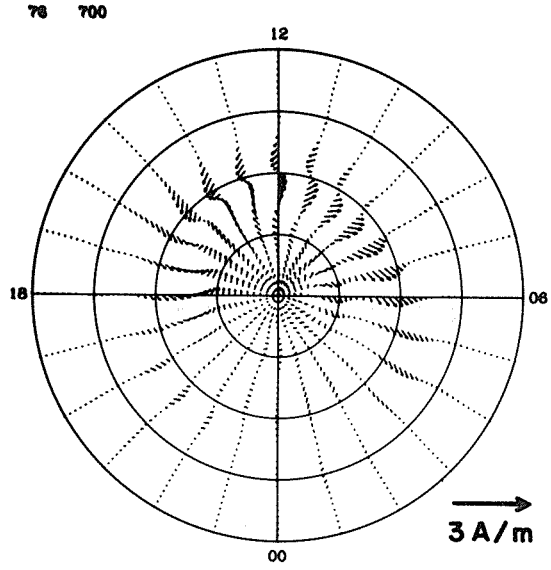

JOULE HEATING

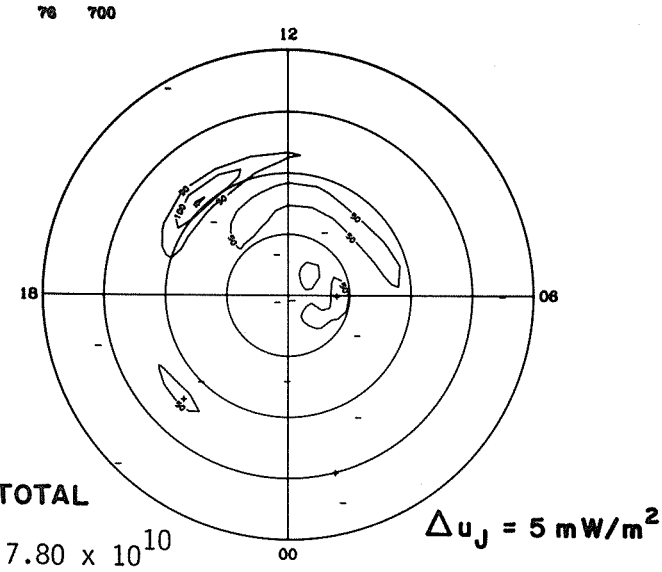

TOTAL

7.80×10^{10}

FIELD-ALIGNED CURRENT

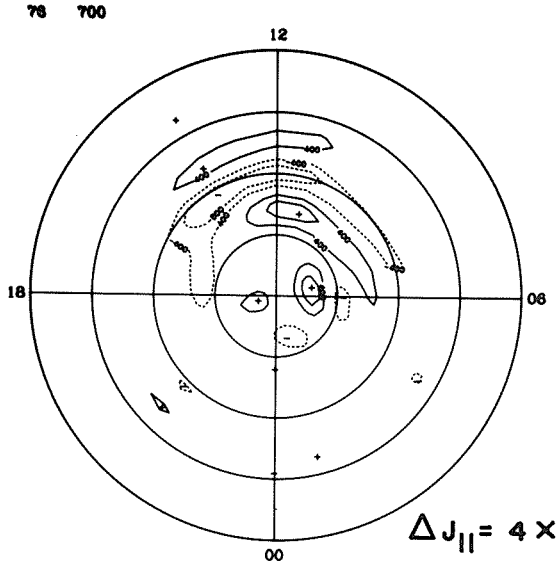

EQUIVALENT CURRENT

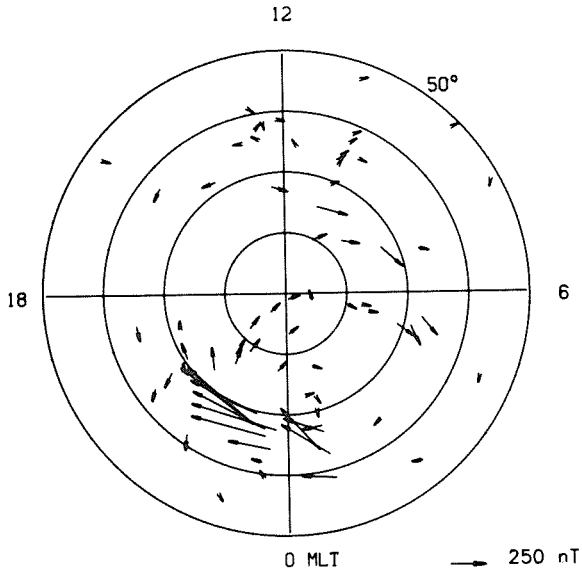

EQUIVALENT CURRENT SYSTEM

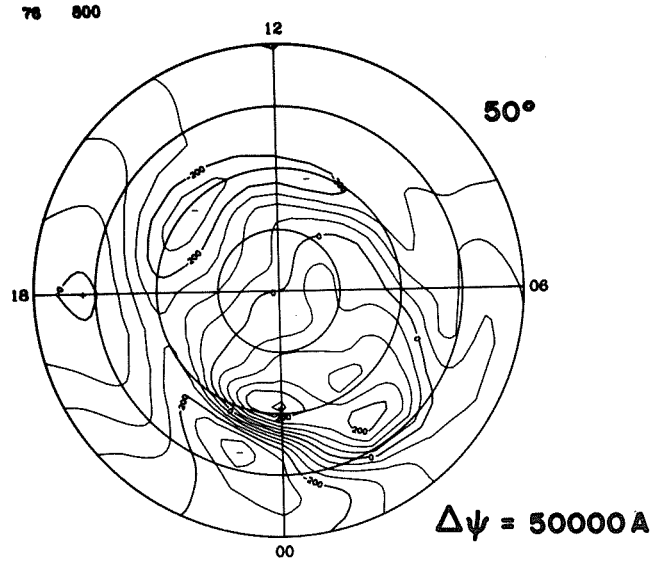

ELECTRIC POTENTIAL

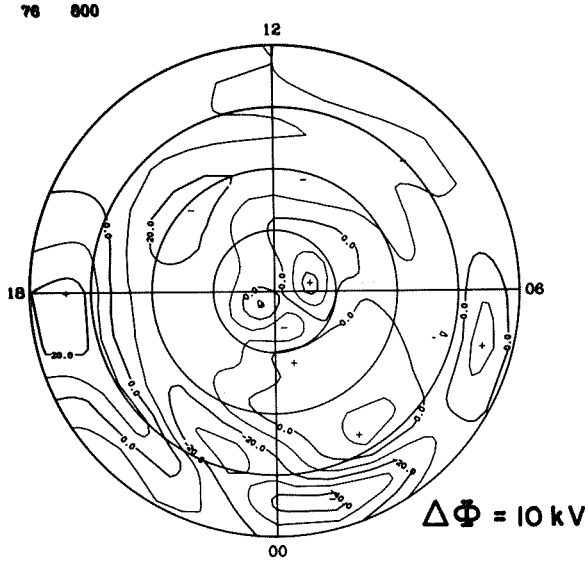

IONOSPHERIC CURRENT

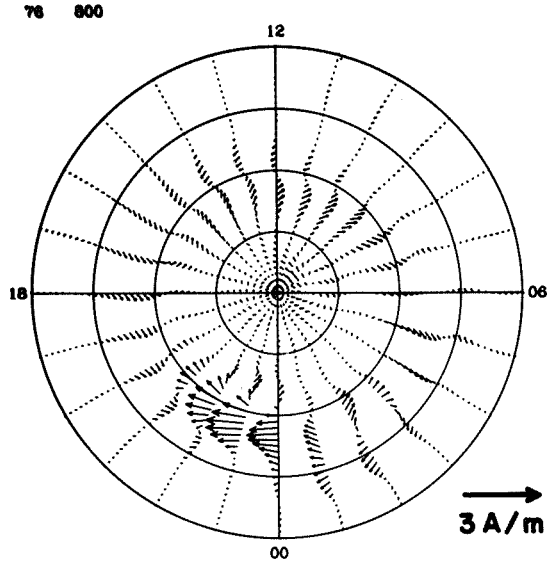

JOULE HEATING

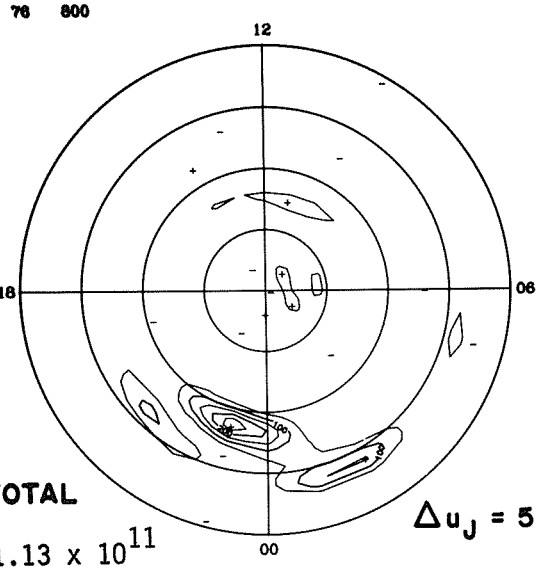

FIELD-ALIGNED CURRENT

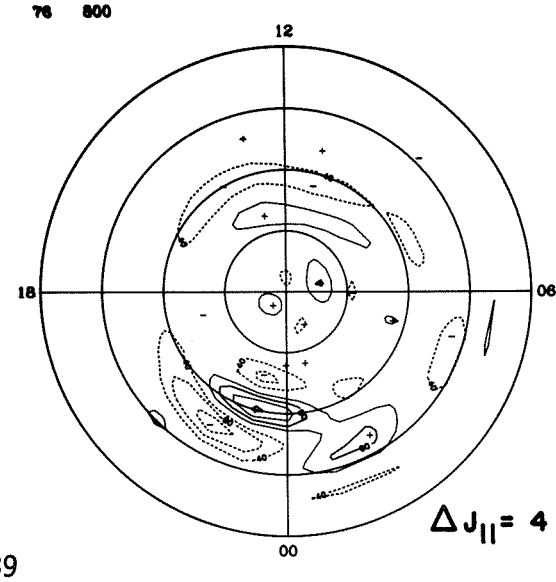

EQUIVALENT CURRENT

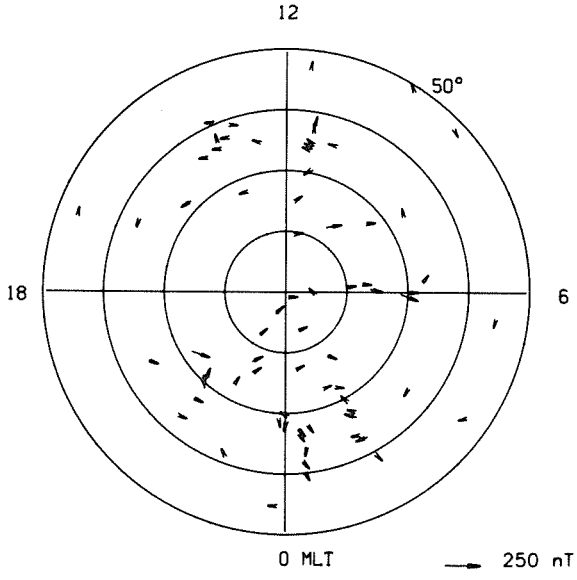

EQUIVALENT CURRENT SYSTEM

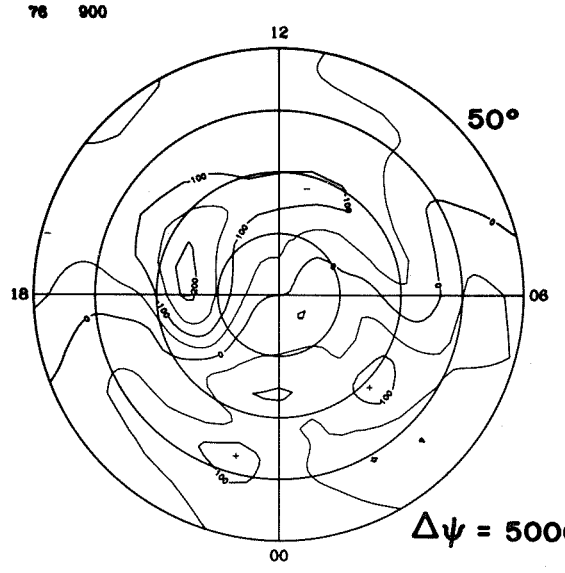

ELECTRIC POTENTIAL

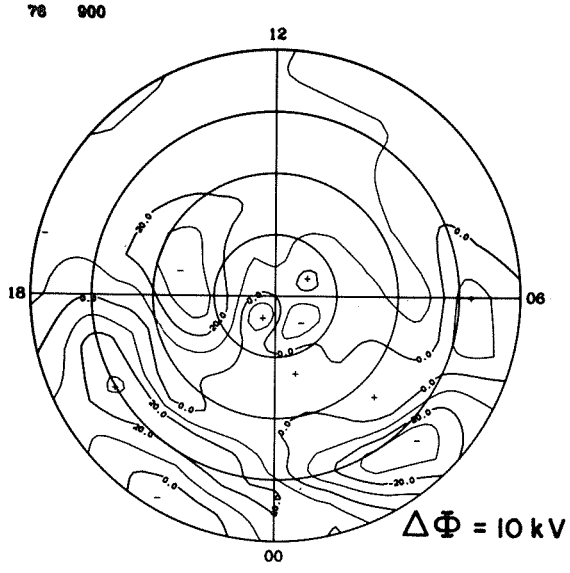

IONOSPHERIC CURRENT

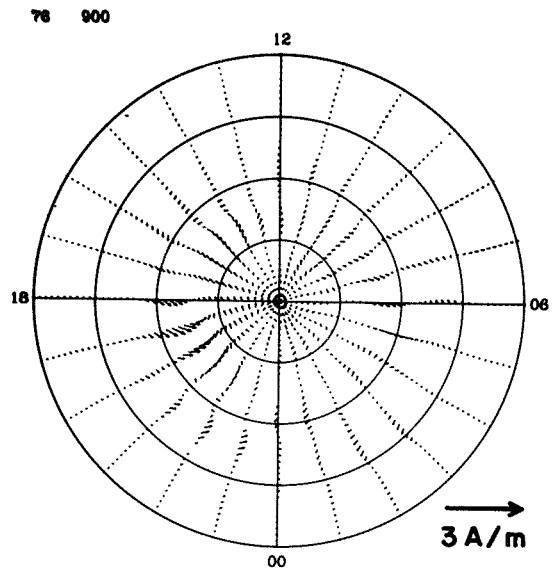

JOULE HEATING

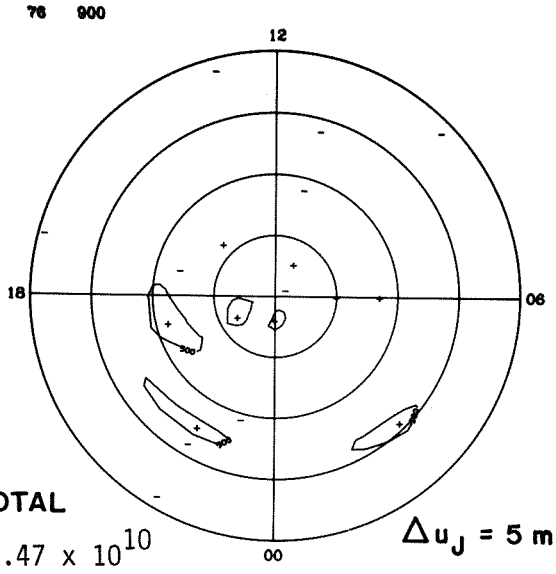

TOTAL

6.47×10^{10}

FIELD-ALIGNED CURRENT

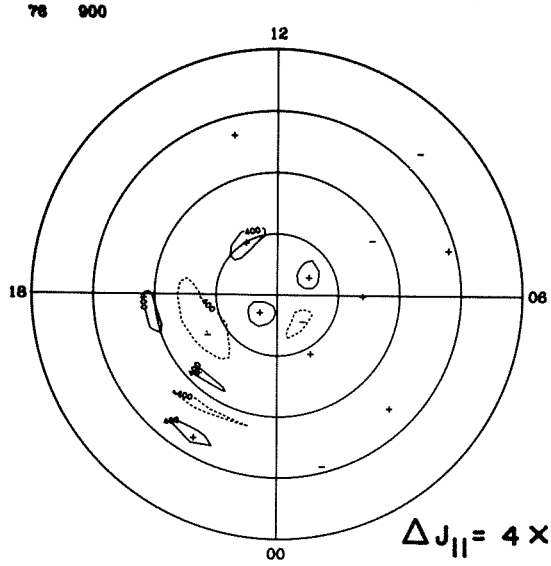

EQUIVALENT CURRENT

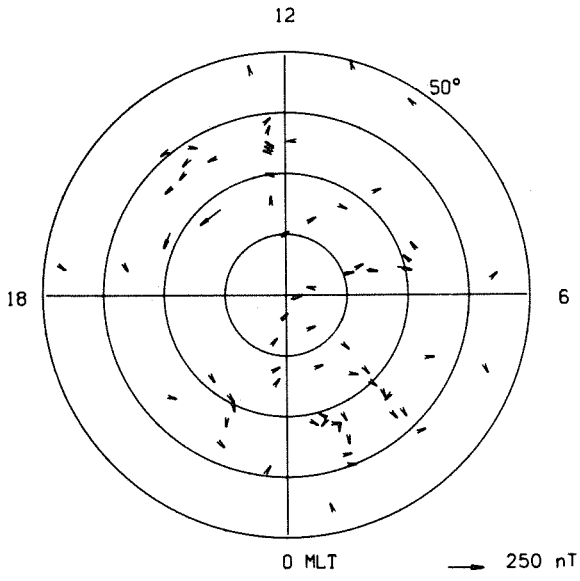

EQUIVALENT CURRENT SYSTEM

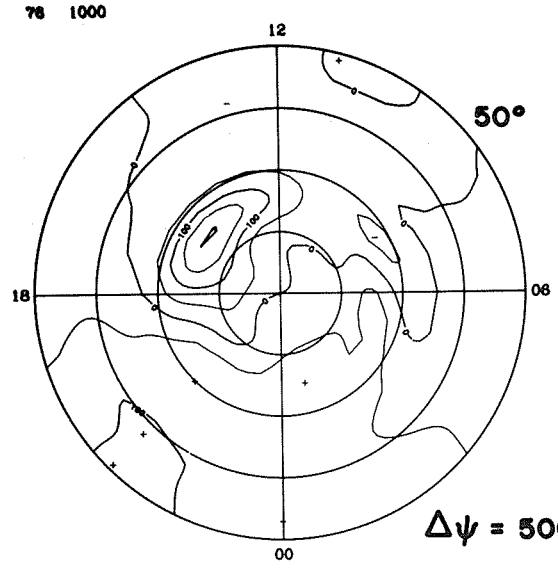

ELECTRIC POTENTIAL

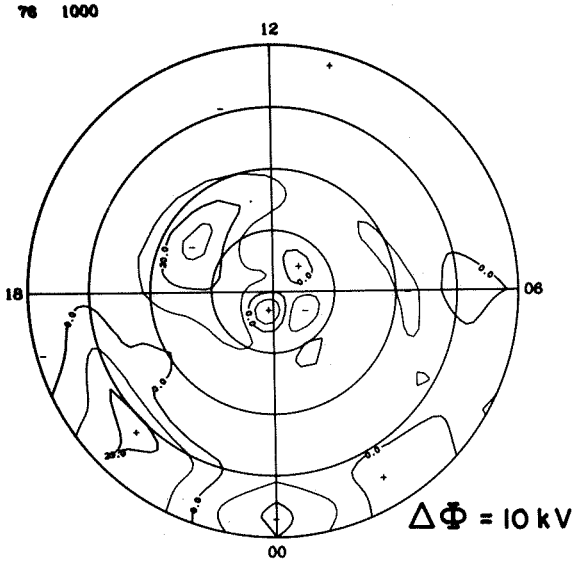

IONOSPHERIC CURRENT

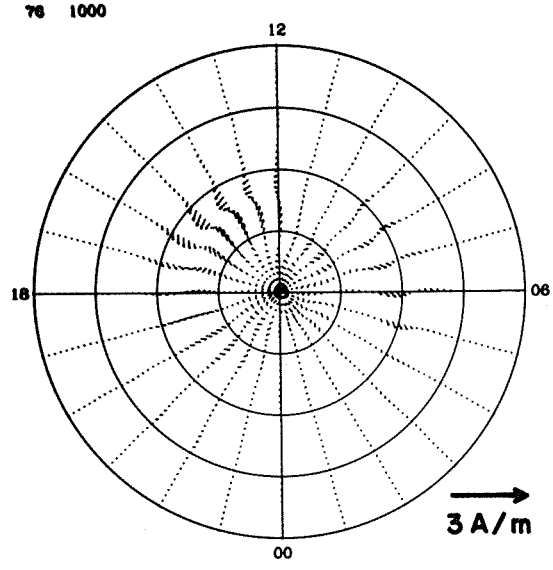

JOULE HEATING

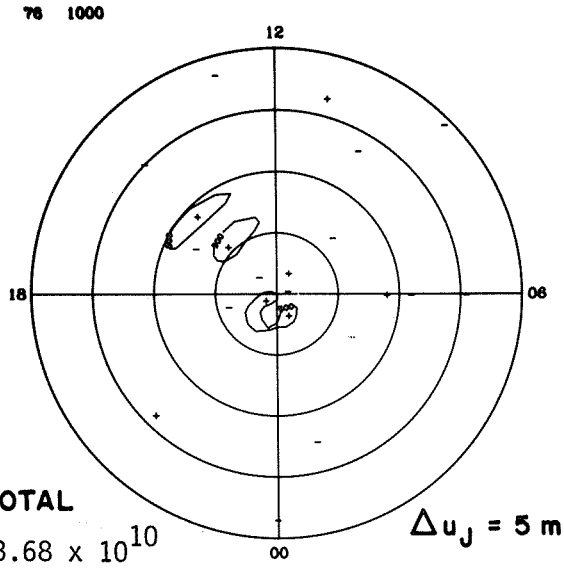

FIELD-ALIGNED CURRENT

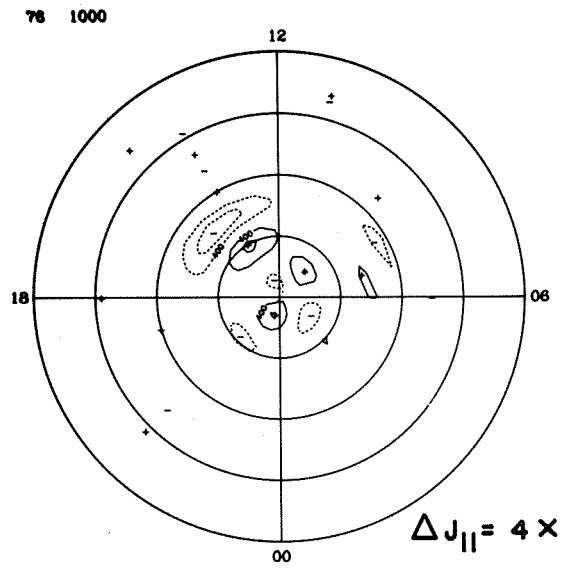

EQUIVALENT CURRENT

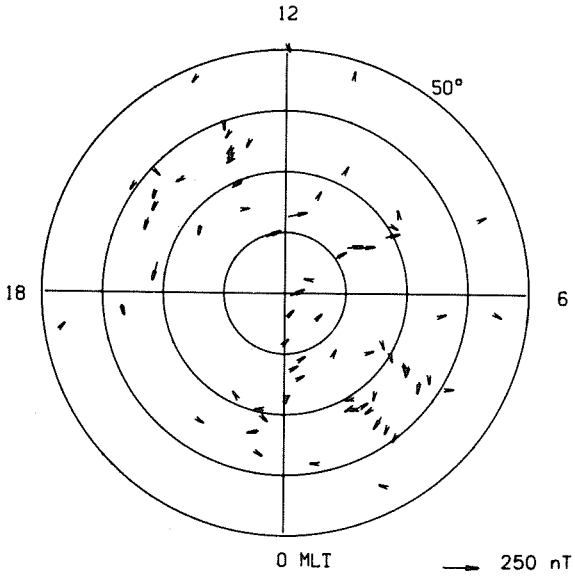

EQUIVALENT CURRENT SYSTEM

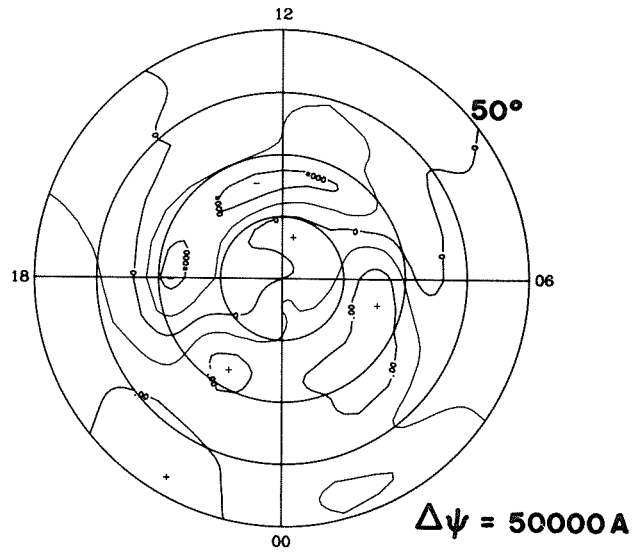

ELECTRIC POTENTIAL

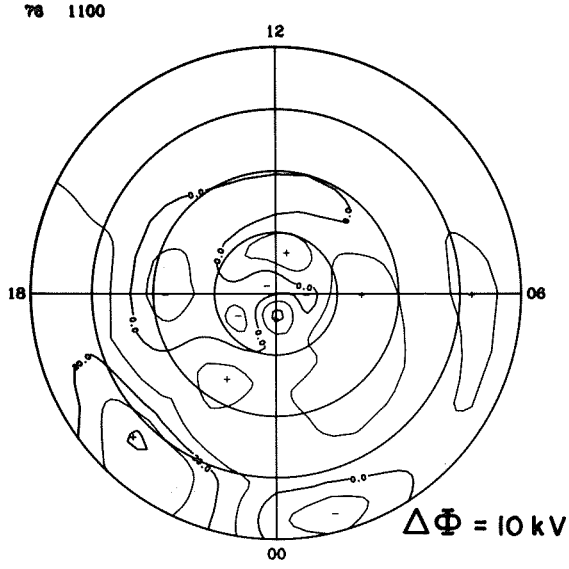

IONOSPHERIC CURRENT

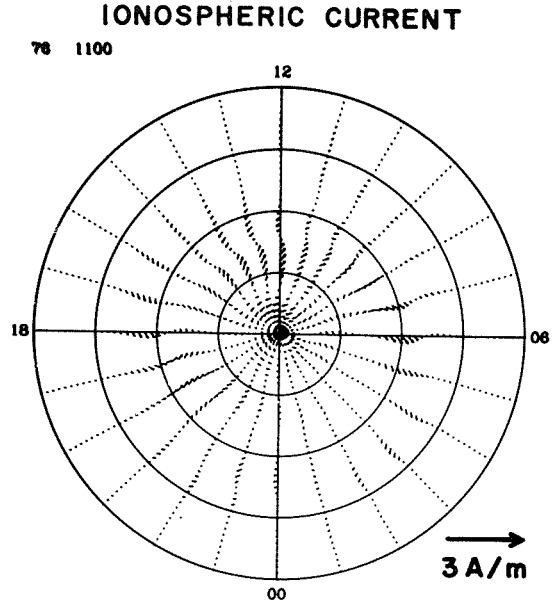

JOULE HEATING

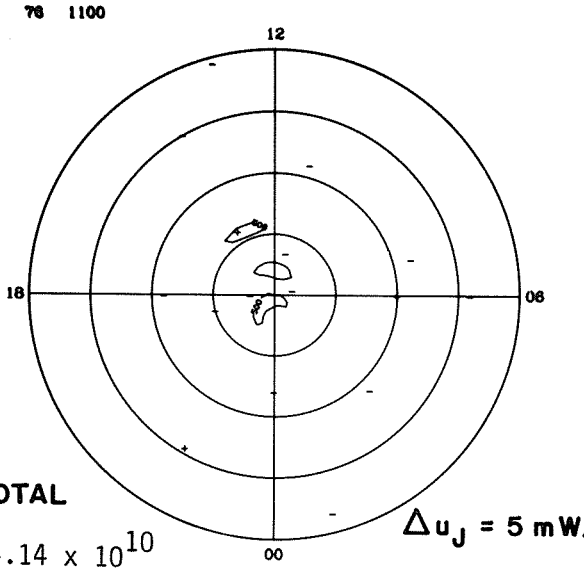

TOTAL

4.14×10^{10}

FIELD-ALIGNED CURRENT

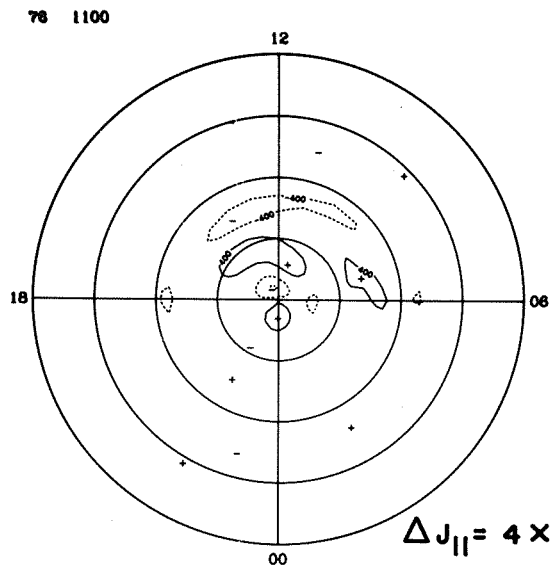

EQUIVALENT CURRENT

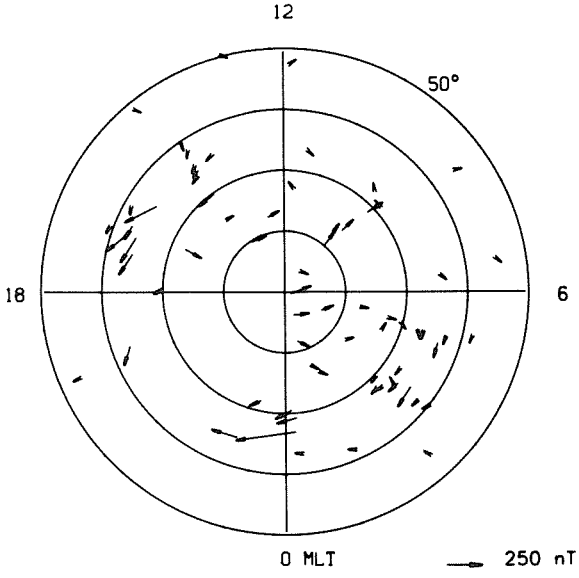

EQUIVALENT CURRENT SYSTEM

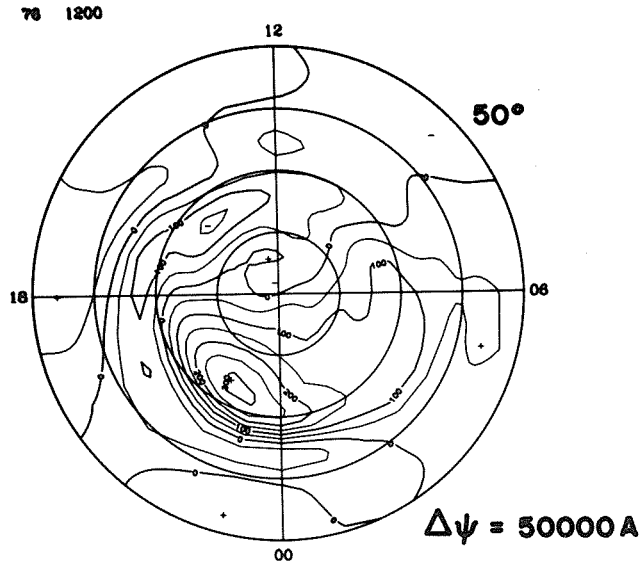

ELECTRIC POTENTIAL

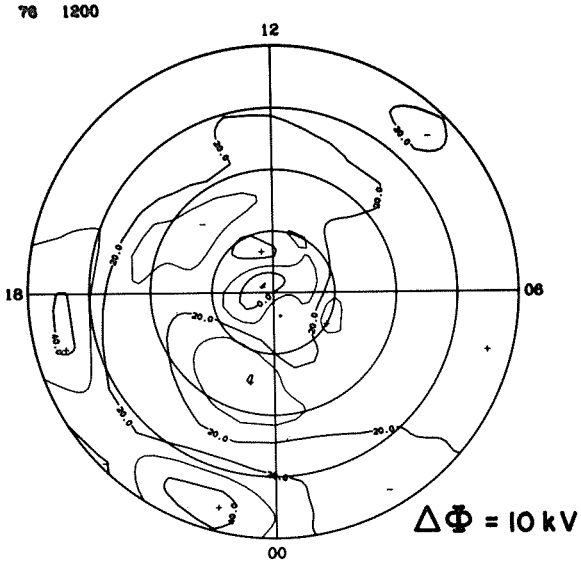

IONOSPHERIC CURRENT

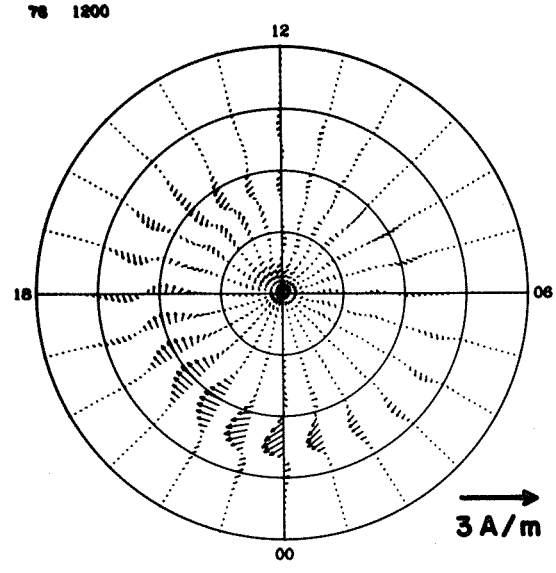

JOULE HEATING

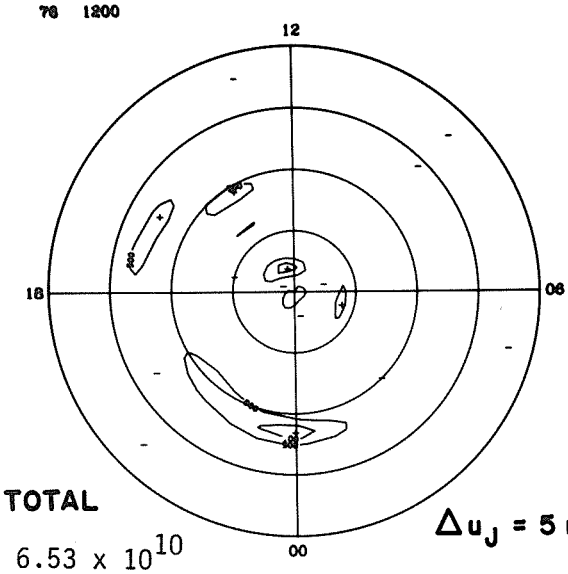

TOTAL

6.53×10^{10}

FIELD-ALIGNED CURRENT

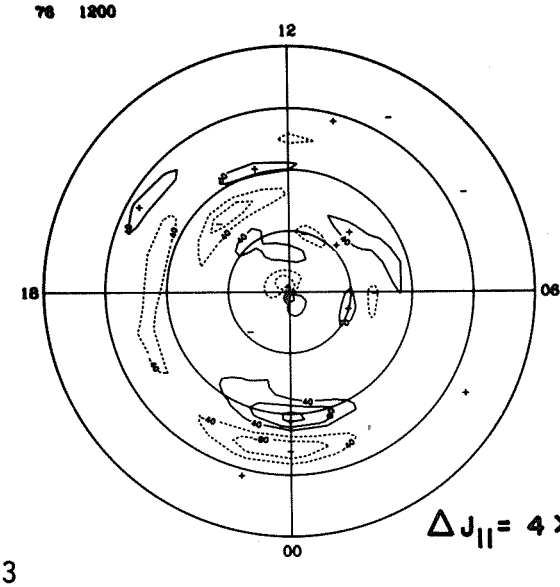

EQUIVALENT CURRENT

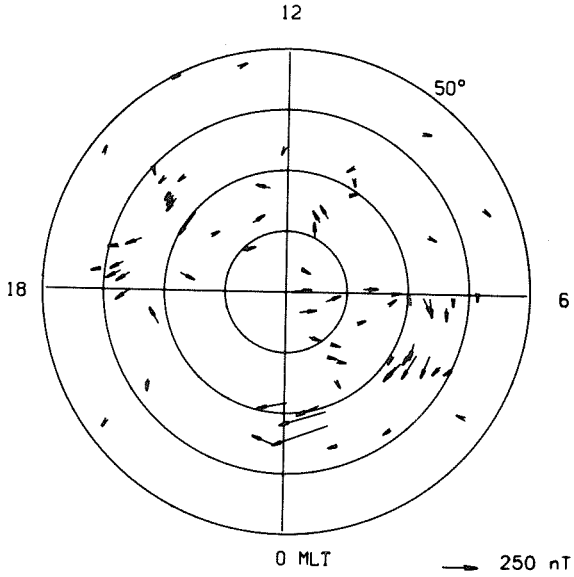

EQUIVALENT CURRENT SYSTEM

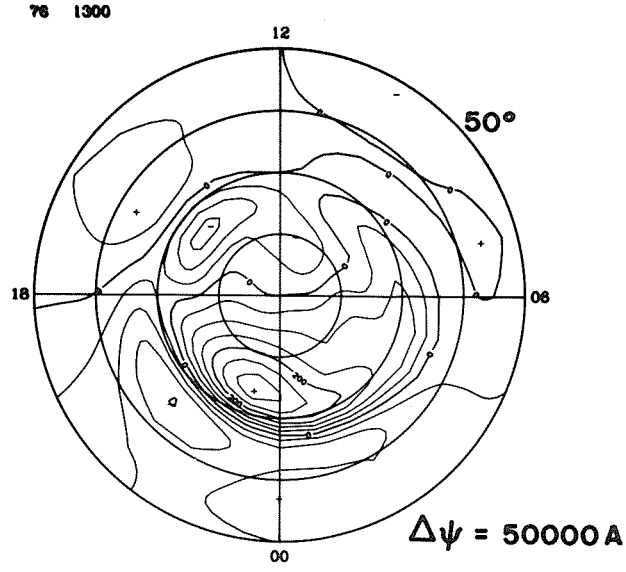

ELECTRIC POTENTIAL

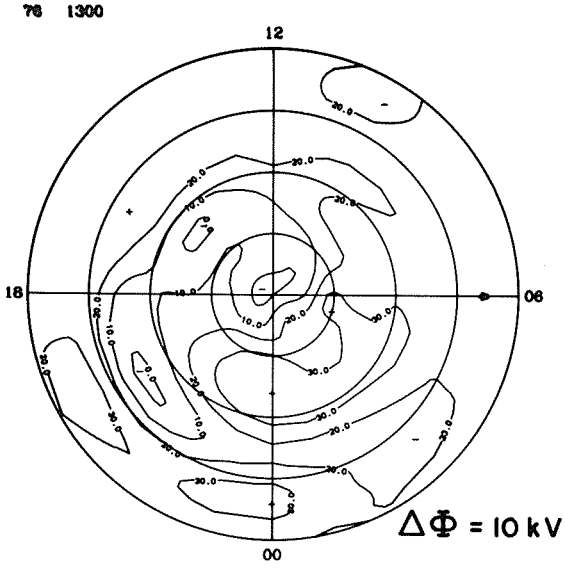

IONOSPHERIC CURRENT

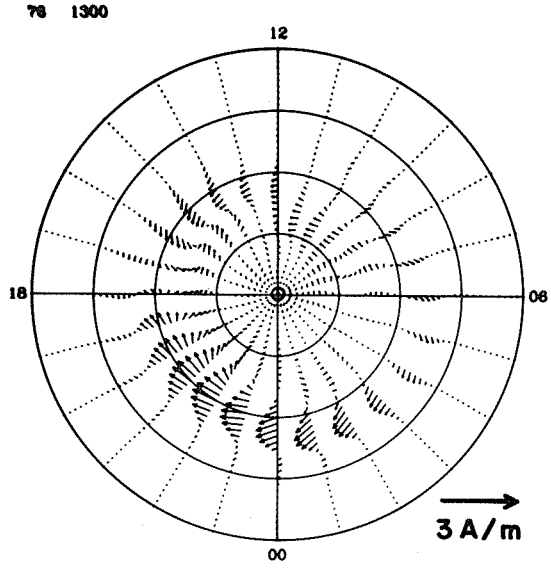

JOULE HEATING

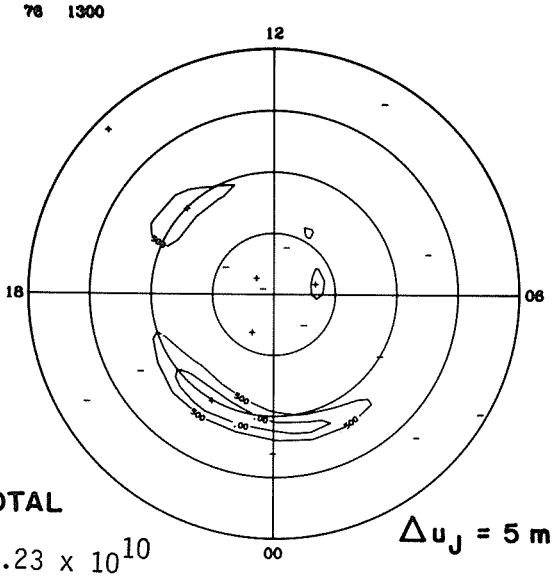

TOTAL

7.23×10^{10}

FIELD-ALIGNED CURRENT

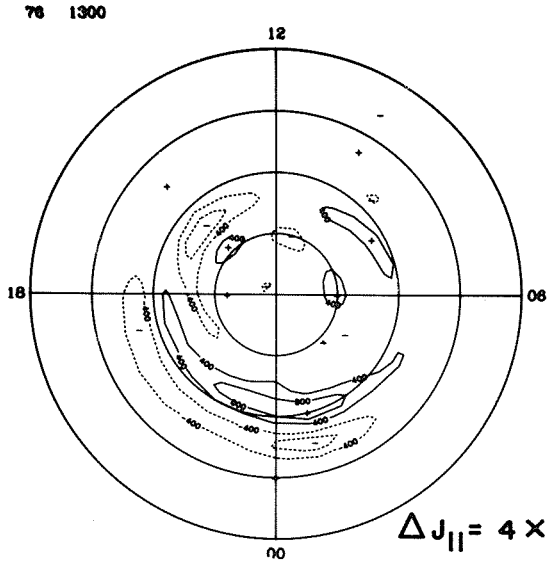

EQUIVALENT CURRENT

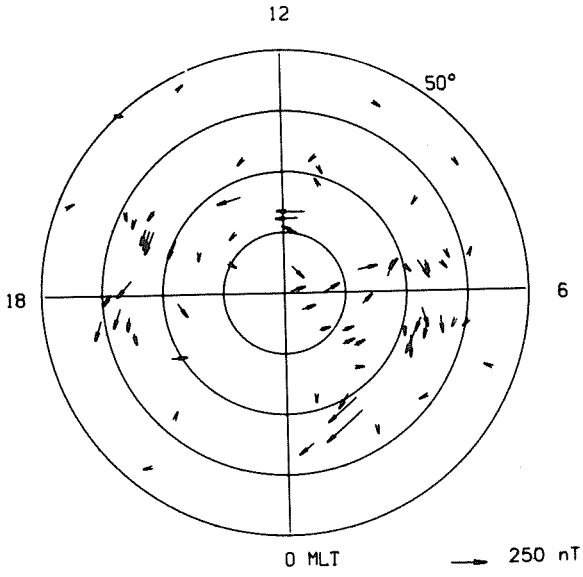

EQUIVALENT CURRENT SYSTEM

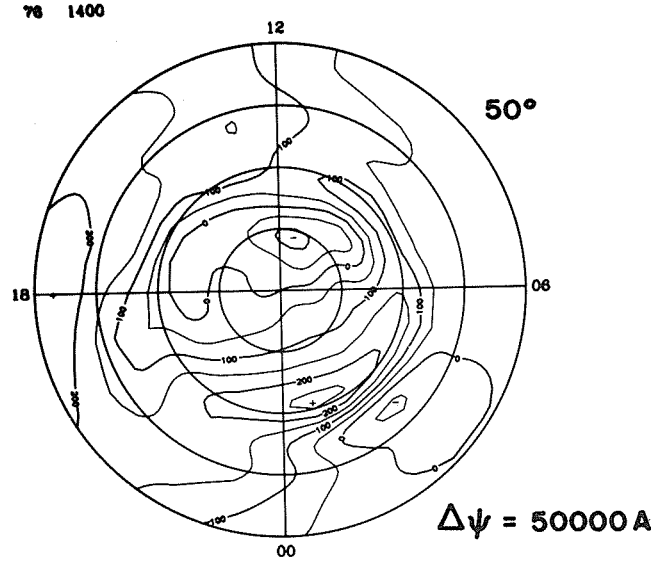

ELECTRIC POTENTIAL

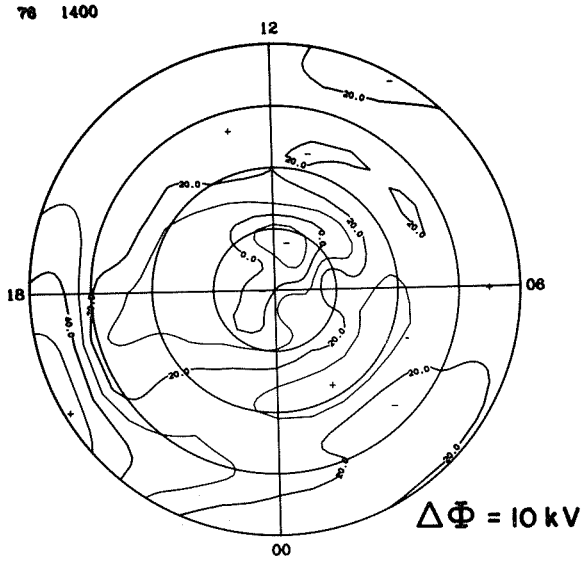

IONOSPHERIC CURRENT

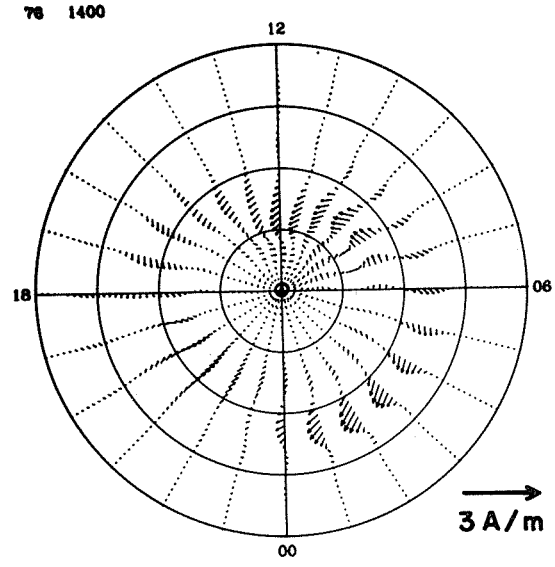

JOULE HEATING

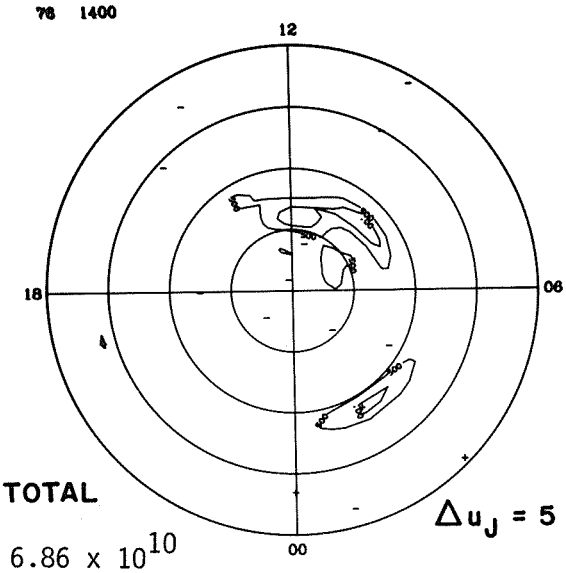

TOTAL

6.86×10^{10}

FIELD-ALIGNED CURRENT

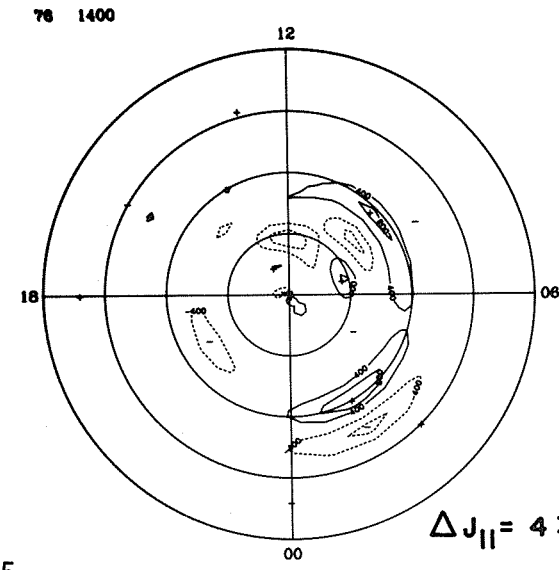

EQUIVALENT CURRENT

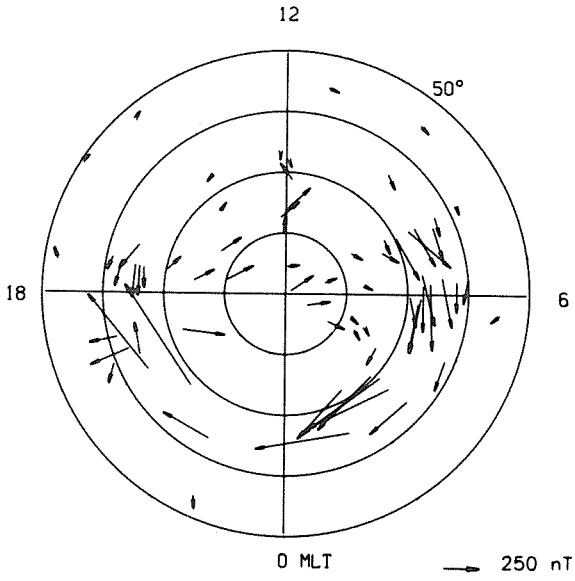

EQUIVALENT CURRENT SYSTEM

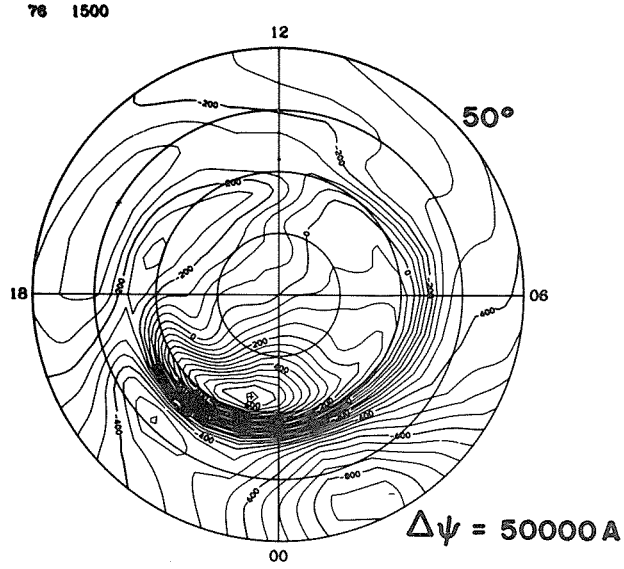

ELECTRIC POTENTIAL

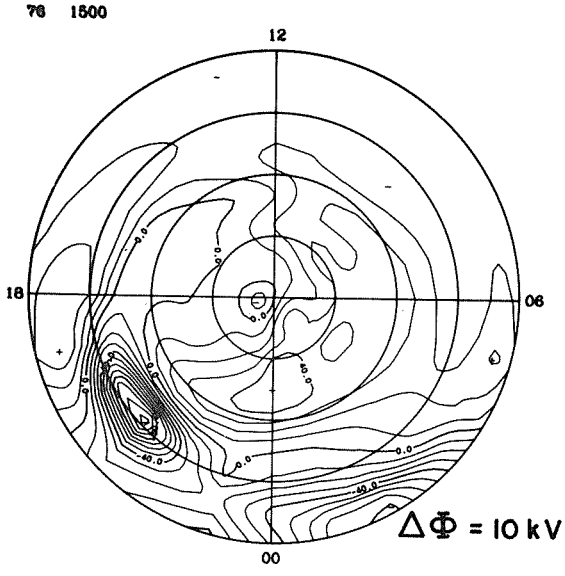

IONOSPHERIC CURRENT

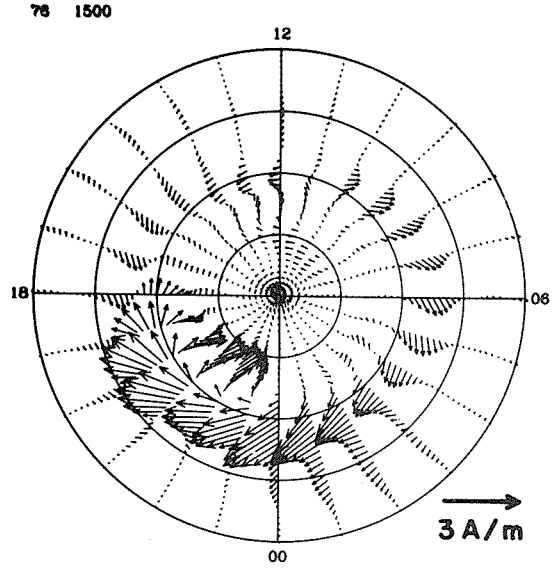

JOULE HEATING

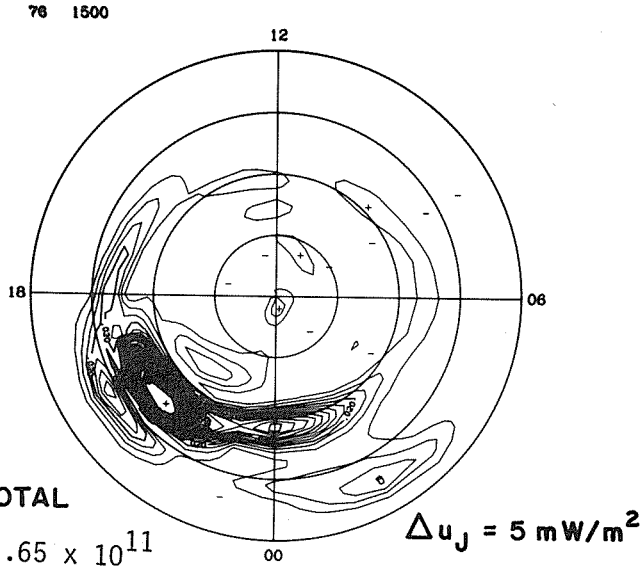

TOTAL

4.65×10^{11}

FIELD-ALIGNED CURRENT

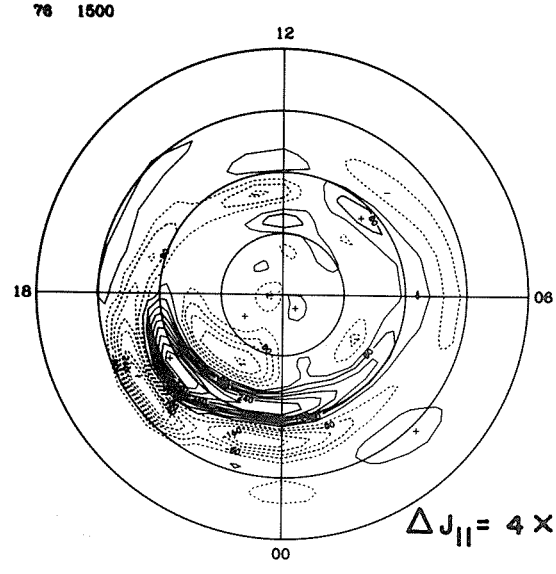

EQUIVALENT CURRENT

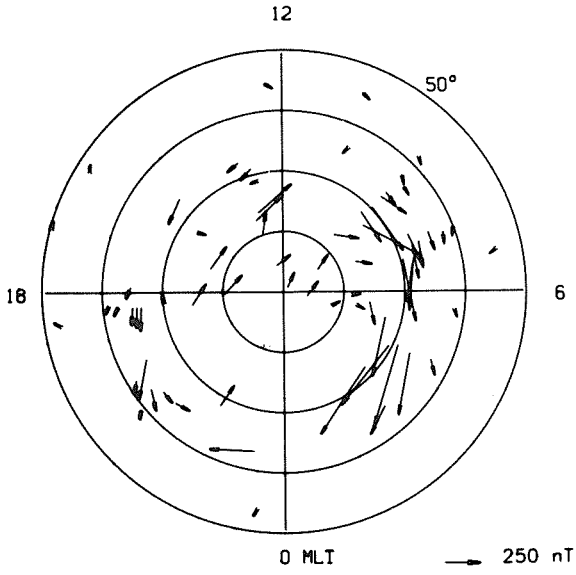

EQUIVALENT CURRENT SYSTEM

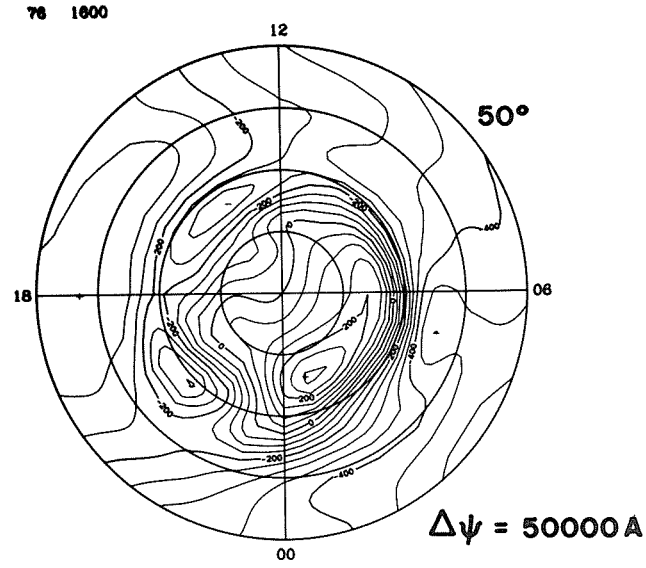

ELECTRIC POTENTIAL

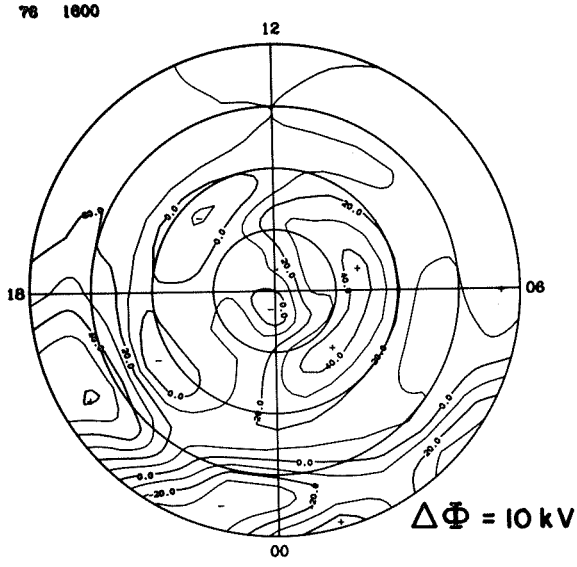

IONOSPHERIC CURRENT

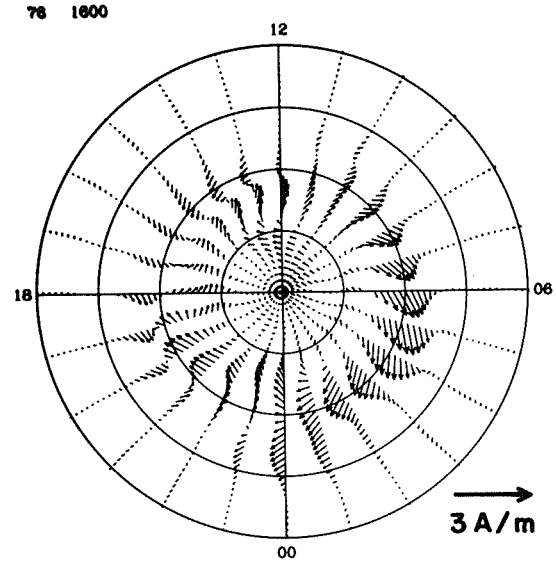

JOULE HEATING

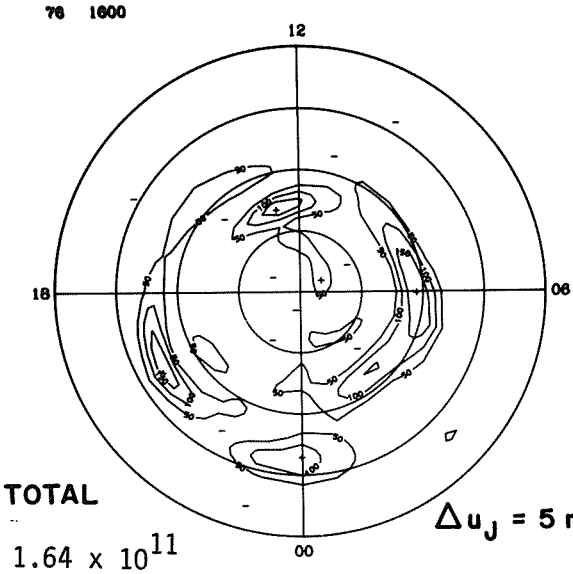

FIELD-ALIGNED CURRENT

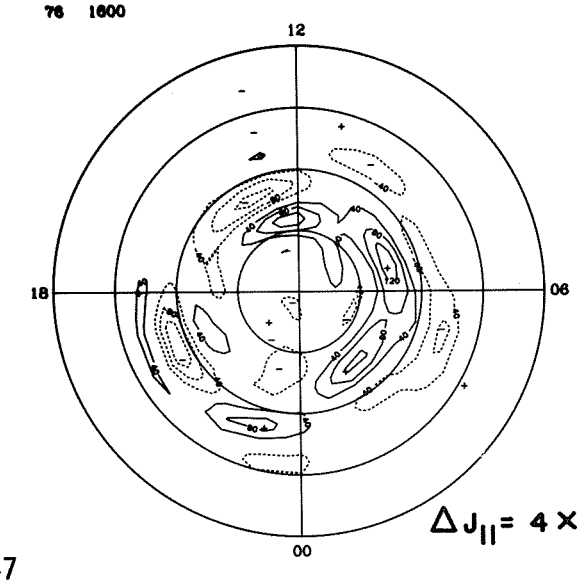

EQUIVALENT CURRENT

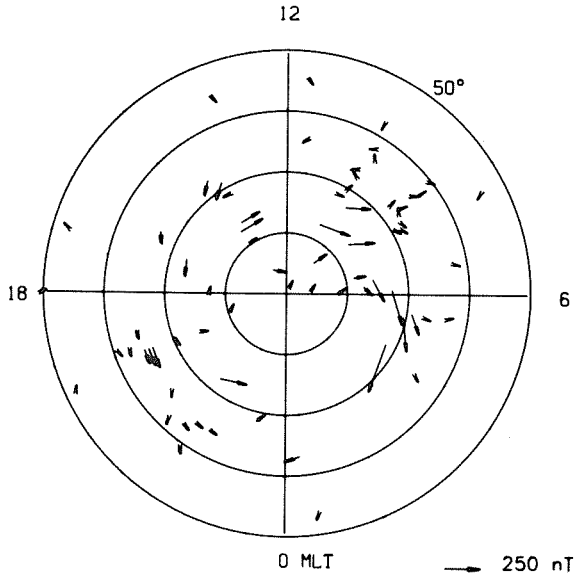

EQUIVALENT CURRENT SYSTEM

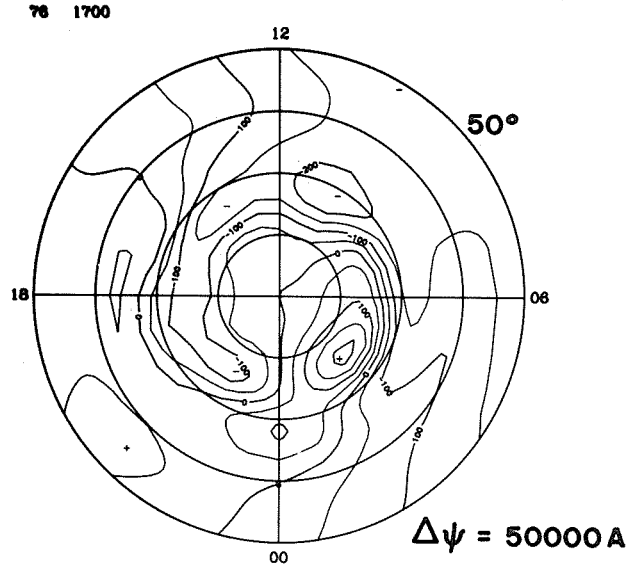

ELECTRIC POTENTIAL

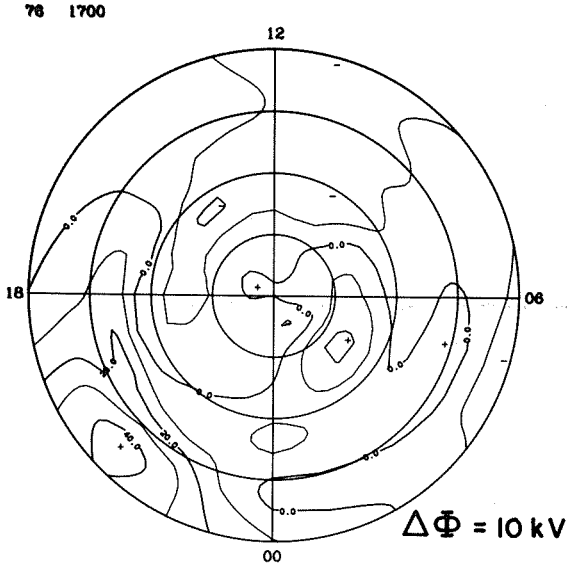

IONOSPHERIC CURRENT

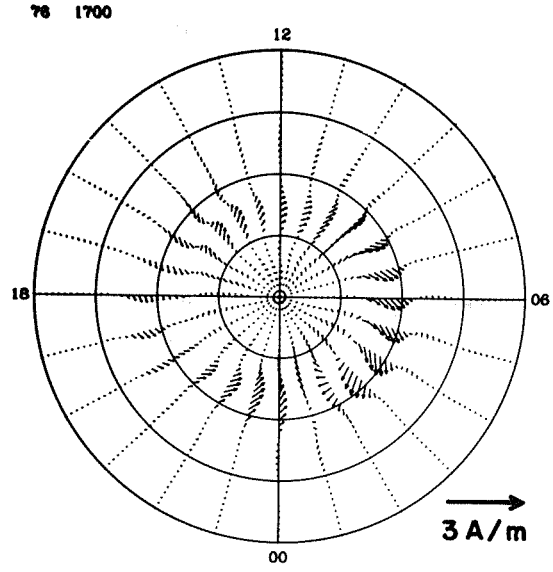

JOULE HEATING

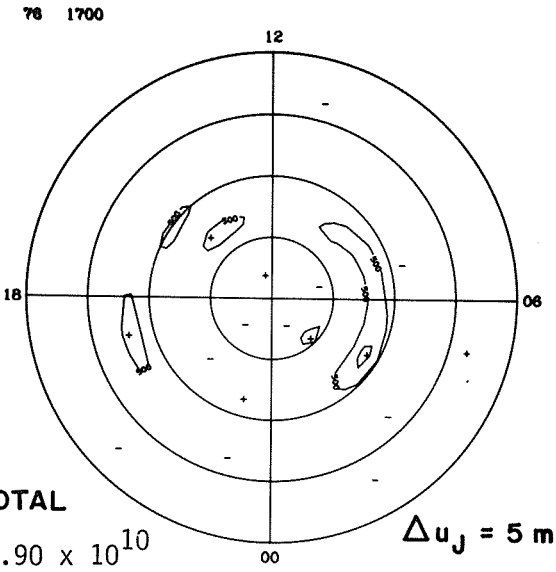

TOTAL

5.90×10^{10}

FIELD-ALIGNED CURRENT

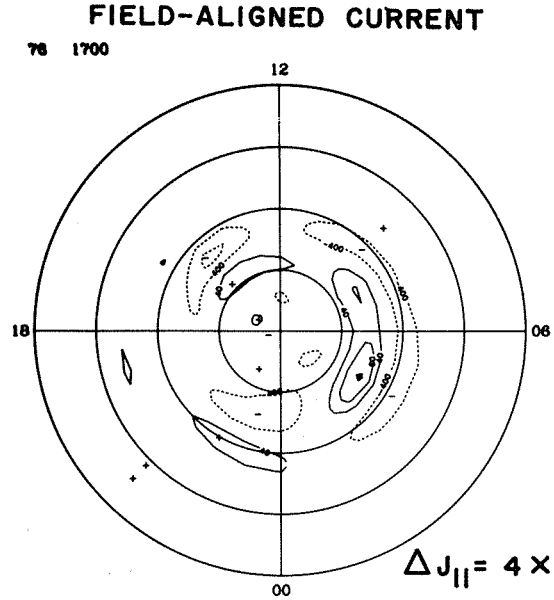

EQUIVALENT CURRENT

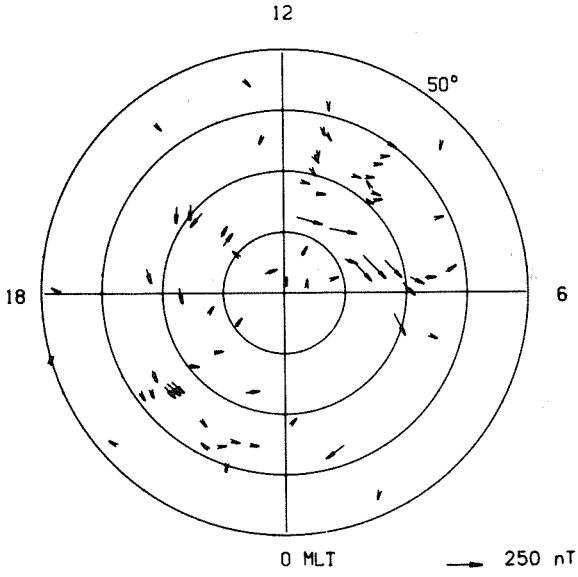

EQUIVALENT CURRENT SYSTEM

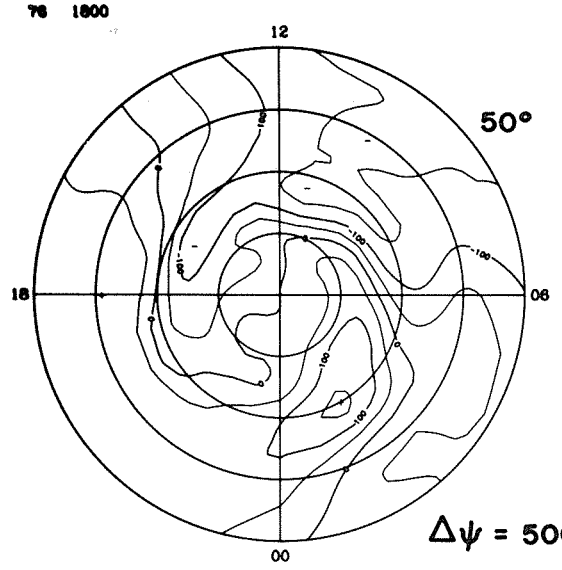

ELECTRIC POTENTIAL

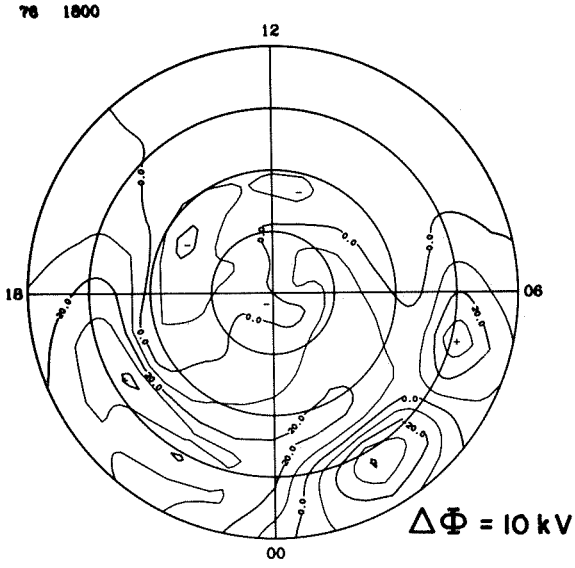

IONOSPHERIC CURRENT

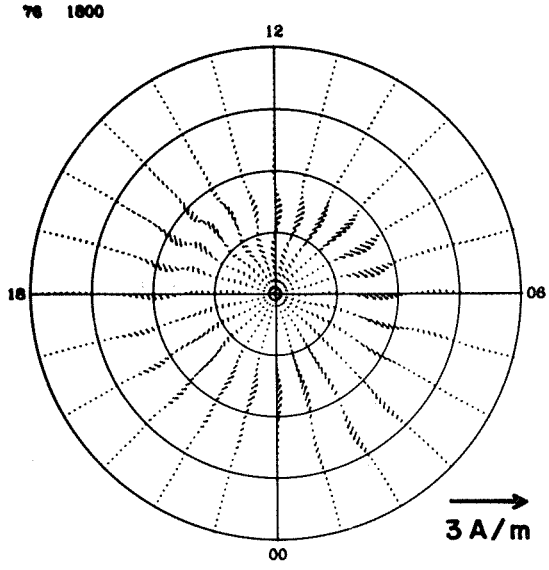

JOULE HEATING

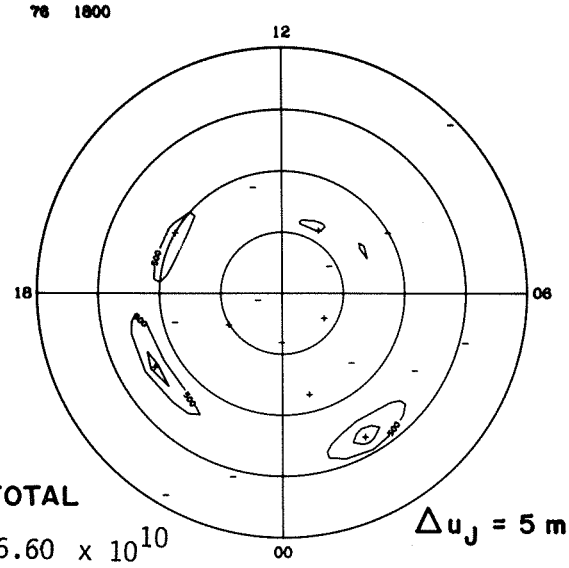

TOTAL

6.60×10^{10}

FIELD-ALIGNED CURRENT

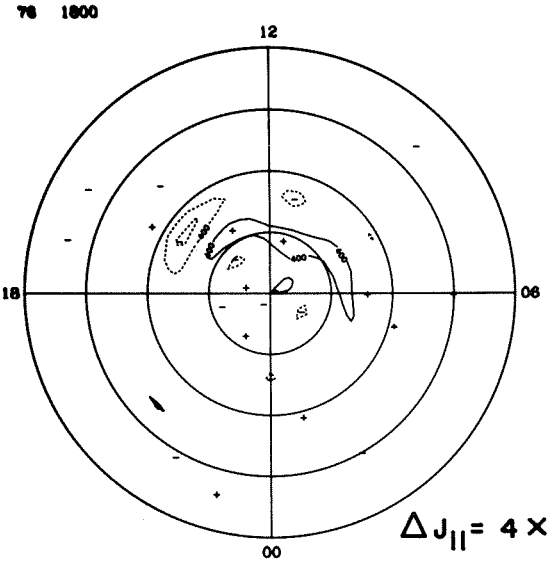

EQUIVALENT CURRENT

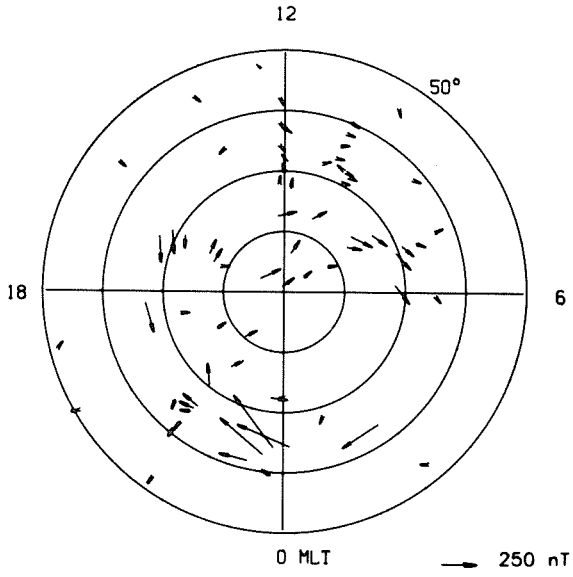

EQUIVALENT CURRENT SYSTEM

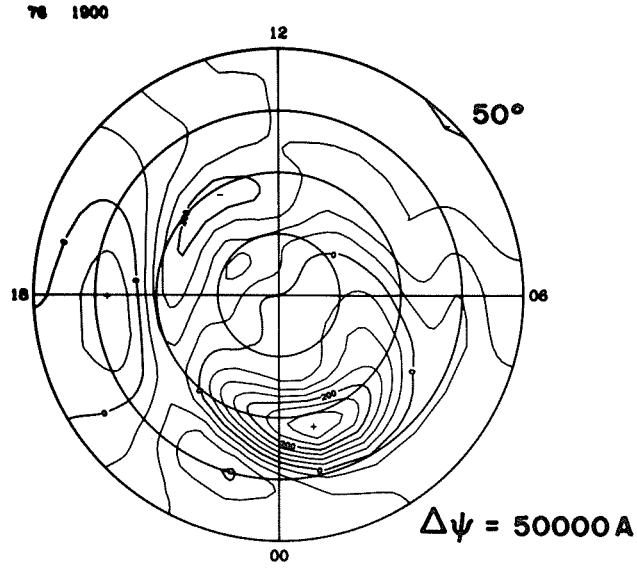

ELECTRIC POTENTIAL

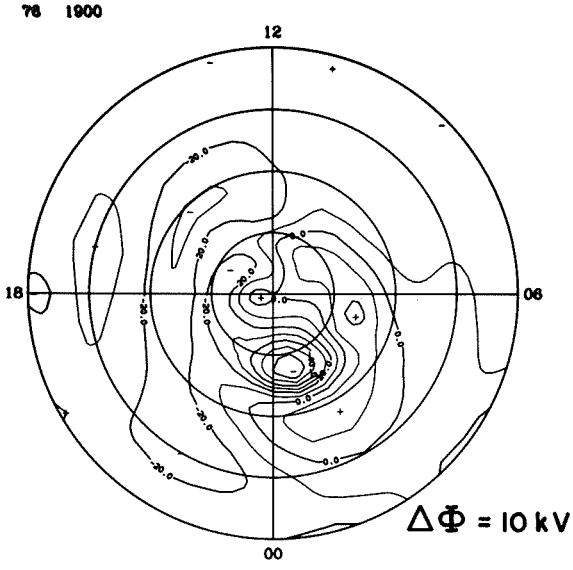

IONOSPHERIC CURRENT

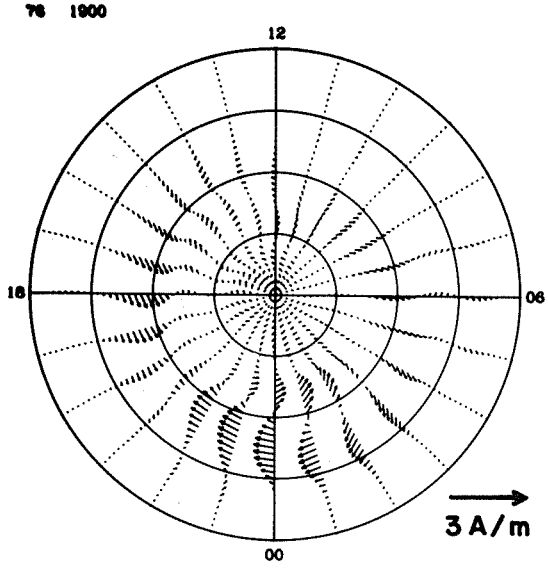

JOULE HEATING

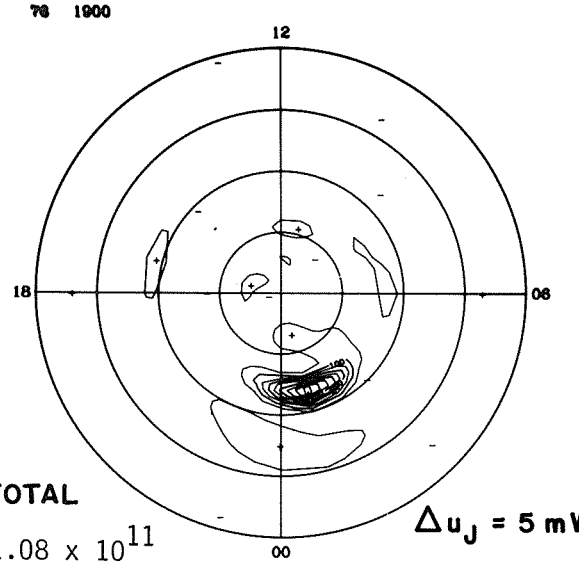

TOTAL

1.08×10^{11}

FIELD-ALIGNED CURRENT

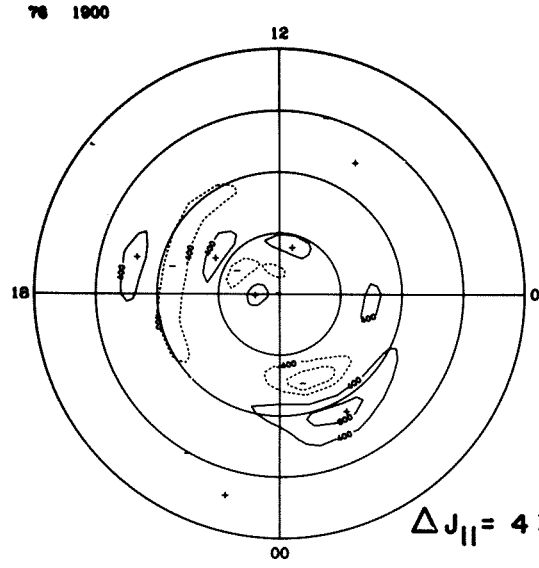

EQUIVALENT CURRENT

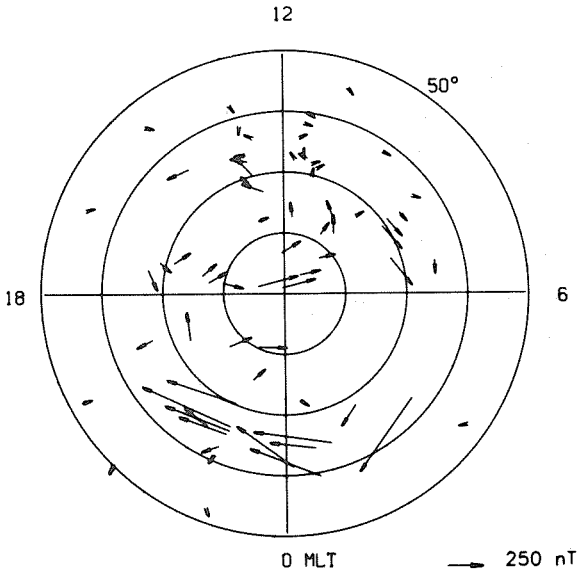

EQUIVALENT CURRENT SYSTEM

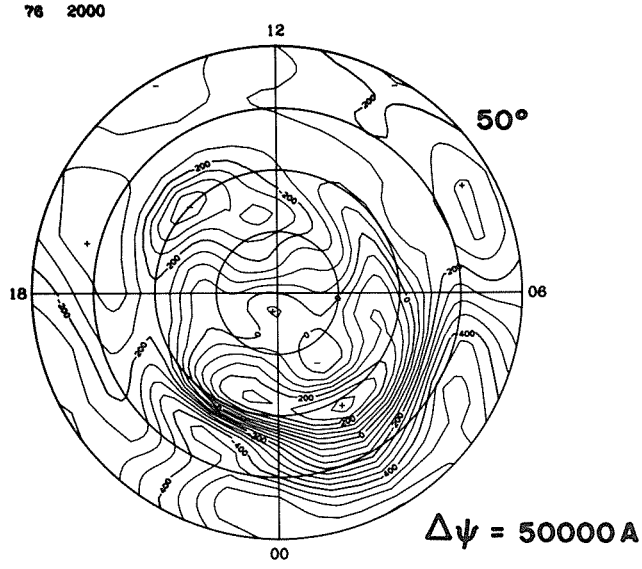

ELECTRIC POTENTIAL

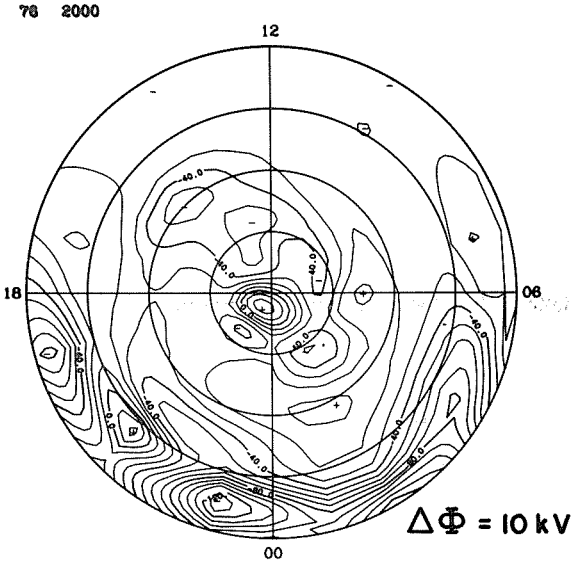

IONOSPHERIC CURRENT

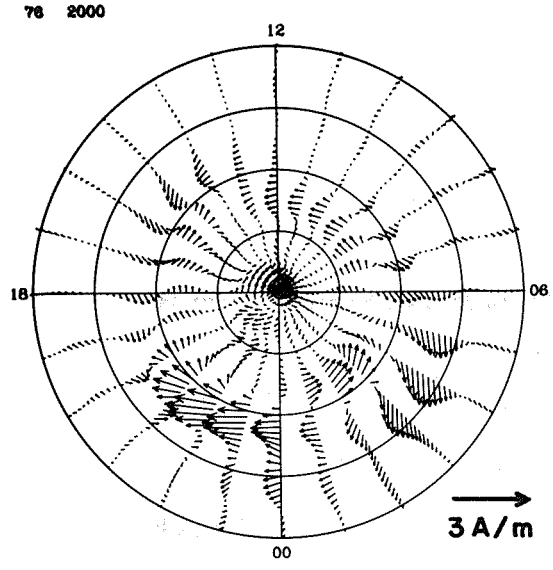

JOULE HEATING

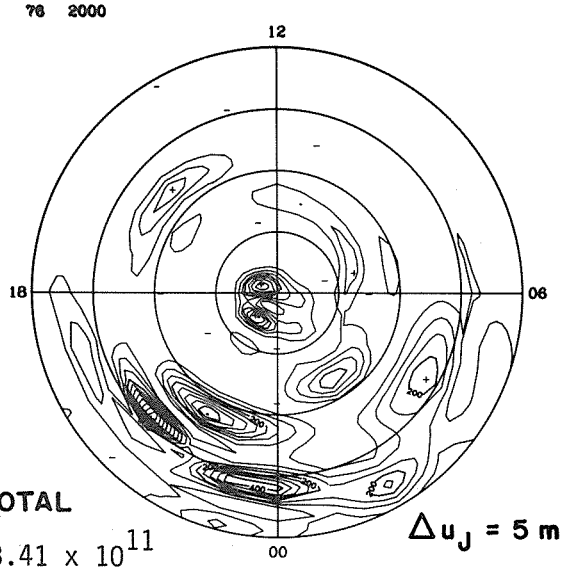

TOTAL

3.41×10^{11}

FIELD-ALIGNED CURRENT

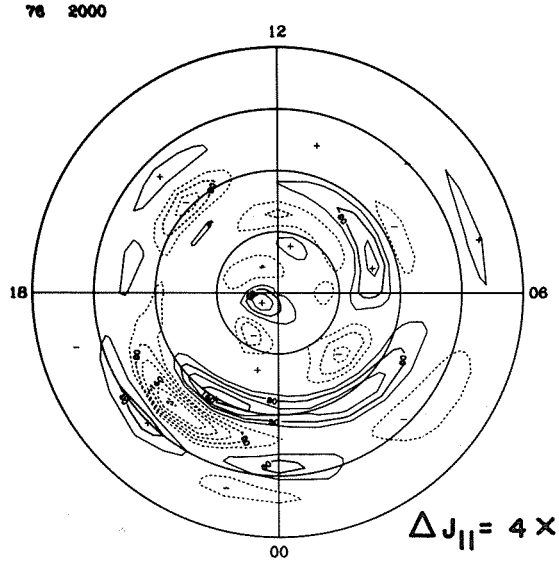

EQUIVALENT CURRENT

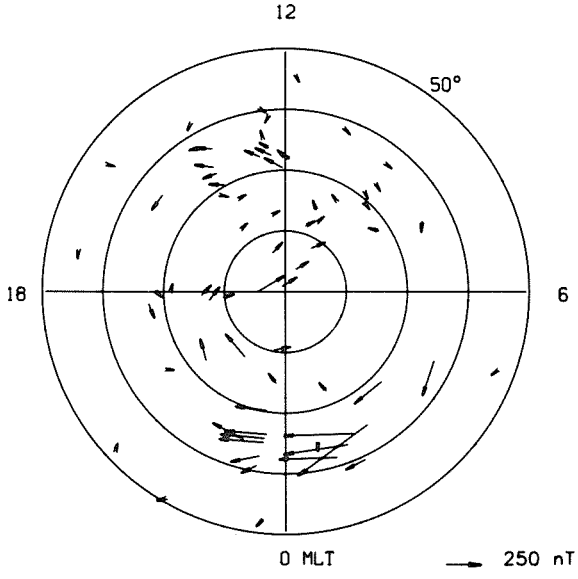

EQUIVALENT CURRENT SYSTEM

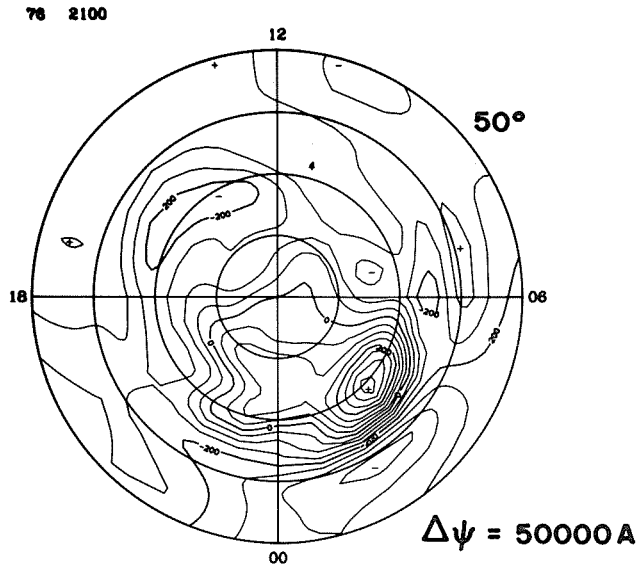

ELECTRIC POTENTIAL

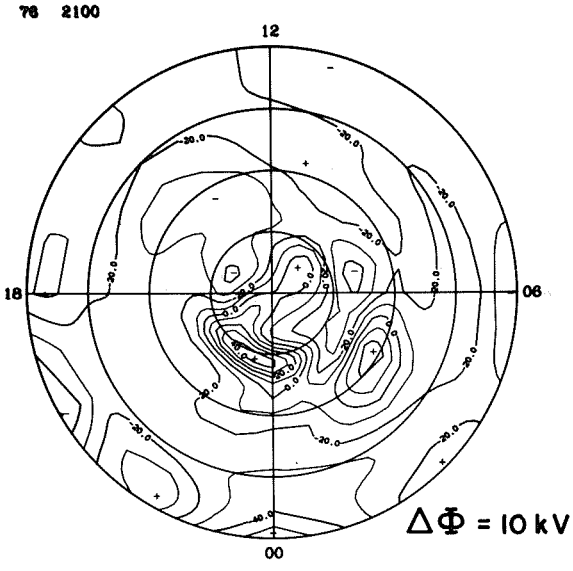

IONOSPHERIC CURRENT

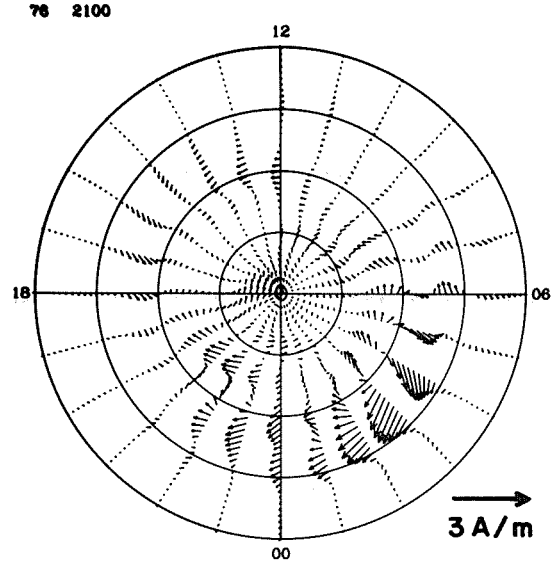

JOULE HEATING

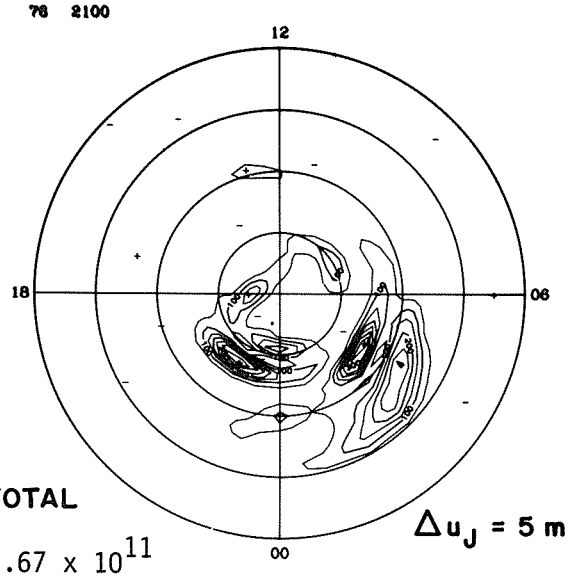

TOTAL

1.67×10^{11}

FIELD-ALIGNED CURRENT

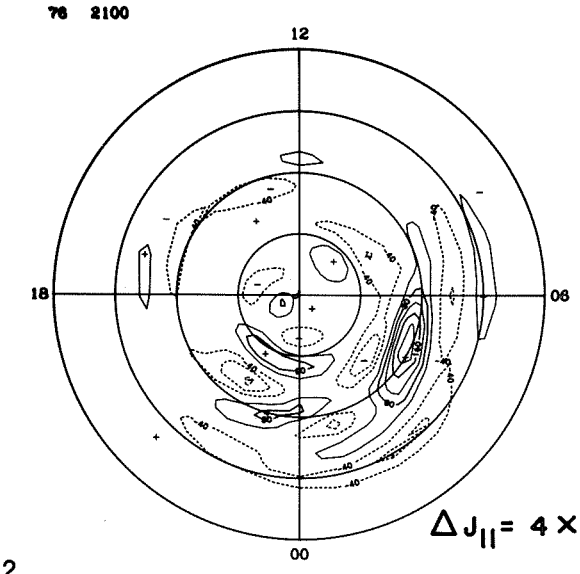

EQUIVALENT CURRENT

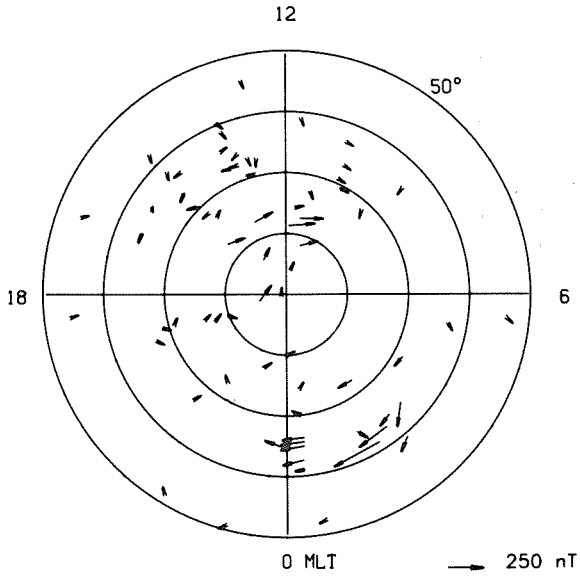

EQUIVALENT CURRENT SYSTEM

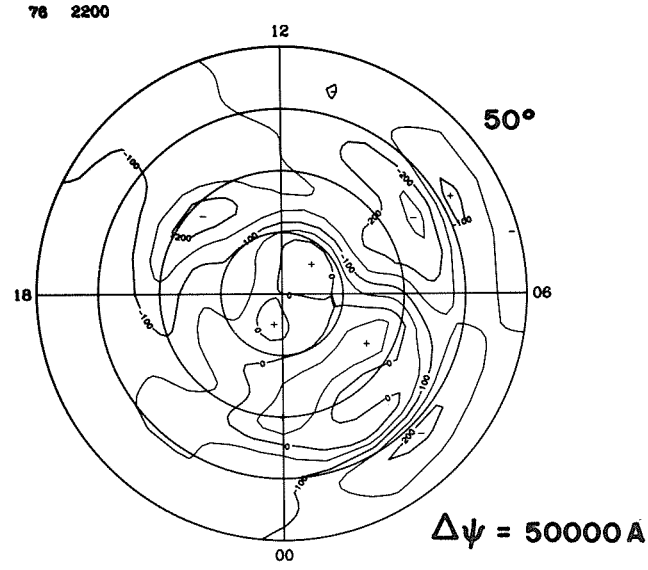

ELECTRIC POTENTIAL

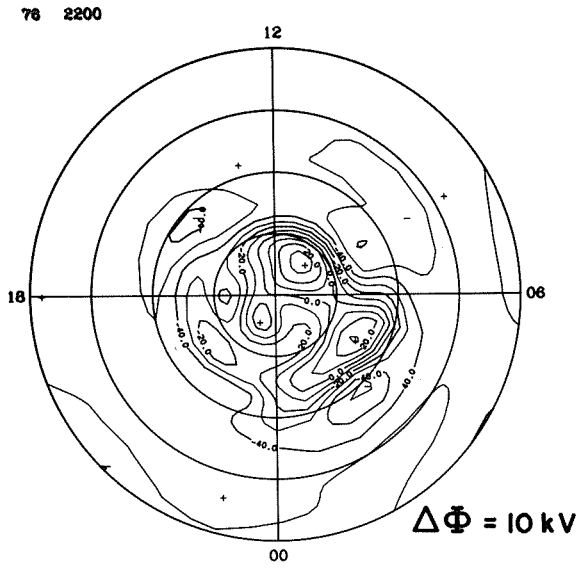

IONOSPHERIC CURRENT

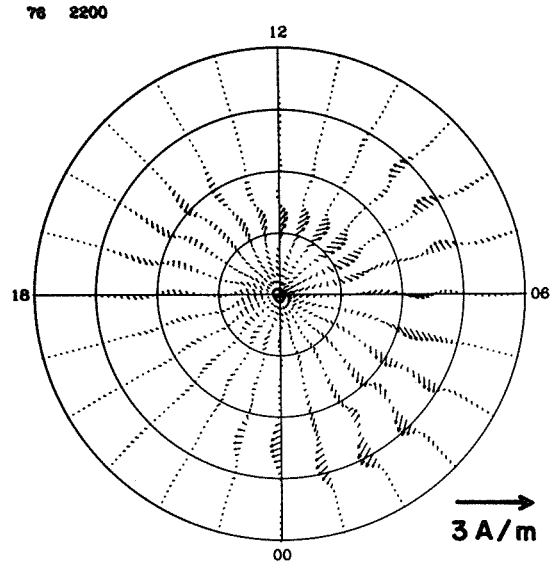

JOULE HEATING

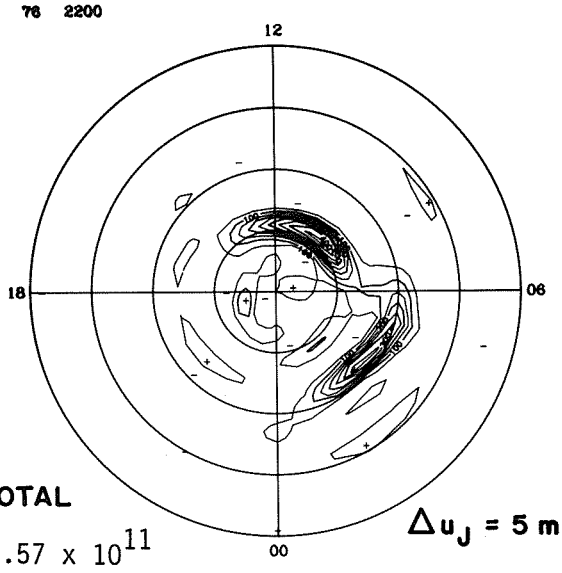

TOTAL

1.57×10^{11}

FIELD-ALIGNED CURRENT

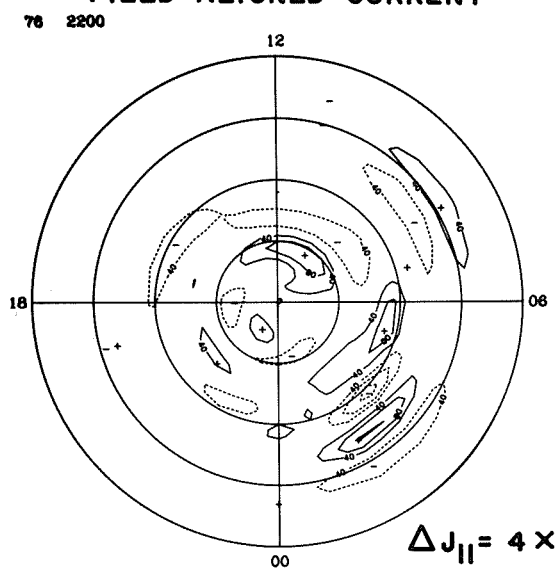

EQUIVALENT CURRENT

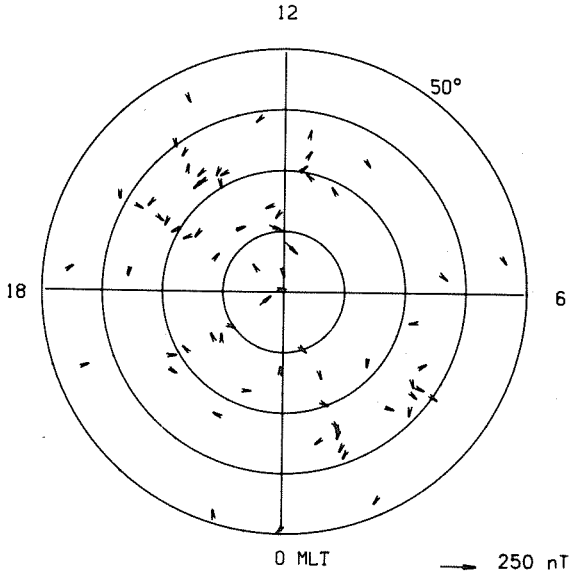

EQUIVALENT CURRENT SYSTEM

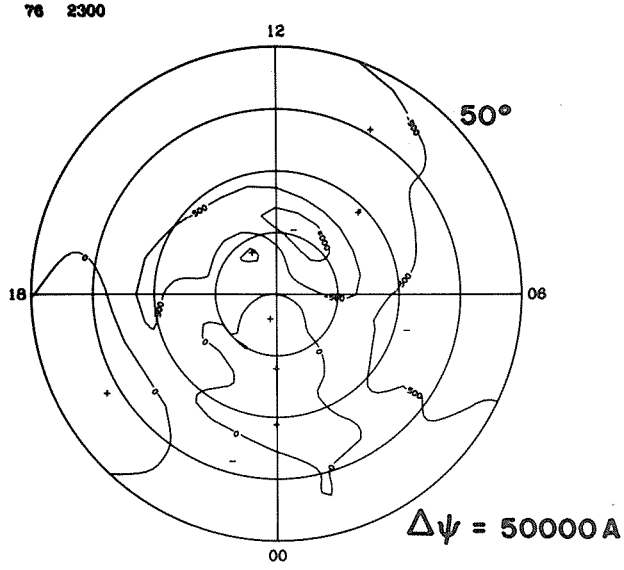

ELECTRIC POTENTIAL

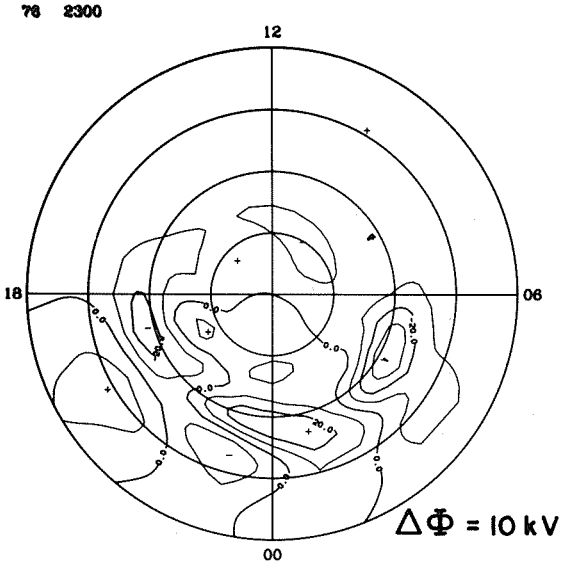

IONOSPHERIC CURRENT

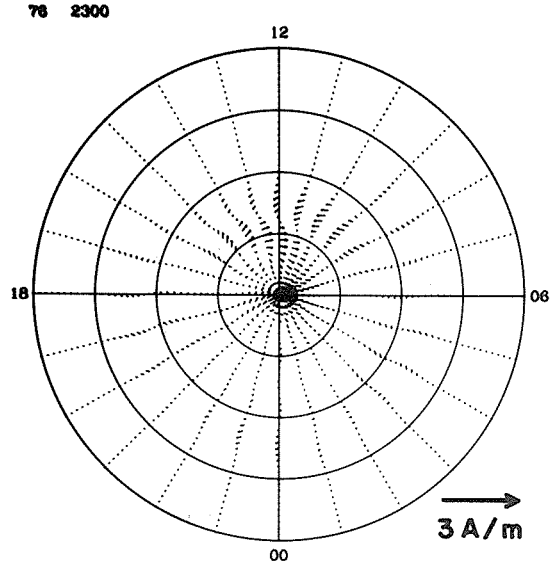

JOULE HEATING

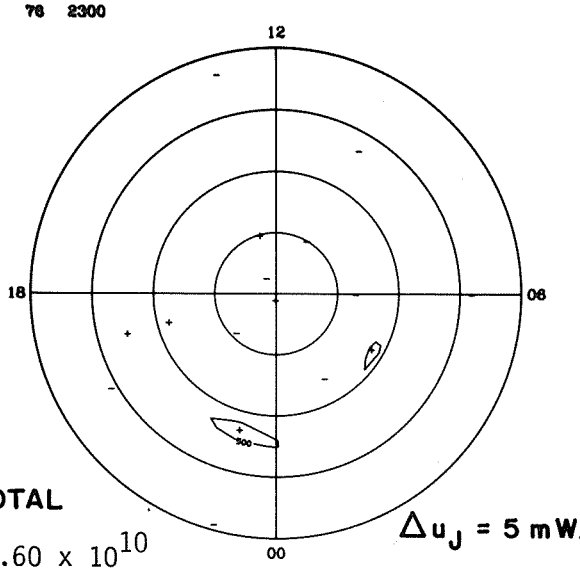

TOTAL

3.60×10^{10}

FIELD-ALIGNED CURRENT

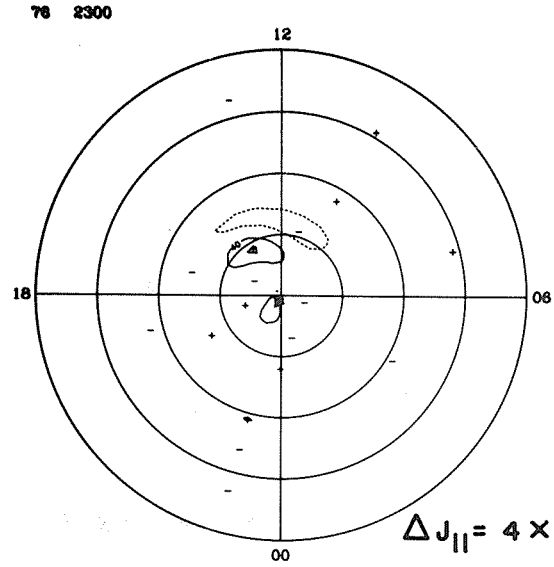

EQUIVALENT CURRENT

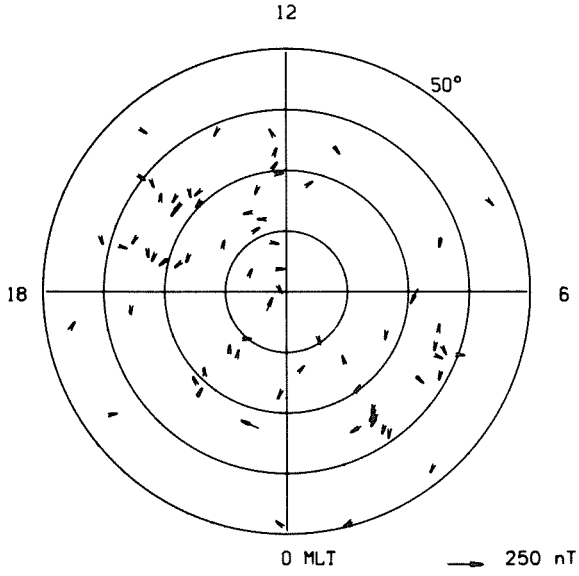

EQUIVALENT CURRENT SYSTEM

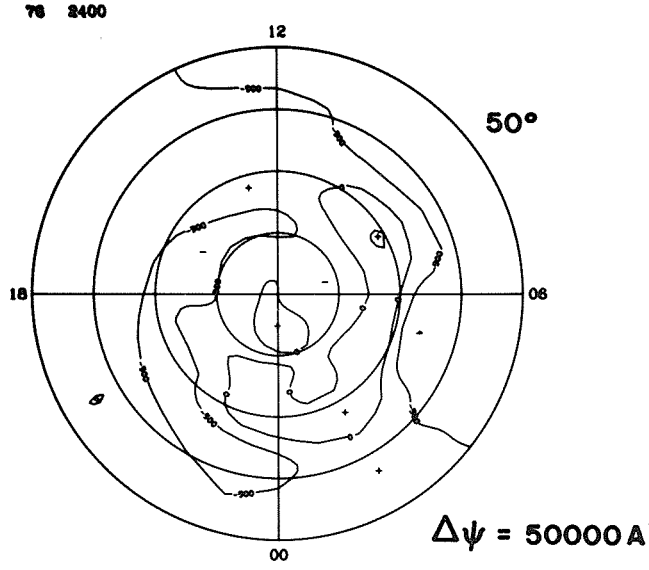

ELECTRIC POTENTIAL

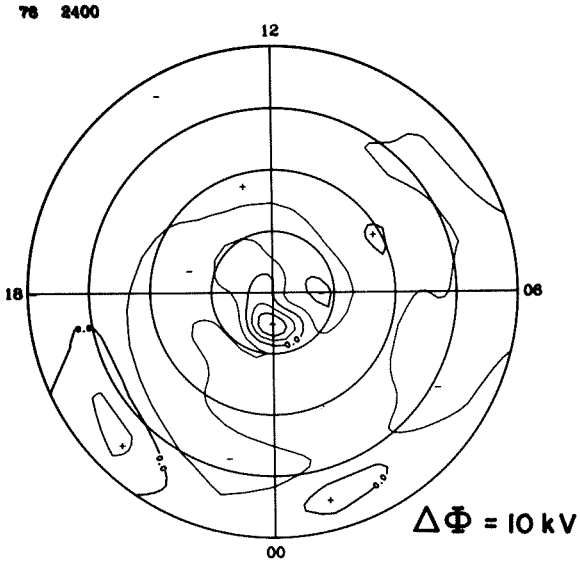

IONOSPHERIC CURRENT

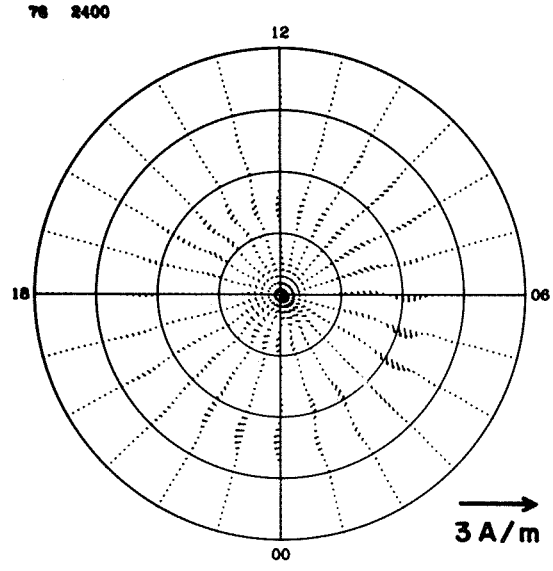

JOULE HEATING

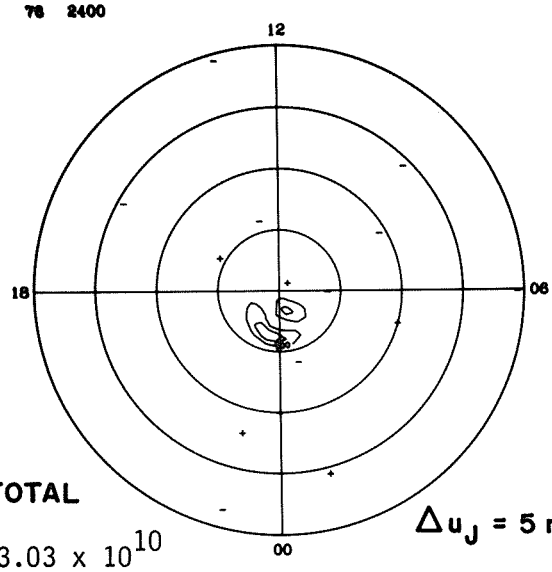

TOTAL

3.03×10^{10}

FIELD-ALIGNED CURRENT

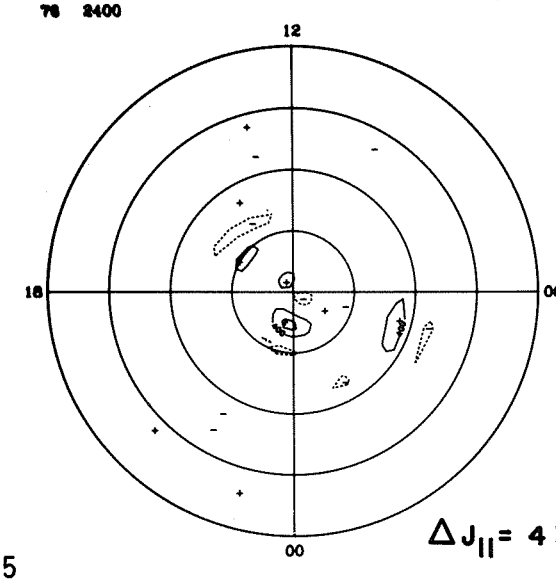

EQUIVALENT CURRENT

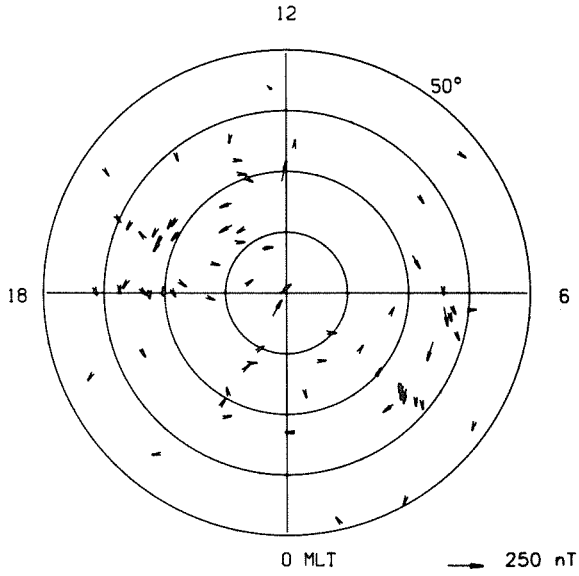

EQUIVALENT CURRENT SYSTEM

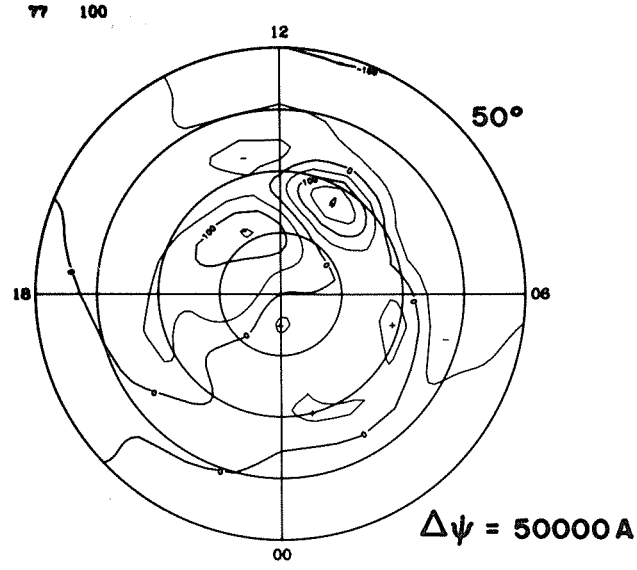

ELECTRIC POTENTIAL

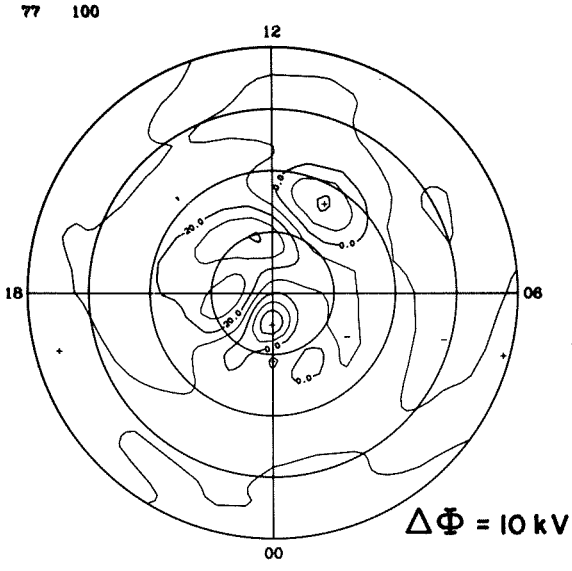

IONOSPHERIC CURRENT

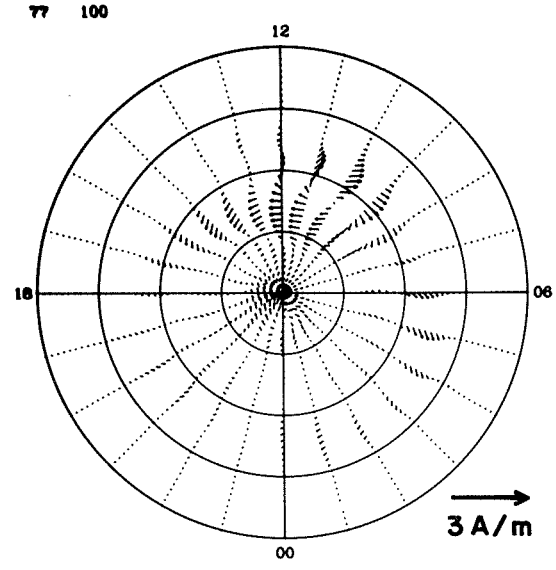

JOULE HEATING

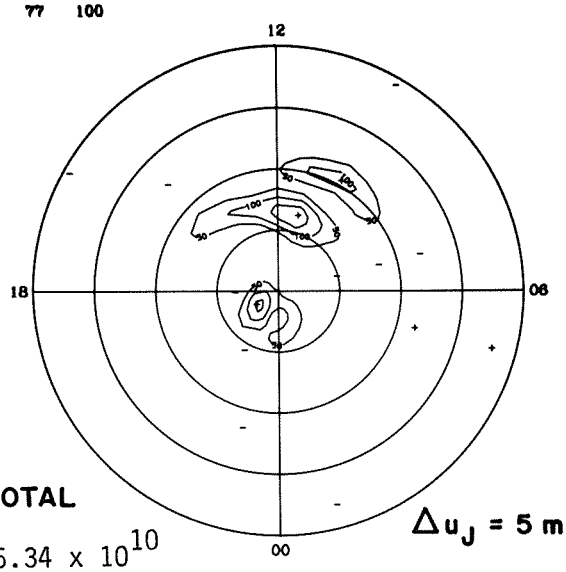

TOTAL

6.34×10^{10}

FIELD-ALIGNED CURRENT

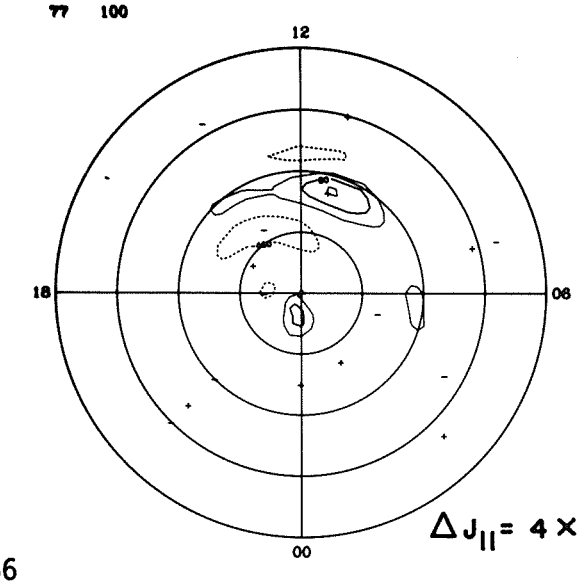

EQUIVALENT CURRENT

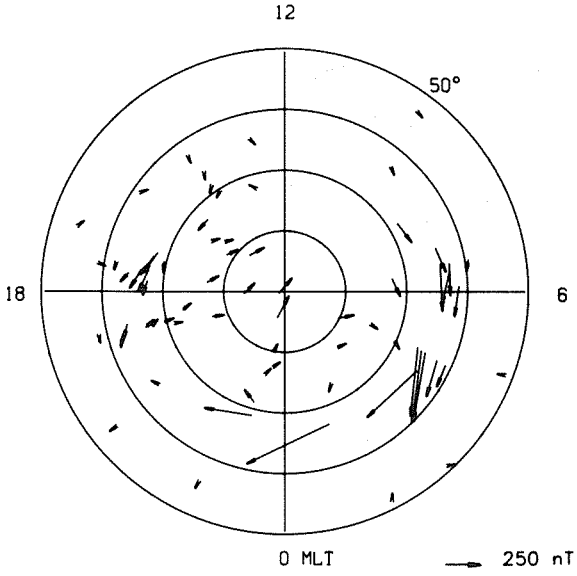

EQUIVALENT CURRENT SYSTEM

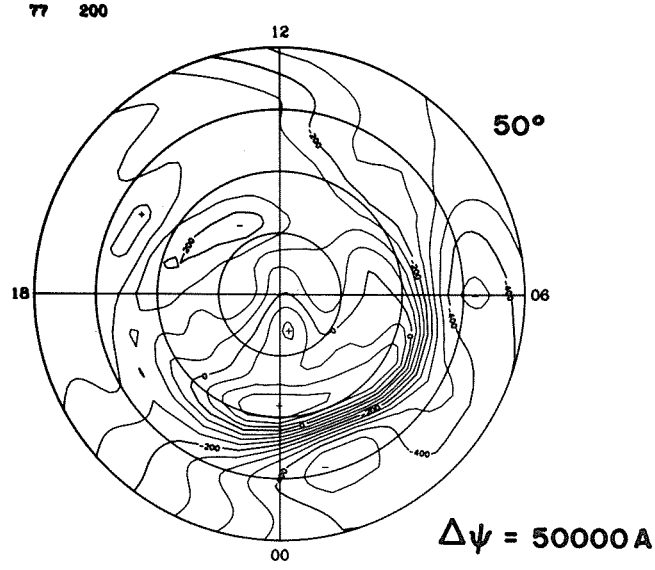

ELECTRIC POTENTIAL

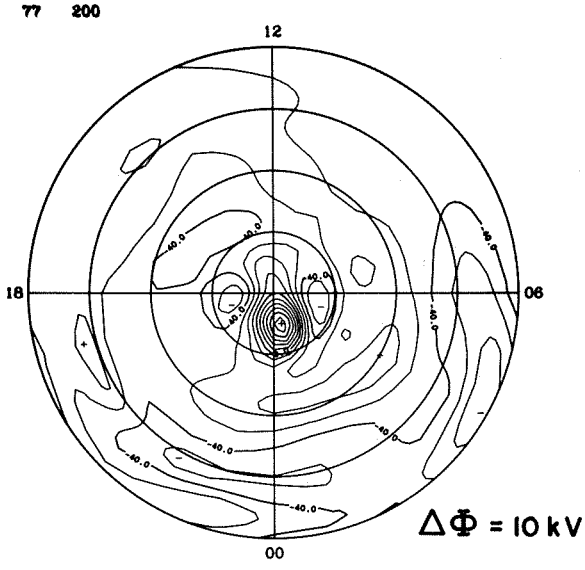

IONOSPHERIC CURRENT

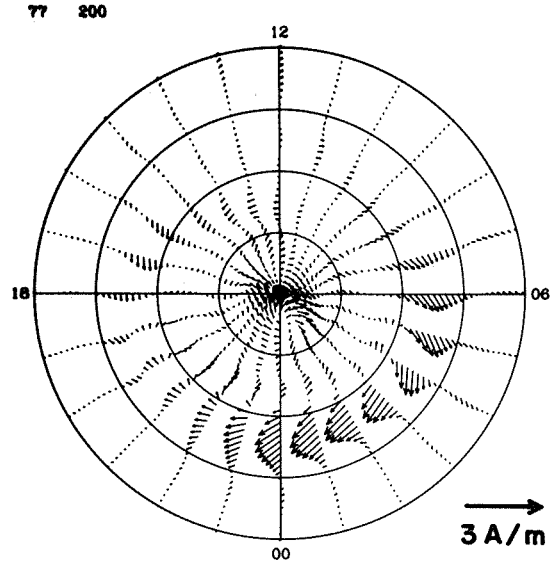

JOULE HEATING

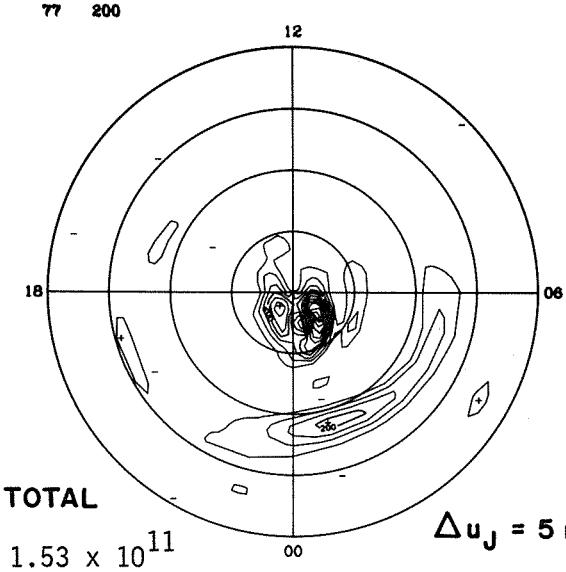

FIELD-ALIGNED CURRENT

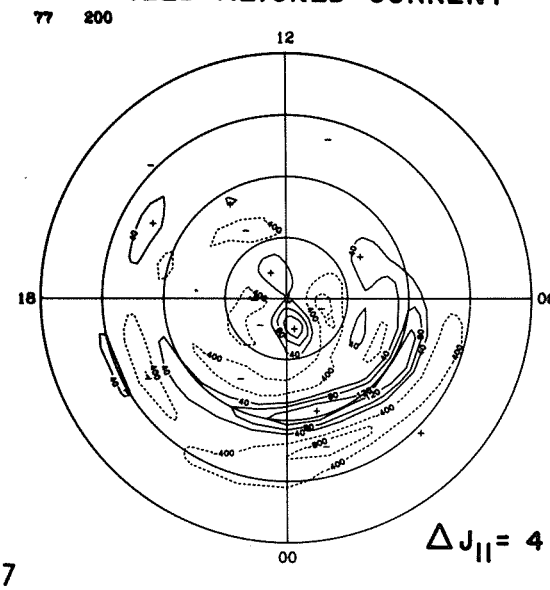

EQUIVALENT CURRENT

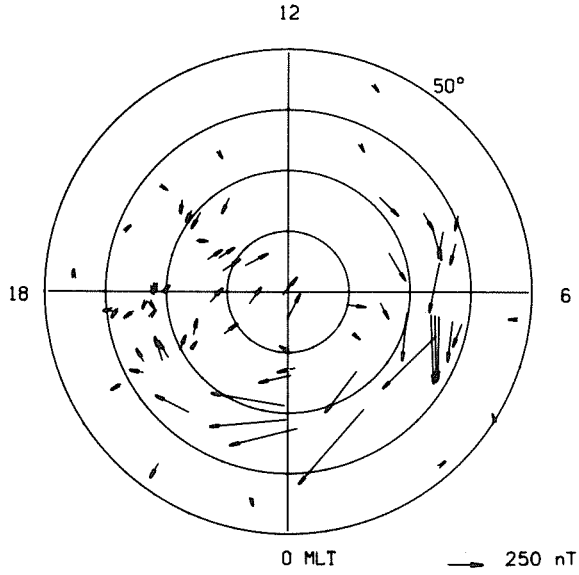

EQUIVALENT CURRENT SYSTEM

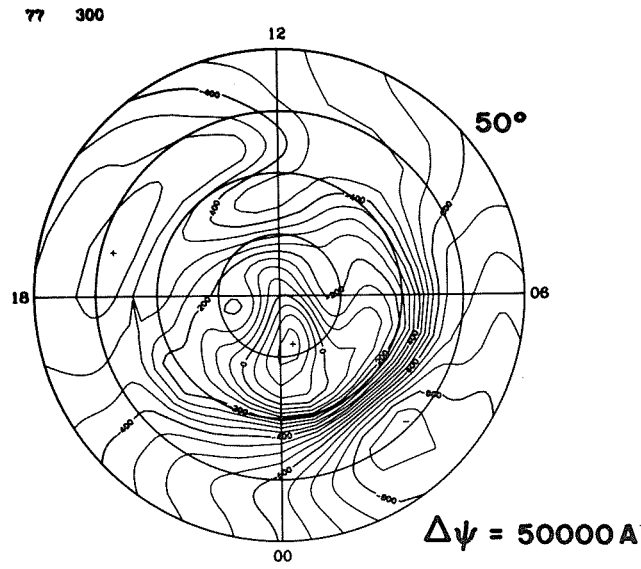

ELECTRIC POTENTIAL

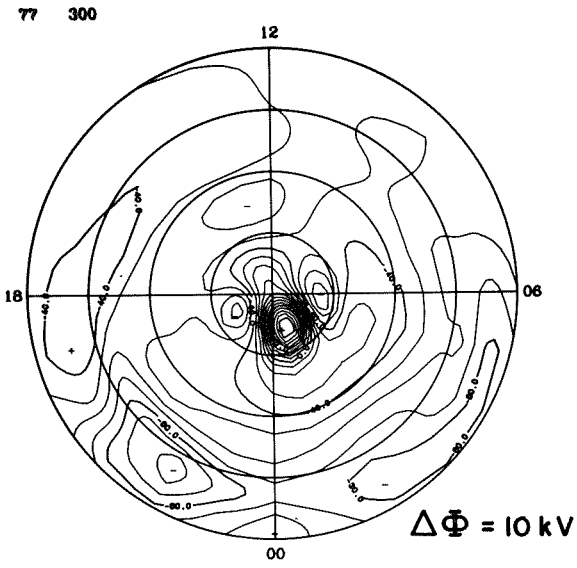

IONOSPHERIC CURRENT

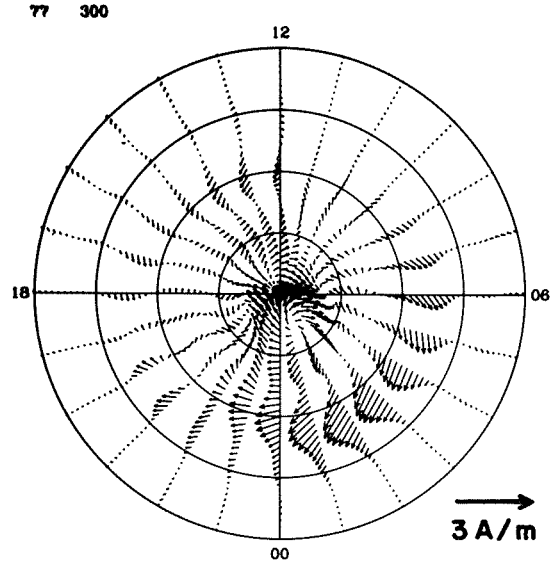

JOULE HEATING

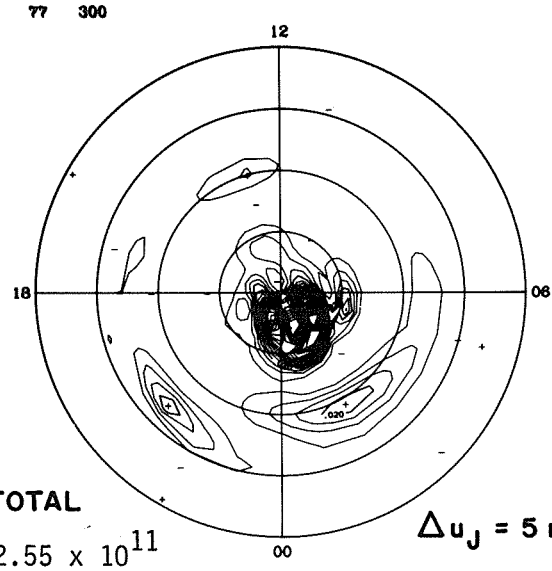

TOTAL

2.55×10^{11}

FIELD-ALIGNED CURRENT

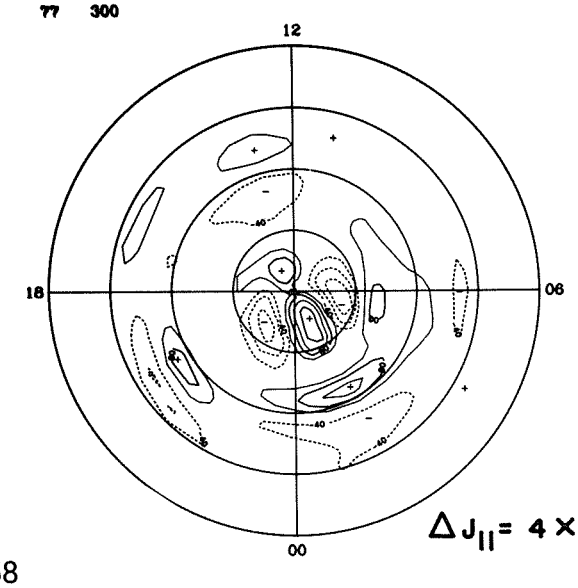

EQUIVALENT CURRENT

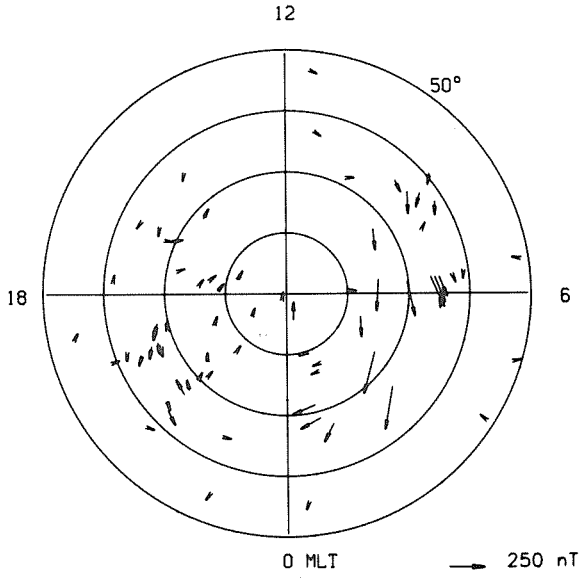

EQUIVALENT CURRENT SYSTEM

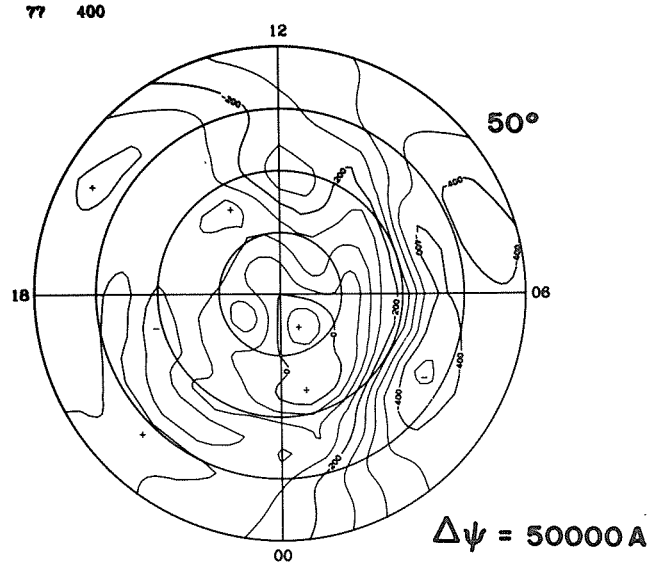

ELECTRIC POTENTIAL

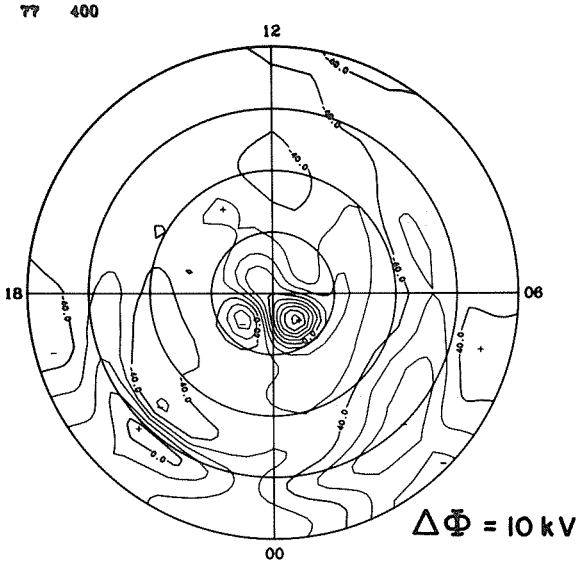

IONOSPHERIC CURRENT

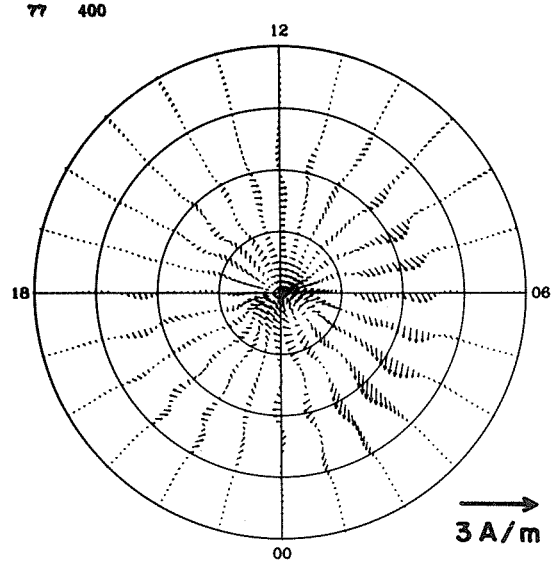

JOULE HEATING

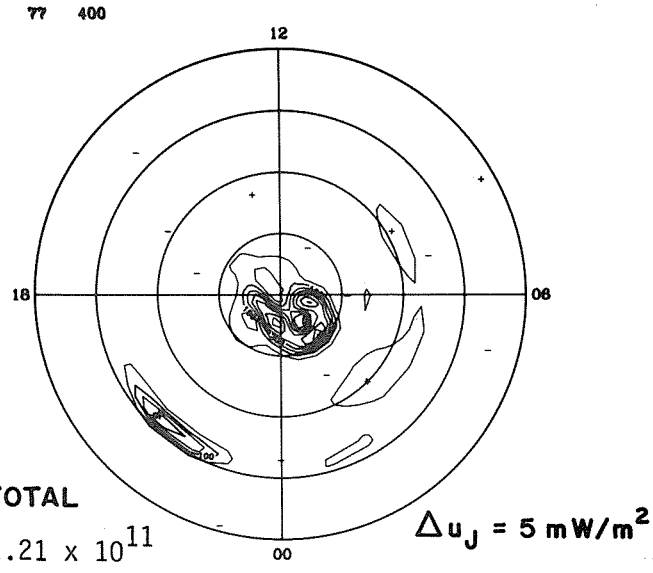

TOTAL

1.21×10^{11}

FIELD-ALIGNED CURRENT

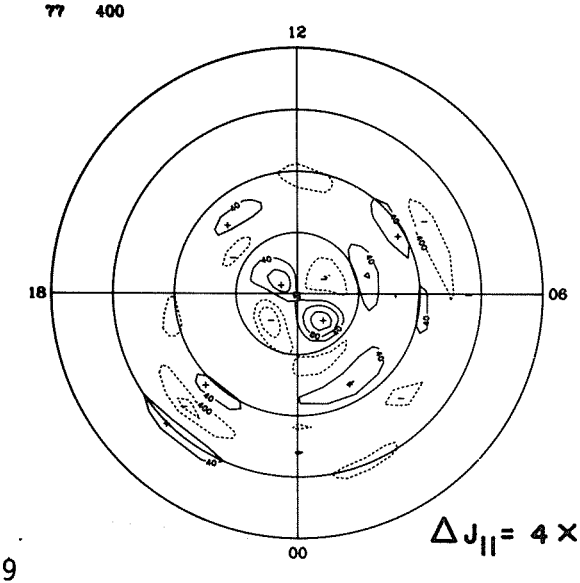

EQUIVALENT CURRENT

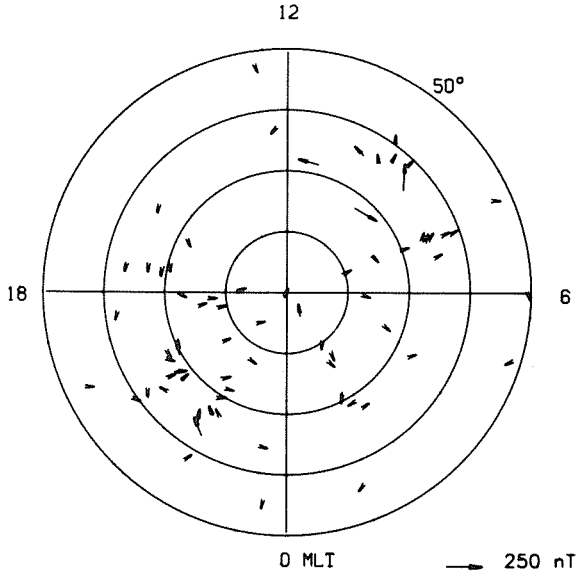

EQUIVALENT CURRENT SYSTEM

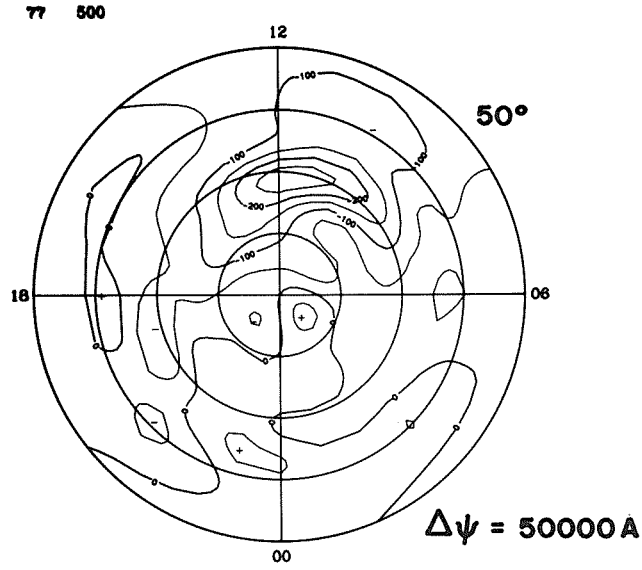

ELECTRIC POTENTIAL

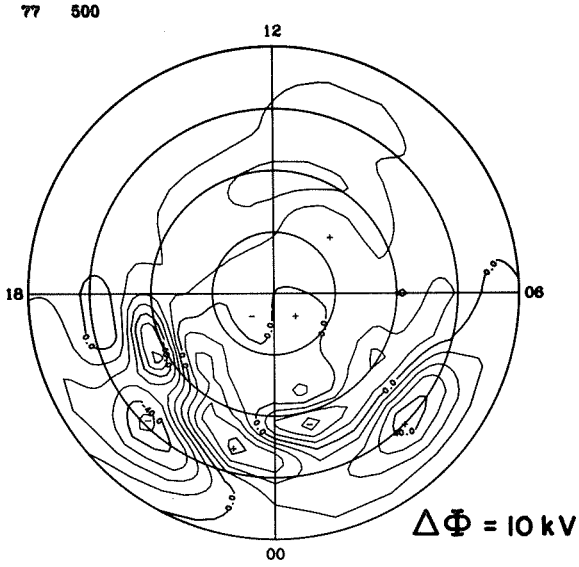

IONOSPHERIC CURRENT

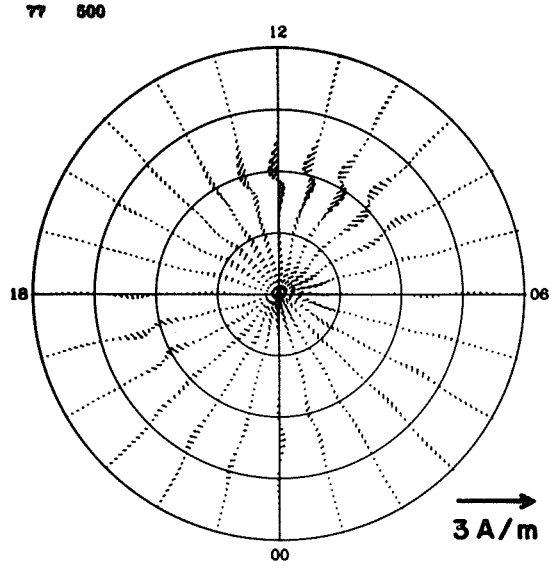

JOULE HEATING

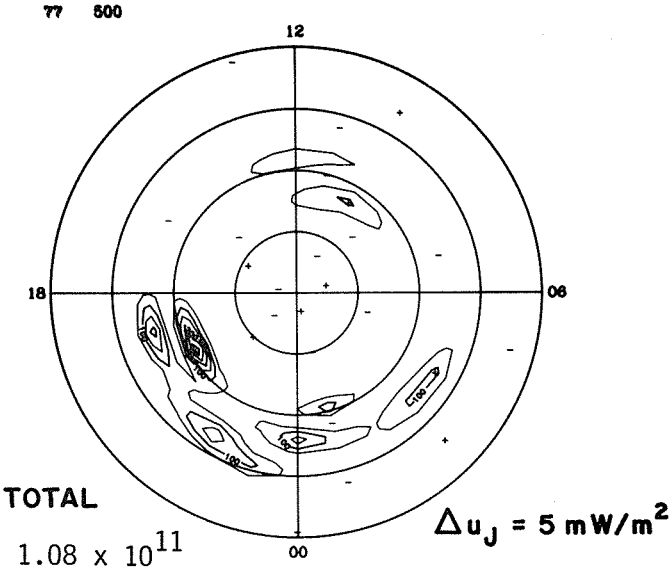

FIELD-ALIGNED CURRENT

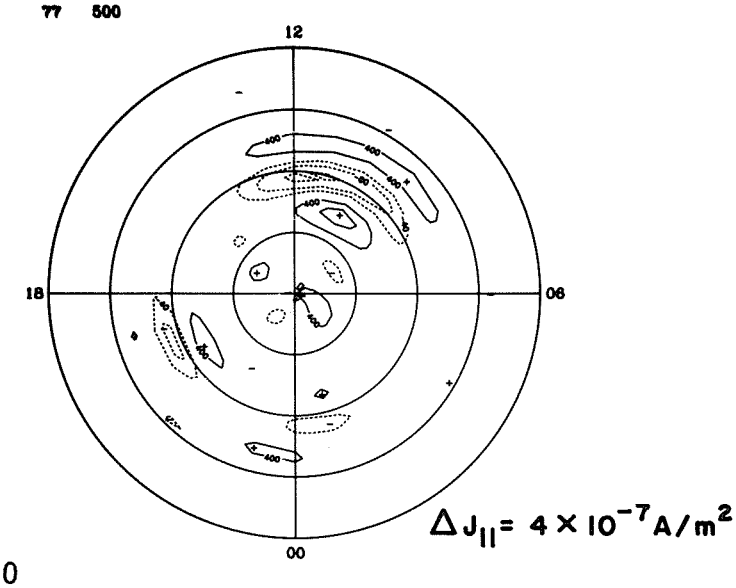

EQUIVALENT CURRENT

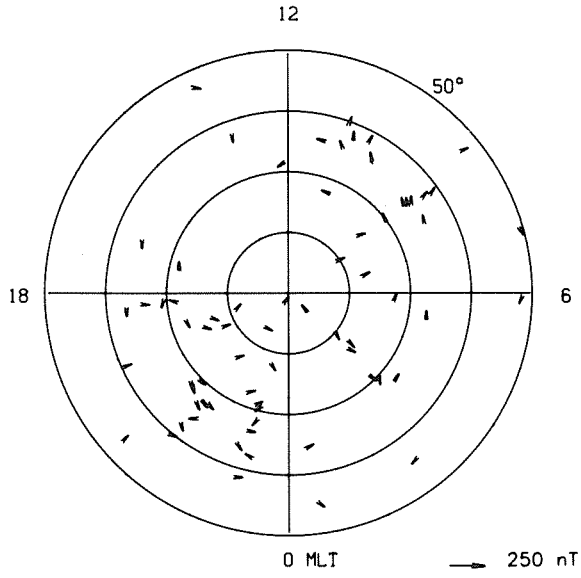

EQUIVALENT CURRENT SYSTEM

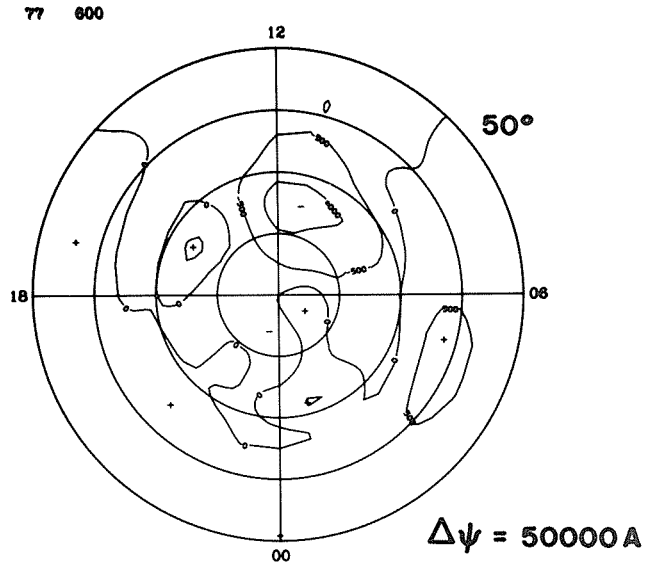

ELECTRIC POTENTIAL

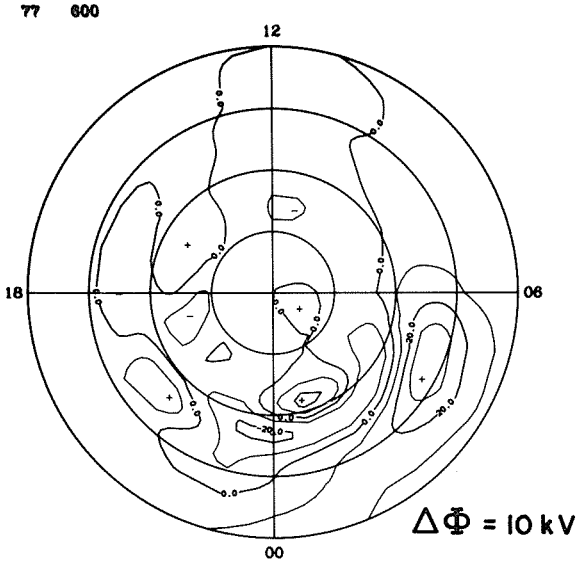

IONOSPHERIC CURRENT

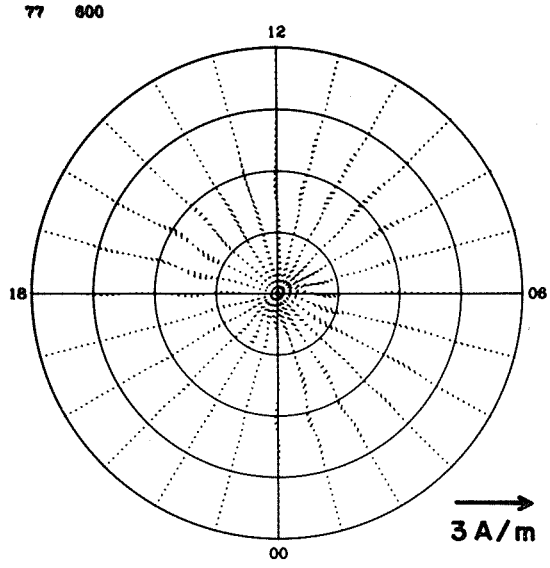

JOULE HEATING

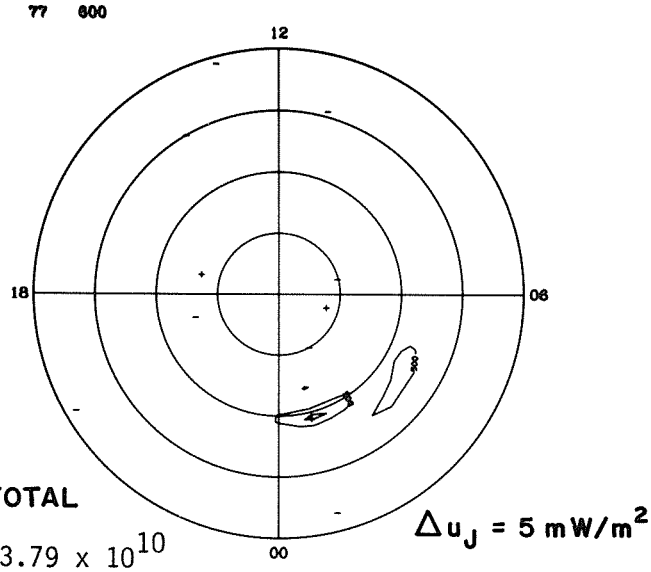

TOTAL

3.79×10^{10}

FIELD-ALIGNED CURRENT

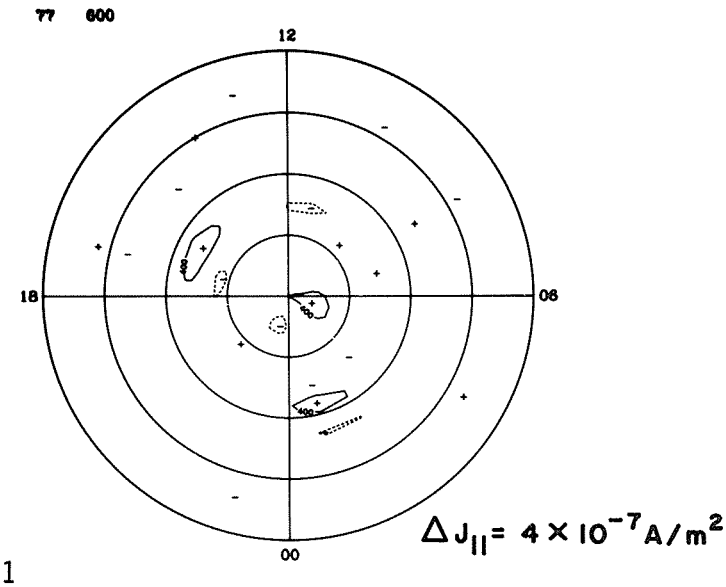

EQUIVALENT CURRENT

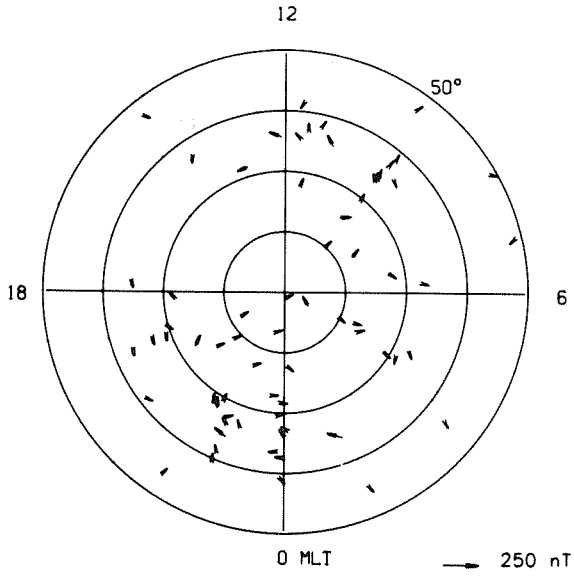

EQUIVALENT CURRENT SYSTEM

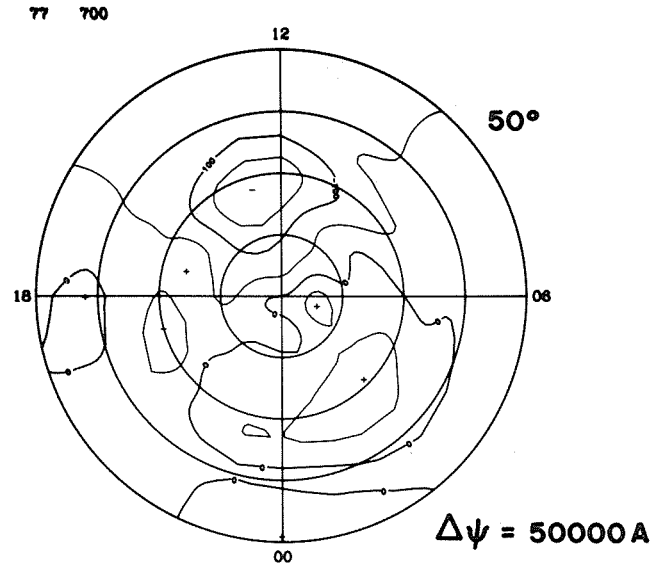

ELECTRIC POTENTIAL

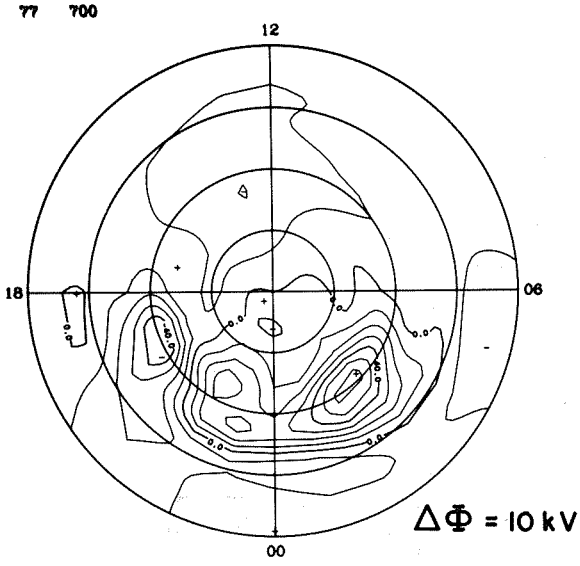

IONOSPHERIC CURRENT

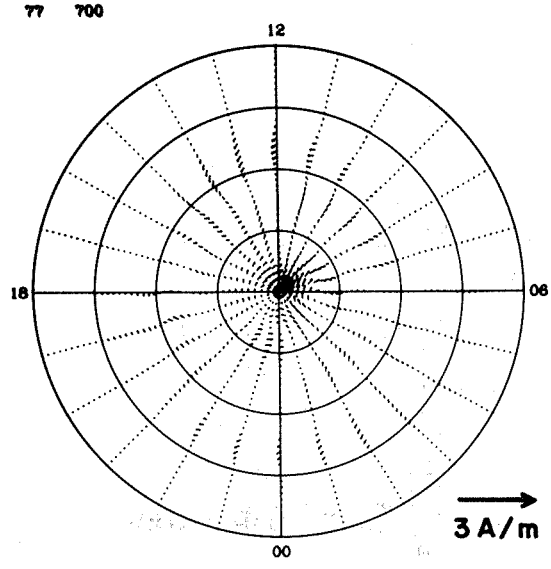

JOULE HEATING

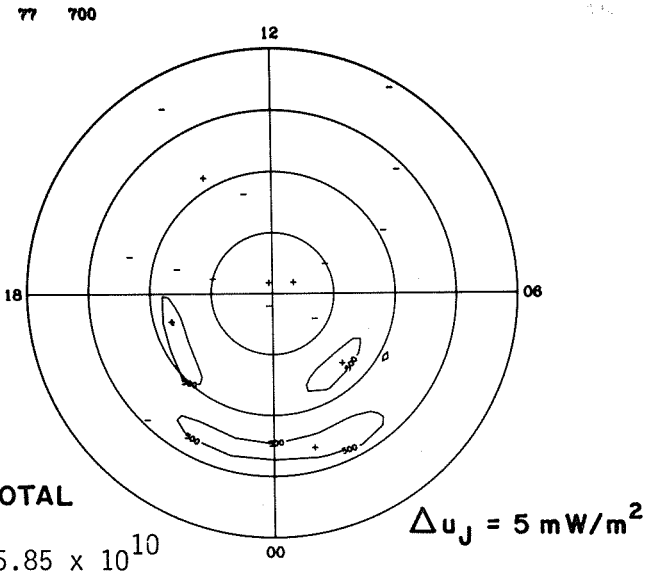

TOTAL

5.85×10^{10}

FIELD-ALIGNED CURRENT

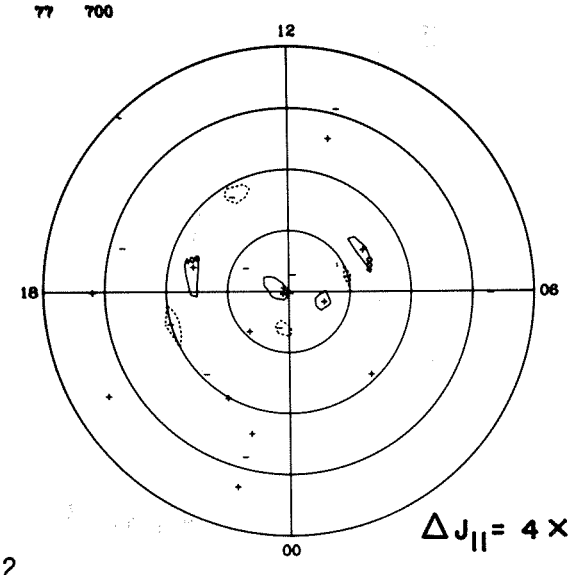

EQUIVALENT CURRENT

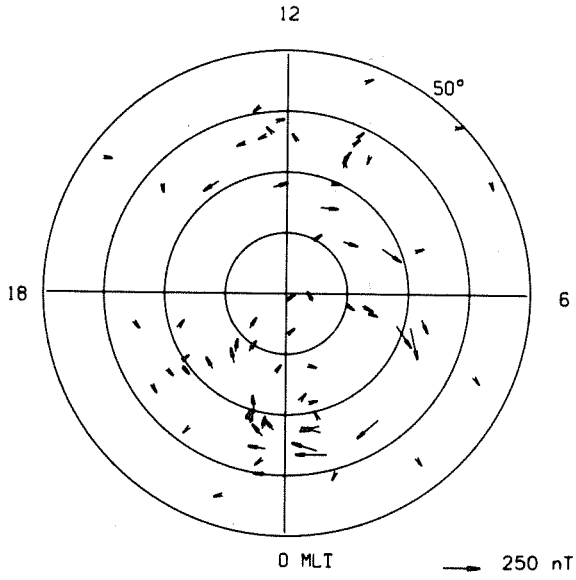

EQUIVALENT CURRENT SYSTEM

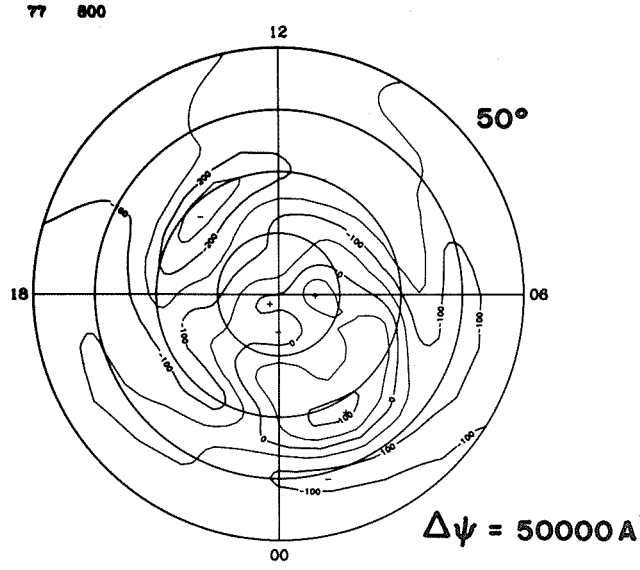

ELECTRIC POTENTIAL

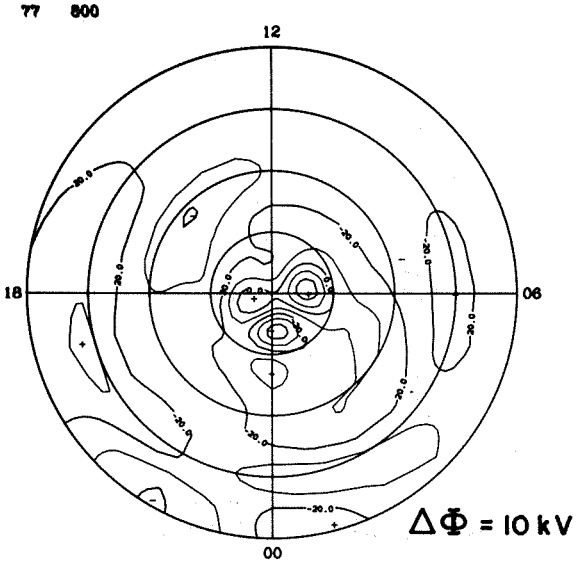

IONOSPHERIC CURRENT

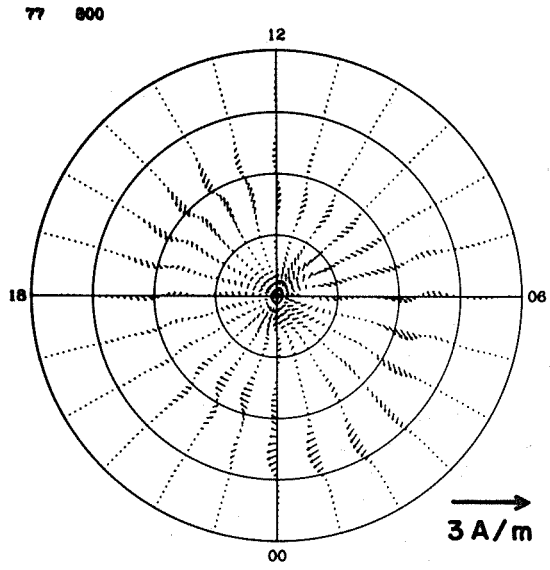

JOULE HEATING

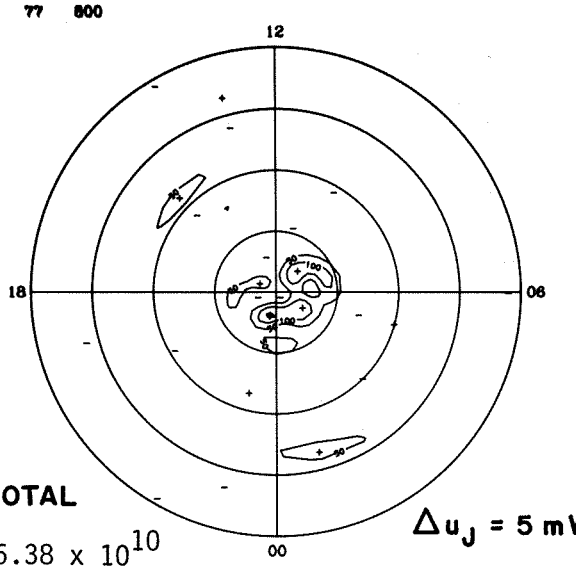

TOTAL

6.38×10^{10}

FIELD-ALIGNED CURRENT

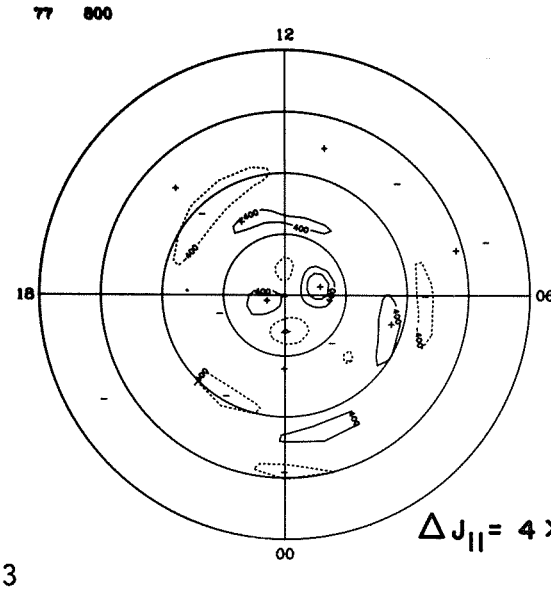

EQUIVALENT CURRENT

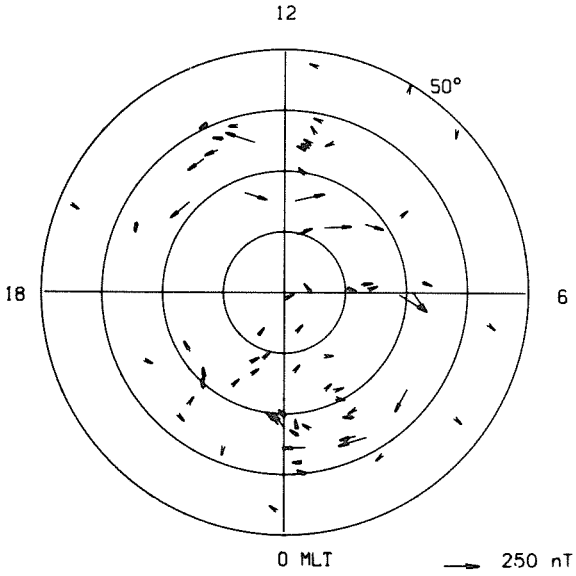

EQUIVALENT CURRENT SYSTEM

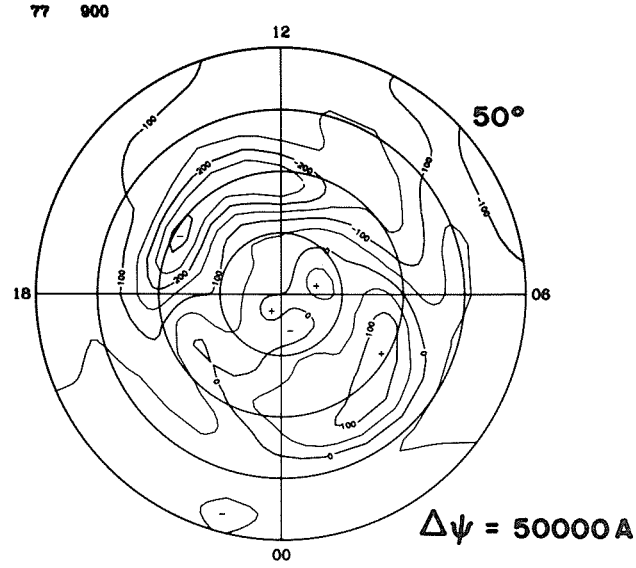

ELECTRIC POTENTIAL

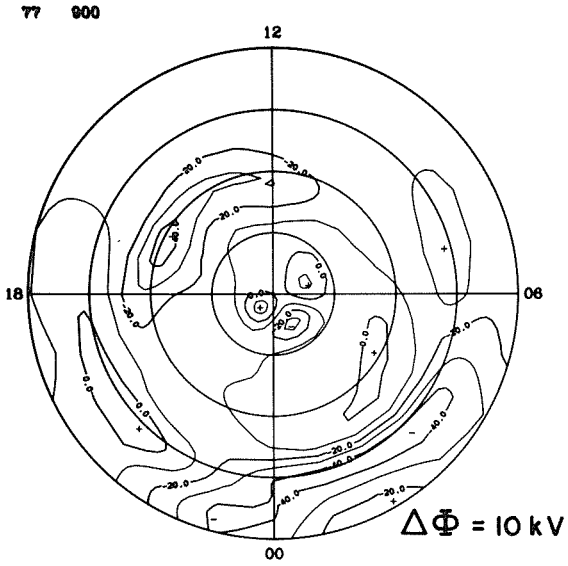

IONOSPHERIC CURRENT

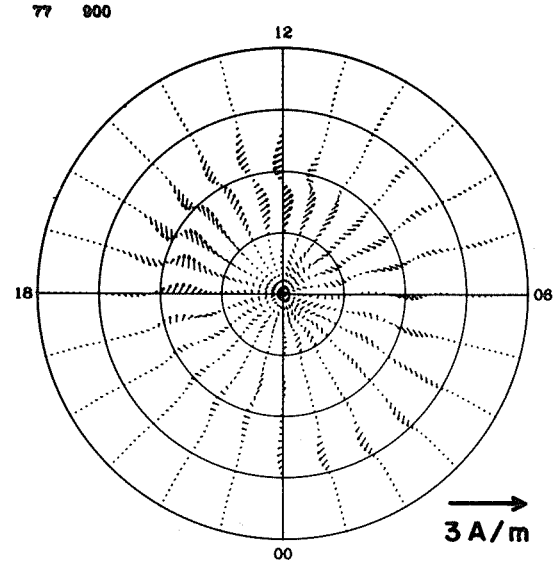

JOULE HEATING

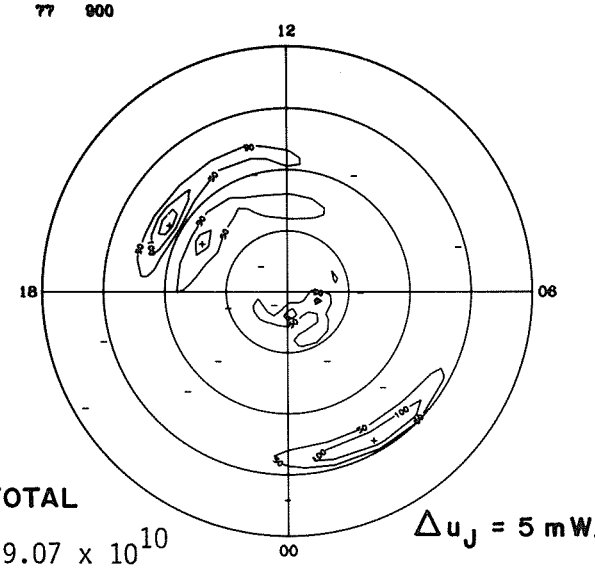

TOTAL

9.07×10^{10}

FIELD-ALIGNED CURRENT

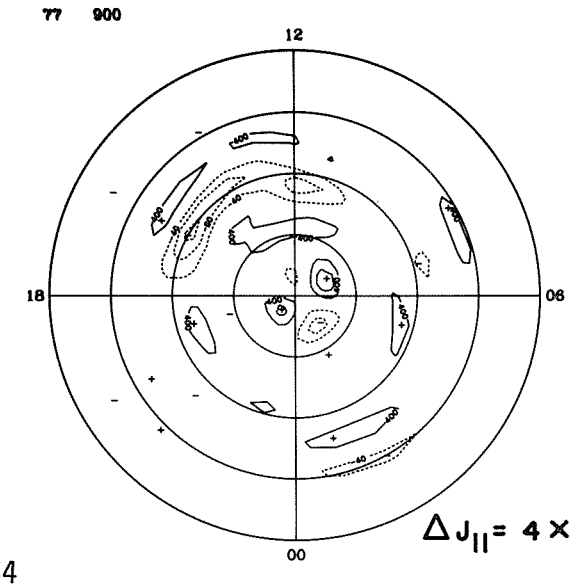

EQUIVALENT CURRENT

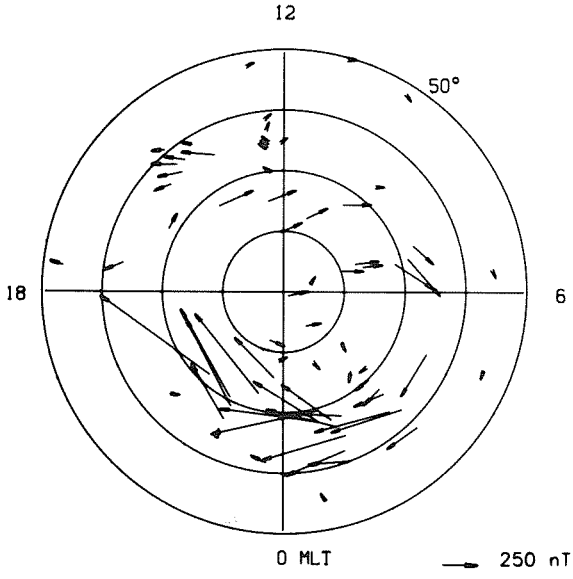

EQUIVALENT CURRENT SYSTEM

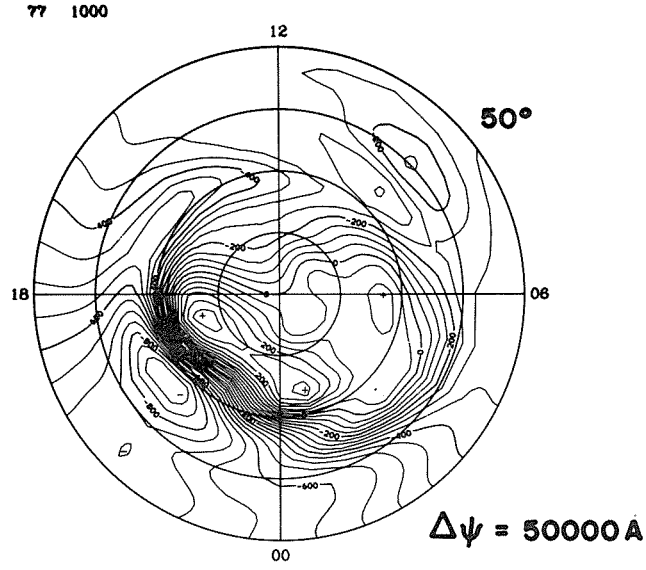

ELECTRIC POTENTIAL

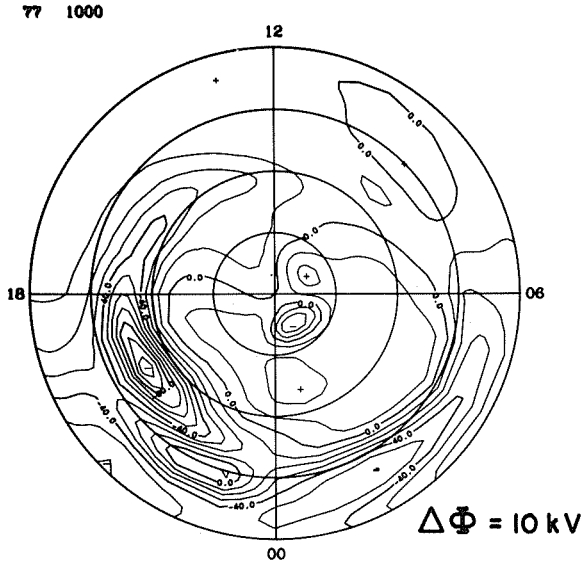

IONOSPHERIC CURRENT

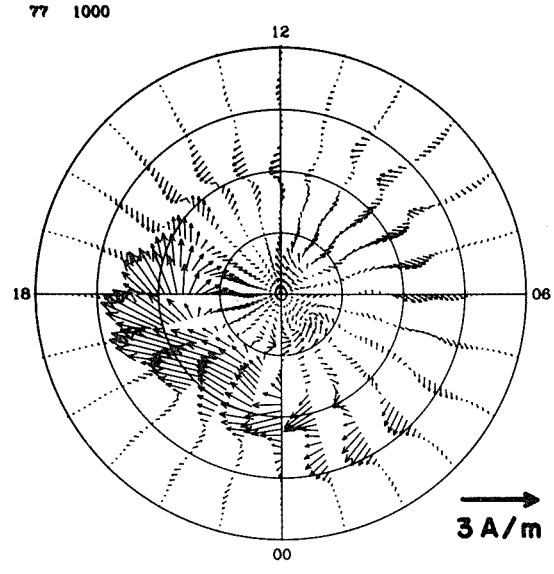

JOULE HEATING

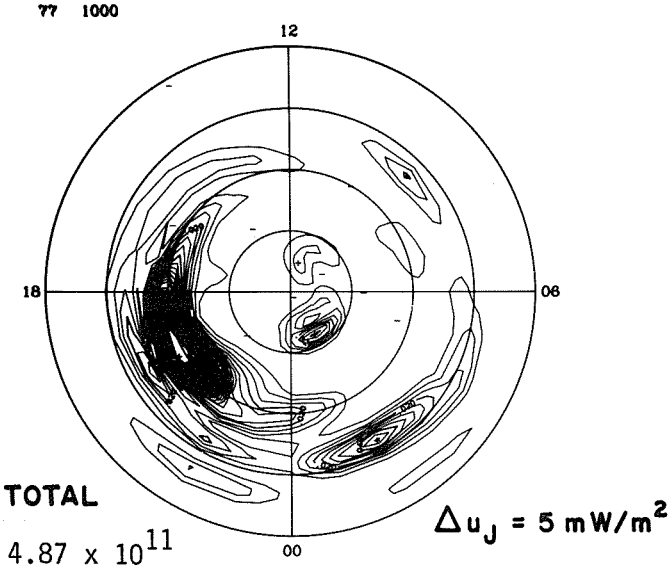

TOTAL

4.87×10^{11}

FIELD-ALIGNED CURRENT

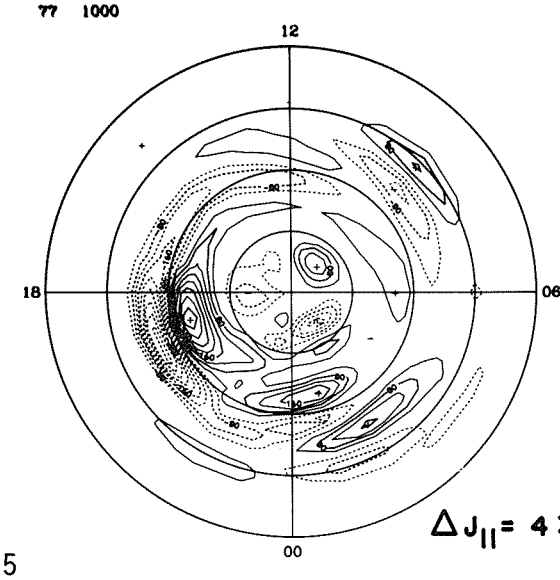

EQUIVALENT CURRENT

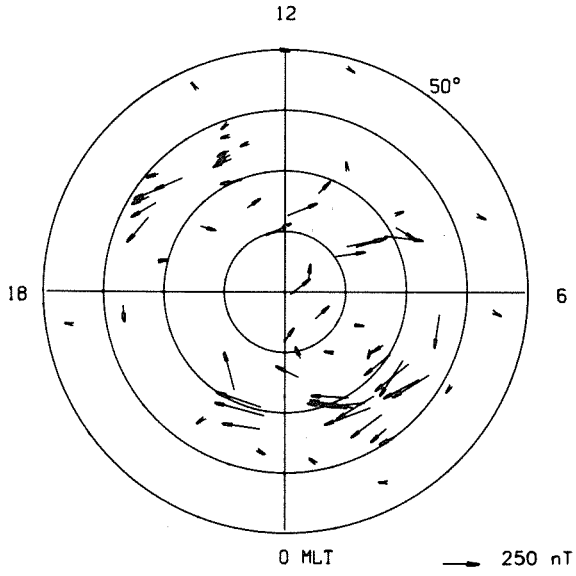

EQUIVALENT CURRENT SYSTEM

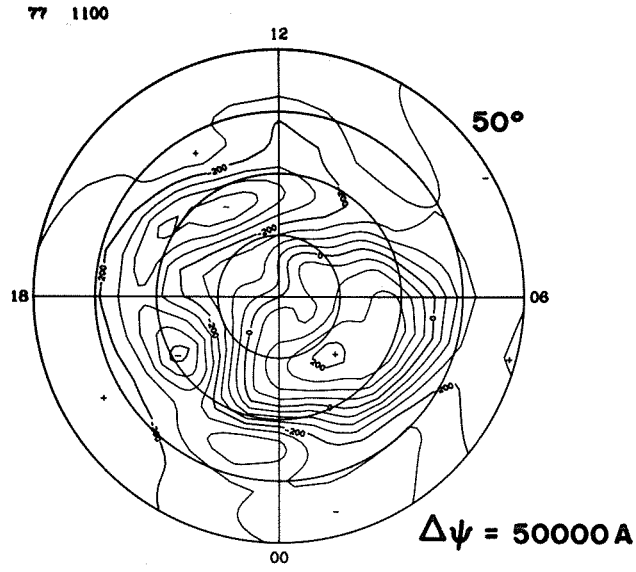

ELECTRIC POTENTIAL

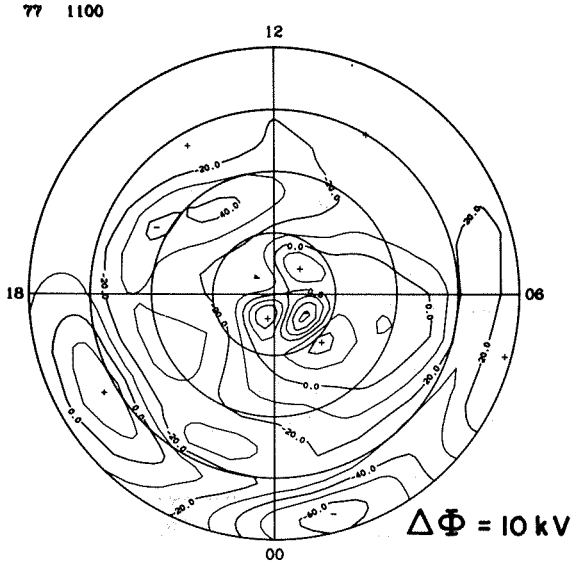

IONOSPHERIC CURRENT

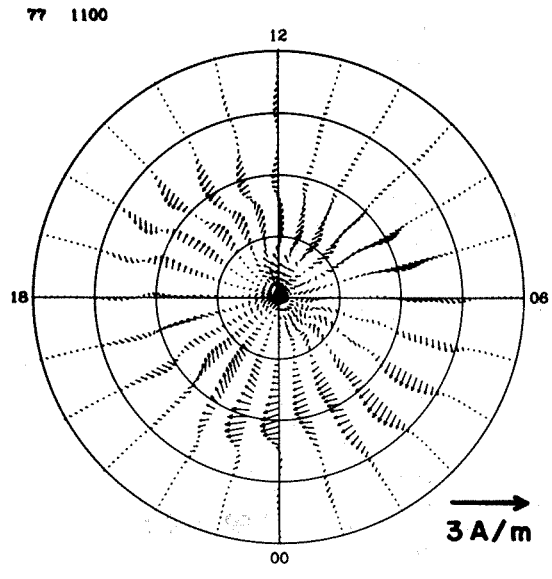

JOULE HEATING

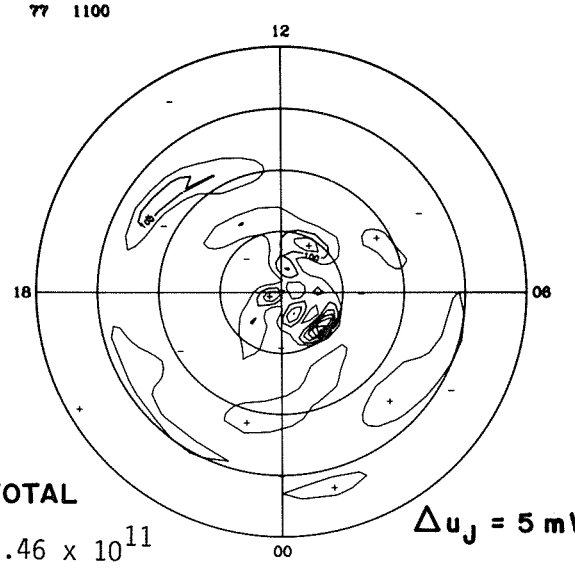

FIELD-ALIGNED CURRENT

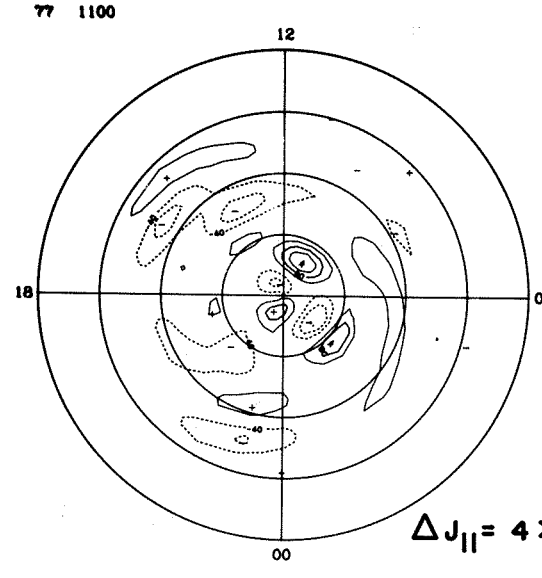

EQUIVALENT CURRENT

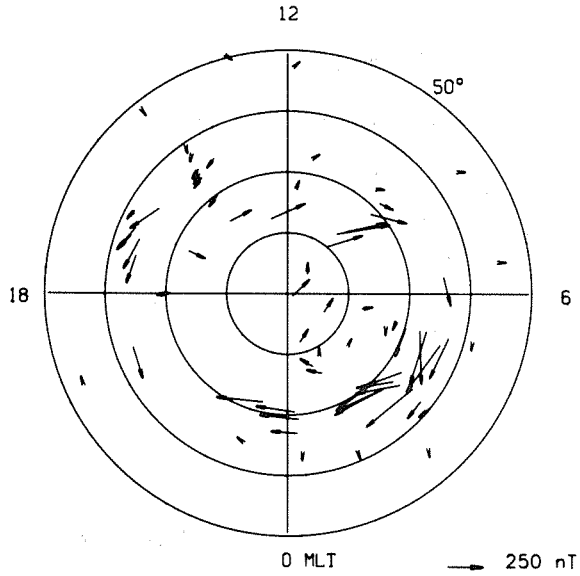

EQUIVALENT CURRENT SYSTEM

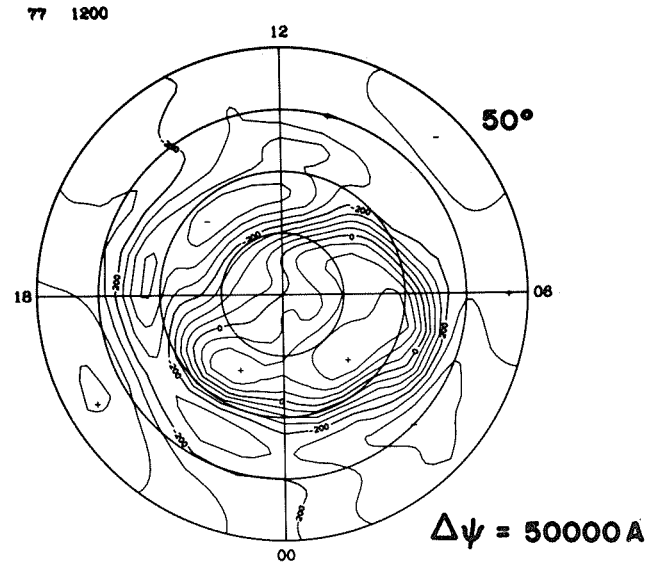

ELECTRIC POTENTIAL

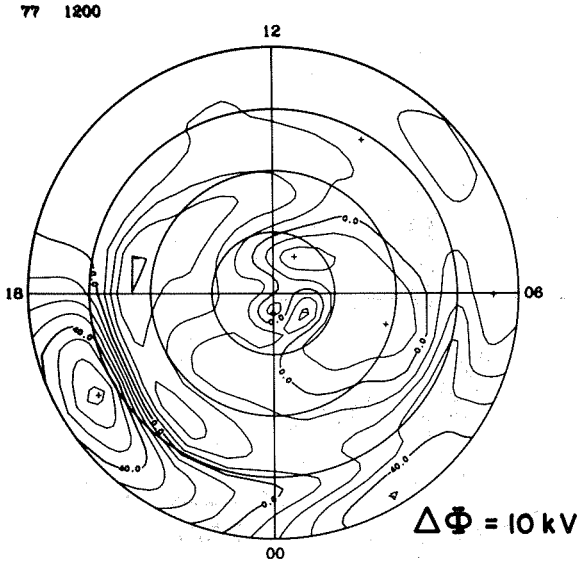

IONOSPHERIC CURRENT

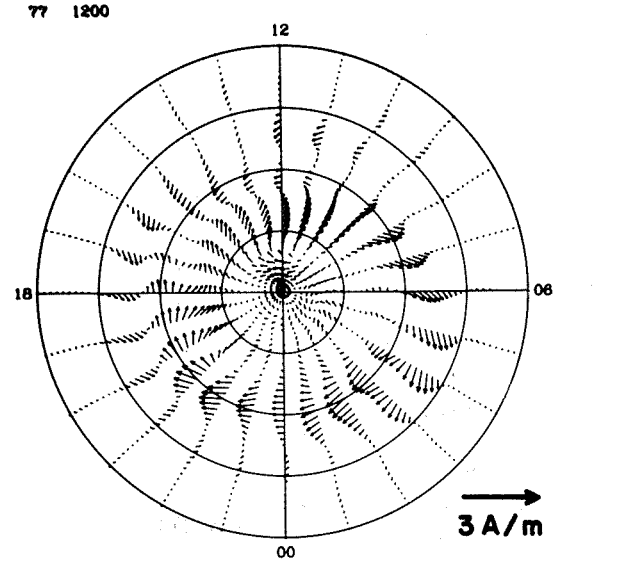

JOULE HEATING

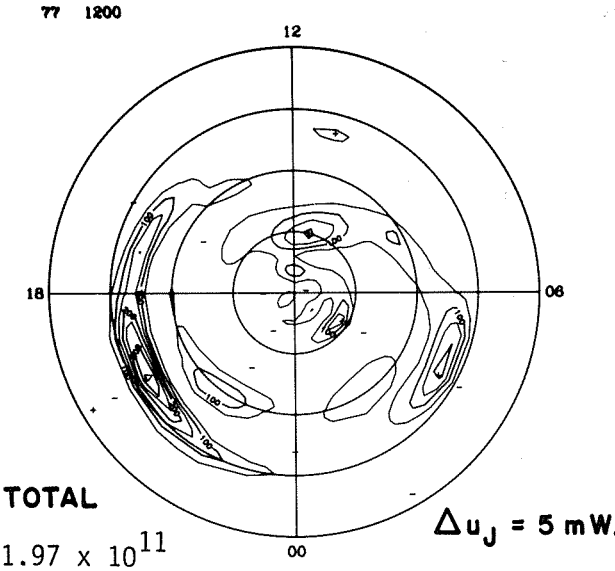

TOTAL

1.97×10^{11}

FIELD-ALIGNED CURRENT

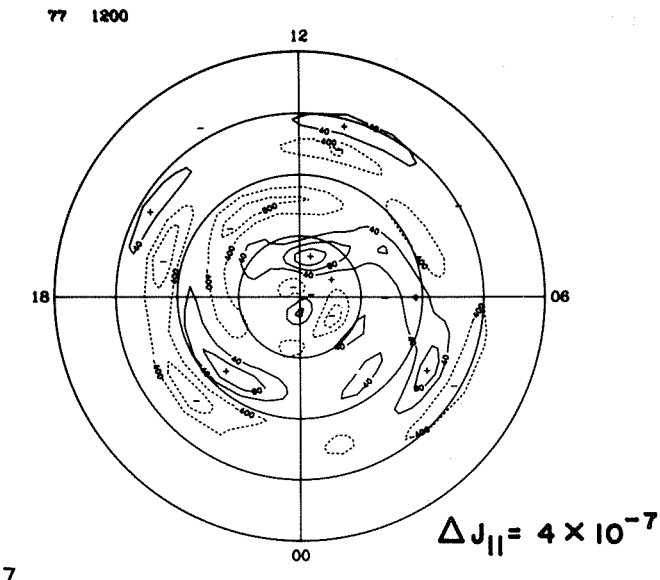

EQUIVALENT CURRENT

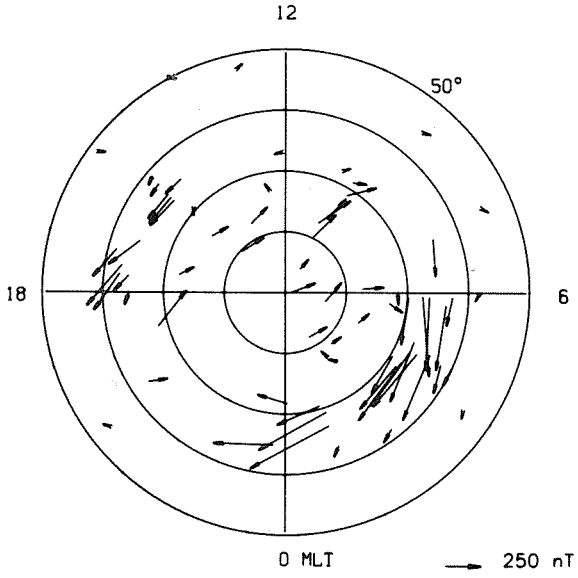

EQUIVALENT CURRENT SYSTEM

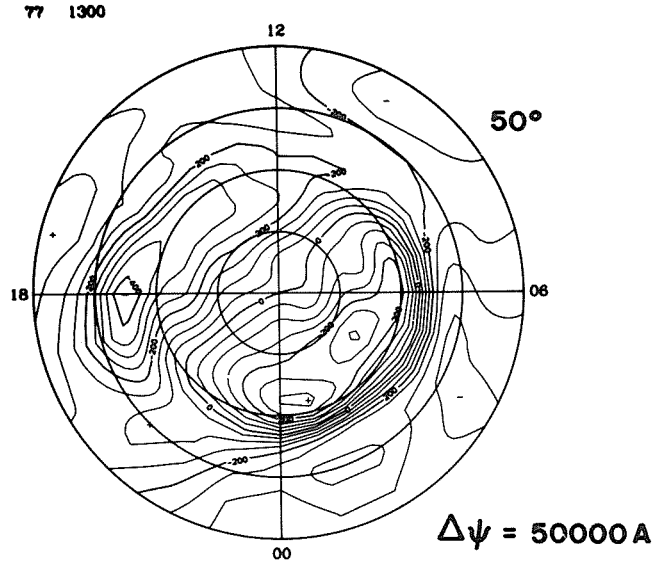

ELECTRIC POTENTIAL

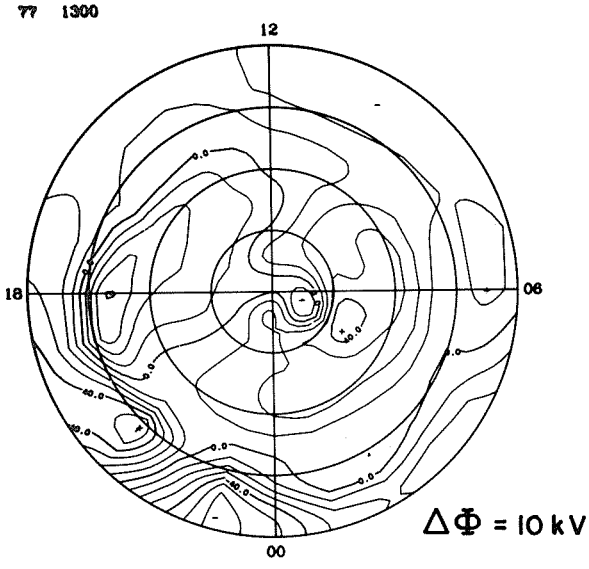

IONOSPHERIC CURRENT

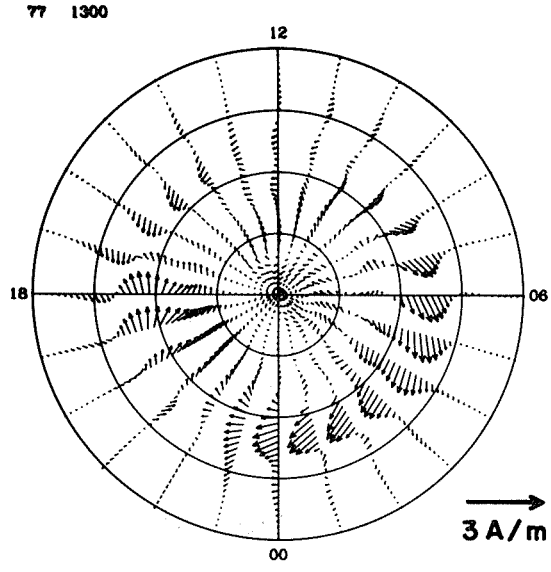

JOULE HEATING

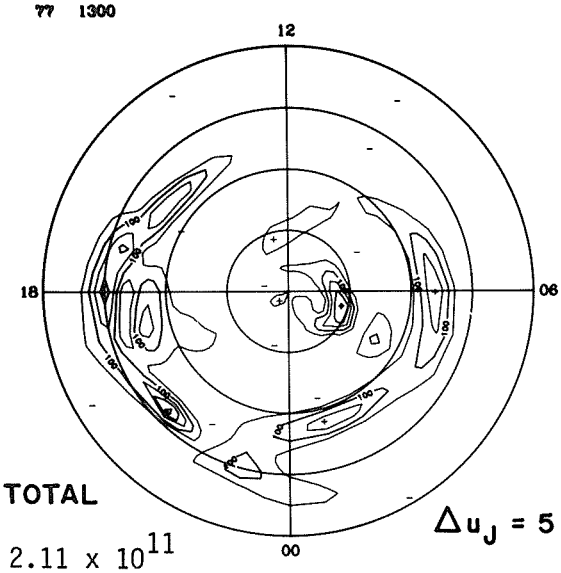

TOTAL

2.11×10^{11}

FIELD-ALIGNED CURRENT

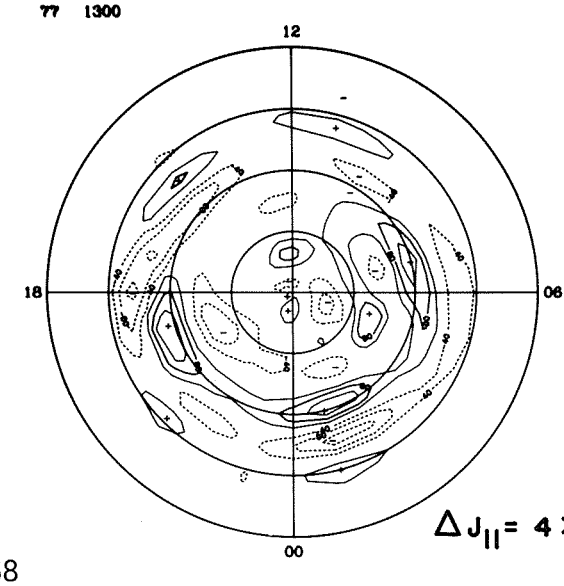

EQUIVALENT CURRENT

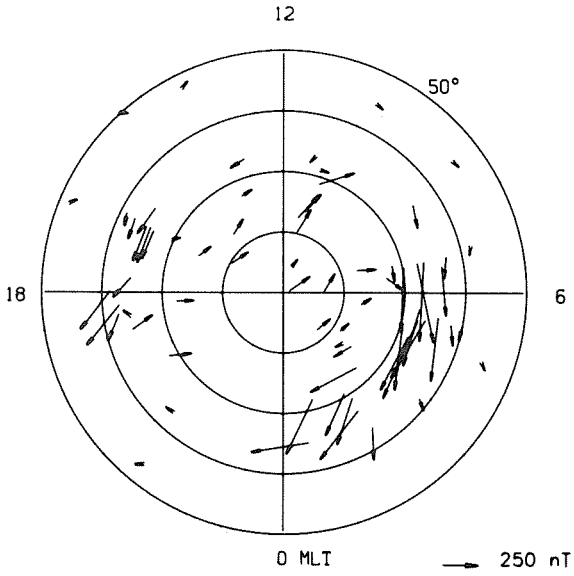

EQUIVALENT CURRENT SYSTEM

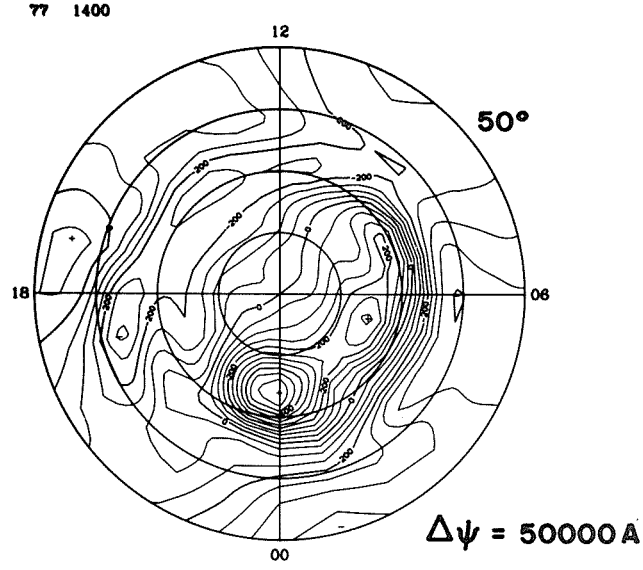

ELECTRIC POTENTIAL

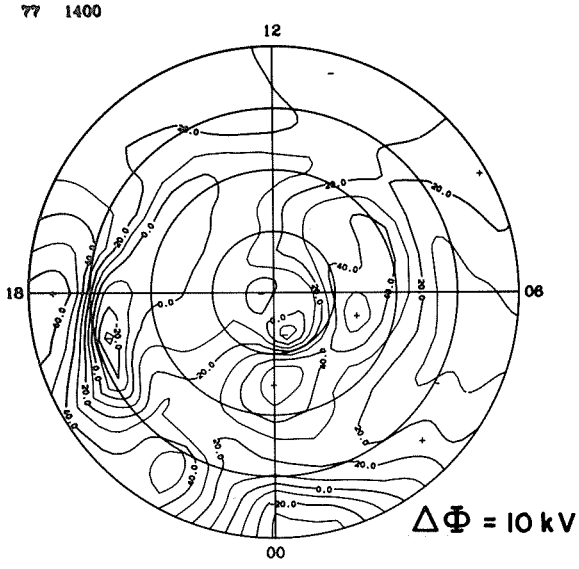

IONOSPHERIC CURRENT

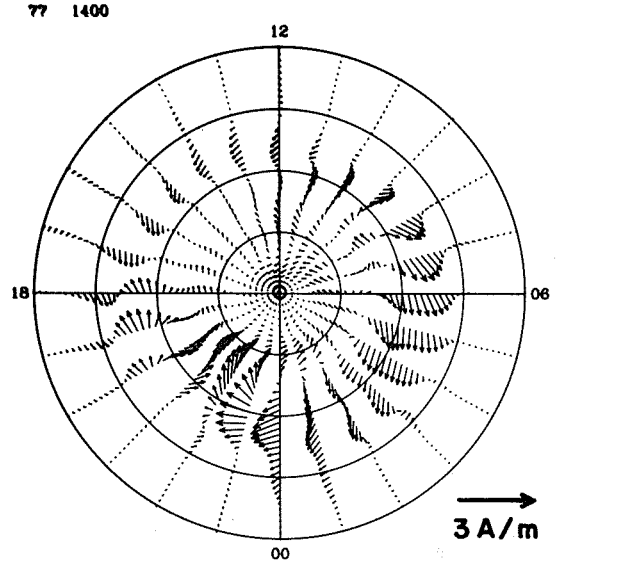

JOULE HEATING

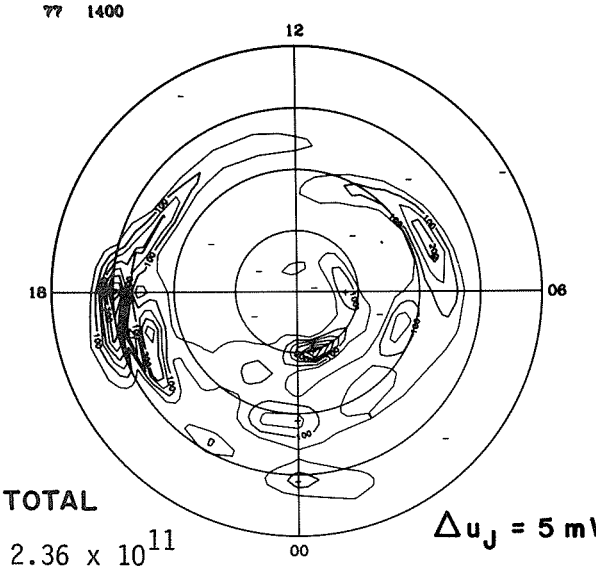

TOTAL

2.36×10^{11}

FIELD-ALIGNED CURRENT

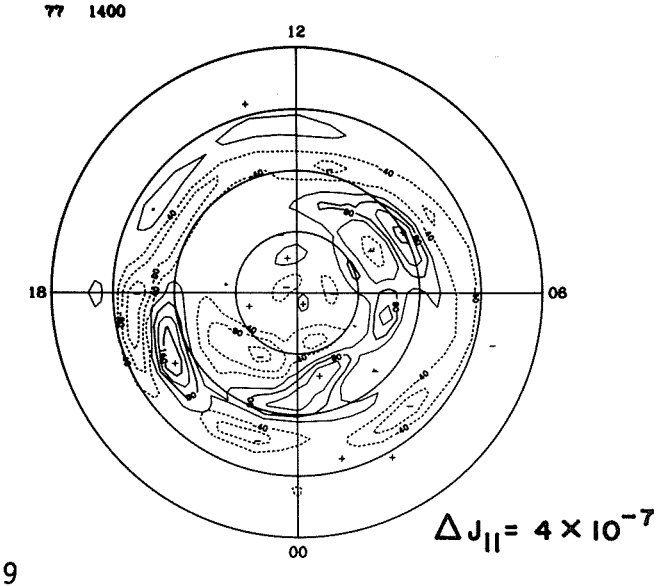

EQUIVALENT CURRENT

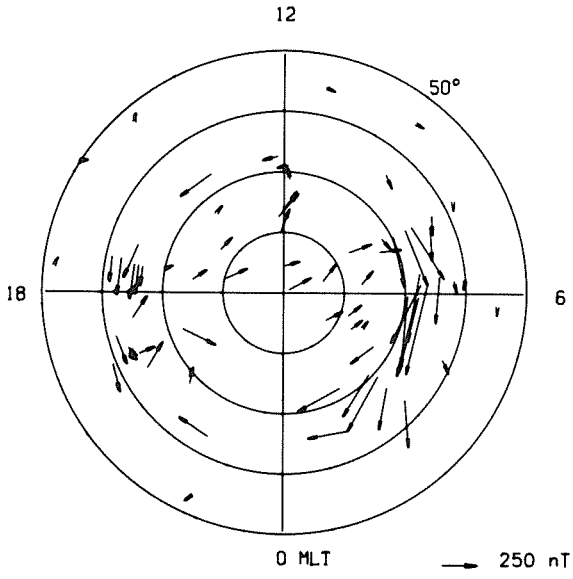

EQUIVALENT CURRENT SYSTEM

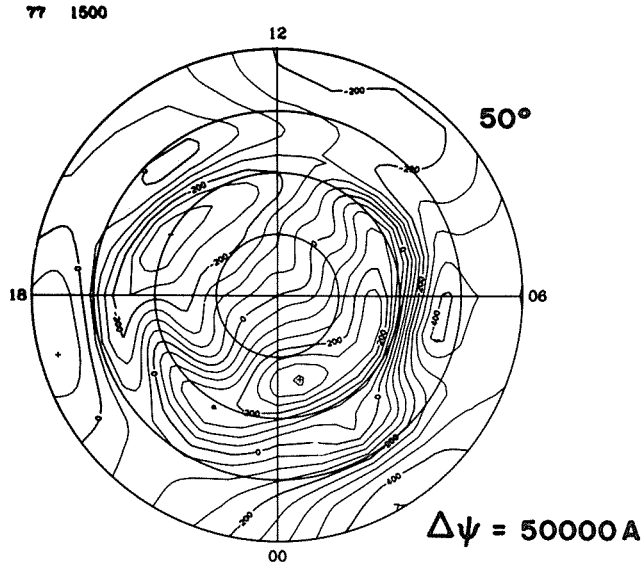

ELECTRIC POTENTIAL

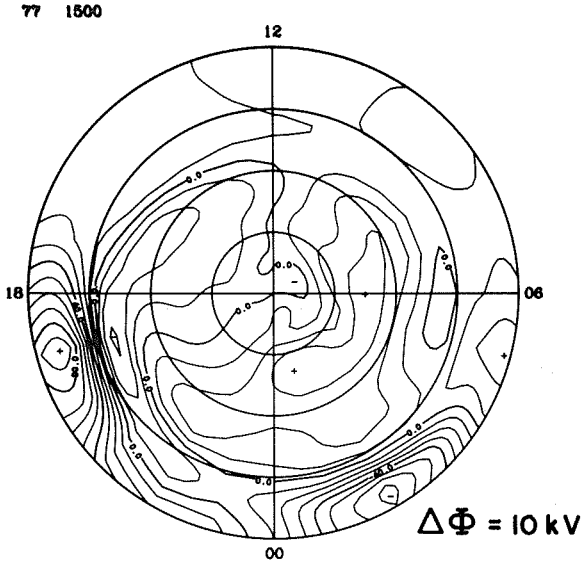

IONOSPHERIC CURRENT

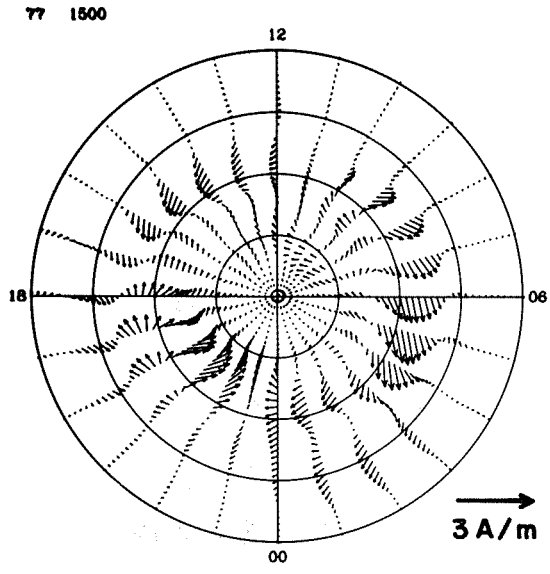

JOULE HEATING

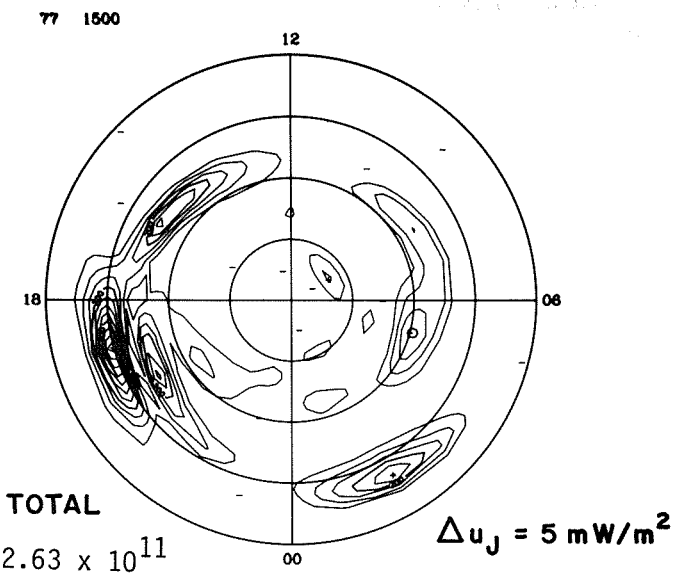

FIELD-ALIGNED CURRENT

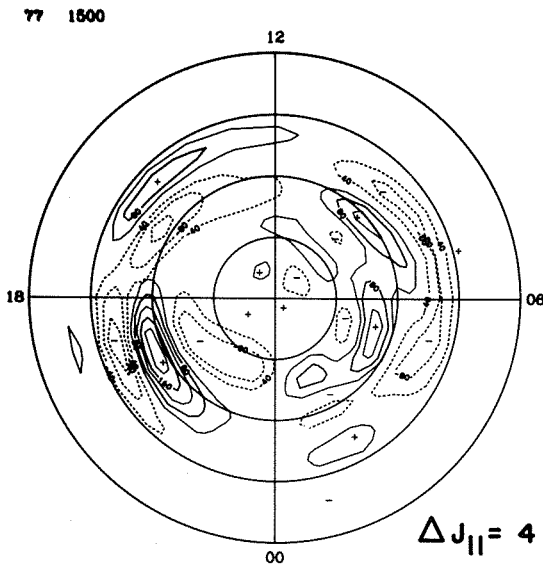

EQUIVALENT CURRENT

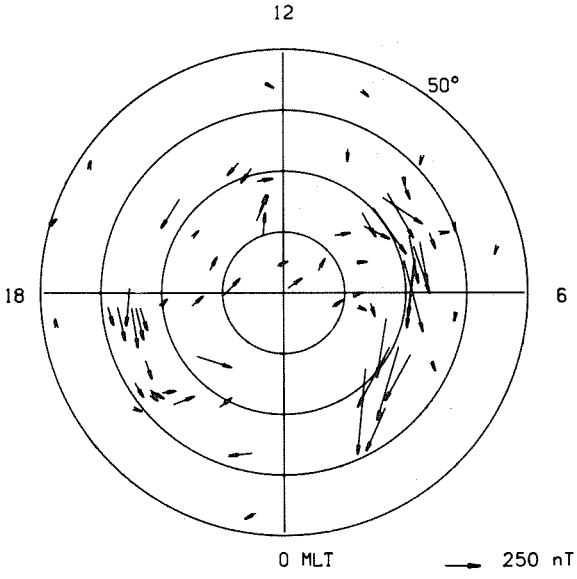

EQUIVALENT CURRENT SYSTEM

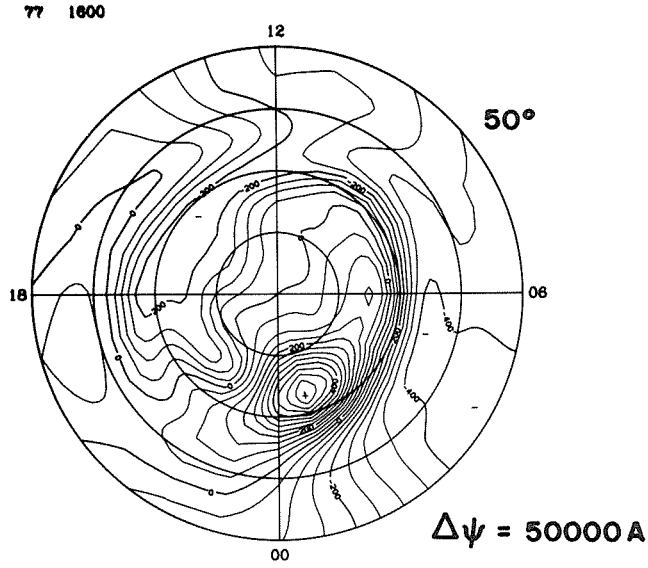

ELECTRIC POTENTIAL

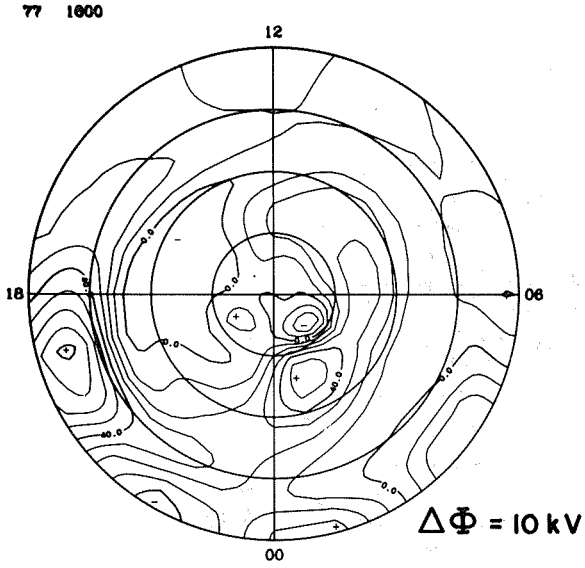

IONOSPHERIC CURRENT

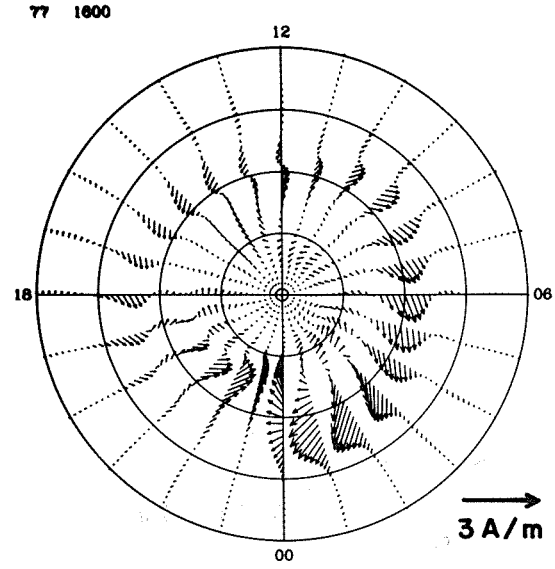

JOULE HEATING

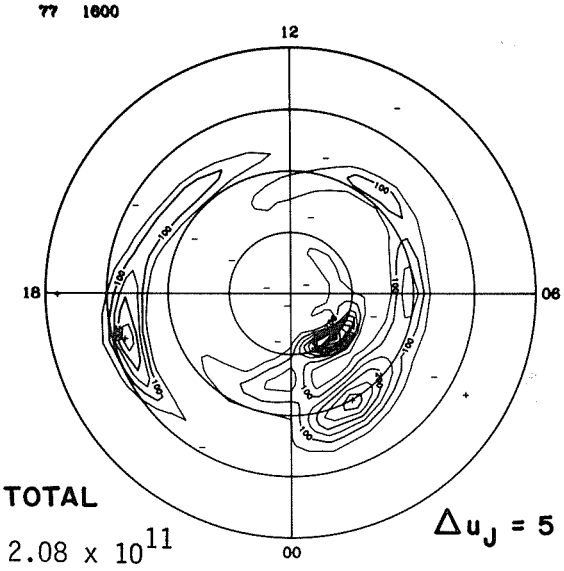

FIELD-ALIGNED CURRENT

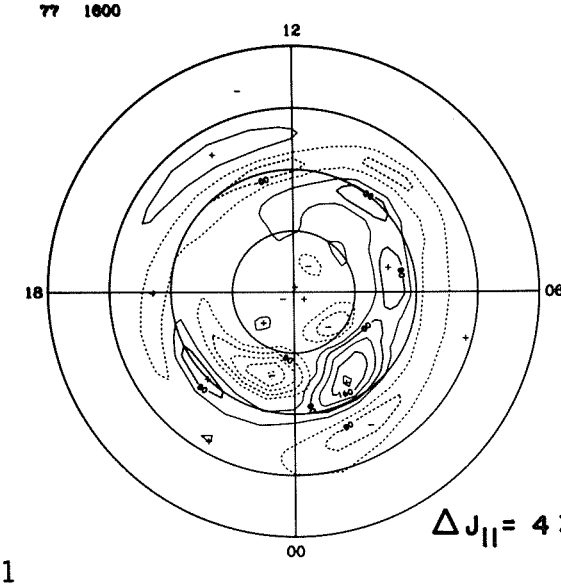

EQUIVALENT CURRENT

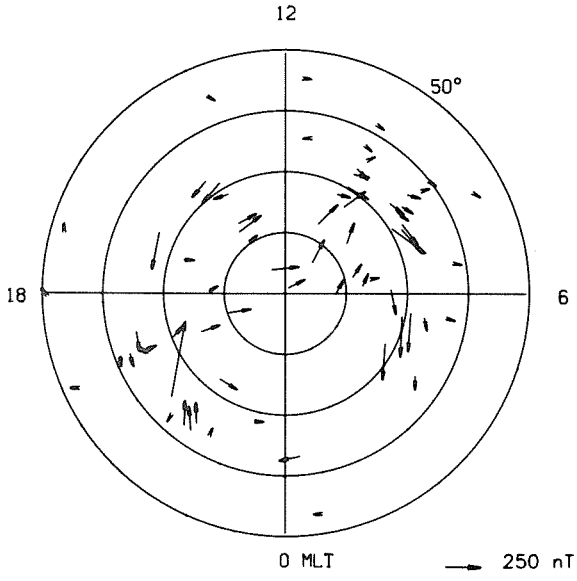

EQUIVALENT CURRENT SYSTEM

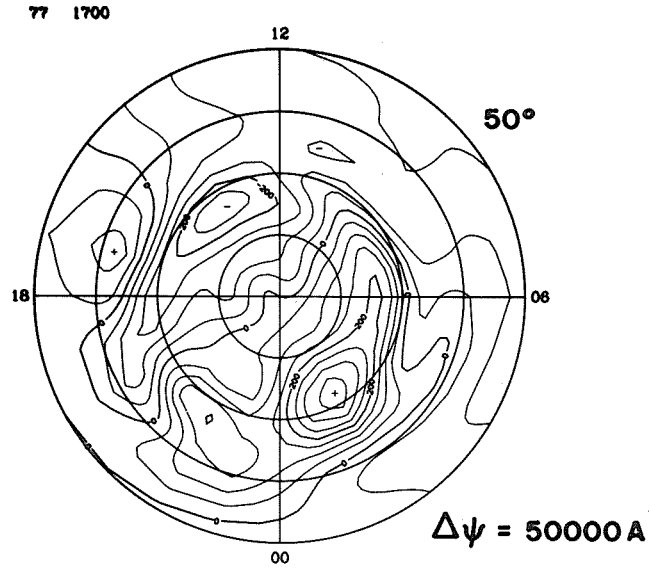

ELECTRIC POTENTIAL

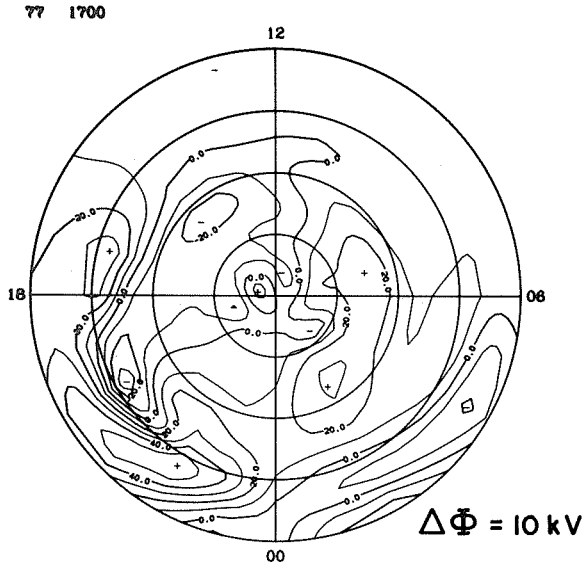

IONOSPHERIC CURRENT

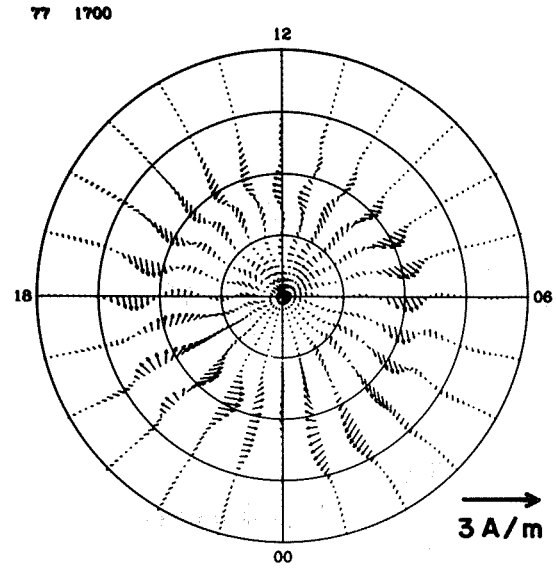

JOULE HEATING

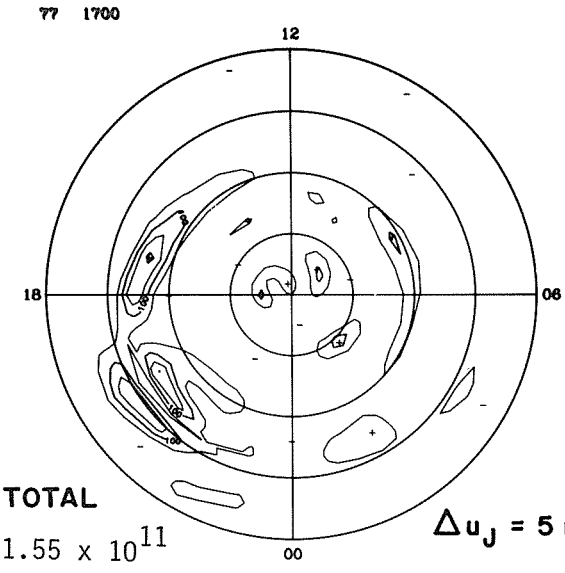

FIELD-ALIGNED CURRENT

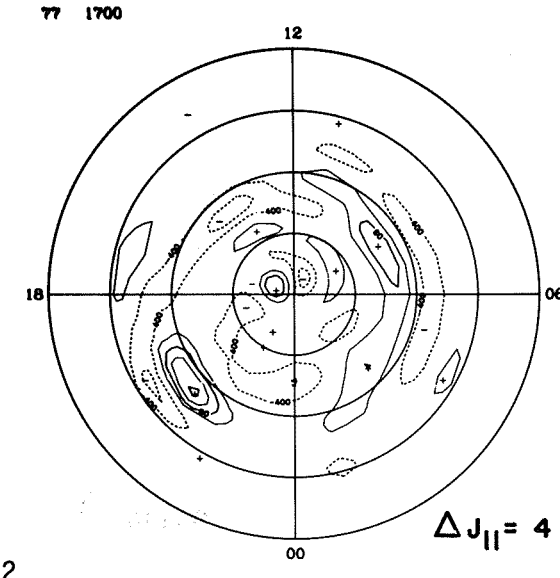

EQUIVALENT CURRENT

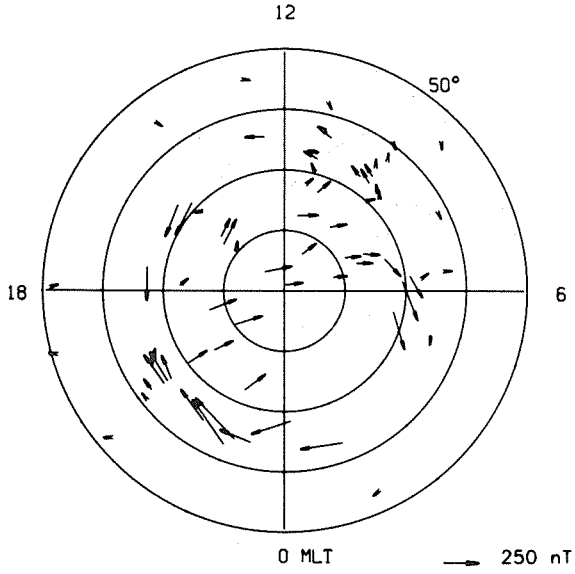

EQUIVALENT CURRENT SYSTEM

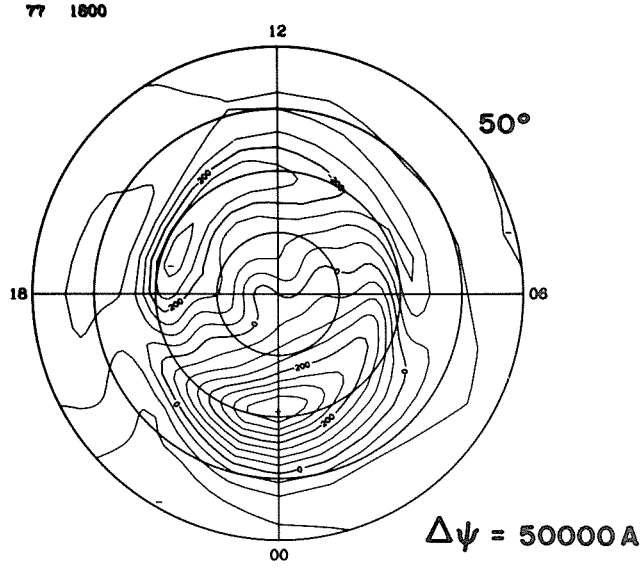

ELECTRIC POTENTIAL

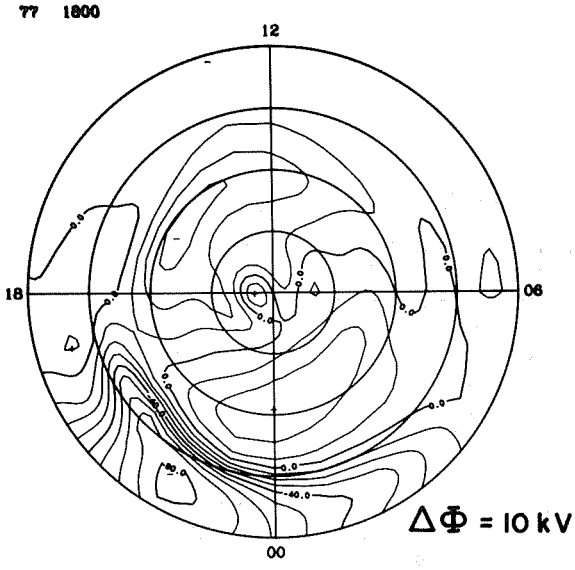

IONOSPHERIC CURRENT

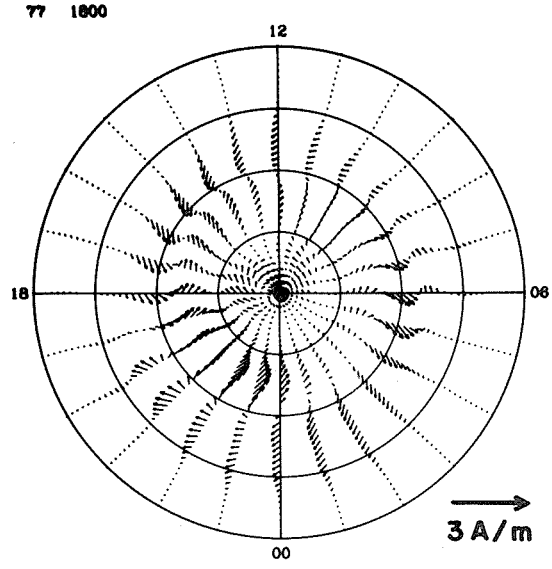

JOULE HEATING

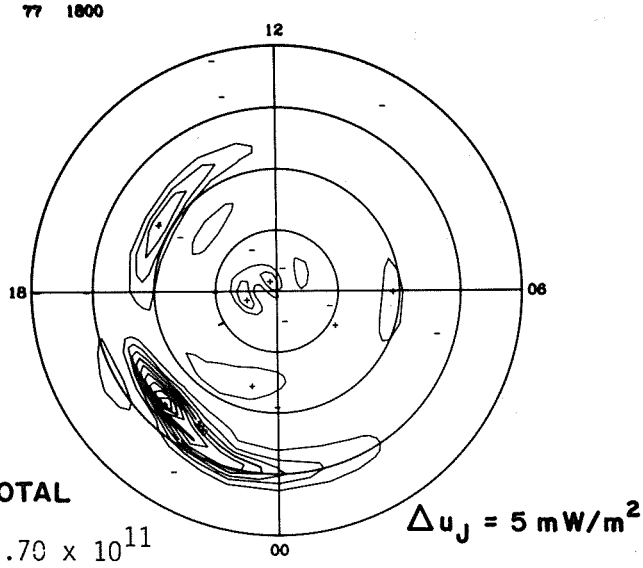

TOTAL

1.70×10^{11}

FIELD-ALIGNED CURRENT

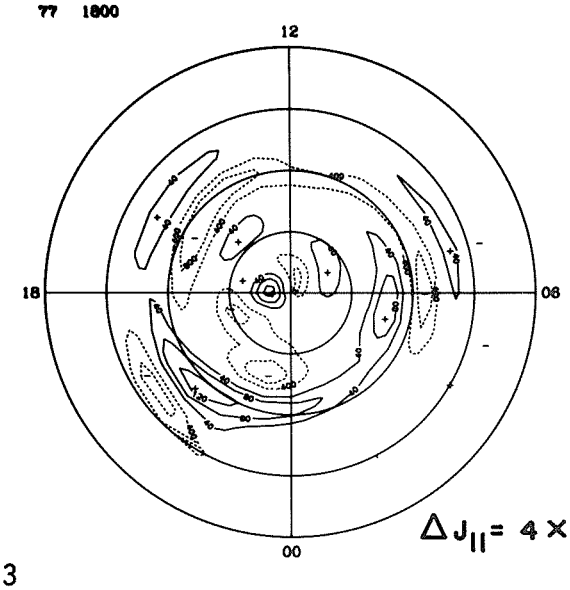

EQUIVALENT CURRENT

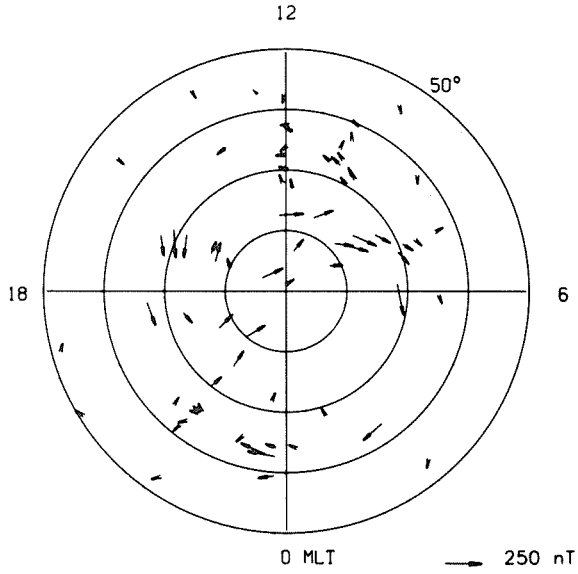

EQUIVALENT CURRENT SYSTEM

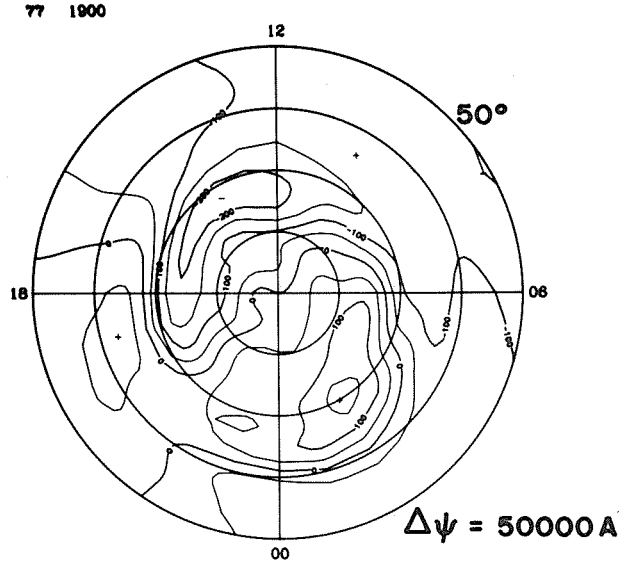

ELECTRIC POTENTIAL

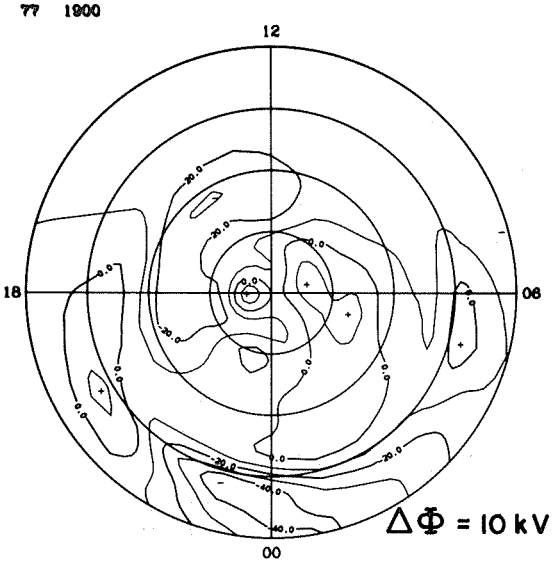

IONOSPHERIC CURRENT

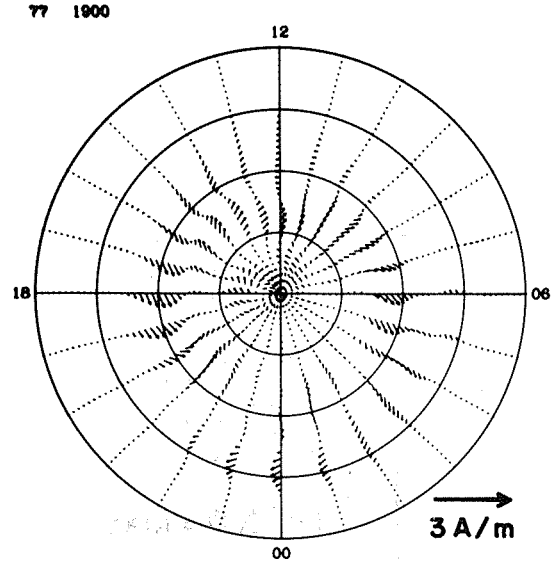

JOULE HEATING

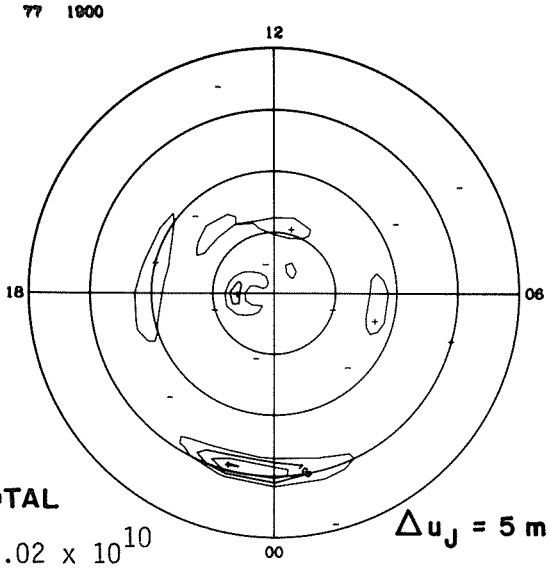

TOTAL

8.02×10^{10}

FIELD-ALIGNED CURRENT

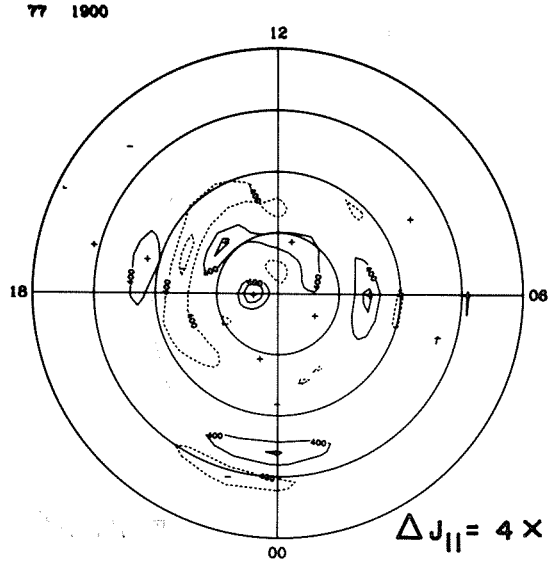

EQUIVALENT CURRENT

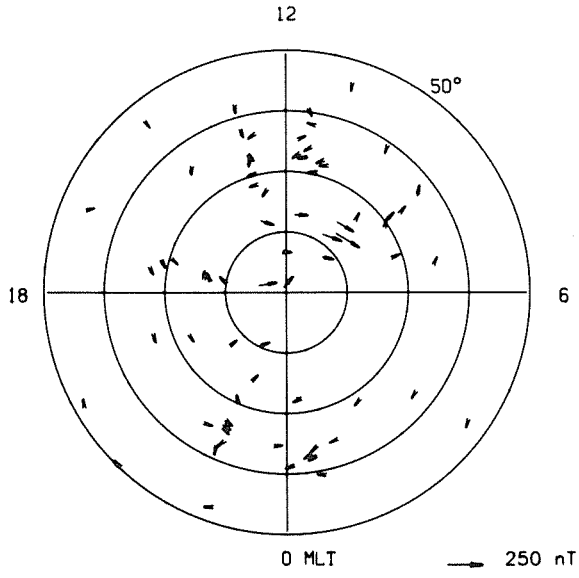

EQUIVALENT CURRENT SYSTEM

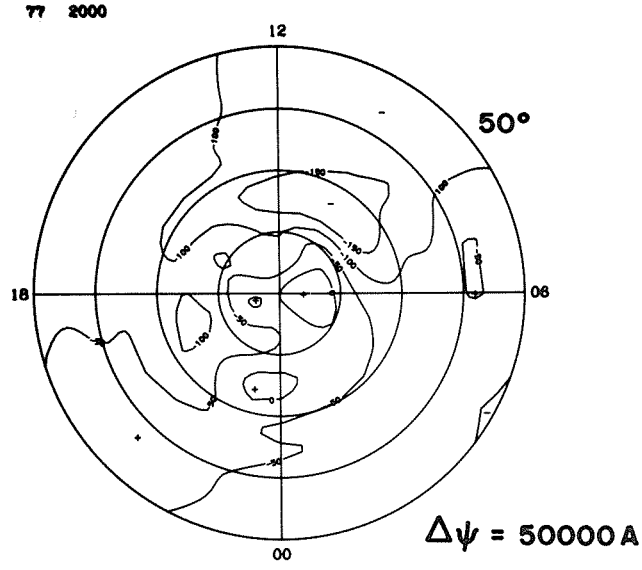

ELECTRIC POTENTIAL

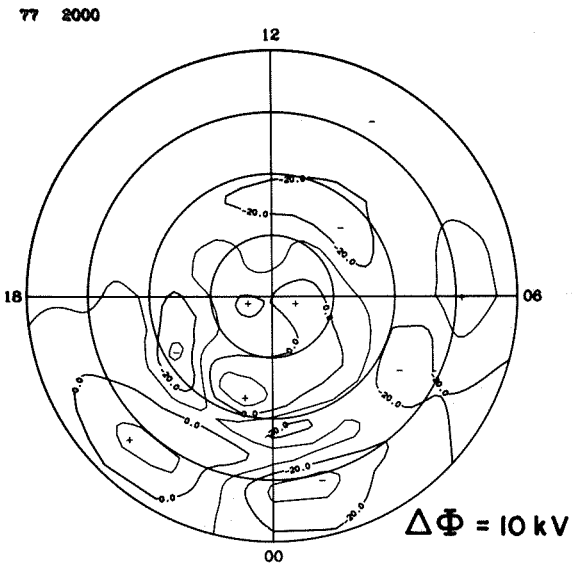

IONOSPHERIC CURRENT

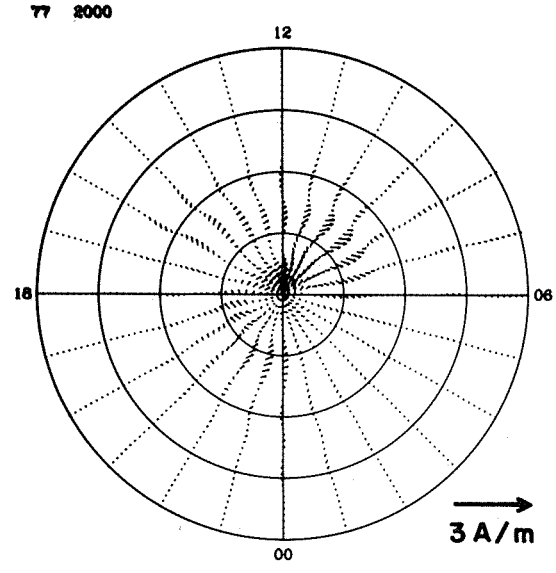

JOULE HEATING

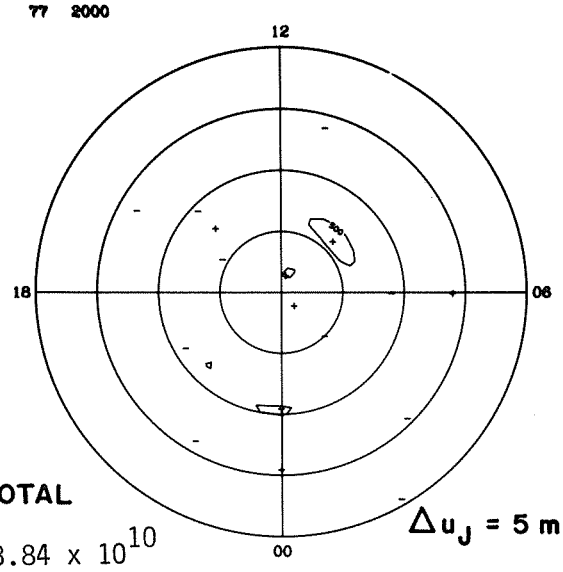

TOTAL

3.84×10^{10}

FIELD-ALIGNED CURRENT

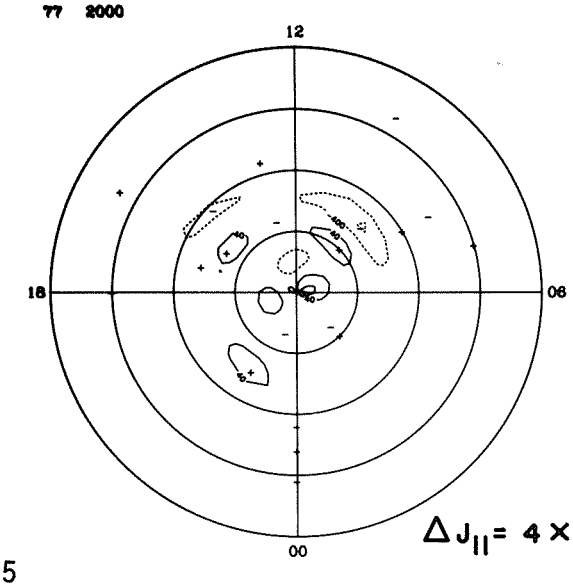

EQUIVALENT CURRENT

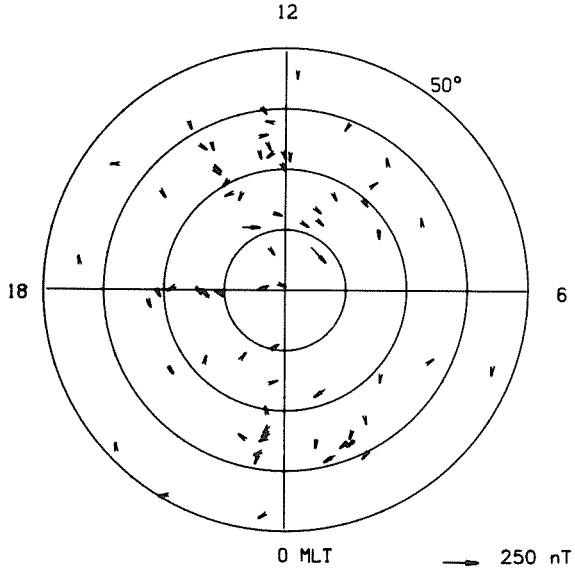

EQUIVALENT CURRENT SYSTEM

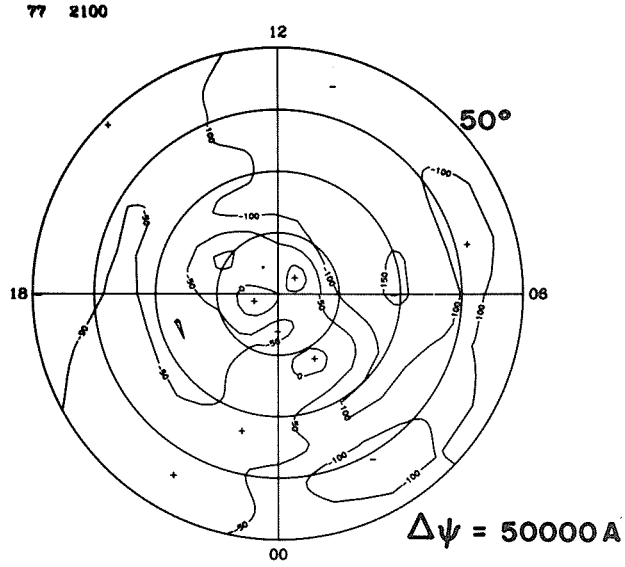

ELECTRIC POTENTIAL

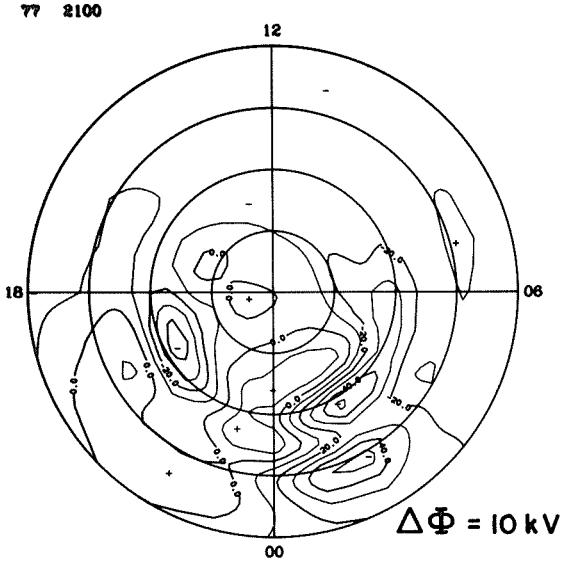

IONOSPHERIC CURRENT

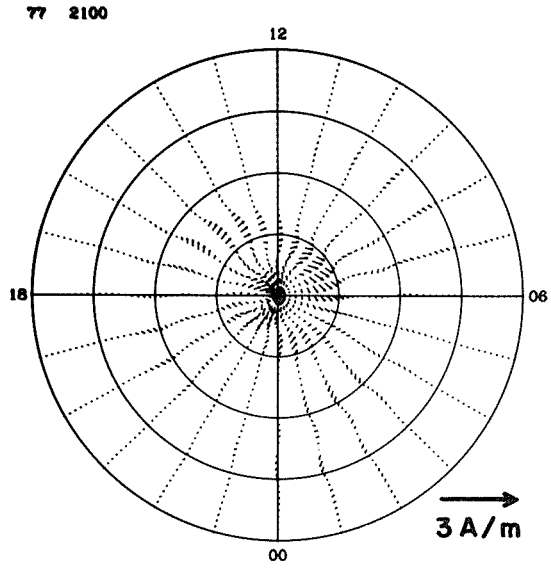

JOULE HEATING

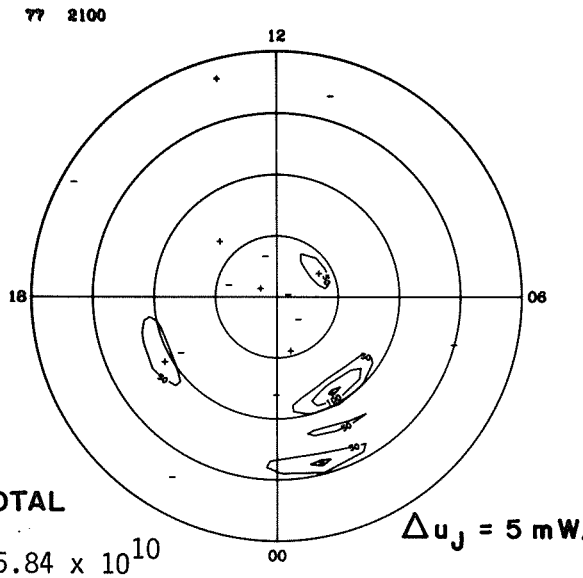

TOTAL

5.84×10^{10}

FIELD-ALIGNED CURRENT

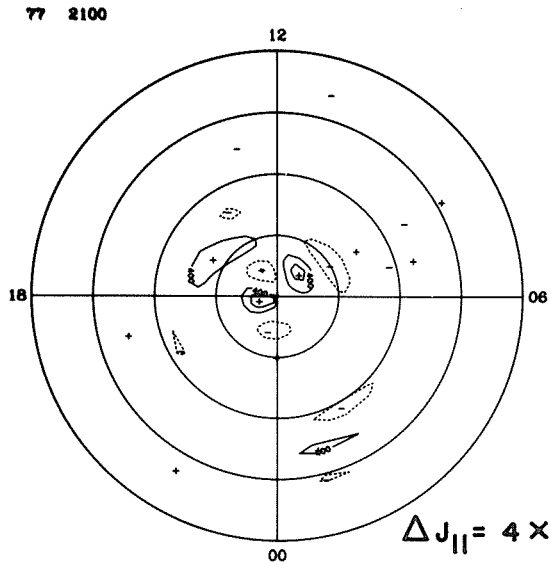

EQUIVALENT CURRENT

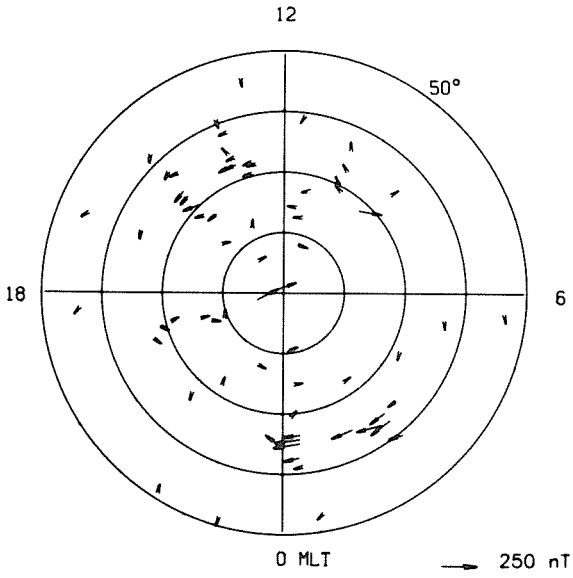

EQUIVALENT CURRENT SYSTEM

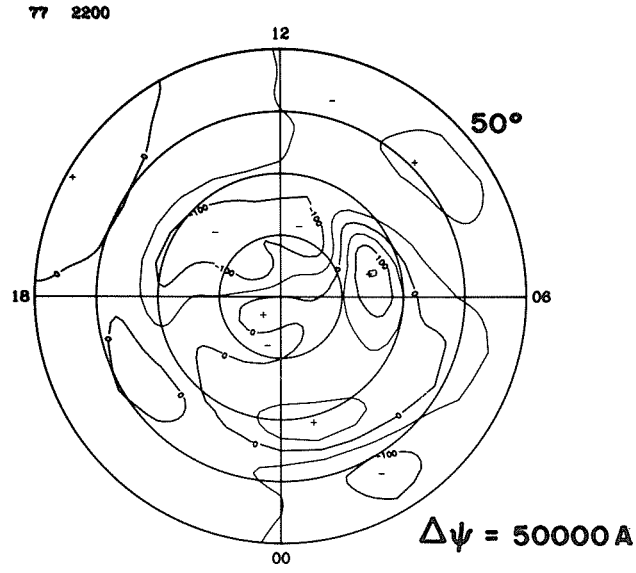

ELECTRIC POTENTIAL

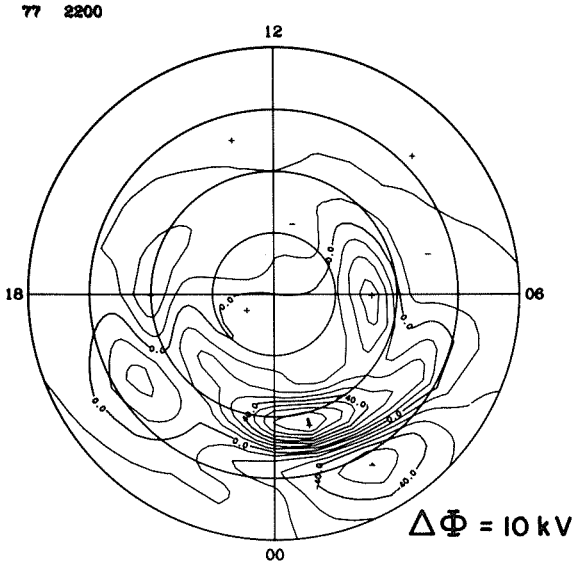

IONOSPHERIC CURRENT

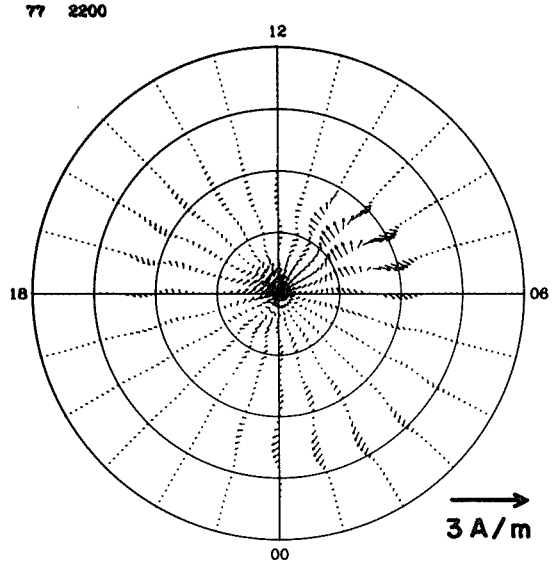

JOULE HEATING

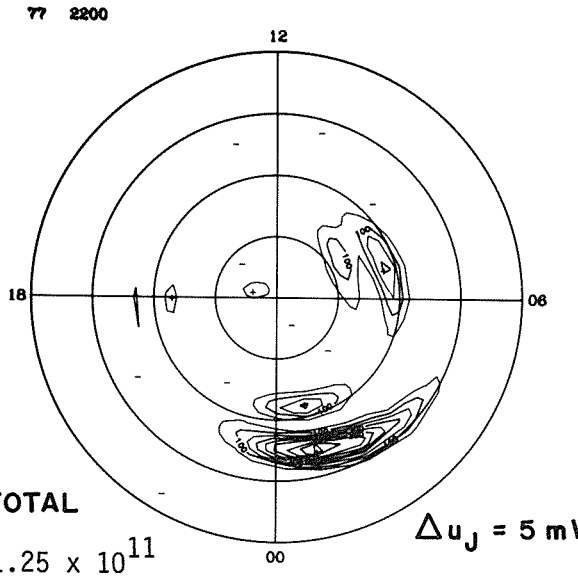

FIELD-ALIGNED CURRENT

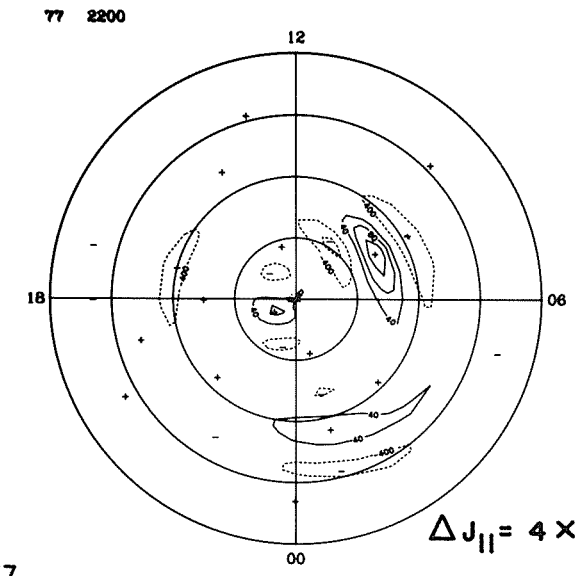

EQUIVALENT CURRENT

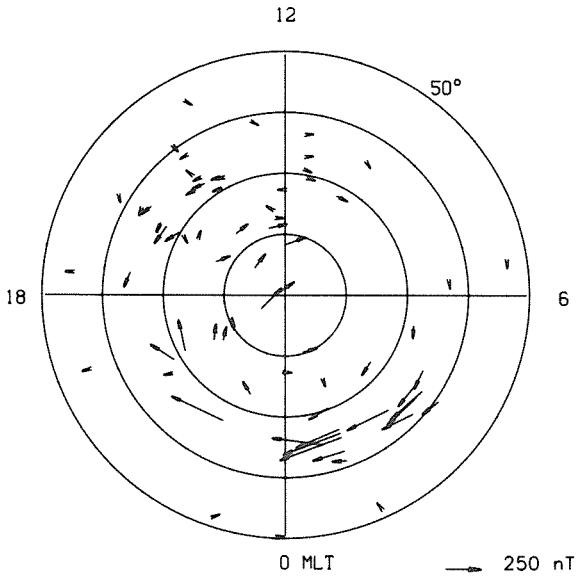

EQUIVALENT CURRENT SYSTEM

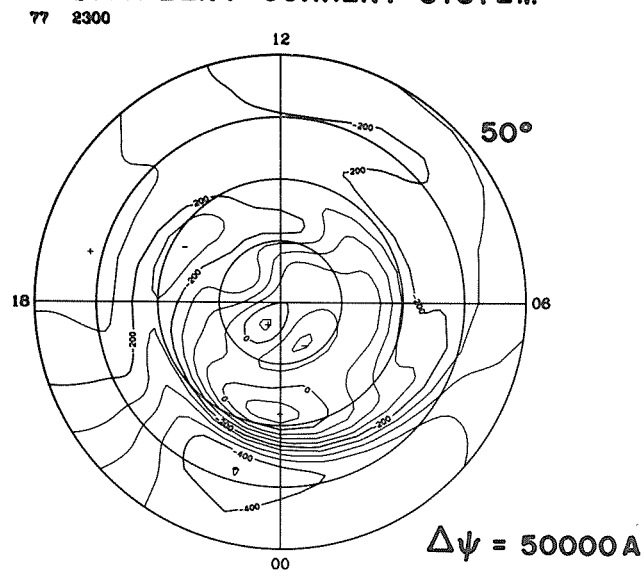

ELECTRIC POTENTIAL

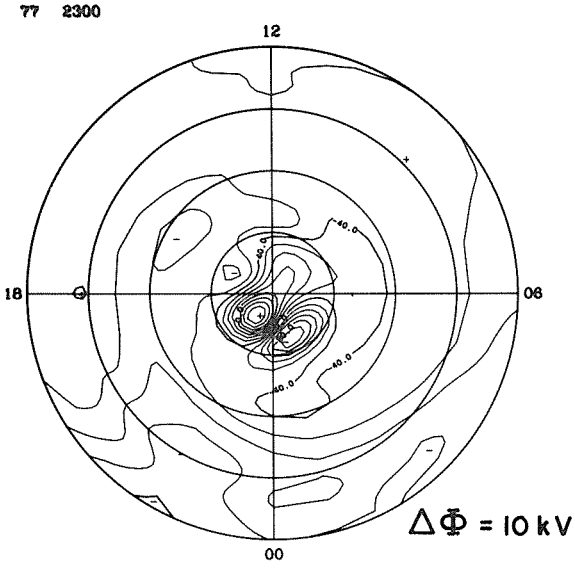

IONOSPHERIC CURRENT

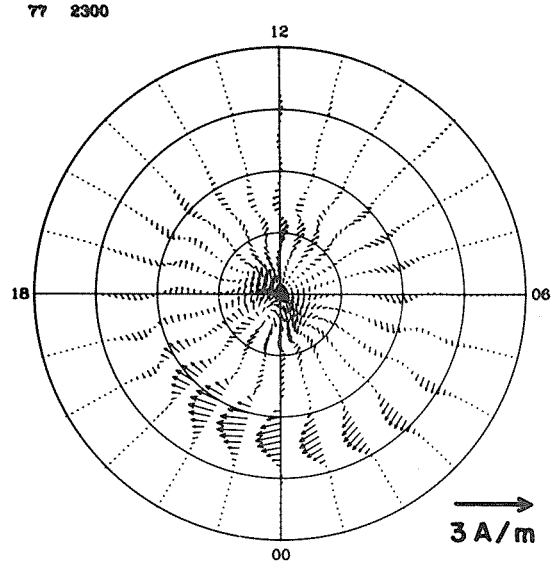

JOULE HEATING

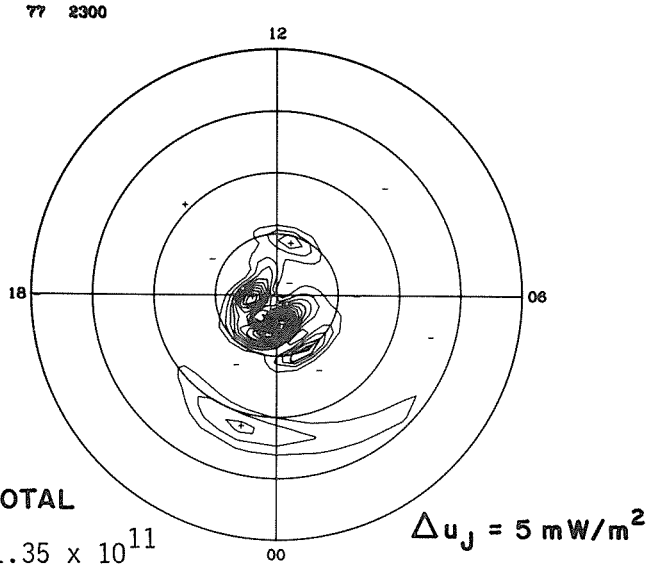

FIELD-ALIGNED CURRENT

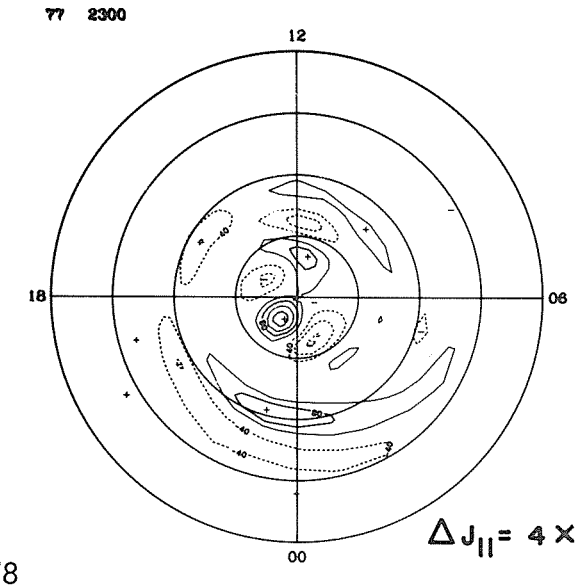

EQUIVALENT CURRENT

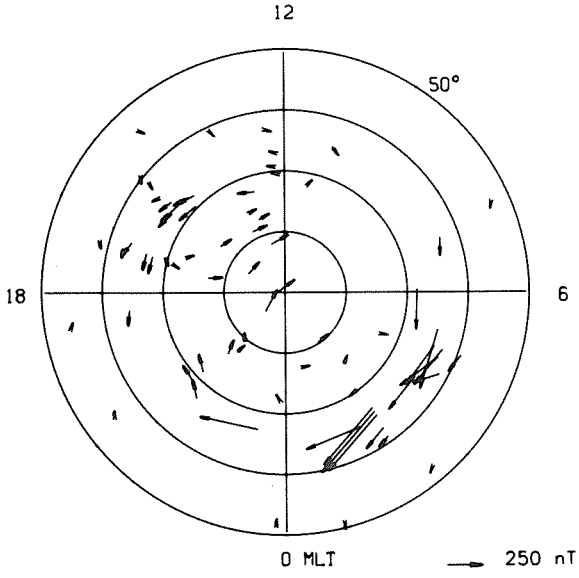

EQUIVALENT CURRENT SYSTEM

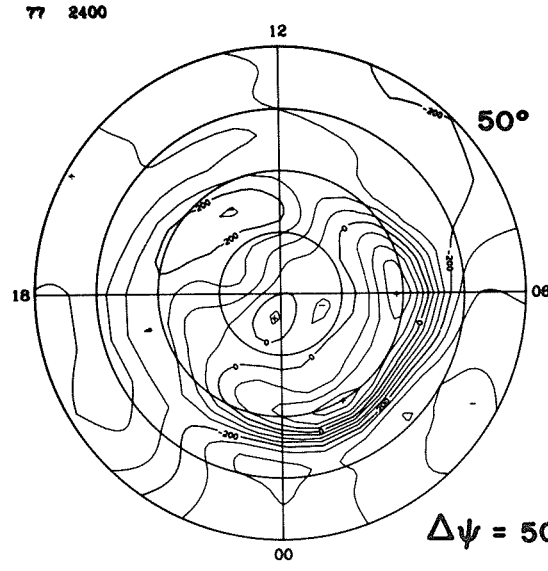

ELECTRIC POTENTIAL

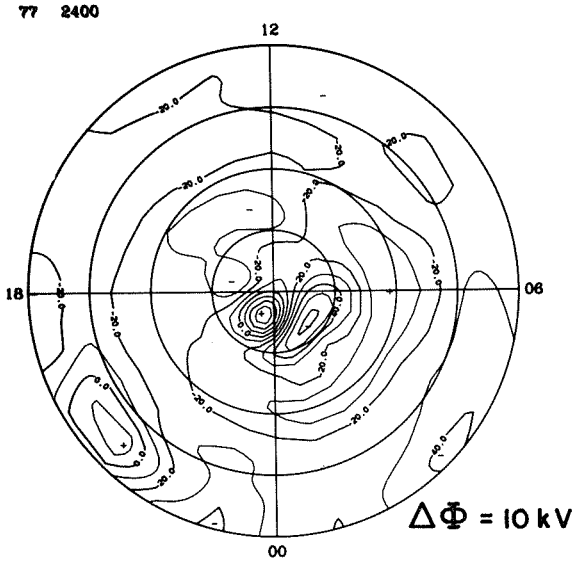

IONOSPHERIC CURRENT

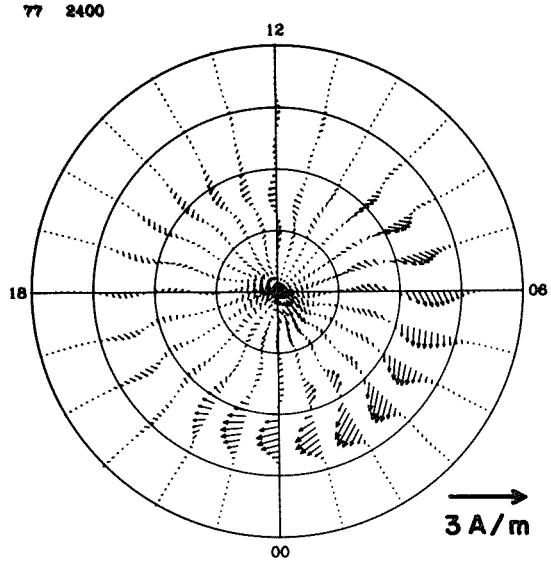

JOULE HEATING

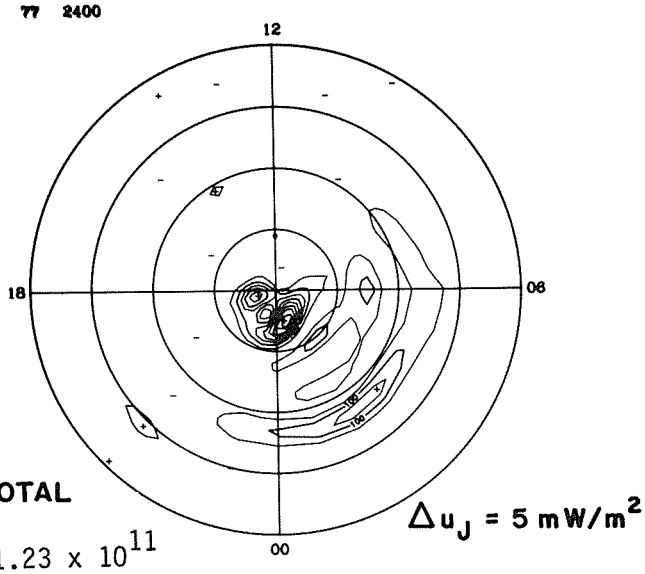

TOTAL

1.23×10^{11}

FIELD-ALIGNED CURRENT

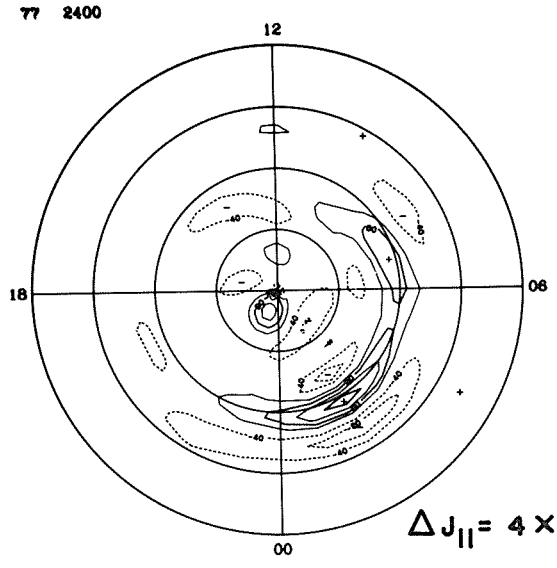

EQUIVALENT CURRENT

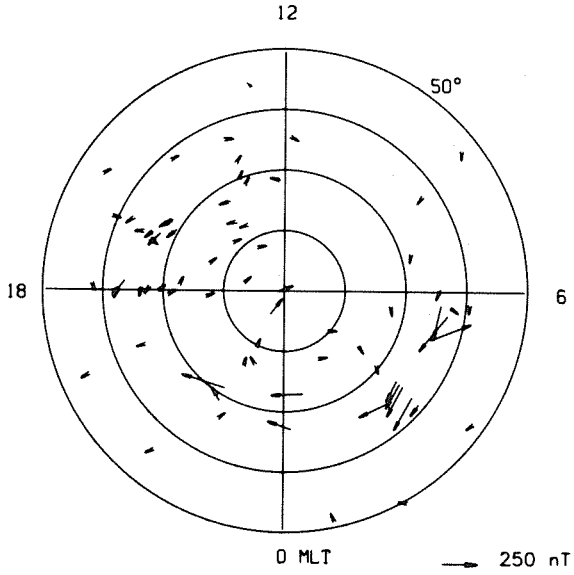

EQUIVALENT CURRENT SYSTEM

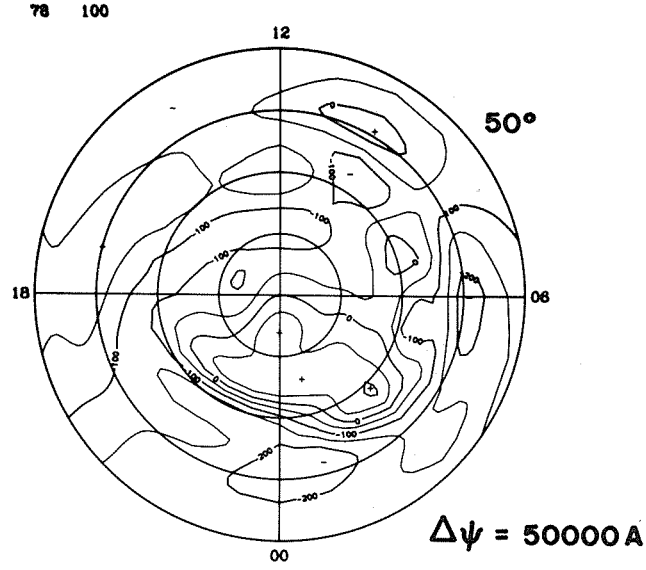

ELECTRIC POTENTIAL

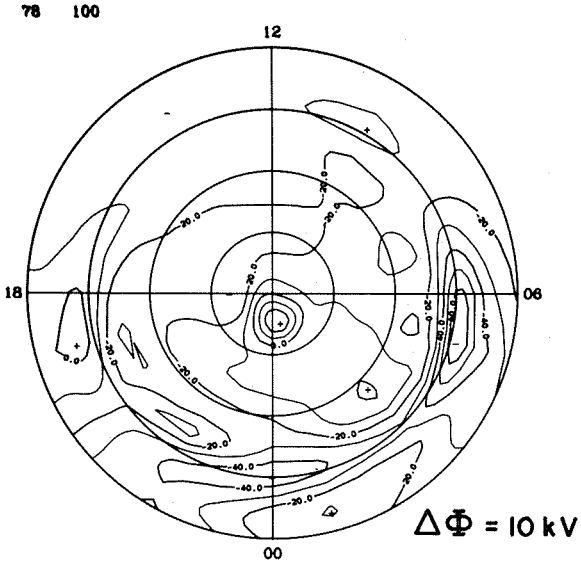

IONOSPHERIC CURRENT

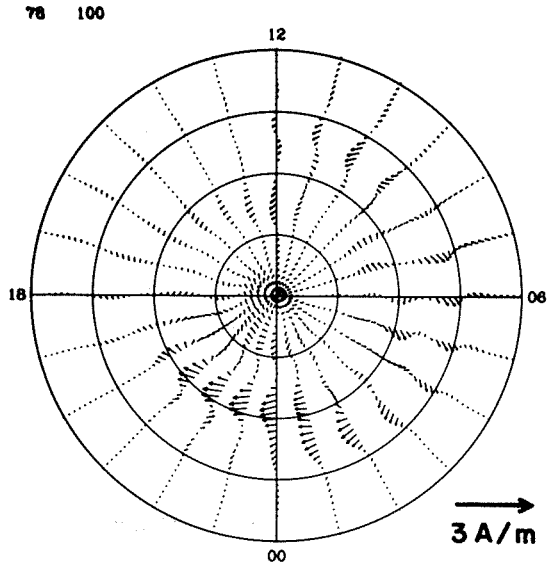

JOULE HEATING

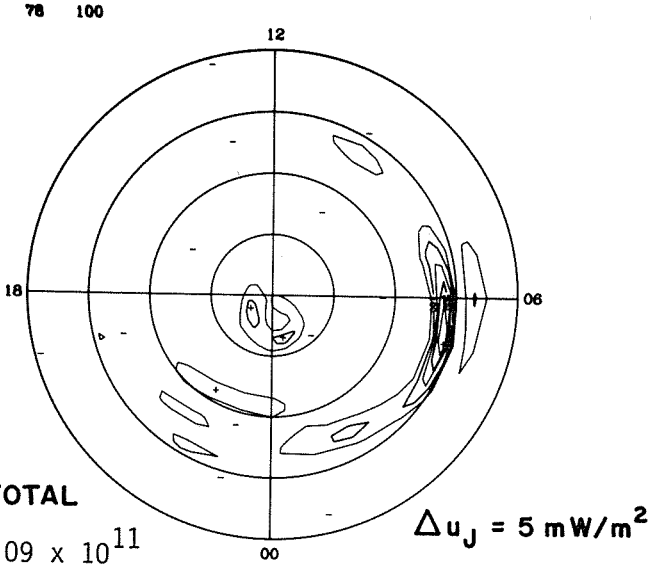

TOTAL

1.09×10^{11}

FIELD-ALIGNED CURRENT

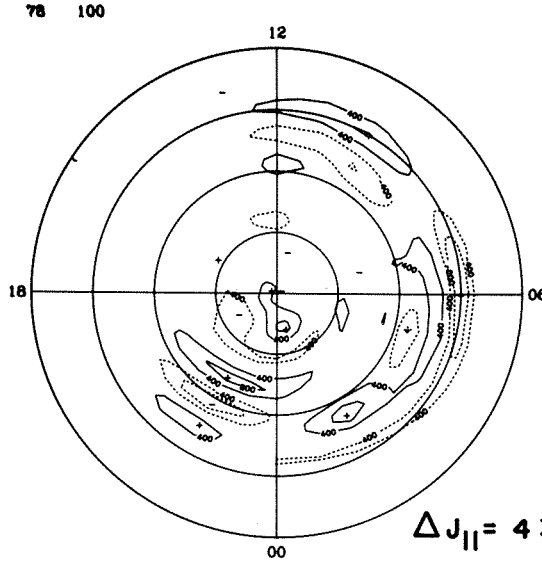

EQUIVALENT CURRENT

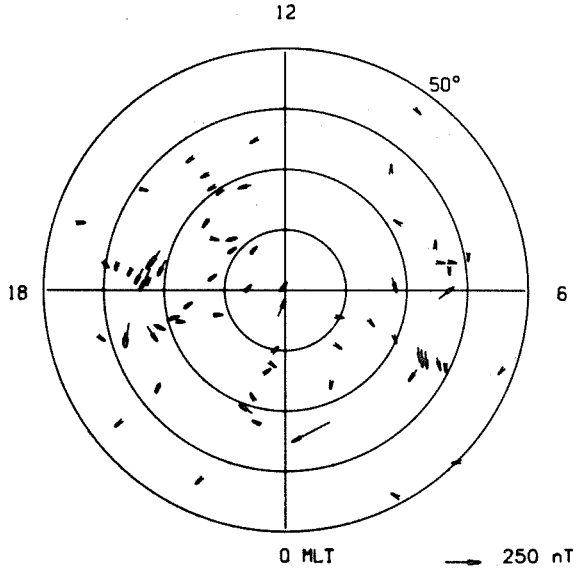

EQUIVALENT CURRENT SYSTEM

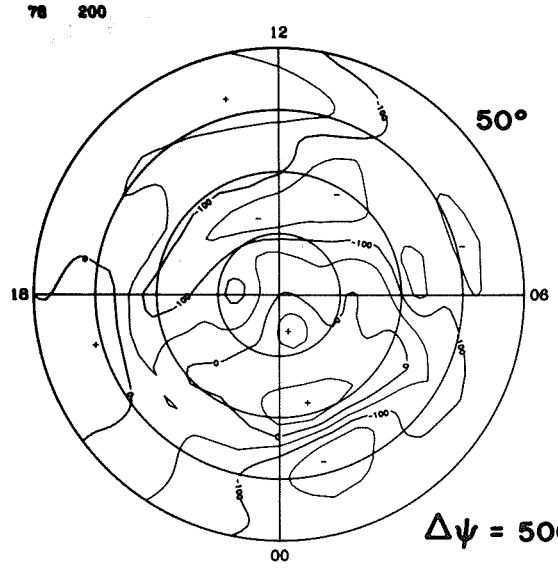

ELECTRIC POTENTIAL

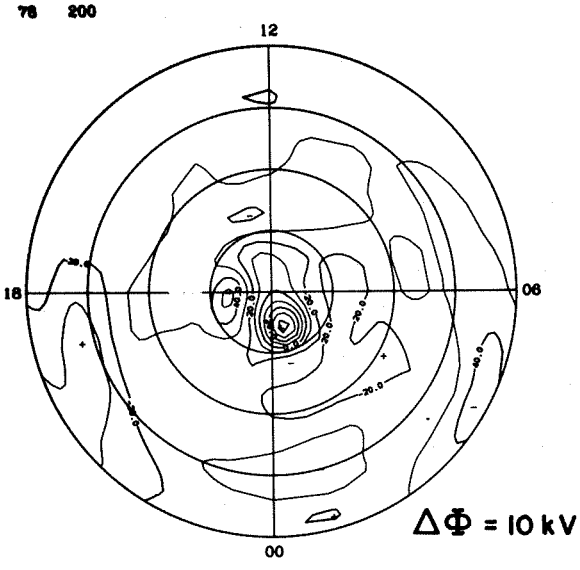

IONOSPHERIC CURRENT

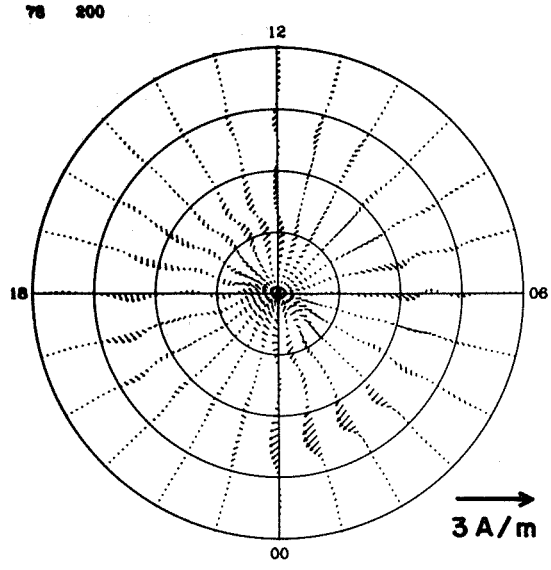

JOULE HEATING

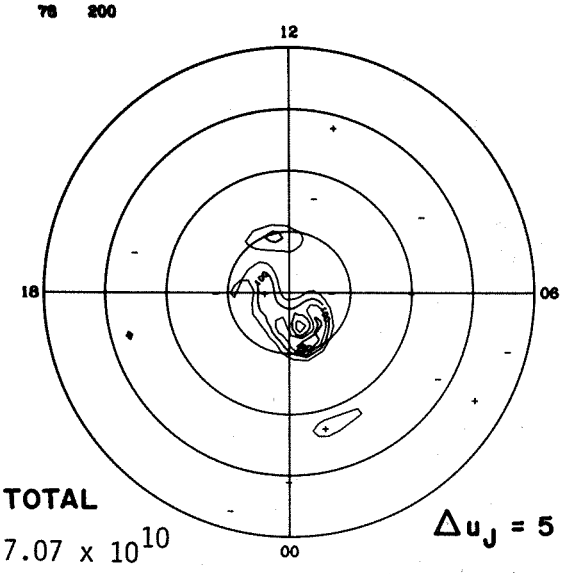

TOTAL

7.07×10^{10}

FIELD-ALIGNED CURRENT

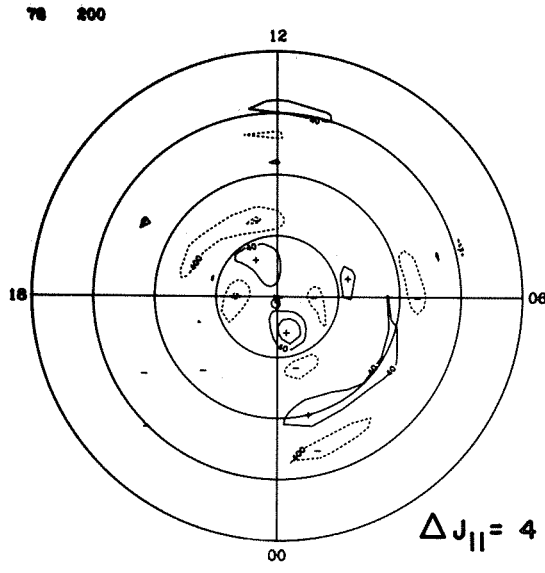

EQUIVALENT CURRENT

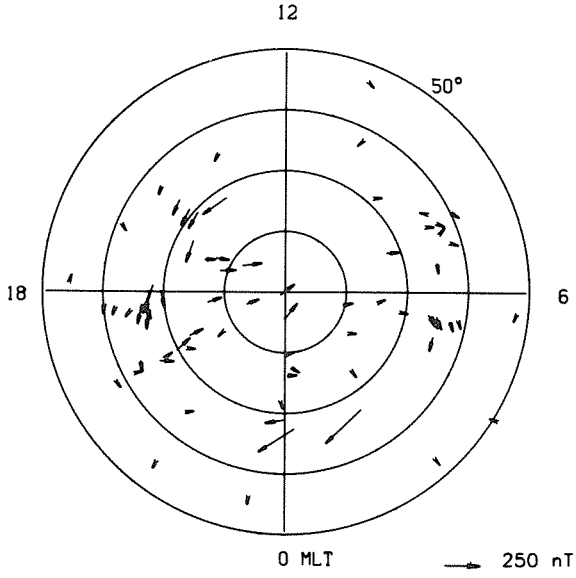

EQUIVALENT CURRENT SYSTEM

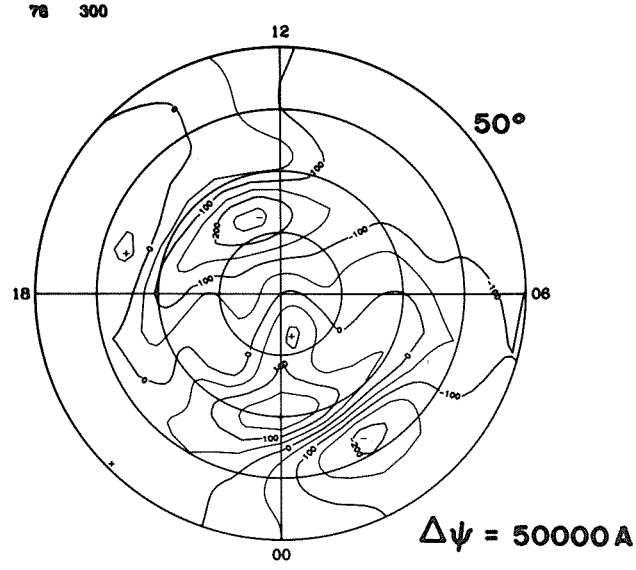

ELECTRIC POTENTIAL

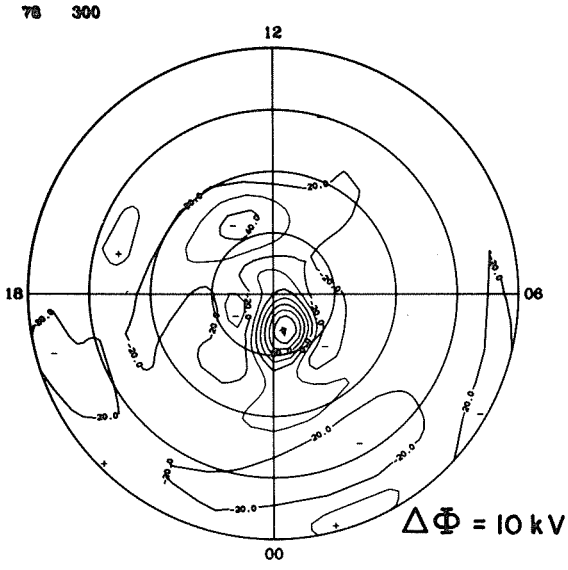

IONOSPHERIC CURRENT

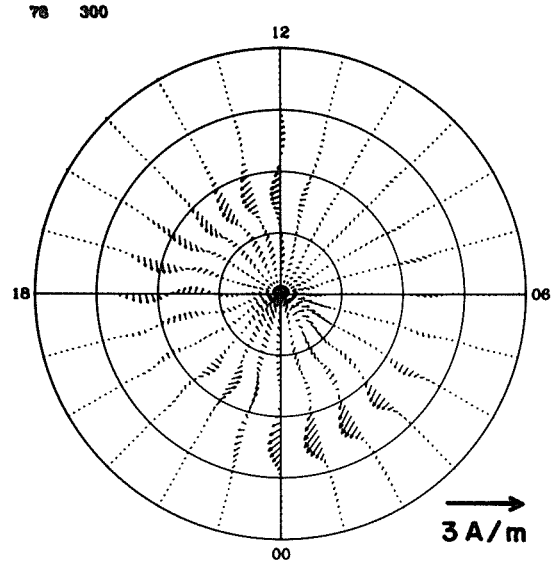

JOULE HEATING

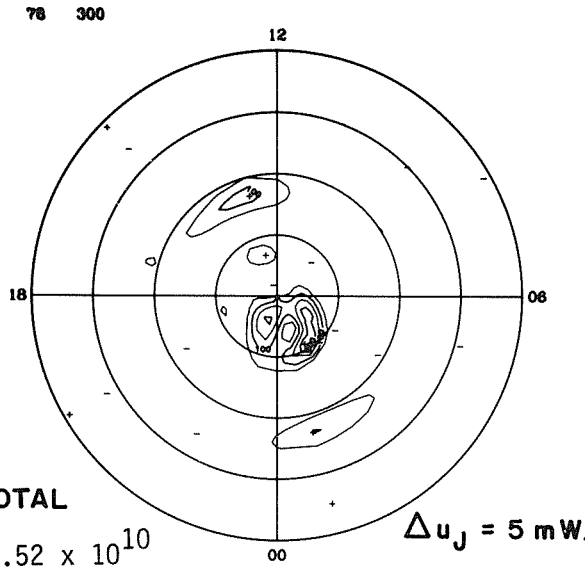

TOTAL

7.52×10^{10}

FIELD-ALIGNED CURRENT

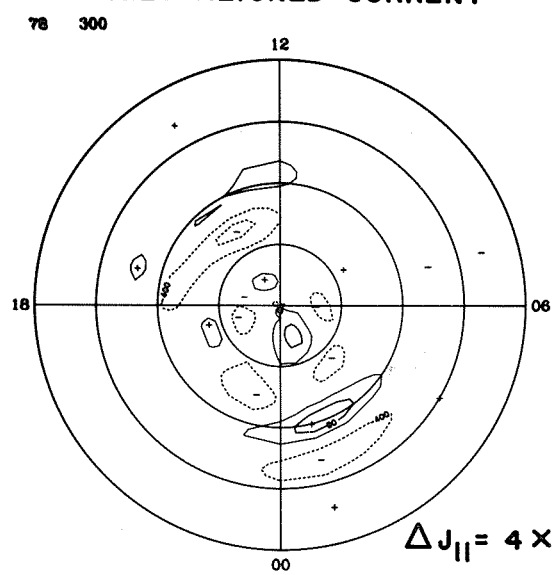

EQUIVALENT CURRENT

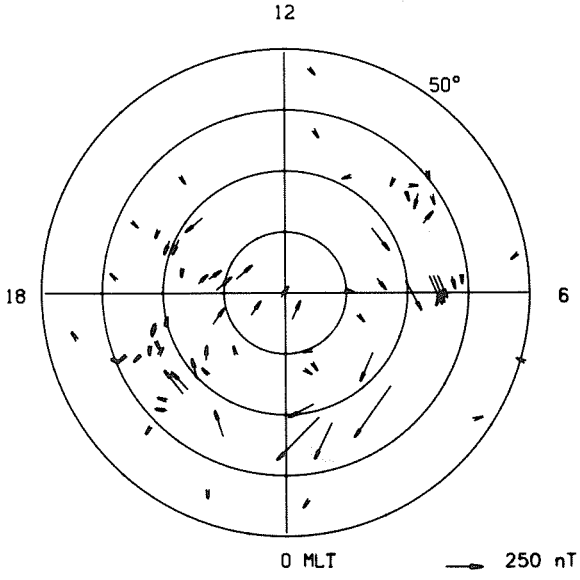

EQUIVALENT CURRENT SYSTEM

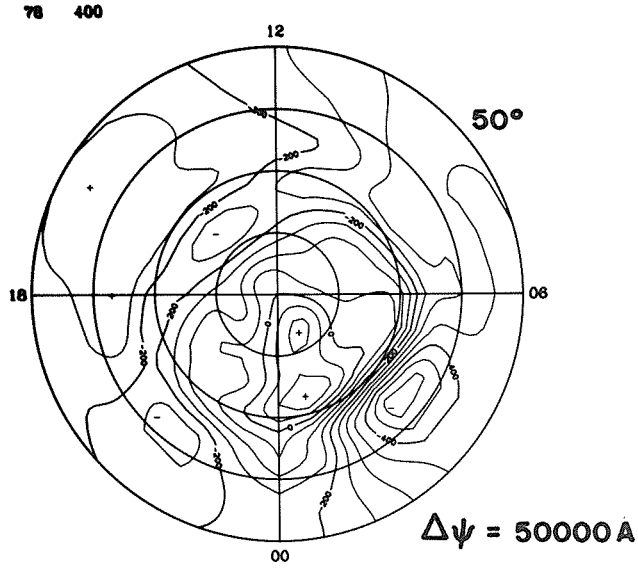

ELECTRIC POTENTIAL

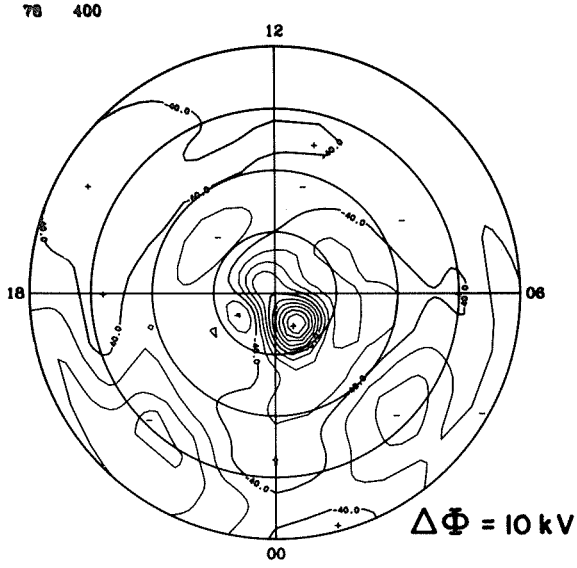

IONOSPHERIC CURRENT

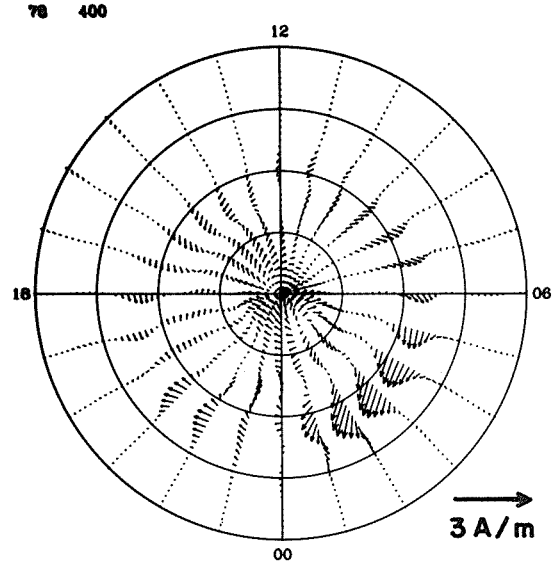

JOULE HEATING

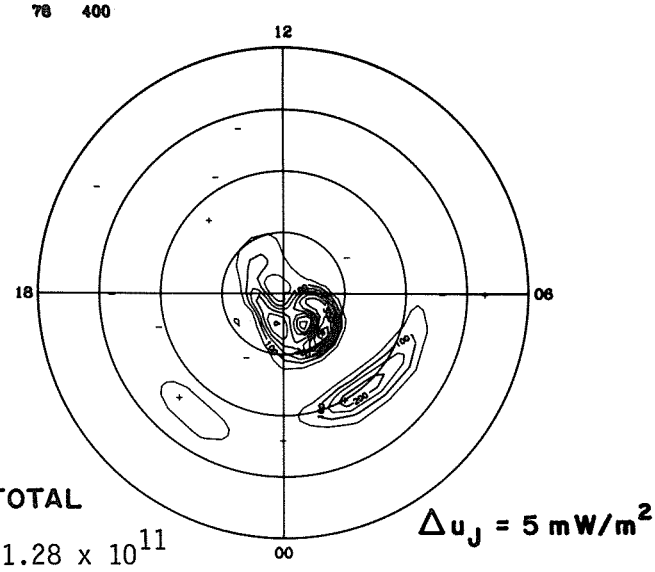

TOTAL

1.28×10^{11}

FIELD-ALIGNED CURRENT

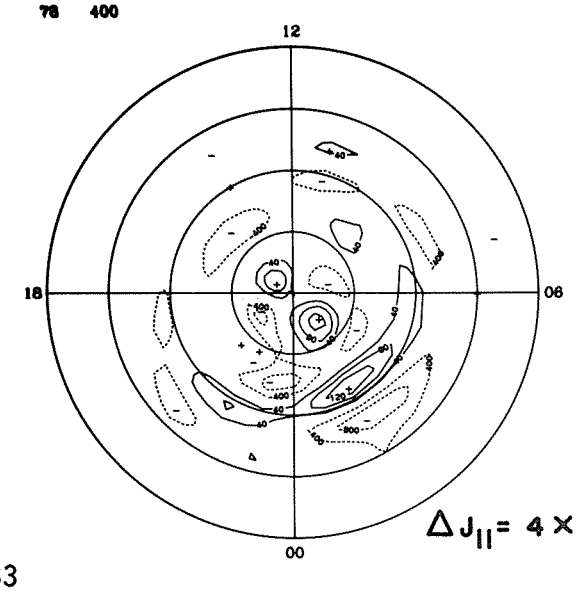

EQUIVALENT CURRENT

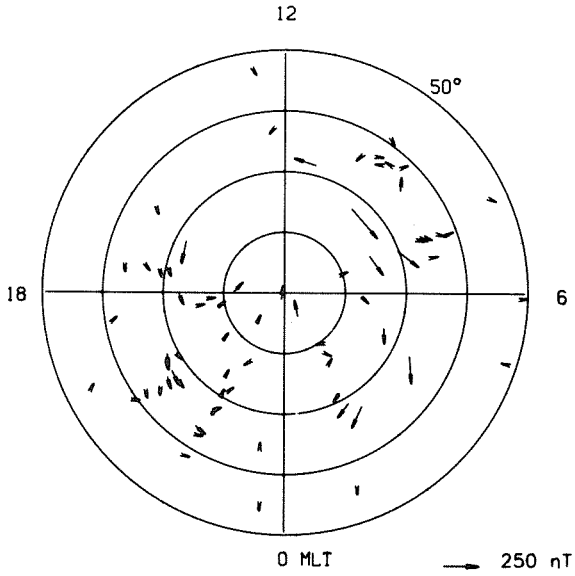

EQUIVALENT CURRENT SYSTEM

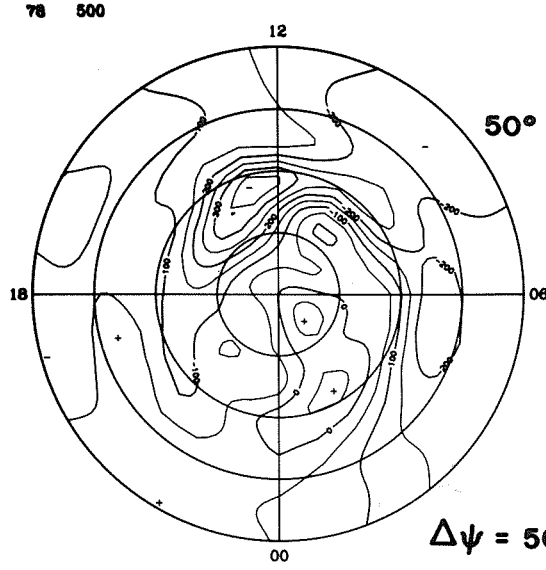

ELECTRIC POTENTIAL

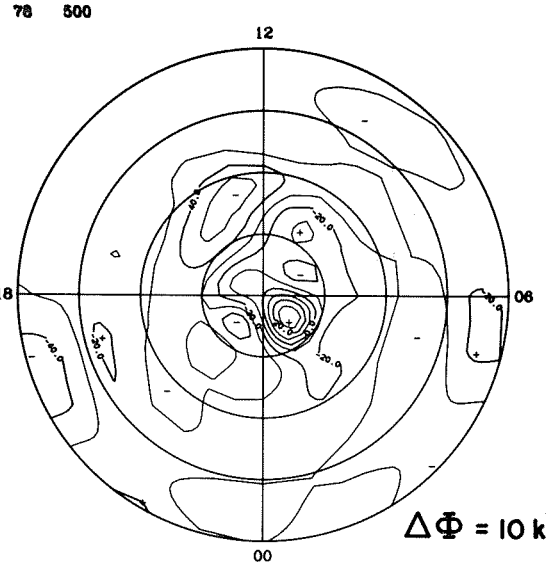

IONOSPHERIC CURRENT

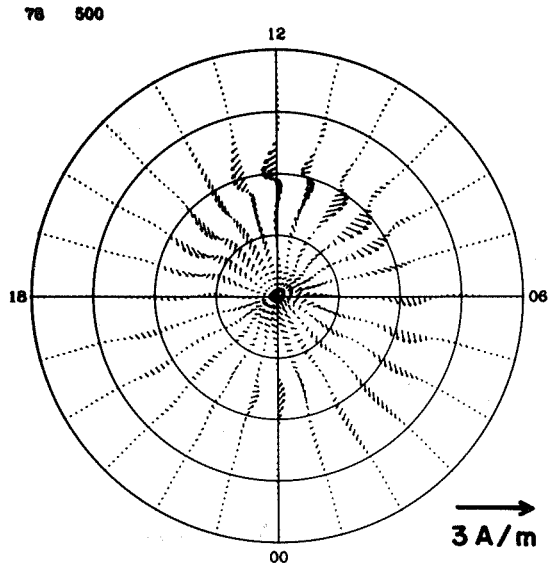

JOULE HEATING

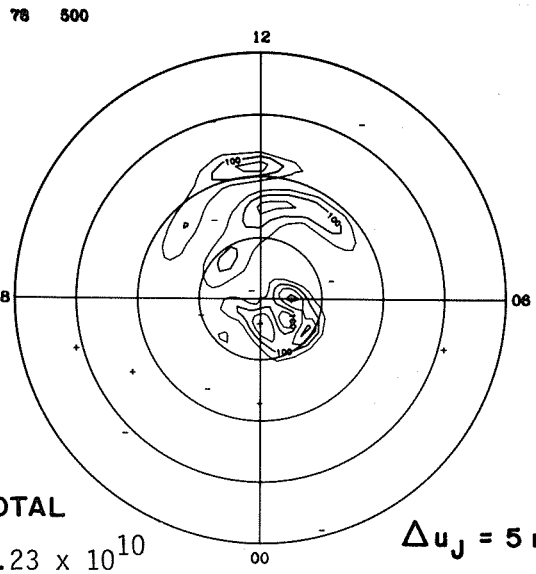

TOTAL

9.23×10^{10}

FIELD-ALIGNED CURRENT

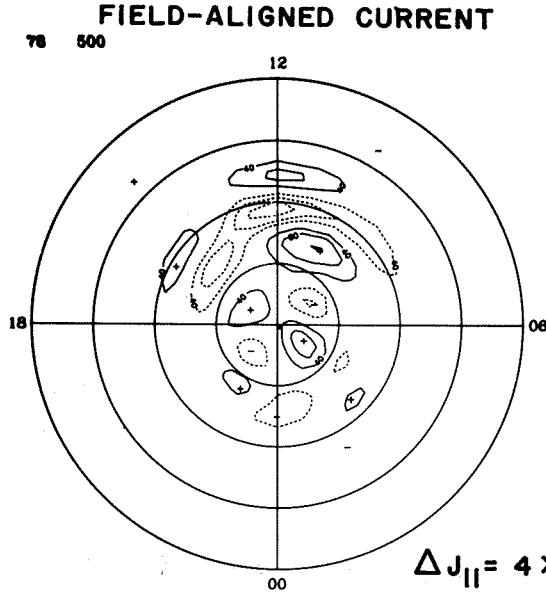

EQUIVALENT CURRENT

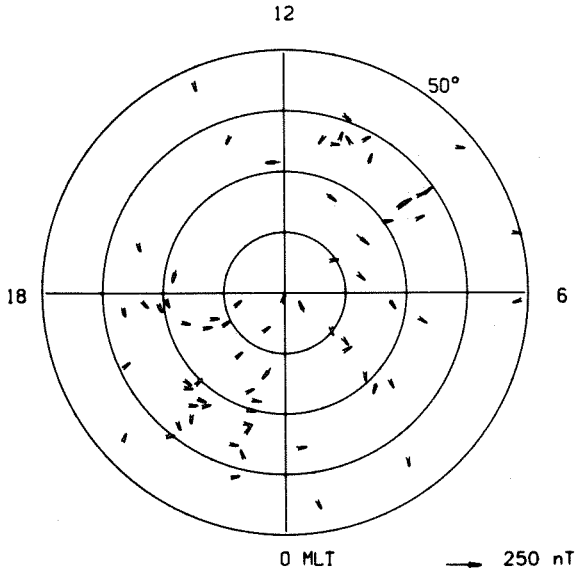

EQUIVALENT CURRENT SYSTEM

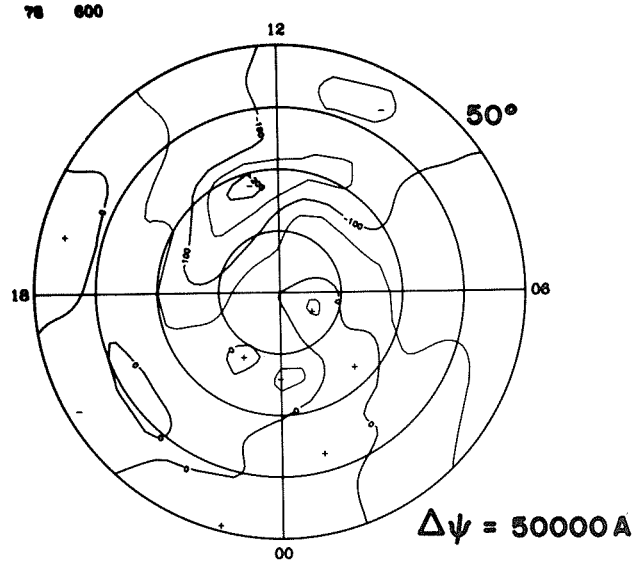

ELECTRIC POTENTIAL

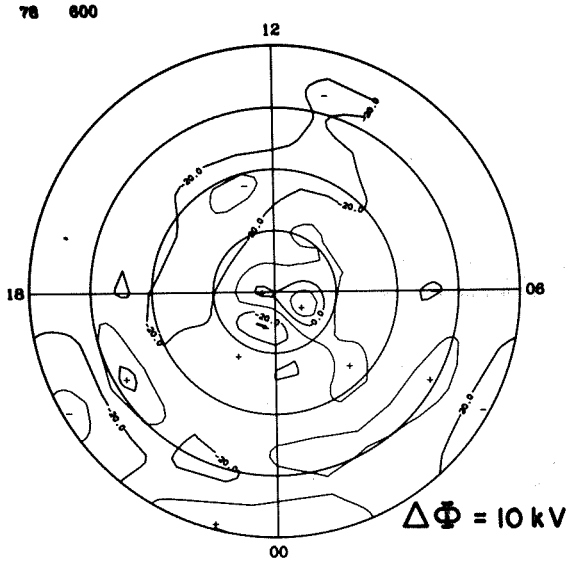

IONOSPHERIC CURRENT

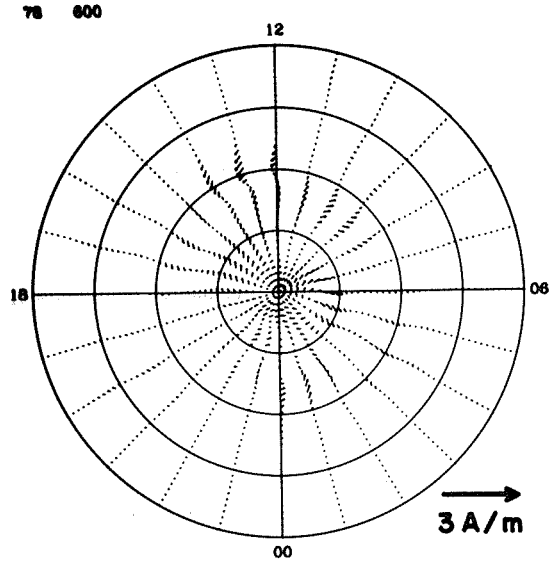

JOULE HEATING

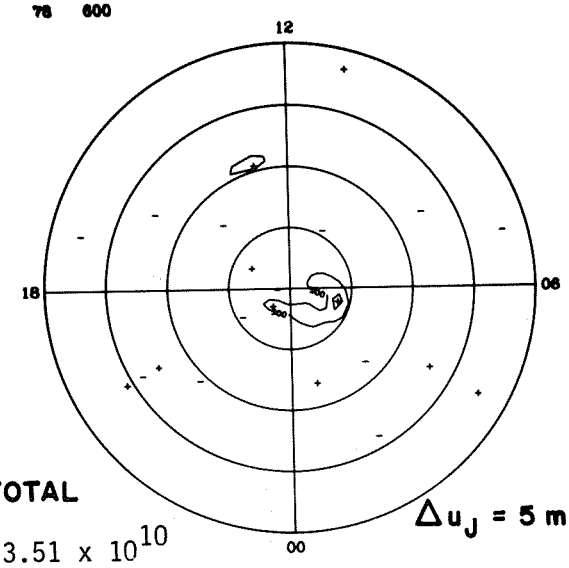

FIELD-ALIGNED CURRENT

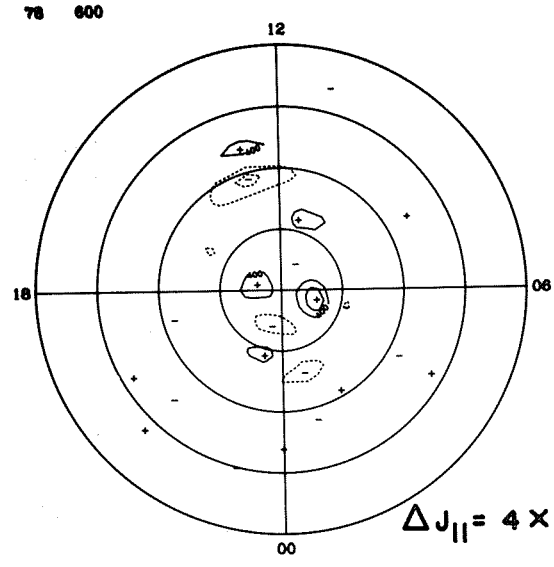

EQUIVALENT CURRENT

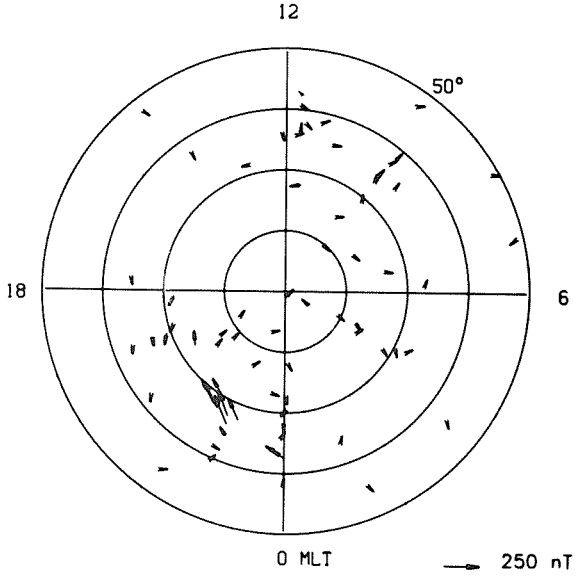

EQUIVALENT CURRENT SYSTEM

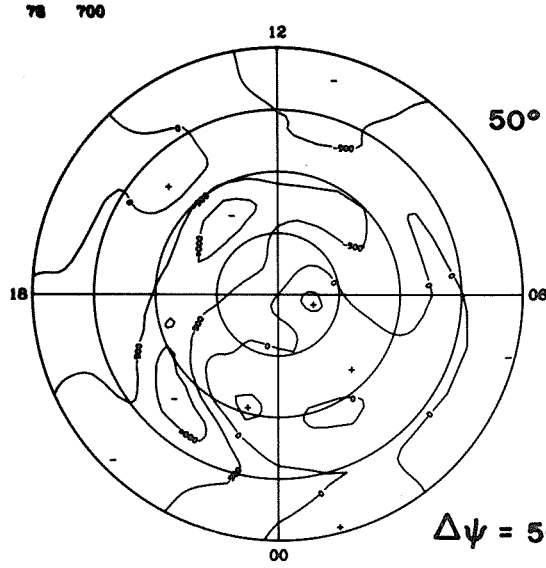

ELECTRIC POTENTIAL

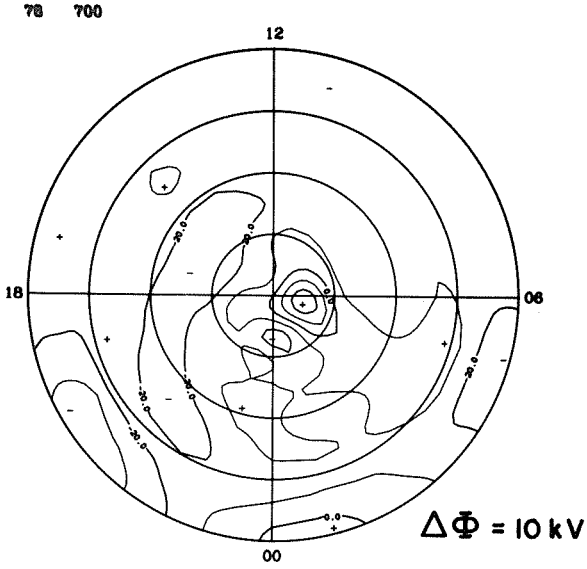

IONOSPHERIC CURRENT

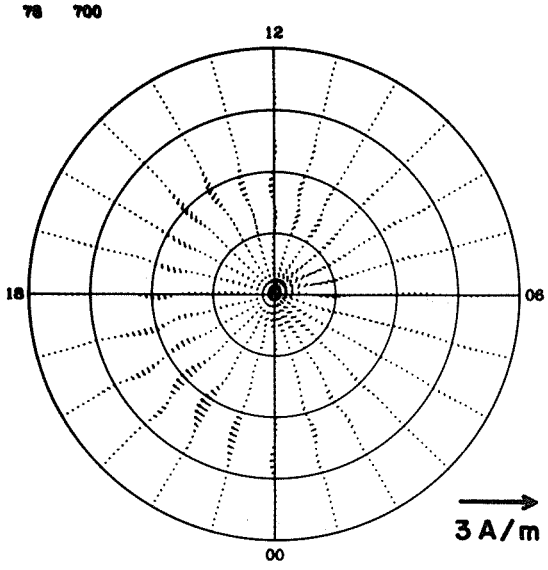

JOULE HEATING

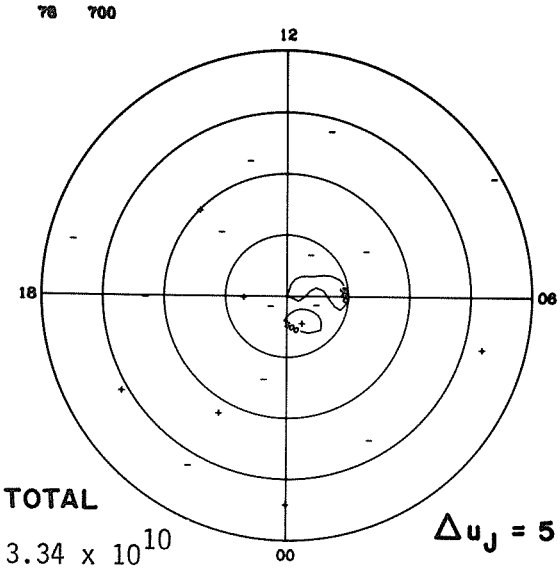

FIELD-ALIGNED CURRENT

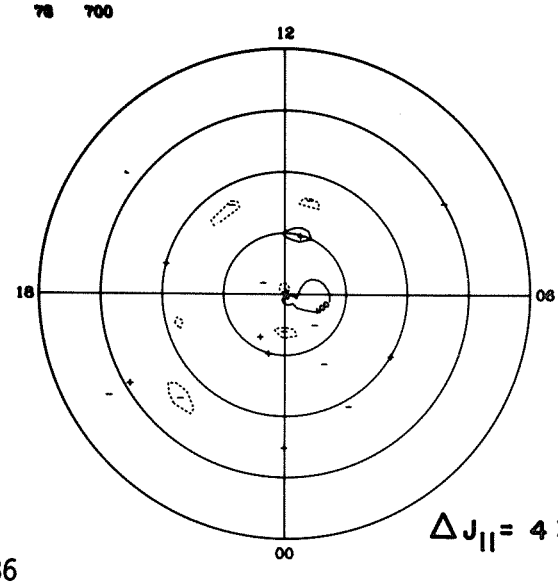

EQUIVALENT CURRENT

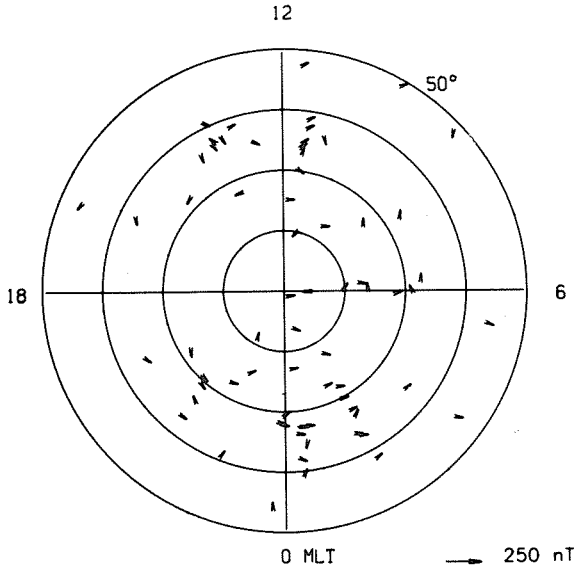

EQUIVALENT CURRENT SYSTEM

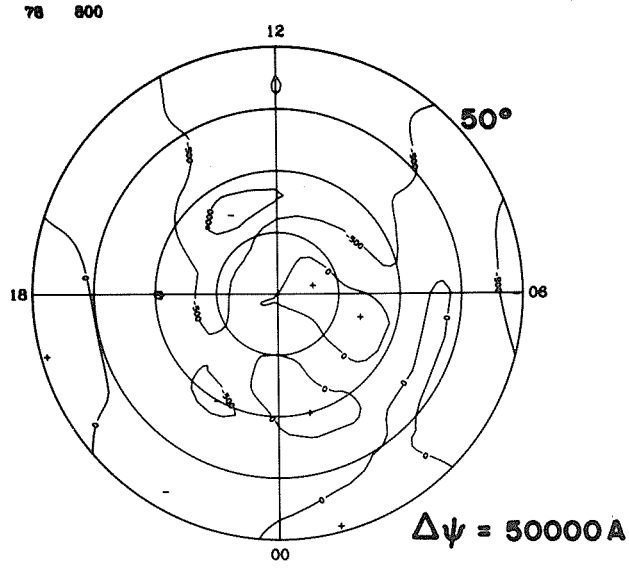

ELECTRIC POTENTIAL

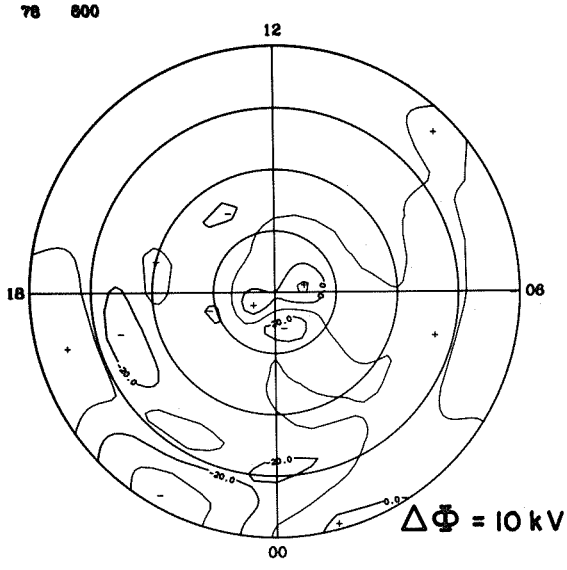

IONOSPHERIC CURRENT

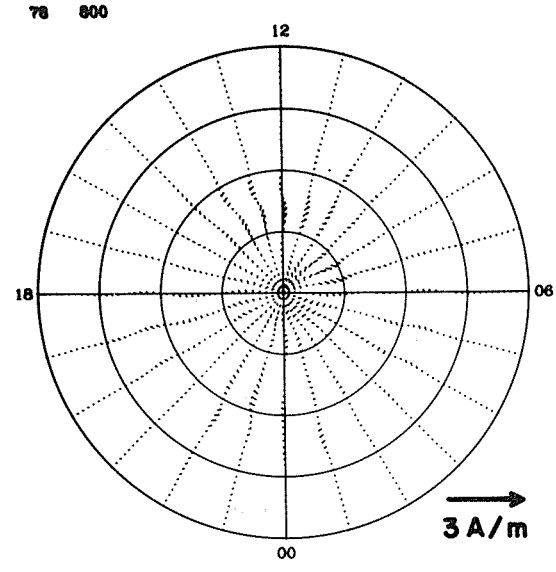

JOULE HEATING

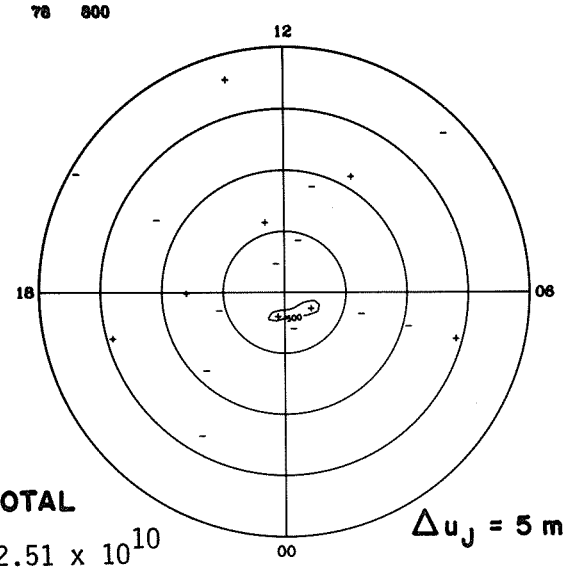

FIELD-ALIGNED CURRENT

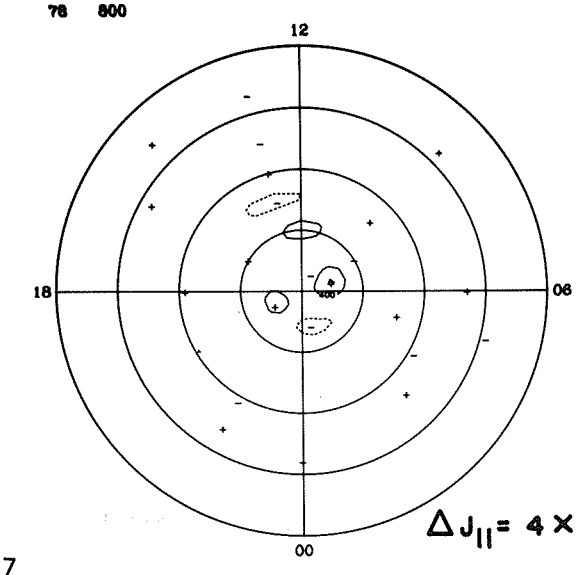

EQUIVALENT CURRENT

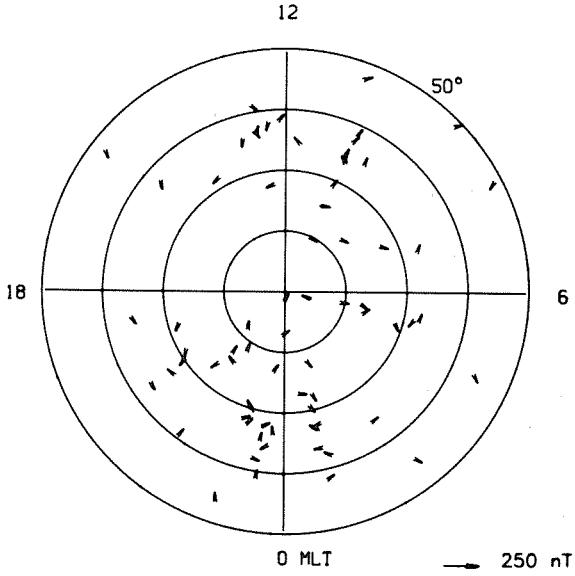

EQUIVALENT CURRENT SYSTEM

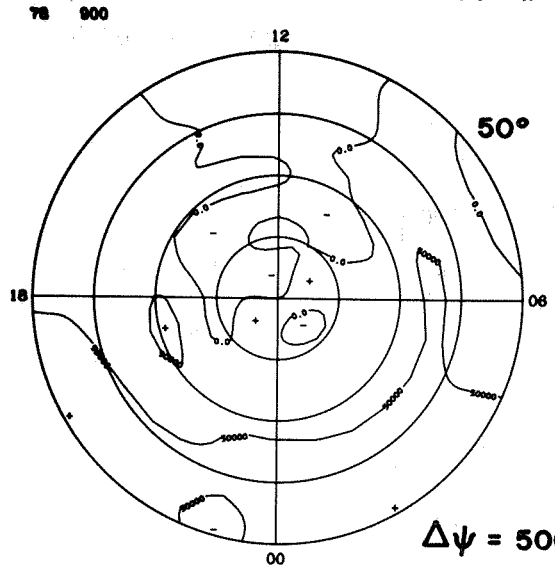

ELECTRIC POTENTIAL

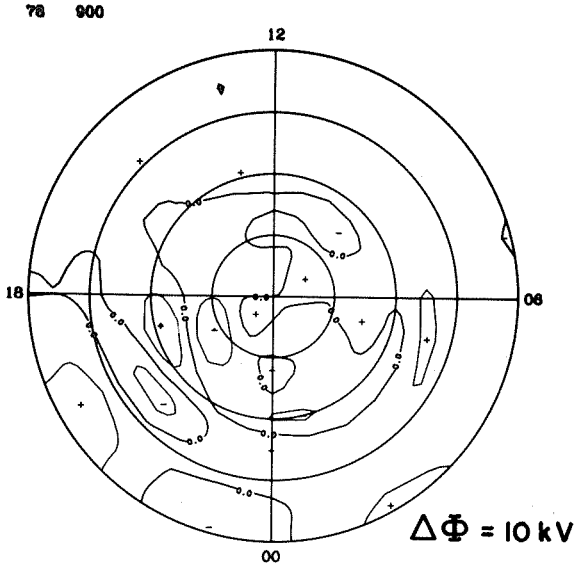

IONOSPHERIC CURRENT

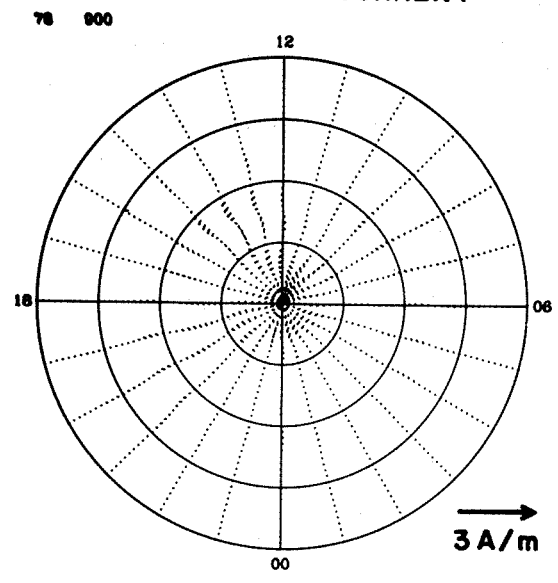

JOULE HEATING

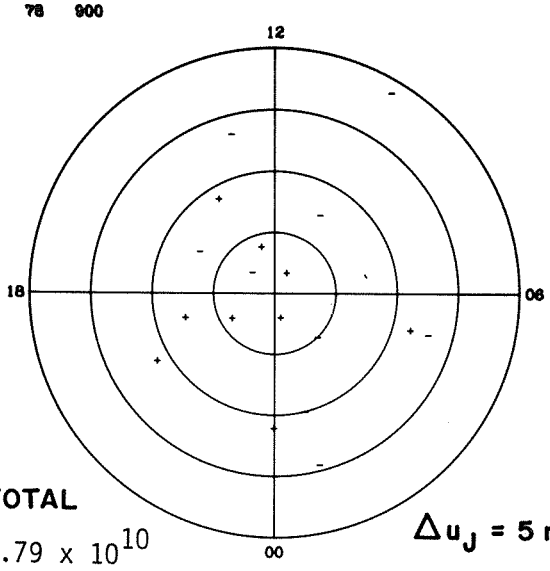

TOTAL

1.79×10^{10}

FIELD-ALIGNED CURRENT

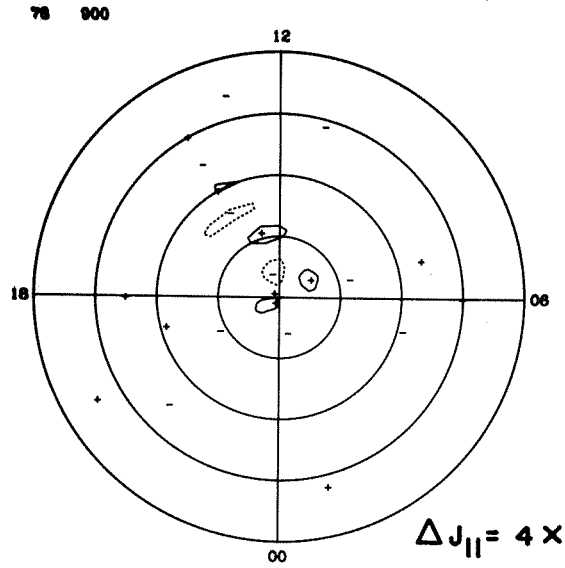

EQUIVALENT CURRENT

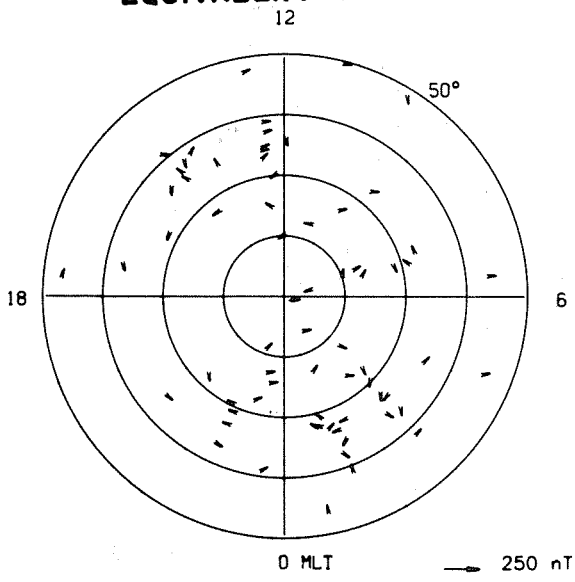

EQUIVALENT CURRENT SYSTEM

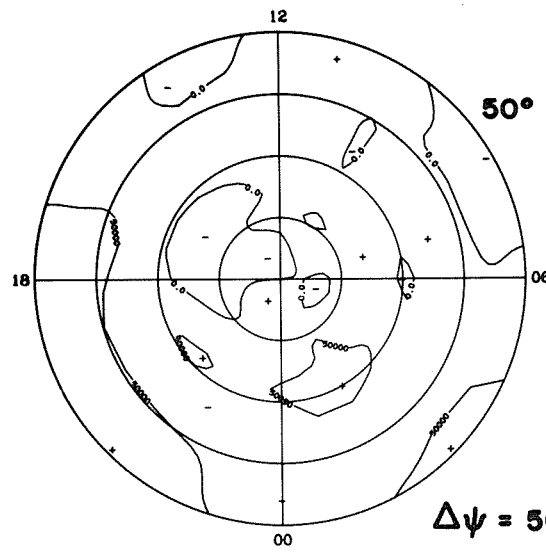

ELECTRIC POTENTIAL

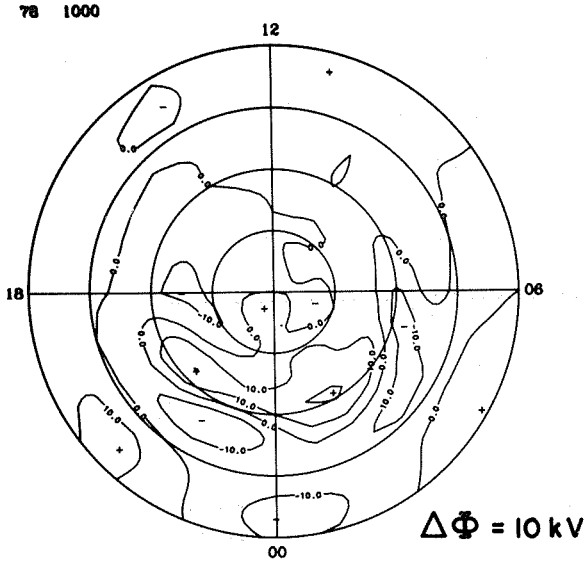

IONOSPHERIC CURRENT

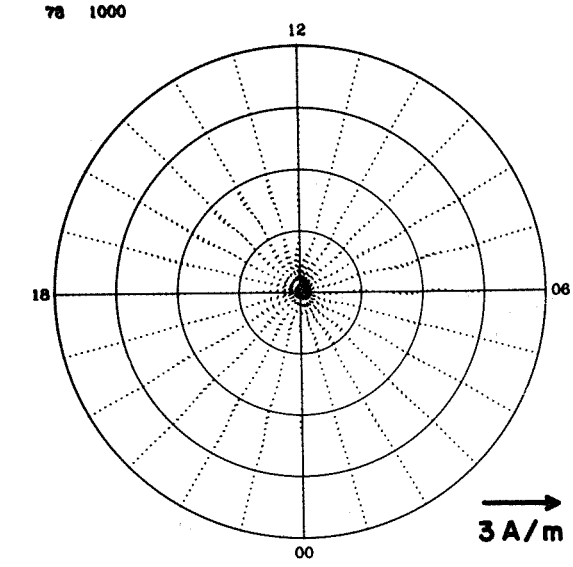

JOULE HEATING

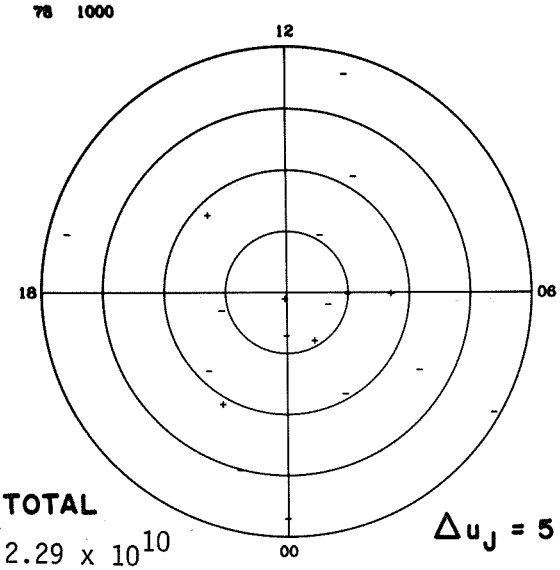

TOTAL

2.29×10^{10}

FIELD-ALIGNED CURRENT

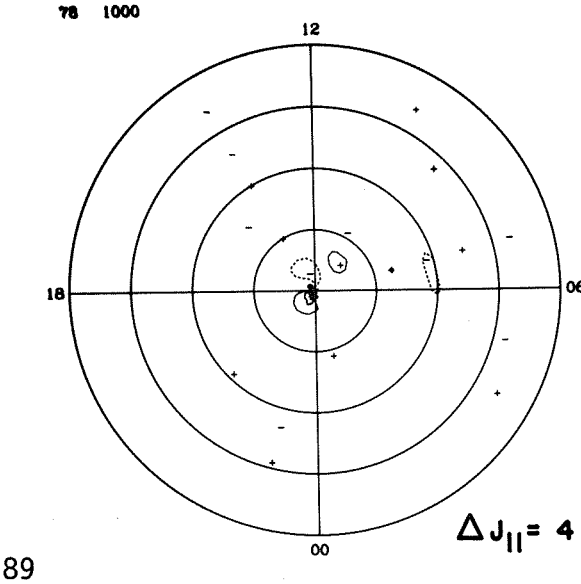

EQUIVALENT CURRENT

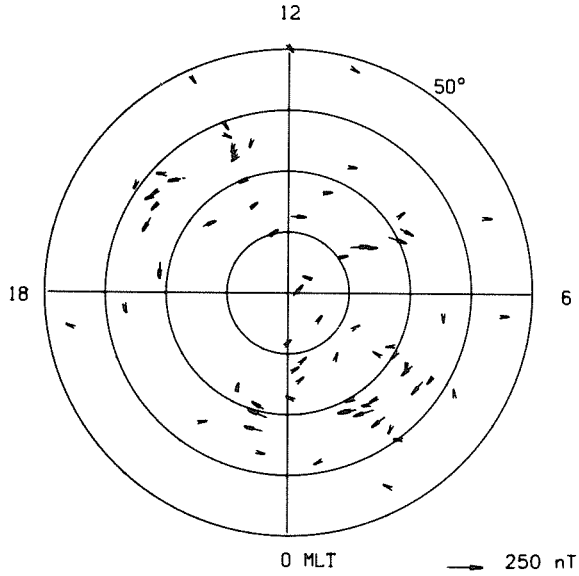

EQUIVALENT CURRENT SYSTEM

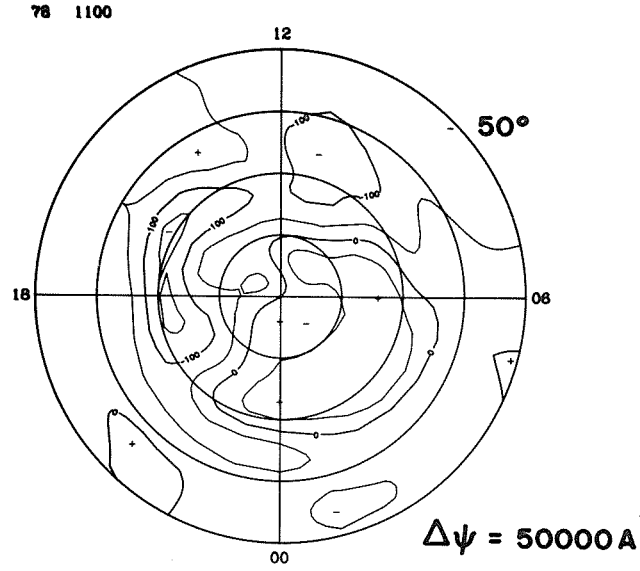

ELECTRIC POTENTIAL

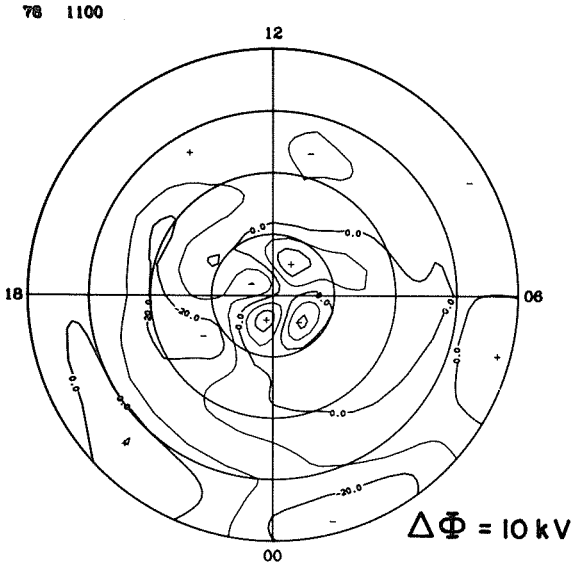

IONOSPHERIC CURRENT

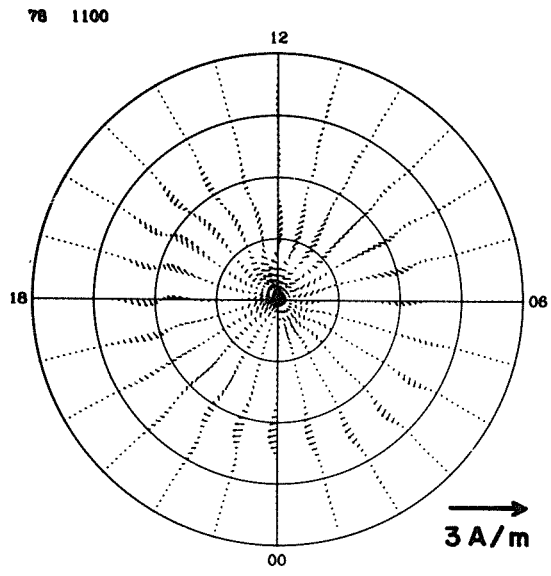

JOULE HEATING

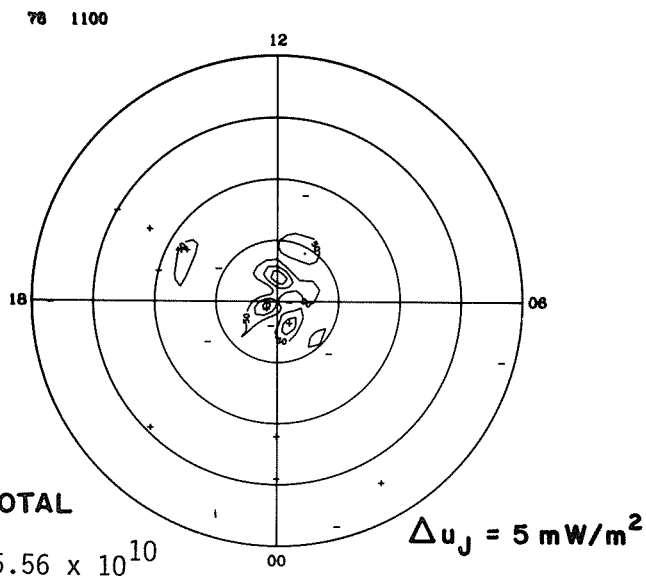

TOTAL

5.56×10^{10}

FIELD-ALIGNED CURRENT

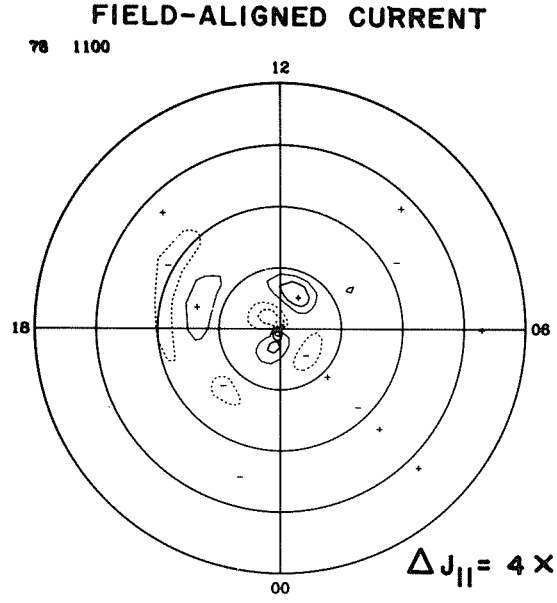

EQUIVALENT CURRENT

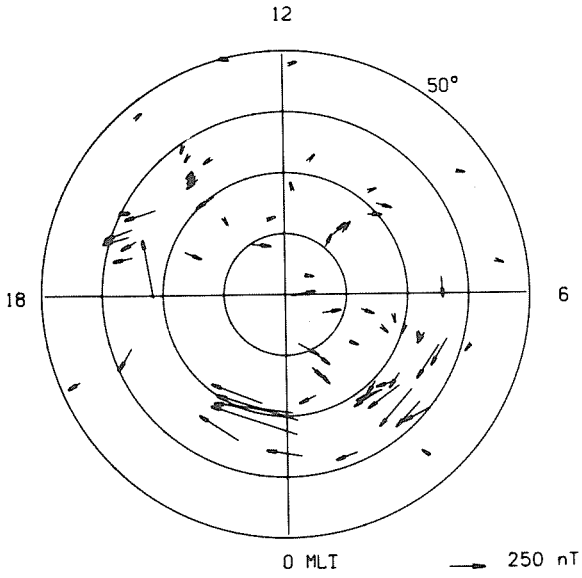

EQUIVALENT CURRENT SYSTEM

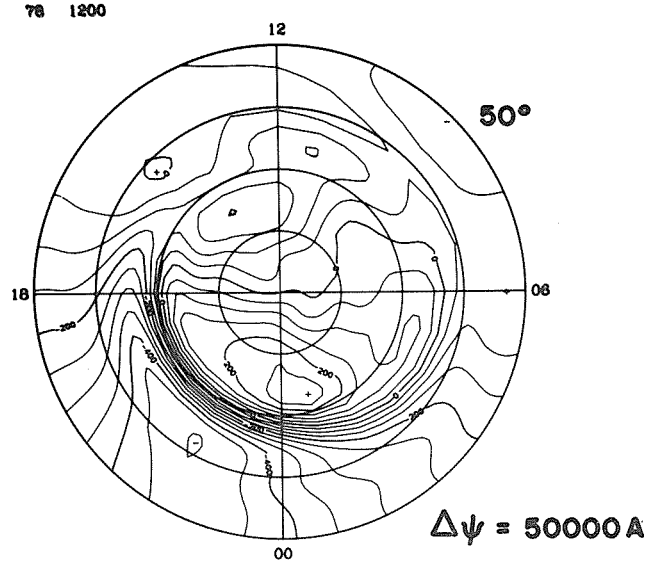

ELECTRIC POTENTIAL

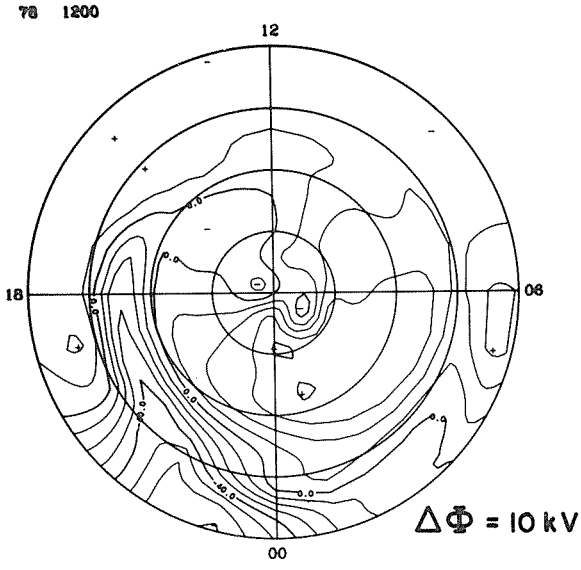

IONOSPHERIC CURRENT

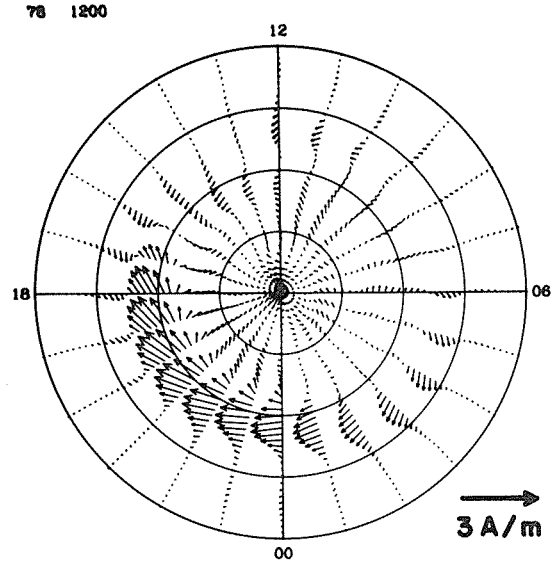

JOULE HEATING

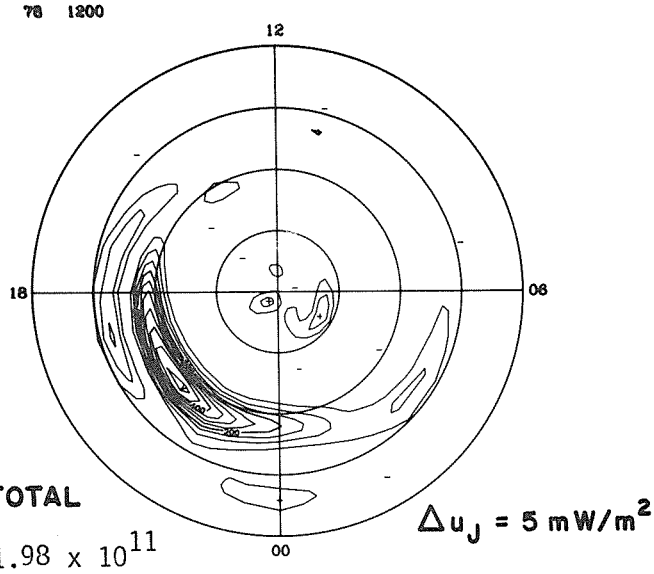

TOTAL

1.98×10^{11}

FIELD-ALIGNED CURRENT

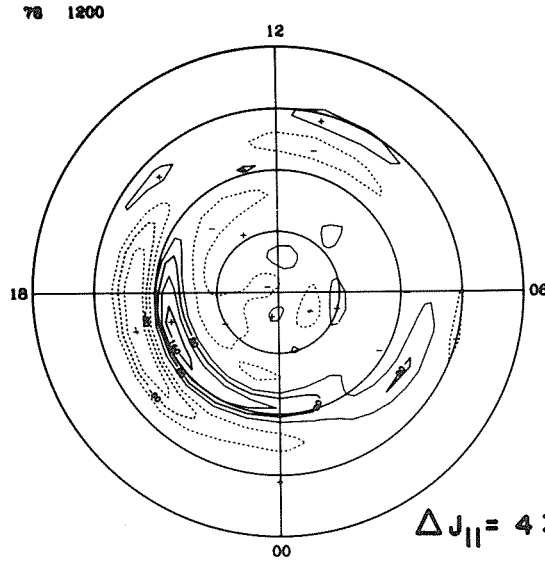

EQUIVALENT CURRENT

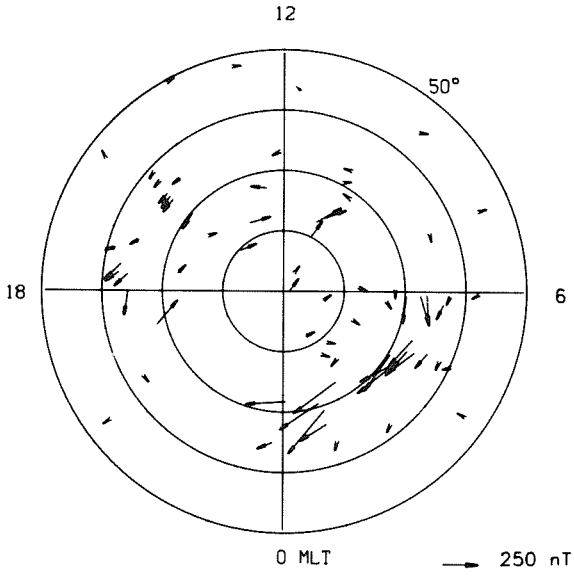

EQUIVALENT CURRENT SYSTEM

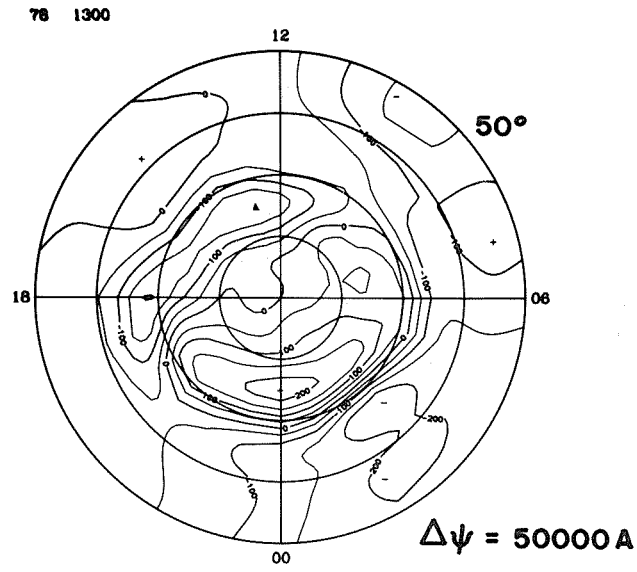

ELECTRIC POTENTIAL

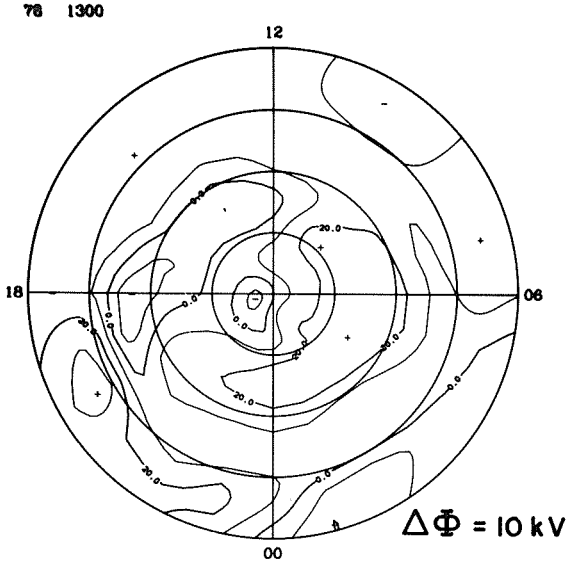

IONOSPHERIC CURRENT

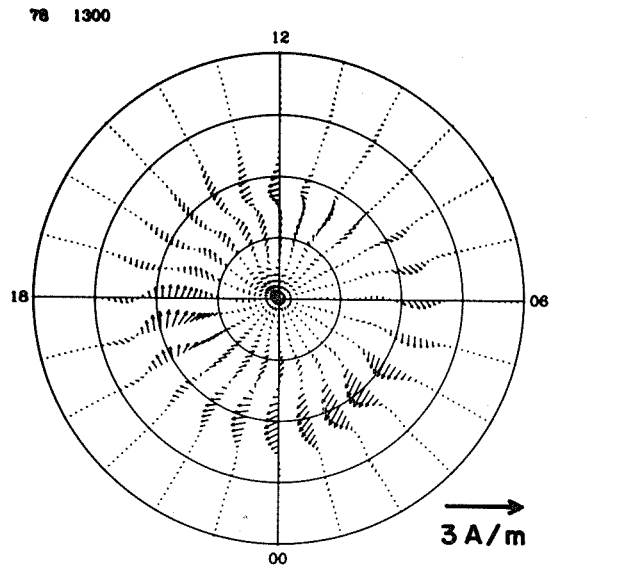

JOULE HEATING

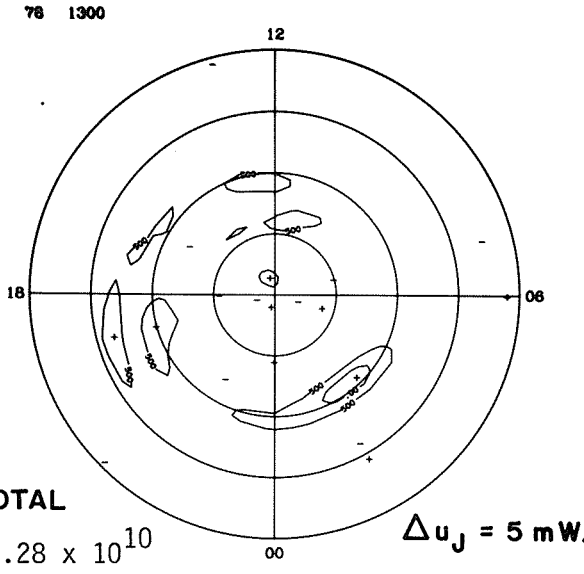

TOTAL

8.28×10^{10}

FIELD-ALIGNED CURRENT

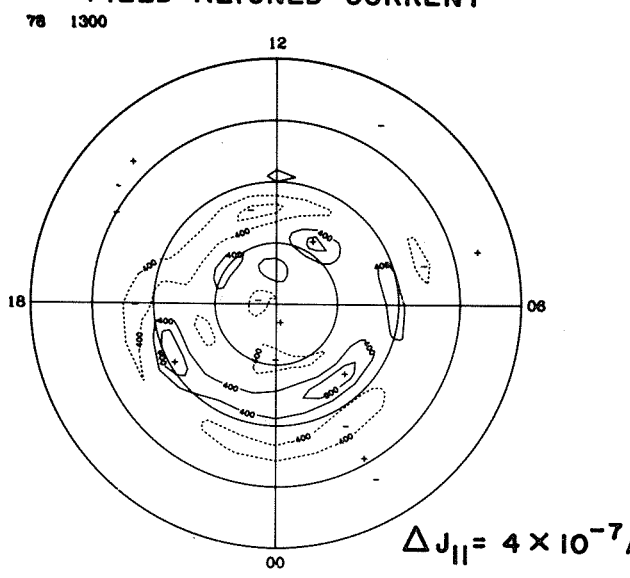

EQUIVALENT CURRENT

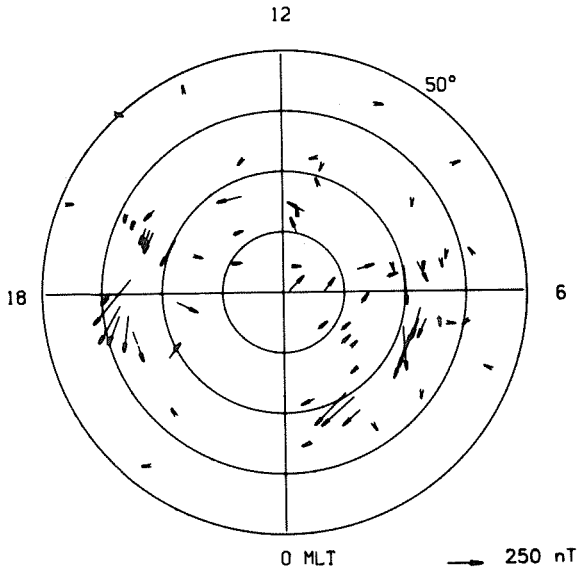

EQUIVALENT CURRENT SYSTEM

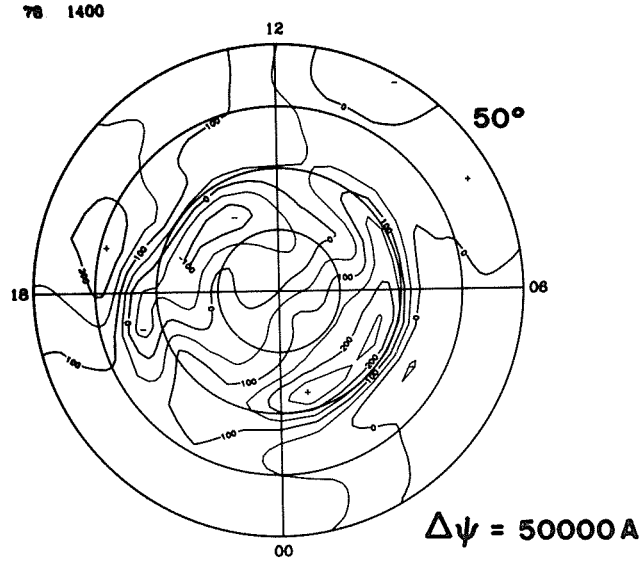

ELECTRIC POTENTIAL

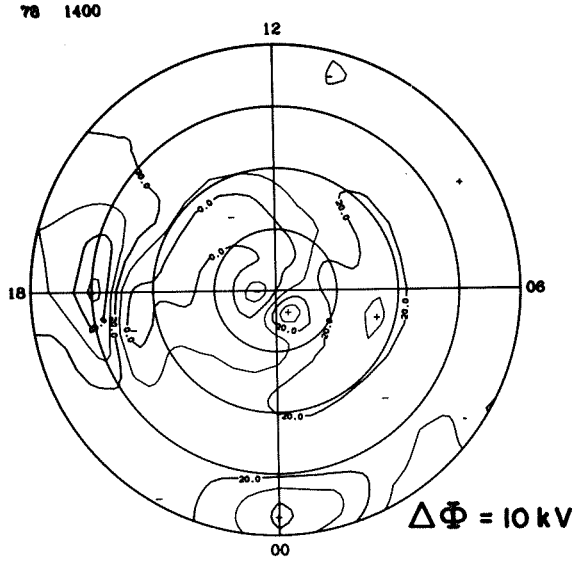

IONOSPHERIC CURRENT

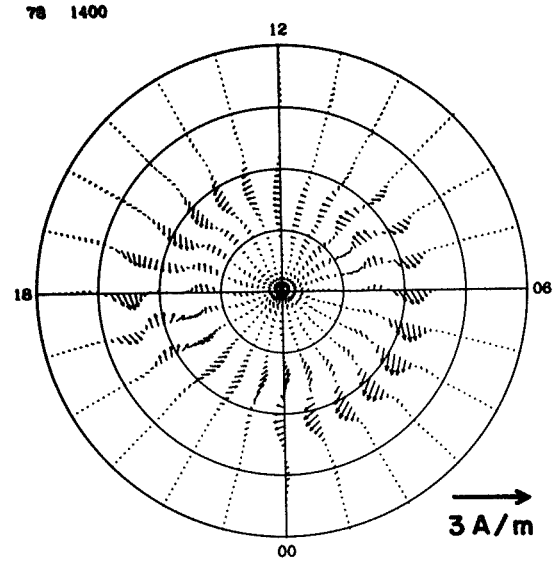

JOULE HEATING

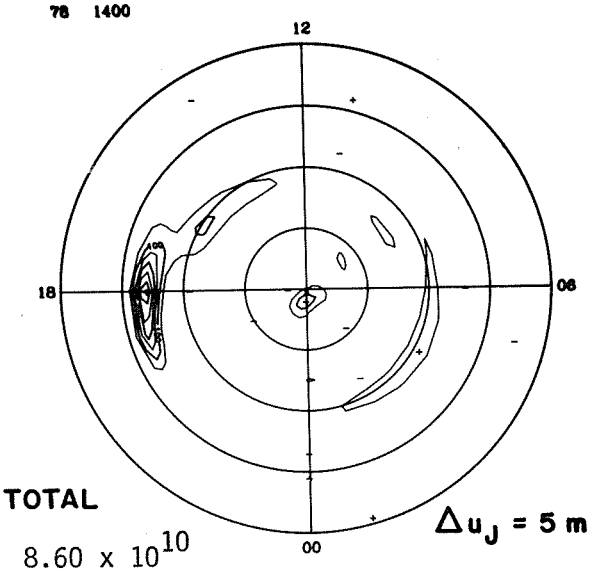

FIELD-ALIGNED CURRENT

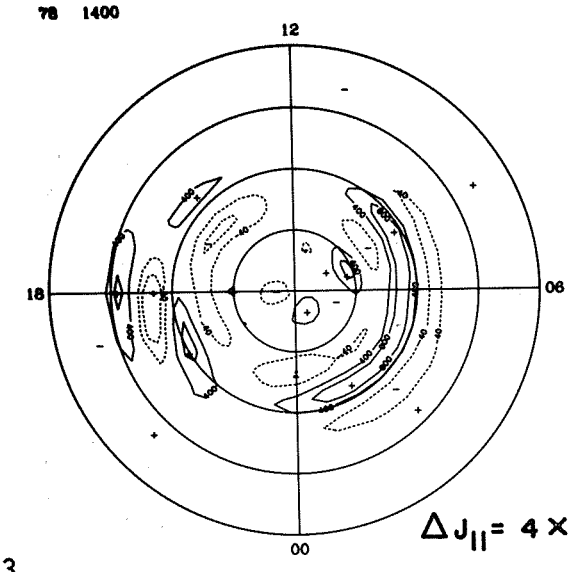

EQUIVALENT CURRENT

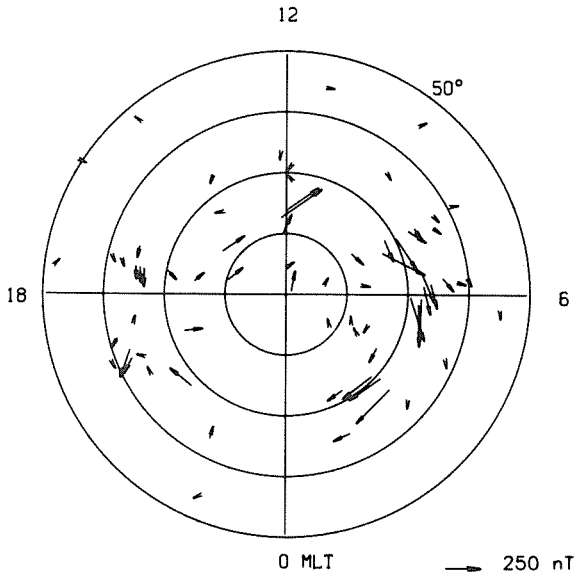

EQUIVALENT CURRENT SYSTEM

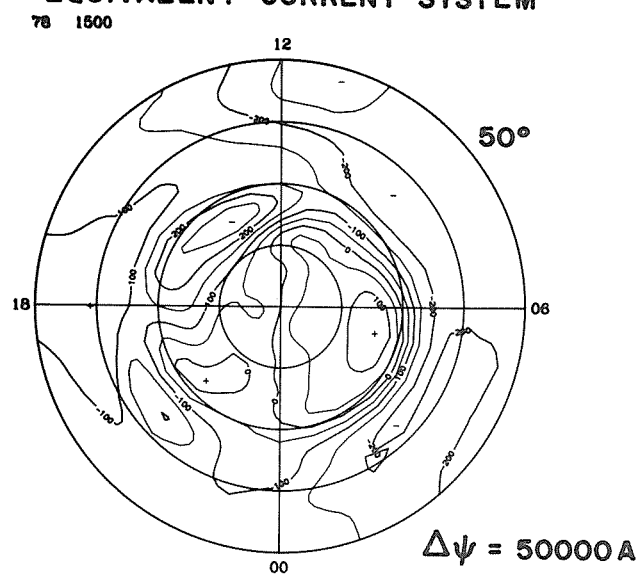

ELECTRIC POTENTIAL

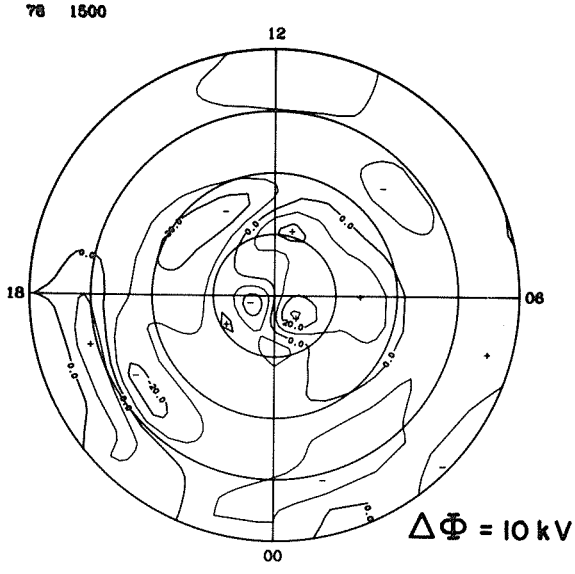

IONOSPHERIC CURRENT

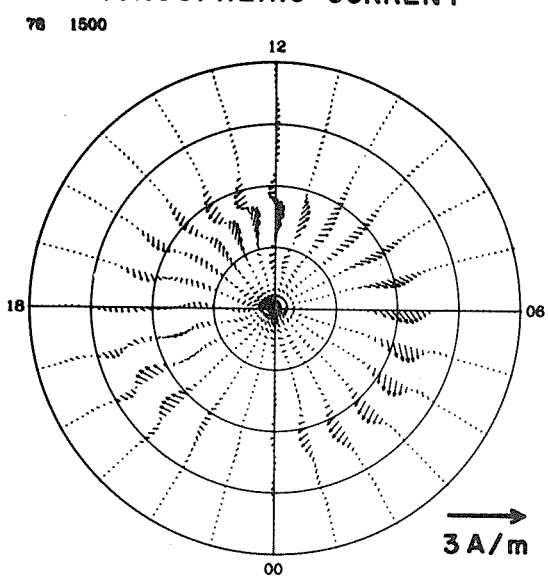

JOULE HEATING

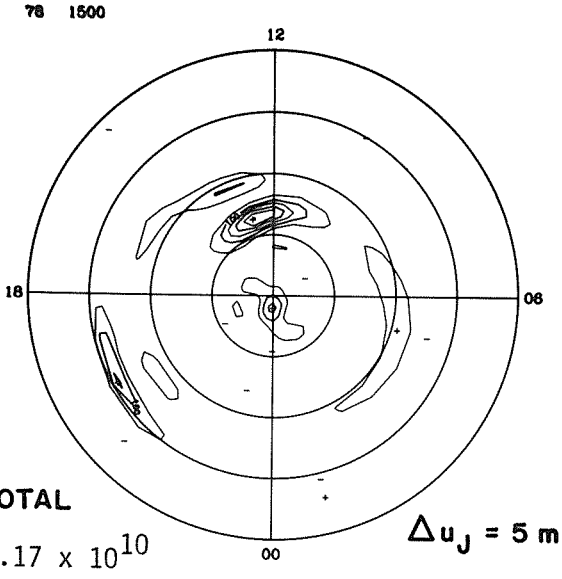

TOTAL

9.17×10^{10}

FIELD-ALIGNED CURRENT

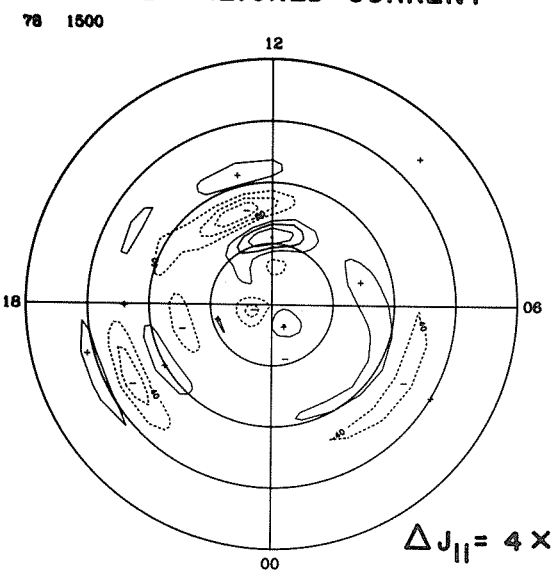

EQUIVALENT CURRENT

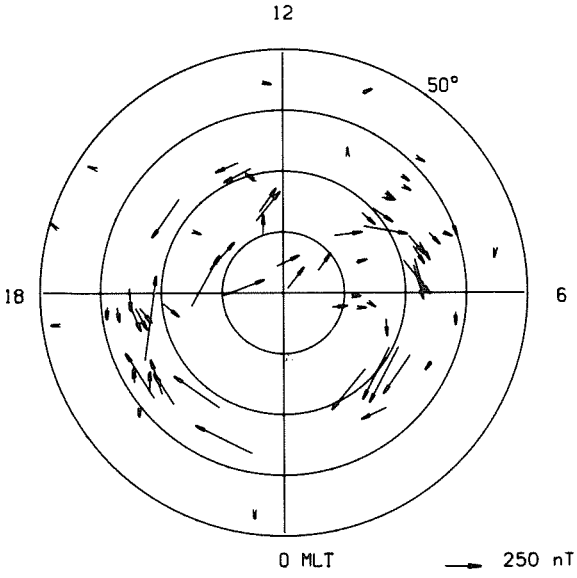

EQUIVALENT CURRENT SYSTEM

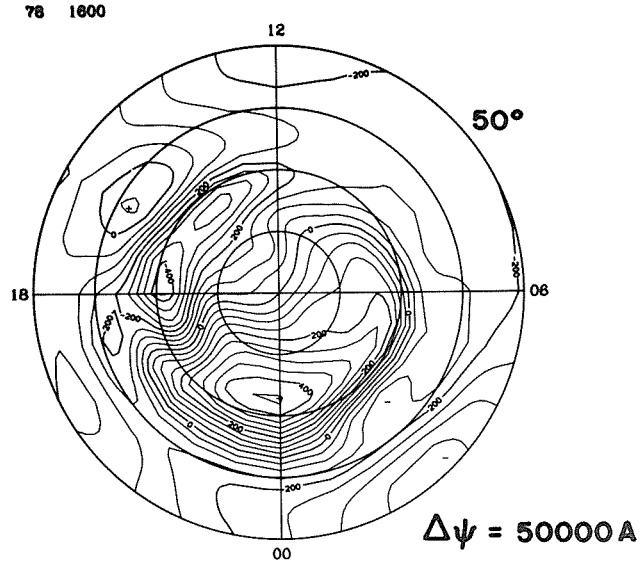

ELECTRIC POTENTIAL

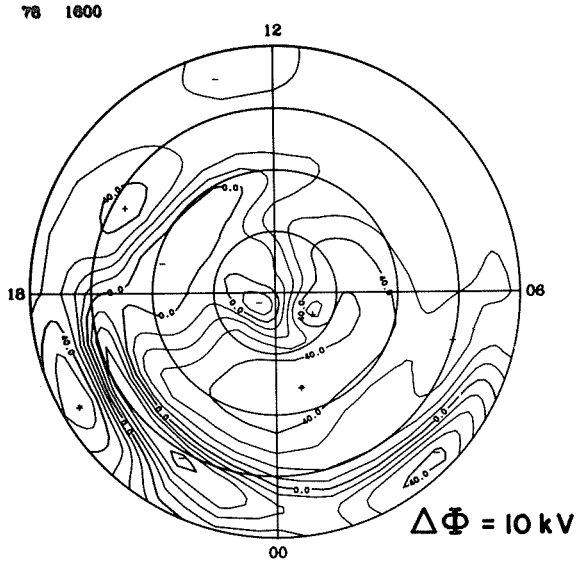

IONOSPHERIC CURRENT

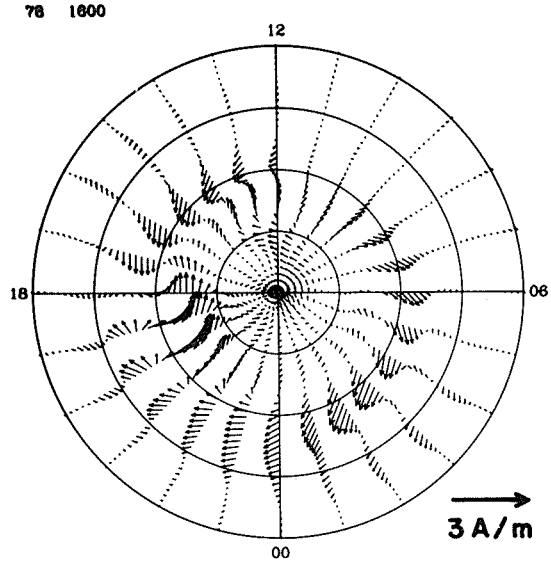

JOULE HEATING

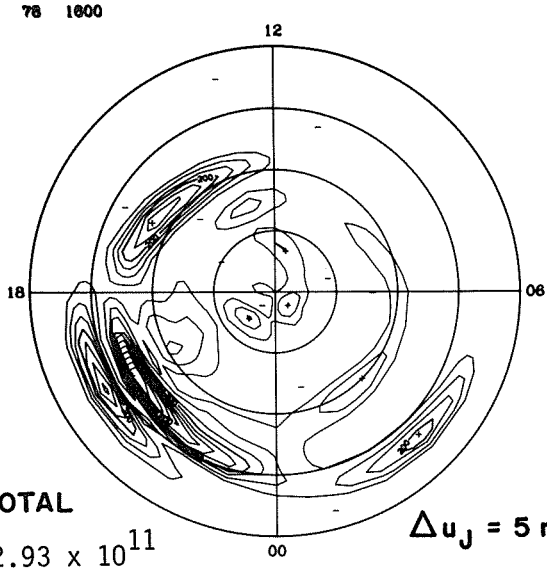

FIELD-ALIGNED CURRENT

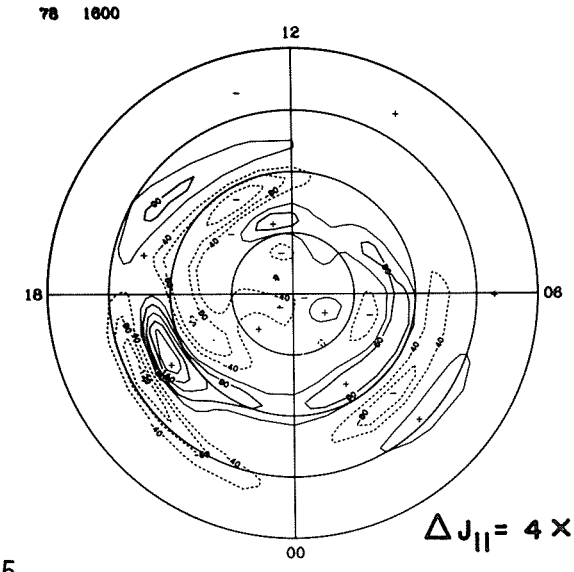

EQUIVALENT CURRENT

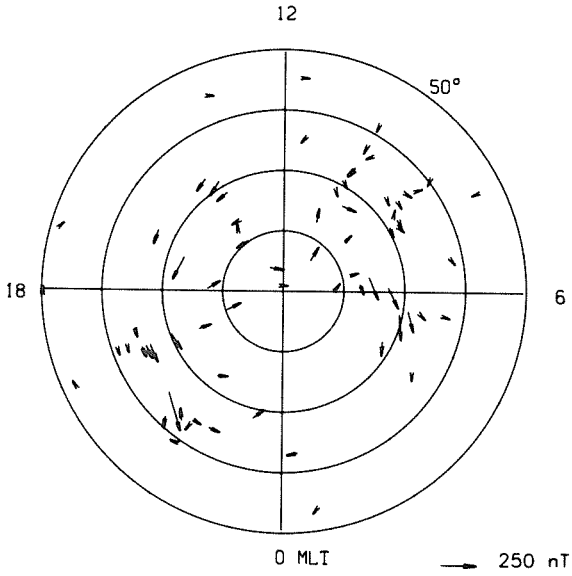

EQUIVALENT CURRENT SYSTEM

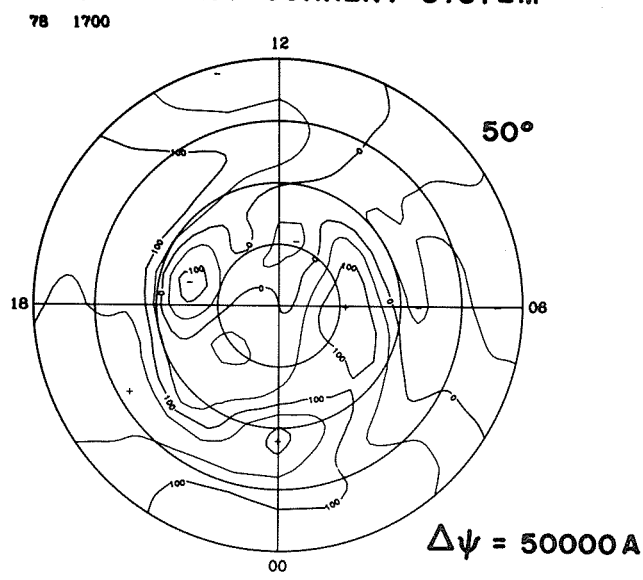

ELECTRIC POTENTIAL

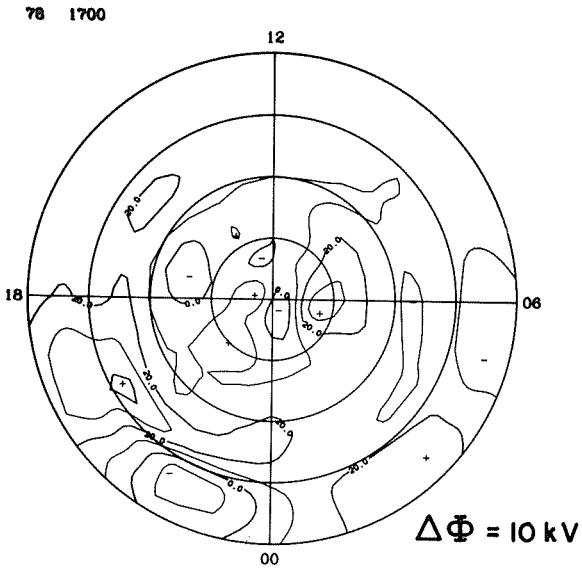

IONOSPHERIC CURRENT

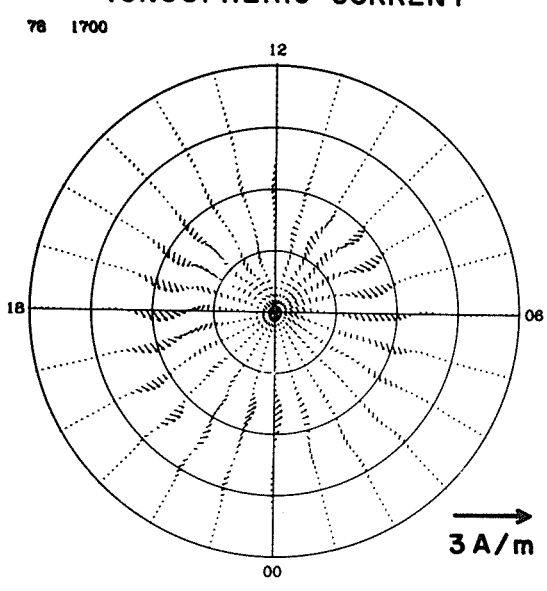

JOULE HEATING

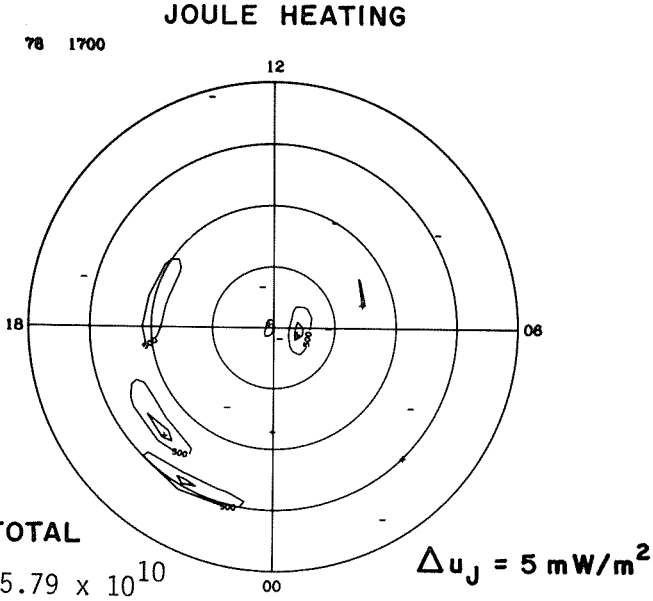

TOTAL

5.79×10^{10}

FIELD-ALIGNED CURRENT

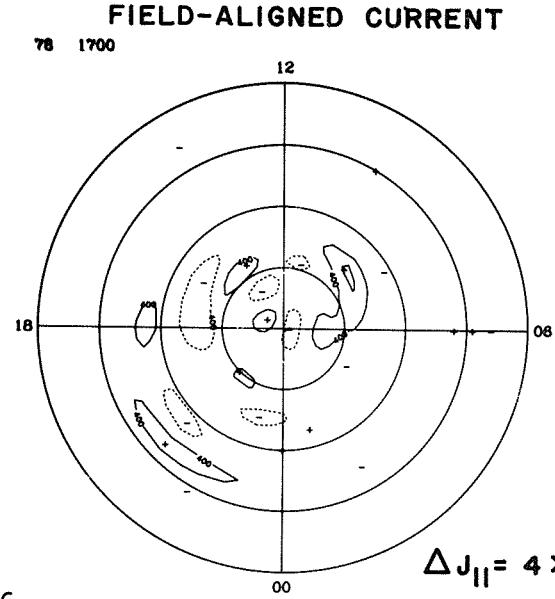

EQUIVALENT CURRENT

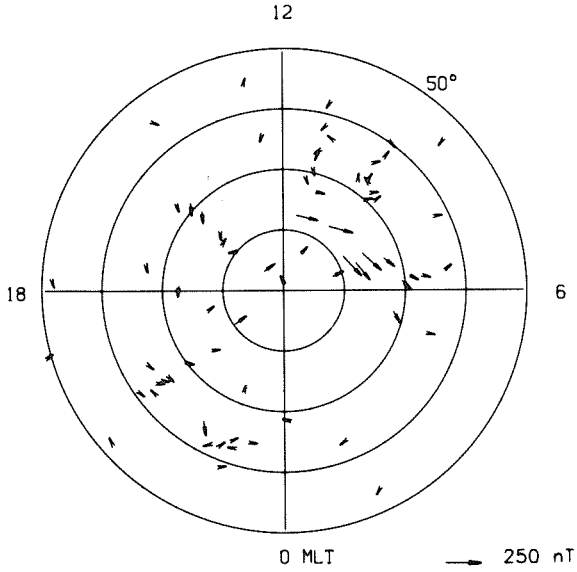

EQUIVALENT CURRENT SYSTEM

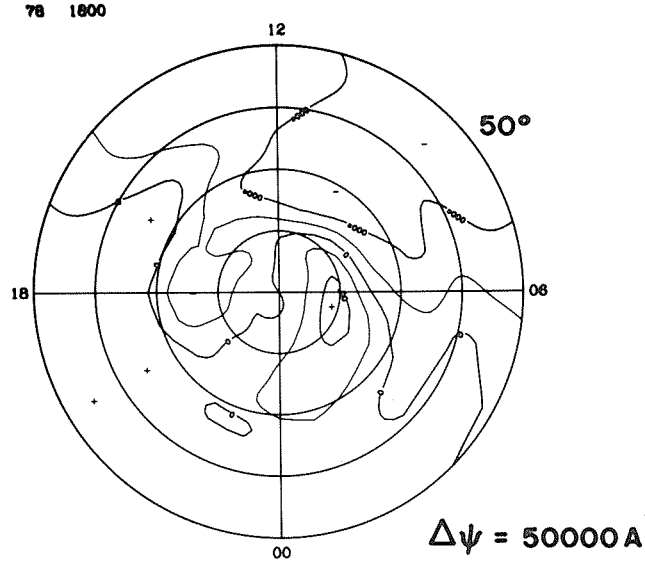

ELECTRIC POTENTIAL

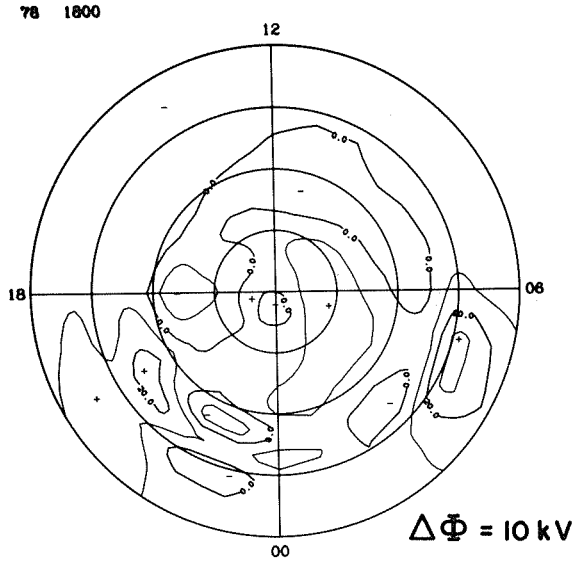

IONOSPHERIC CURRENT

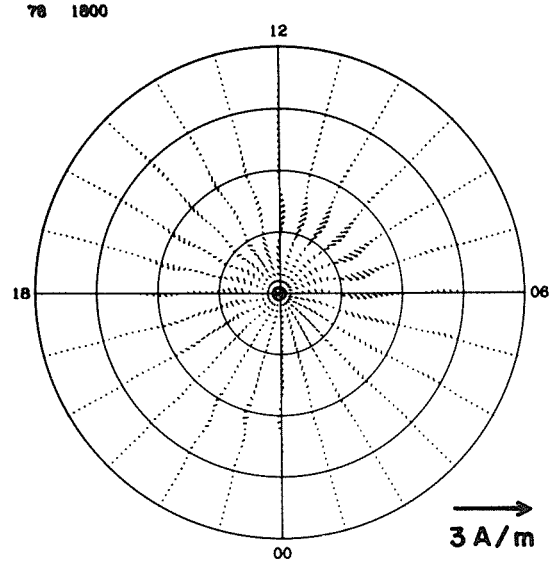

JOULE HEATING

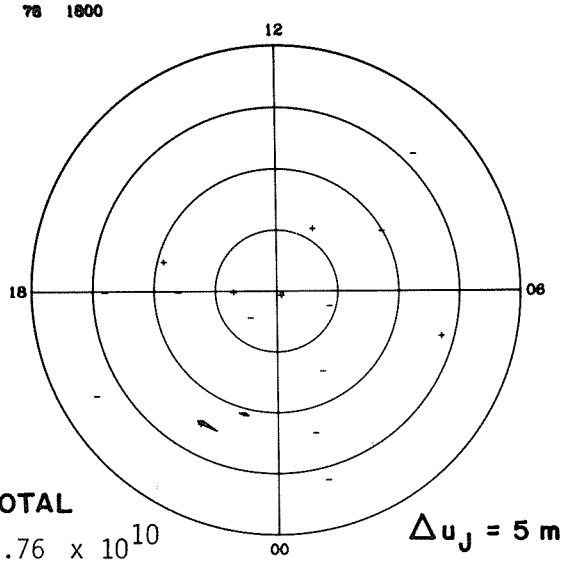

TOTAL

3.76×10^{10}

FIELD-ALIGNED CURRENT

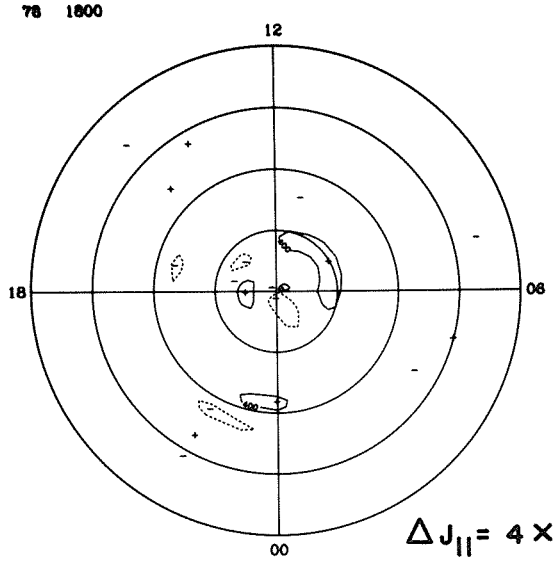

EQUIVALENT CURRENT

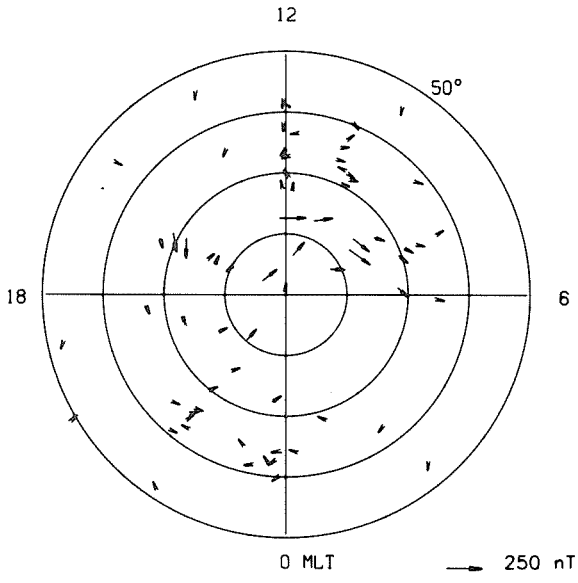

EQUIVALENT CURRENT SYSTEM

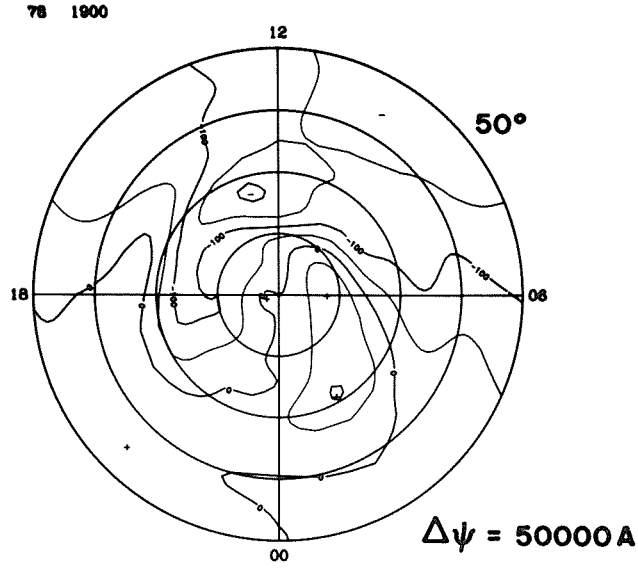

ELECTRIC POTENTIAL

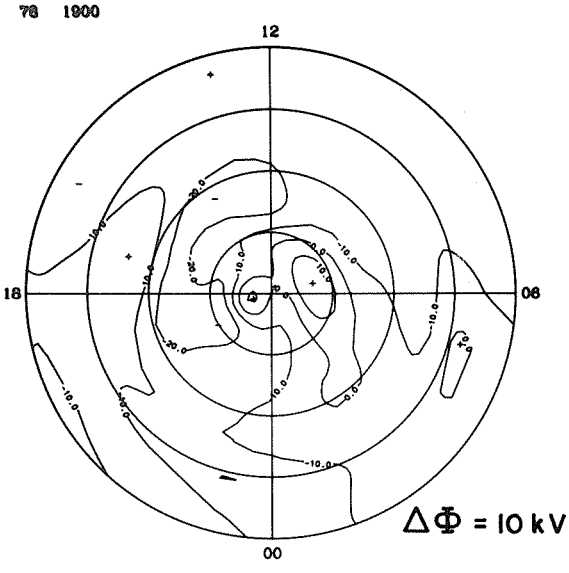

IONOSPHERIC CURRENT

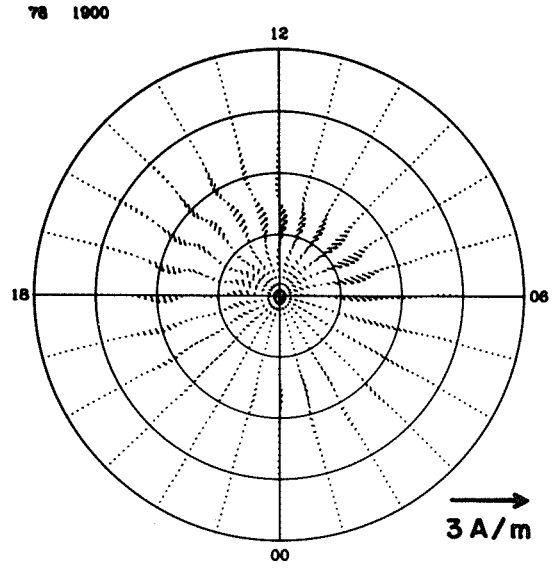

JOULE HEATING

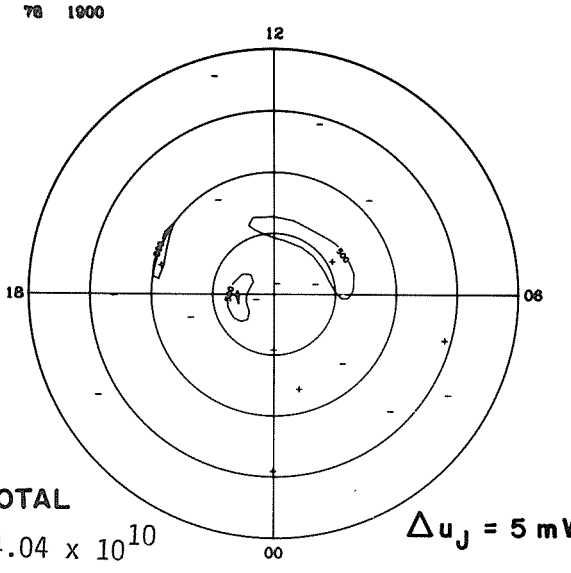

FIELD-ALIGNED CURRENT

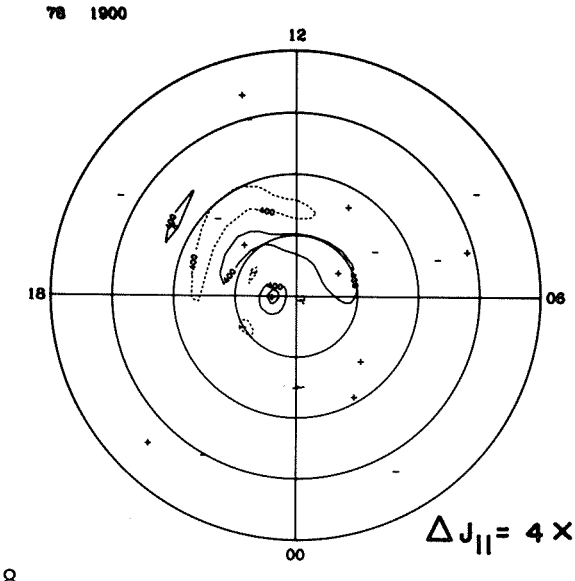

EQUIVALENT CURRENT

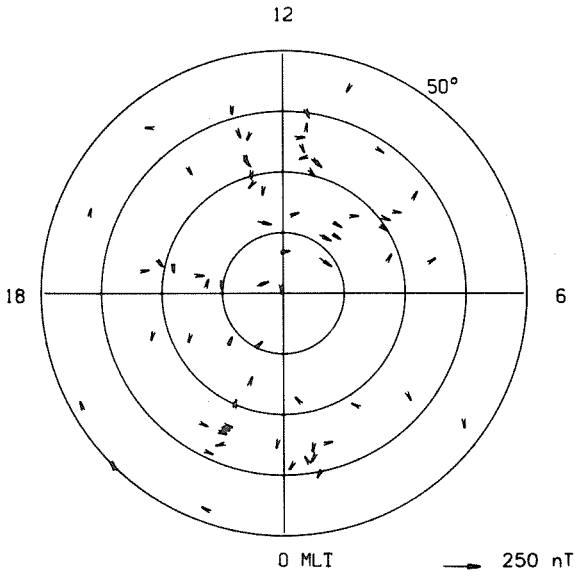

EQUIVALENT CURRENT SYSTEM

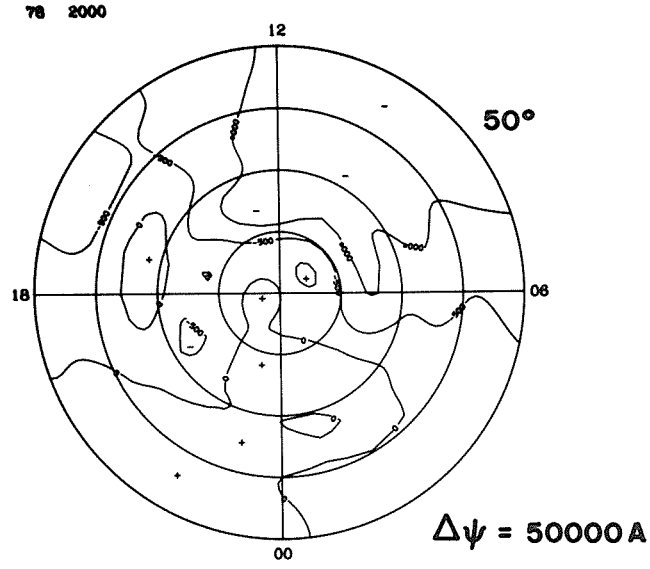

ELECTRIC POTENTIAL

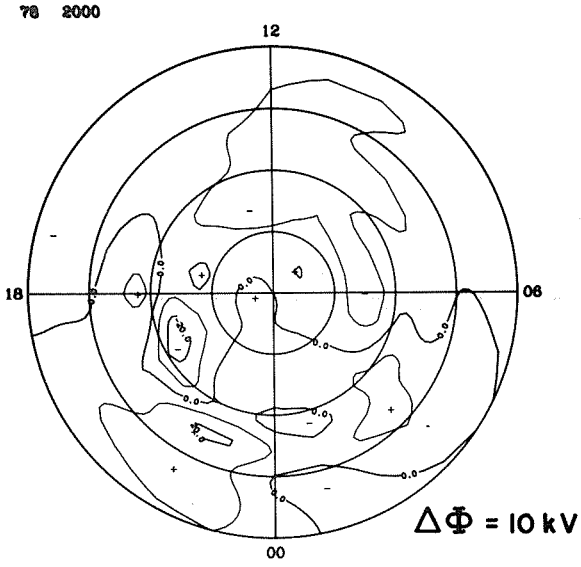

IONOSPHERIC CURRENT

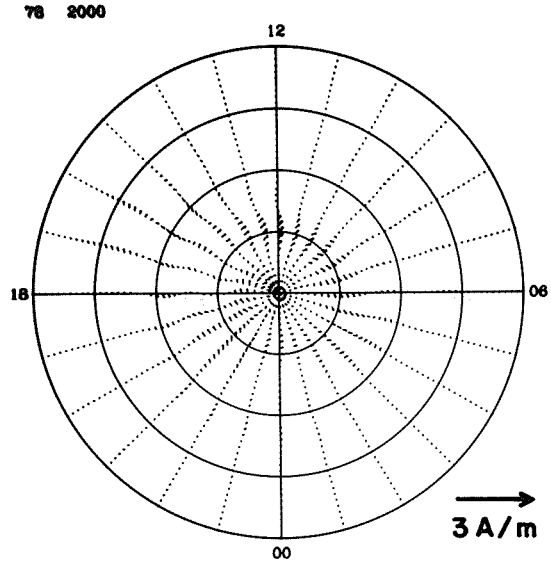

JOULE HEATING

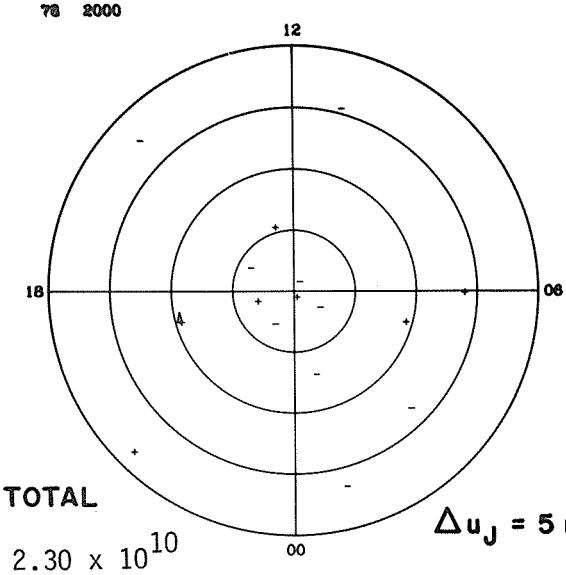

FIELD-ALIGNED CURRENT

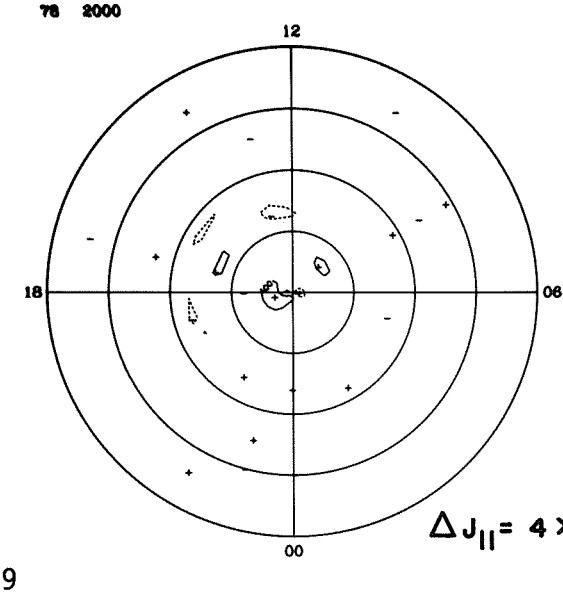

EQUIVALENT CURRENT

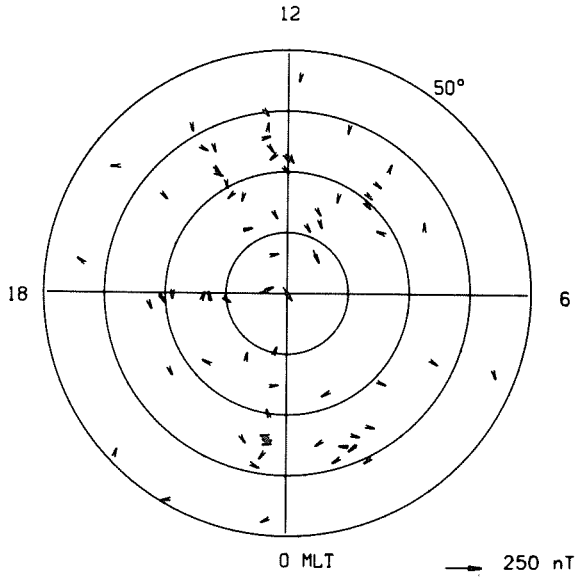

EQUIVALENT CURRENT SYSTEM

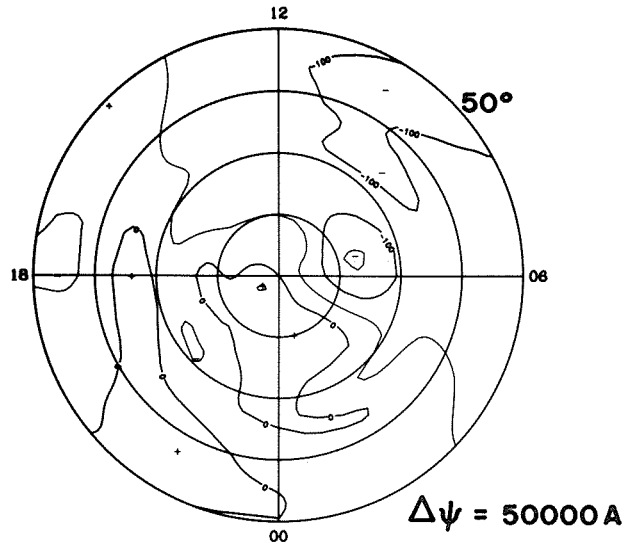

ELECTRIC POTENTIAL

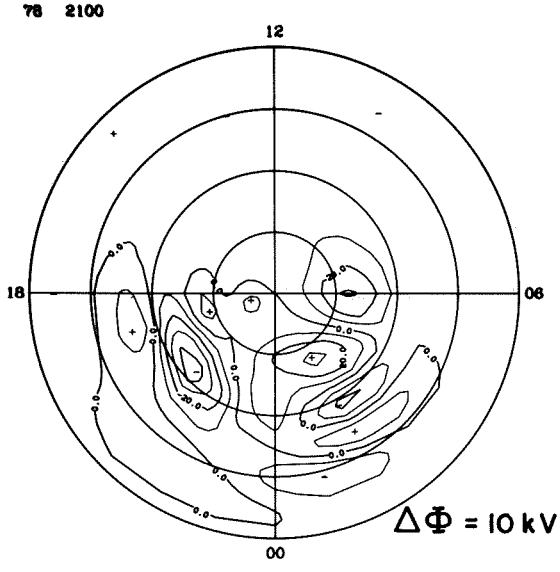

IONOSPHERIC CURRENT

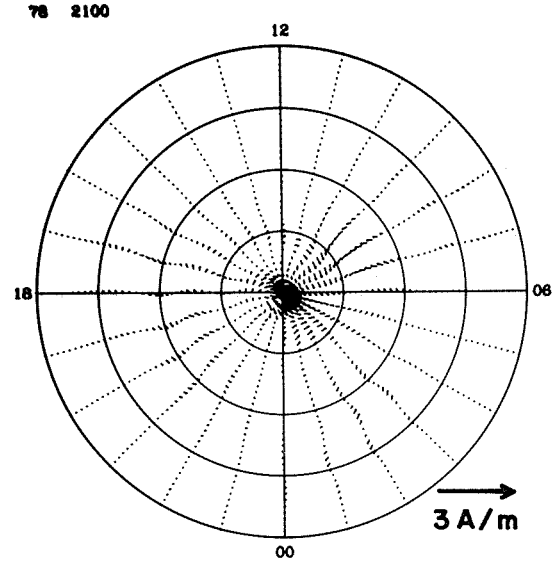

JOULE HEATING

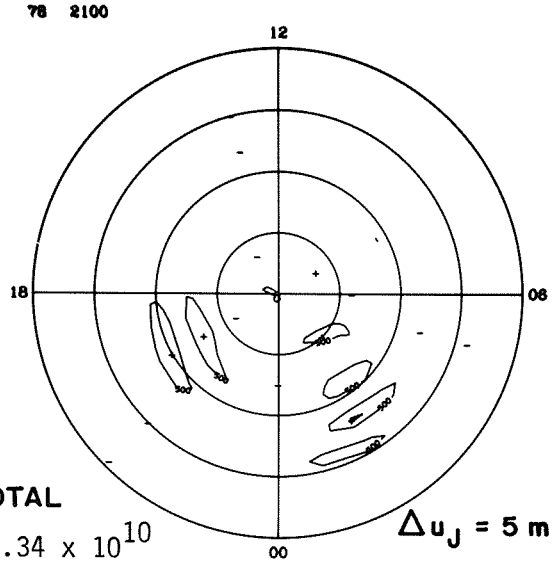

TOTAL

5.34×10^{10}

FIELD-ALIGNED CURRENT

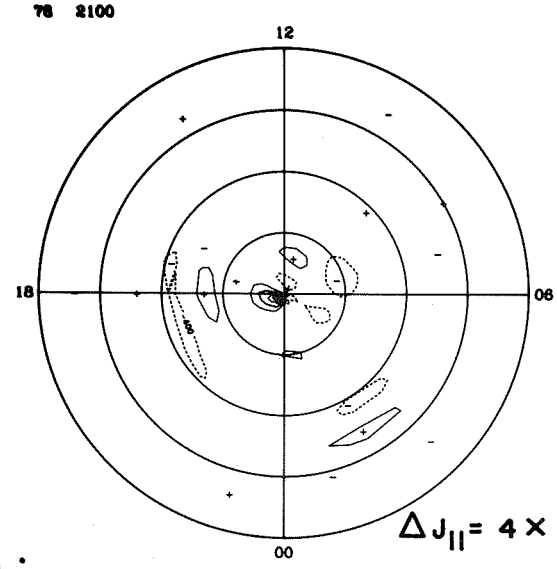

EQUIVALENT CURRENT

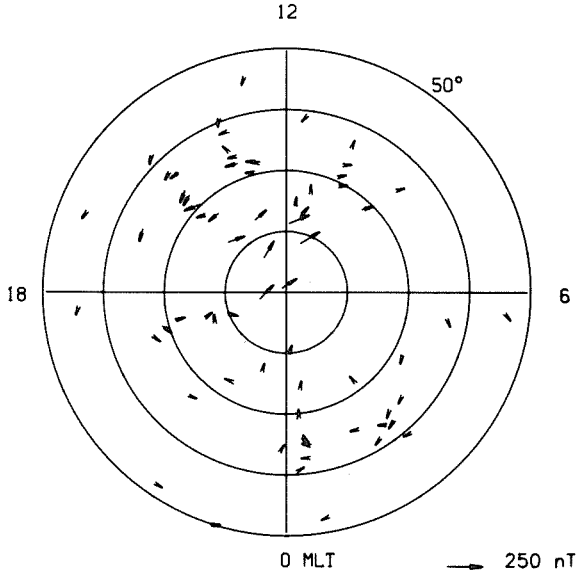

EQUIVALENT CURRENT SYSTEM

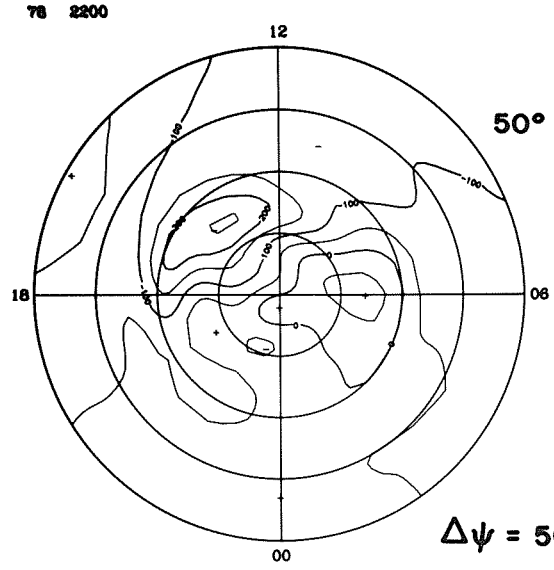

ELECTRIC POTENTIAL

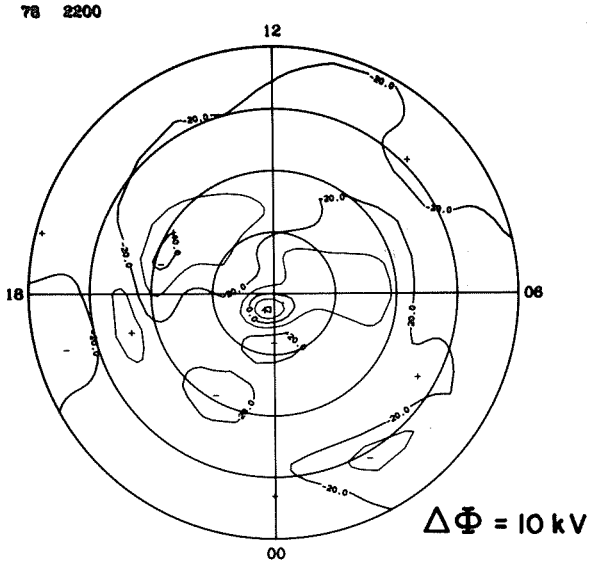

IONOSPHERIC CURRENT

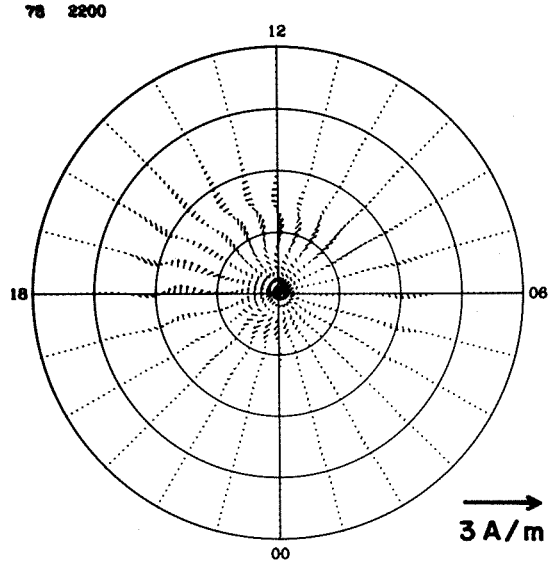

JOULE HEATING

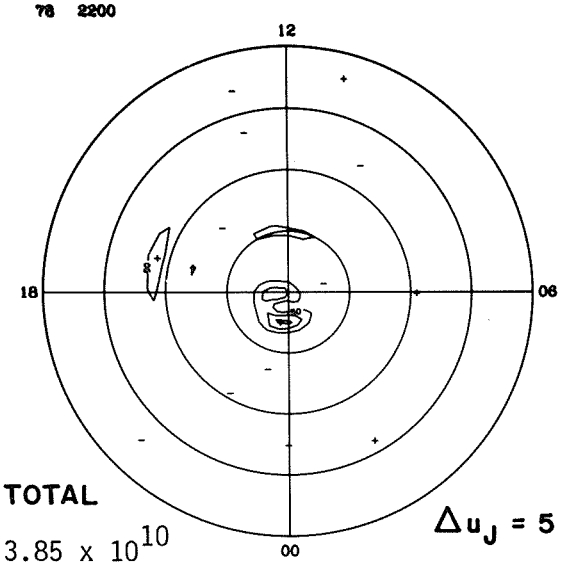

TOTAL

3.85×10^{10}

FIELD-ALIGNED CURRENT

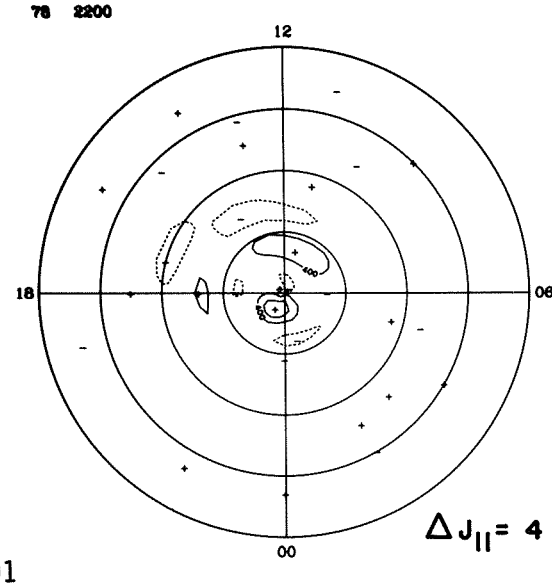

EQUIVALENT CURRENT

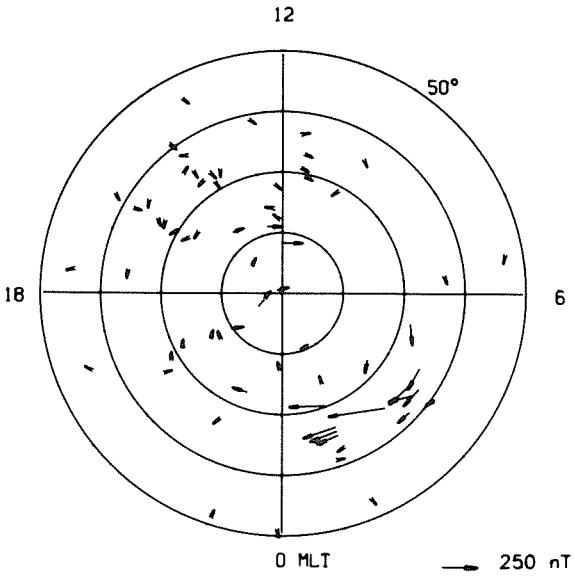

EQUIVALENT CURRENT SYSTEM

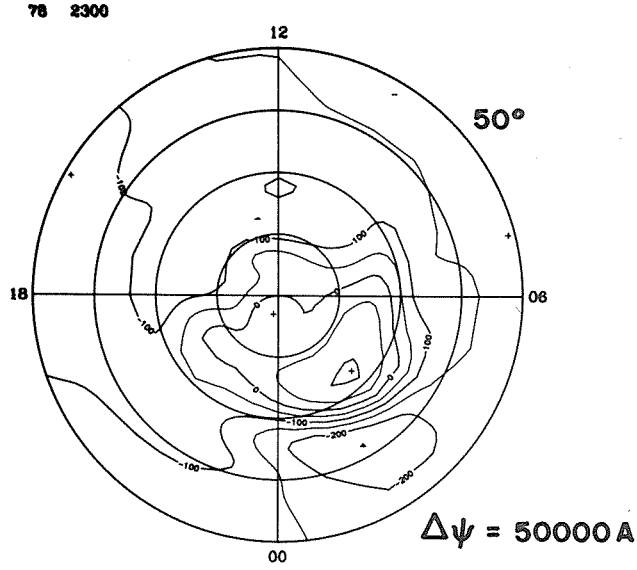

ELECTRIC POTENTIAL

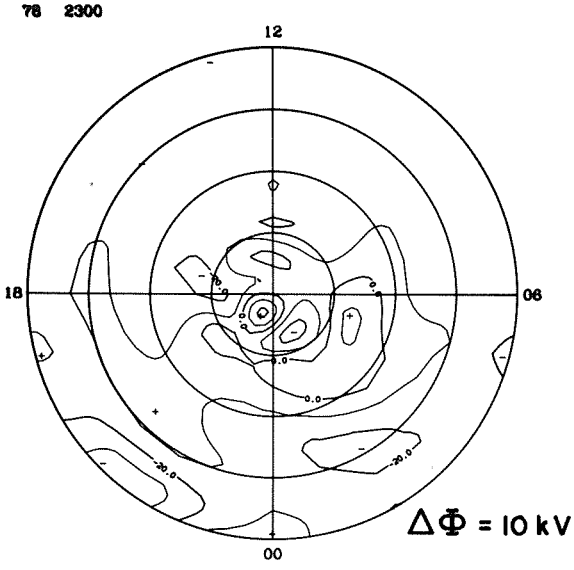

IONOSPHERIC CURRENT

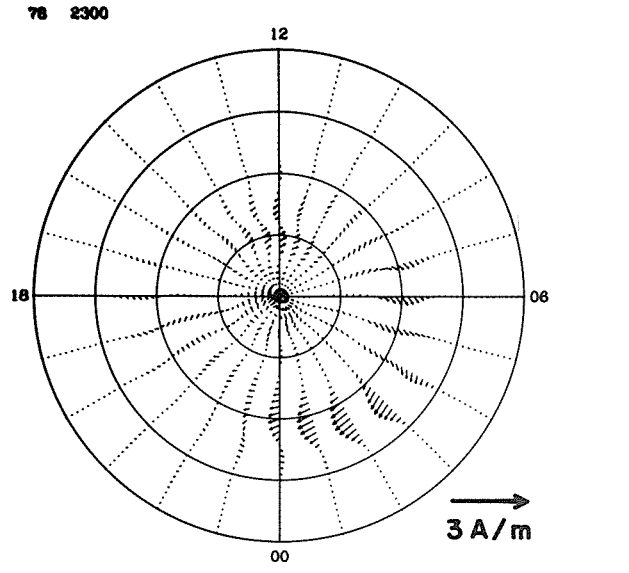

JOULE HEATING

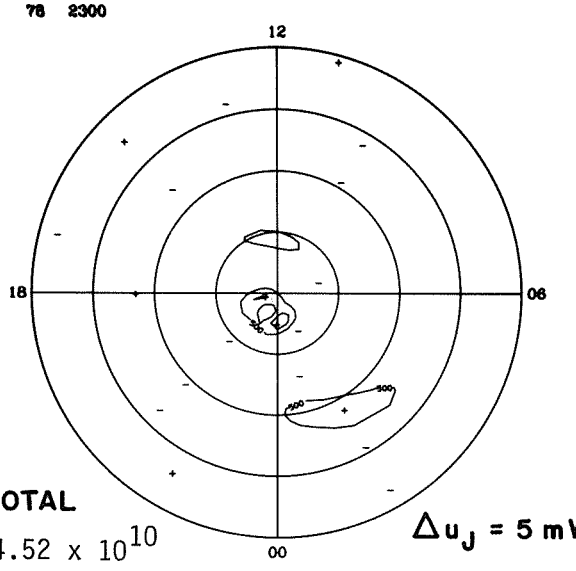

TOTAL

4.52×10^{10}

FIELD-ALIGNED CURRENT

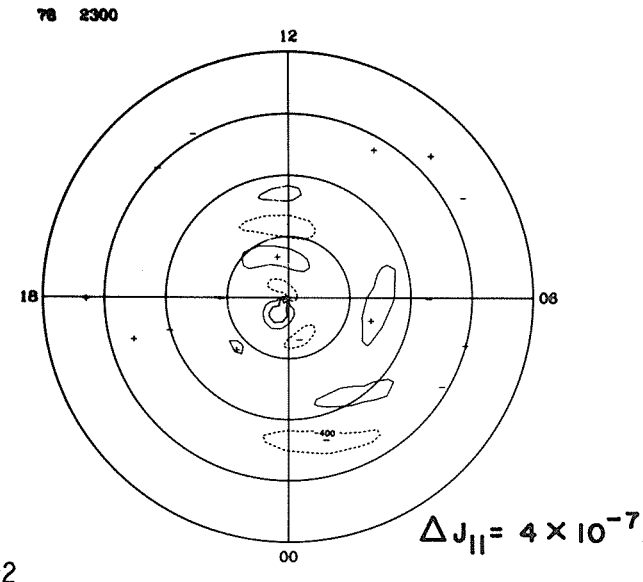

UAG SERIES OF REPORTS

Fewer than four UAG Reports are published at irregular intervals each year. Copies of these publications may be purchased through World Data Center A for Solar-Terrestrial Physics, Environmental Data and Information Service, NOAA, D63, 325 Broadway, Boulder, Colorado 80303, USA. A $4.00 handling charge per order will be added to the single-copy prices listed below. Please note, too, that some reports are available on microfiche only. Orders must include check or money order payable in U.S. currency to the Department of Commerce, NOAA/NGDC.

UAG-1 "IQSY Night Airglow Data," by L.L. Smith, F.E. Roach, and J.M. McKennan, ESSA Aeronomy Laboratory, Boulder, CO, July 1968, 305 pp, $1.75.

UAG-2 "A Reevaluation of Solar Flares, 1964-1966," by Helen W. Dodson and E. Ruth Hedeman, McMath-Hulbert Observatory, University of Michigan, Pontiac, MI, August 1968, 28 pp, $0.30.

UAG-3 "Observations of Jupiter's Sporadic Radio Emission in the Range 7.6-41 MHz, 6 July 1966 through 8 September 1968," by James W. Warwick and George A. Dulk, University of Colorado, Boulder, CO, October 1968, 35 pp, $0.55.

UAG-4 "Abbreviated Calendar Record 1966-1967," by J. Virginia Lincoln, Hope I. Leighton and Dorothy K. Kropp, ESSA now NOAA, Aeronomy and Space Data Center, Boulder, CO, January 1969, 170 pp, $1.25.

UAG-5 "Data on Solar Event of May 23, 1967 and its Geophysical Effects," compiled by J. Virginia Lincoln, World Data Center A, Upper Atmosphere Geophysics, ESSA now NOAA, Boulder, CO, February 1969, 120 pp, $0.65.

UAG-6 "International Geophysical Calendars 1957-1969," by A.H. Shapley and J. Virginia Lincoln, ESSA Research Laboratories, now NOAA, Boulder, CO, March 1969, 25 pp, $0.30.

UAG-7 "Observations of the Solar Electron Corona: February 1964 - January 1968," by Richard T. Hansen, High Altitude Observatory, NCAR, Boulder, CO, and Kamuela, HI, October 1969, 12 pp, $0.15.

UAG-8 "Data on Solar-Geophysical Activity October 24 - November 6, 1968," Parts 1 and 2, compiled by J. Virginia Lincoln, World Data Center A, Upper Atmosphere Geophysics, ESSA now NOAA, Boulder, CO, March 1970, 312 pp, $1.75 (includes Parts 1 and 2).

UAG-9 "Data on Cosmic Ray Event of November 18, 1968 and Associated Phenomena," compiled by J. Virginia Lincoln, World Data Center A, Upper Atmosphere Geophysics, ESSA now NOAA, Boulder, CO, April 1970, 109 pp, $0.55.

UAG-10 "Atlas of Ionograms," edited by A.H. Shapley, ESSA Research Laboratories now NOAA, Boulder, CO, May 1970, 243 pp, $1.50.

UAG-12 "Solar-Geophysical Activity Associated with the Major Geomagnetic Storm of March 8, 1970," Parts 1, 2 and 3, compiled by J. Virginia Lincoln and Dale B. Bucknam, World Data Center A, Upper Atmosphere Geophysics, ESSA now NOAA, Boulder, CO, April 1971, 466 pp, $3.00 (includes Parts 1-3).

UAG-13 "Data on the Solar Proton Event of November 2, 1969 through the Geomagnetic Storm of November 8-10, 1969," compiled by Dale B. Bucknam and J. Virginia Lincoln, World Data Center A, Upper Atmosphere Geophysics, ESSA now NOAA, Boulder, CO, May 1971, 76 pp, $0.90.

UAG-14 "An Experimental, Comprehensive Flare Index and Its Derivation for 'Major" Flares, 1955-1969," by Helen W. Dodson and E. Ruth Hedeman, McMath-Hulbert Observatory, University of Michigan, Pontiac, MI, July 1971, 25 pp, $0.30.

UAG-16 "Temporal Development of the Geophysical Distribution of Auroral Absorption for 30 Substorm Events in each of IQSY (1964-65) and IASY (1960)," by F.T. Berkey, University of Alaska, Fairbanks, AK; V.M. Driatskiy, Arctic and Antarctic Research Institute, Leningrad, USSR; K. Henriksen, Auroral Observatory, Tromson, Norway; D.H. Jelly, Communications Research Center, Ottawa, Canada; T.I. Shchuka, Arctic and Antarctic Research Institute, Leningrad, USSR; A. Theander, Kiruna Geophysical Observatory, Kiruna, Sweden; and J. Yliniemi, University of Oulu, Oulu, Finland, September 1971, 131 pp, $0.70 (microfiche only).

UAG-17 "Ionospheric Drift Velocity Measurements at Jicamarca, Peru (July 1967 - March 1970)," by Ben B. Balsley, NOAA Aeronomy Laboratory, Boulder, CO, and Ronald F. Woodman, Jicamarca Radar Observatory, Instituto Geofisico del Peru, Lima, Peru, October 1971, 45 pp, $0.55 (microfiche only).

UAG-18 "A Study of Polar Cap and Auroral Zone Magnetic Variations," by K. Kawasaki and S.-I. Akasofu, University of Alaska, Fairbanks, AK, June 1972, 21 pp, $0.20.

UAG-19 "Reevaluation of Solar Flares 1967," by Helen W. Dodson and E. Ruth Hedeman, McMath-Hulbert Observatory, University of Michigan, Pontiac, MI, and Marta Rovira de Miceli, San Miguel Observatory, Argentina, June 1972, 15 pp, $0.15.

UAG-21 "Preliminary Compilation of Data for Retrospective World Interval July 26 - August 14, 1972," by J. Virginia Lincoln and Hope I. Leighton, World Data Center A for Solar-Terrestrial Physics, NOAA, Boulder, CO, November 1972, 128 pp, $0.70.

UAG-22 "Auroral Electrojet Magnetic Activity Indices (AE) for 1970," by Joe Haskell Allen, National Geophysical and Solar-Terrestrial Data Center, Boulder, CO, November 1972, 146 pp, $0.75.

UAG-23 "U.R.S.I. Handbook of Ionogram Interpretation and Reduction," Second Edition, November 1972, edited by W.R. Piggott, Radio and Space Research Station, Slough, UK, and K. Rawer, Arbeitsgruppe fur Physikalische Weltraumforschung, Freiburg, GFR, November 1972, 324 pp, $1.75.

UAG-23A "U.R.S.I. Handbook of Ionogram Interpretation and Reduction," Second Edition, Revision of Chapters 1-4, edited by W.R. Piggott, Radio and Space Research Station, Slough, UK, and K. Rawer, Arbeitsgruppe fur Physikalische Weltraumforschung, Freiburg, GFR, November 1972, 135 pp, $2.14.

UAG-24 "Data on Solar-Geophysical Activity Associated with the Major Ground Level Cosmic Ray Events of 24 January and 1 September 1971," Parts 1 and 2, compiled by Helen E. Coffey and J. Virginia Lincoln, World Data Center A for Solar-Terrestrial Physics, NOAA, Boulder, CO, December 1972, 462 pp, $2.00 (includes Parts 1 and 2).

UAG-25 "Observations of Jupiter's Sporadic Radio Emission in the Range 7.6-41 MHz, 9 September 1968 through 9 December 1971," by James W. Warwick, George A. Dulk and David G. Swann, University of Colorado, Boulder, CO, February 1973, 35 pp, $0.35.

UAG-26 "Data Compilation for the Magnetospherically Quiet Periods February 19-23 and November 29 - December 3, 1970," compiled by Helen E. Coffey and J. Virginia Lincoln, World Data Center A for Solar-Terrestrial Physics, NOAA, Boulder, CO, May 1973, 129 pp, $0.70.

UAG-27 "High Speed Streams in the Solar Wind," by D.S. Intriligator, University of Southern California, Los Angeles, CA, June 1973, 16 pp, $0.15.

UAG-28 "Collected Data Reports on August 1972 Solar-Terrestrial Events," Parts 1, 2 and 3, edited by Helen E. Coffey, World Data Center A for Solar-Terrestrial Physics, NOAA, Boulder, CO, July 1973, 932 pp, $4.50.

UAG-29 "Auroral Electrojet Magnetic Activity Indices AE(11) for 1968," by Joe Haskell Allen, Carl C. Abston and Leslie D. Morris, National Geophysical and Solar-Terrestrial Data Center, Boulder, CO, October 1973, 148 pp, $0.75.

UAG-30 "Catalogue of Data on Solar-Terrestrial Physics," prepared by NOAA Environmental Data Service, Boulder, CO, October 1973, $1.50. Supersedes UAG-11, 15, and 20 catalogs.

UAG-31 "Auroral Electrojet Magnetic Activity Indices AE(11) for 1969," by Joe Haskell Allen, Carl C. Abston and Leslie D. Morris, National Geophysical and Solar-Terrestrial Data Center, Boulder, CO, February 1974, 142 pp, $0.75.

UAG-32 "Synoptic Radio Maps of the Sun at 3.3 mm for the Years 1967-1969," by Earle B. Mayfield, Kennon P. White III, and Fred I. Shimabukuro, Aerospace Corp., El Segundo, CA, April 1974, 26 pp, $0.35.

UAG-33 "Auroral Electrojet Magnetic Activity Indices AE(10) for 1967," by Joe Haskell Allen, Carl C. Abston and Leslie D. Morris, National Geophysical and Solar-Terrestrial Data Center, Boulder, CO, May 1974, 142 pp, $0.75.

UAG-34 "Absorption Data for the IGY/IGC and IQSY," compiled and edited by A.H. Shapley, National Geophysical and Solar-Terrestrial Data Center, Boulder, CO; W.R. Piggott, Appleton Laboratory, Slough, UK; and K. Rawer, Arbeitsgruppe fur Physikalische Weltraumforschung, Freiburg, GFR, June 1974, 381 pp, $2.00.

UAG-35 "Catalogue of Digital Geomagnetic Variation Data at World Data Center A for Solar-Terrestrial Physics," prepared by NOAA Environmental Data Service, Boulder, CO, July 1974, 20 pp, $0.20.

UAG-36 "An Atlas of Extreme Ultraviolet Flashes of Solar Flares Observed via Sudden Frequency Deviations During the ATM-SKYLAB Missions," by R.F. Donnelly and E.L. Berger, NOAA Space Environment Laboratory; Lt. J.D. Busman, NOAA Commissioned Corps; B. Henson, NASA Marshall Space Flight Center; T.B. Jones, University of Leicester, UK; G.M. Lerfald, NOAA Wave Propagation Laboratory; K. Najita, University of Hawaii; W.M. Retallack, NOAA Space Environment Laboratory and W.J. Wagner, Sacramento Peak Observatory, October 1974, 95 pp, $0.55.

UAG-37 "Auroral Electrojet Magnetic Activity Indices AE(10) for 1966," by Joe Haskell Allen, Carl C. Abston and Leslie D. Morris, National Geophysical and Solar-Terrestrial Data Center, Boulder, CO, December 1974, 142 pp, $0.75.

UAG-38 "Master Station List for Solar-Terrestrial Physics Data at WDC-A for Solar-Terrestrial Physics," by R.W. Buhmann, World Data Center A for Solar-Terrestrial Physics, Boulder, CO; Juan D. Roederer, University of Denver, Denver, CO; and M.A. Shea and D.F. Smart, Air Force Cambridge Research Laboratories, Hanscom AFB, MA, December 1974, 110 pp, $1.60.

UAG-39 "Auroral Electrojet Magnetic Activity Indices AE(11) for 1971," by Joe Haskell Allen, Carl C. Abston and Leslie D. Morris, National Geophysical and Solar-Terrestrial Data Center, Boulder, CO, February 1975, 144 pp, $2.05.

UAG-40 "H-Alpha Synoptic Charts of Solar Activity for the Period of Skylab Observations, May 1973 - March 1974," by Patrick S. McIntosh, NOAA Space Environment Laboratory, Boulder, CO, February 1975, 32 pp, $0.56.

UAG-41 "H-Alpha Synoptic Charts of Solar Activity During the First Year of Solar Cycle 20 October 1964 - August 1965," by Patrick S. McIntosh, NOAA Space Environment Laboratory, Boulder, CO and Jerome T. Nolte, American Science and Engineering, Inc., Cambridge, MA, March 1975, 25 pp, $0.48.

UAG-42 "Observations of Jupiter's Sporadic Radio Emission in the Range 7.6-80 MHz, 10 December 1971 through 21 March 1975," by James W. Warwick, George A. Dulk and Anthony C. Riddle, University of Colorado, Boulder, CO, April 1975, 49 pp, $1.15.

UAG-43 "Catalog of Observation Times of Ground-Based Skylab-Coordinated Solar Observing Programs," compiled by Helen E. Coffey, World Data Center A for Solar-Terrestrial Physics, NOAA, Boulder, CO, May 1975, 159 pp, $3.00.

UAG-44 "Synoptic Maps of Solar 9.1 cm Microwave Emission from June 1962 to August 1973," by Werner Graf and Ronald N. Bracewell, Stanford University, Stanford, CA, May 1975, 183 pp, $2.55.

UAG-45 "Auroral Electrojet Magnetic Activity Indices AE(11) for 1972," by Joe Haskell Allen, Carl C. Abston and Leslie D. Morris, National Geophysical and Solar-Terrestrial Data Center, Boulder, CO, May 1975, 144 pp, $2.10 (microfiche only).

UAG-46 "Interplanetary Magnetic Field Data 1963-1964," by Joseph H. King, National Space Science Data Center, NASA Goddard Space Flight Center, Greenbelt, MD, June 1975, 382 pp, $1.95.

UAG-47 "Auroral Electrojet Magnetic Activity Indices AE(11) for 1973," by Joe Haskell Allen, Carl C. Abston and Leslie D. Morris, National Geophysical and Solar-Terrestrial Data Center, Boulder, CO, June 1975, 144 pp, $2.10 (microfiche only).

UAG-48A "Synoptic Observations of the Solar Corona during Carrington Rotations 1580-1596 (11 October 1971 - 15 January 1973)," [Reissue of UAG-48 with quality images], by R.A. Howard, M.J. Koomen, D.J. Michels, R. Tousey, C.R. Detwiler, D.E. Roberts, R.T. Seal, and J.D. Whitney, U.S. Naval Research Laboratory, Washington, DC, and R.T. Hansen and S.F. Hansen, C.J. Garcia and E. Yasukawa, High Altitude Observatory, NCAR, Boulder, CO, February 1976, 200 pp, $4.27.

UAG-49 "Catalog of Standard Geomagnetic Variation Data," prepared by NOAA Environmental Data Service, Boulder, CO, August 1975, 125 pp, $1.85.

UAG-50 "High-Latitude Supplement to the URSI Handbook on Ionogram Interpretation and Rediction," edited by W.R. Piggott, British Antarctic Survey, c/o Appleton Laboratory, Slough, UK, October 1975, 294 pp, $4.00.

UAG-51 "Synoptic Maps of Solar Coronal Hole Boundaries Derived from He II 304A Spectroheliograms from the Manned Skylab Missions," by J.D. Bohlin and D.M. Rubenstein, U.S. Naval Research Laboratory, Washington, DC, November 1975, 30 pp, $0.54.

UAG-52 "Experimental Comprehensive Solar Flare Indices for Certain Flares, 1970-1974," by Helen W. Dodson and E. Ruth Hedeman, McMath-Hulbert Observatory, University of Michigan Pontiac, MI, November 1975, 27 pp, $0.60.

UAG-53 "Description and Catalog of Ionospheric F-Region Data, Jicamarca Radio Observatory (November 1966 - April 1969), by W.L. Clark and T.E. Van Zandt, NOAA Aeronomy Laboratory, Boulder, CO, and J.P. McClure, University of Texas as Dallas, Dallas, TX, April 1976, 10 pp, $0.33.

UAG-54 "Catalog of Ionosphere Vertical Soundings Data," prepared by NOAA Environmental Data Service, Boulder, CO, April 1976, 130 pp, $2.10.

UAG-55 "Equivalent Ionospheric Current Representations by a New Method, Illustrated for 8-9 November 1969 Magnetic Disturbances," by Y. Kamide, Cooperative Institute for Research in Environmental Sciences, University of Colorado, Boulder, CO; H.W. Kroehl, Data Studies Division, National Geophysical and Solar-Terrestrial Data Center, Boulder, CO; M. Kanamitsu, Advanced Study Program, National Center for Atmospheric Research, Boulder, CO; Joe Haskell Allen, Data Studies Division, National Geophysical and Solar-Terrestrial Data Center, Boulder, CO; and S.-I Akasofu, Geophysical Institute, University of Alaska, Fairbanks, AK, April 1976, 91 pp, $1.60 (microfiche only).

UAG-56 "Iso-intensity Contours of Ground Magnetic H Perturbations for the December 16-18, 1971, Geomagnetic Storm," Y. Kamide, Cooperative Institute for Research in Environmental Sciences, University of Colorado, Boulder, CO, April 1976, 37 pp, $1.39.

UAG-57 "Manual on Ionospheric Absorption Measurements," edited by K. Rawer, Institut fur Physikalische Weltraumforschung, Freiburg, GFR, June 1976, 302 pp, $4.27.

UAG-58 "ATS6 Radio Beacon Electron Content Measurements at Boulder, July 1974 - May 1975," by R.B. Fritz, NOAA Space Environment Laboratory, Boulder, CO, September 1976, 61 pp, $1.04.

UAG-59 "Auroral Electrojet Magnetic Activity Indices AE(11) for 1974," by Joe Haskell Allen, Carl C. Abston and Leslie D. Morris, National Geophysical and Solar-Terrestrial Data Center, Boulder, CO, December 1976, 144 pp, $2.16.

UAG-60 "Geomagnetic Data for January 1976 (AE(7) Indices and Stacked Magnetograms)," by Joe Haskell Allen, Carl C. Abston and Leslie D. Morris, National Geophysical and Solar-Terrestrial Data Center, Boulder, CO, July 1977, 57 pp, $1.07.

UAG-61 "Collected Data Reports for STIP Interval II 20 March - 5 May 1976, edited by Helen E. Coffey and John A. McKinnon, World Data Center A for Solar-Terrestrial Physics, Boulder, CO, August 1977, 313 pp, $2.95.

UAG-62 "Geomagnetic Data for February 1976 (AE(7) Indices and Stacked Magnetograms)," by Joe Haskell Allen, Carl C. Abston and Leslie D. Morris, National Geophysical and Solar-Terrestrial Data Center, Boulder, CO, September 1977, 55 pp, $1.11.

UAG-63 "Geomagnetic Data for March 1976 (AE(7) Indices and Stacked Magnetograms)," by Joe Haskell Allen, Carl C. Abston and Leslie D. Morris, National Geophysical and Solar-Terrestrial Data Center, Boulder, CO, September 1977, 57 pp, $1.11.

UAG-64 "Geomagnetic Data for April 1976 (AE(8) Indices and Stacked Magnetograms)," by Joe Haskell Allen, Carl C. Abston and Leslie D. Morris, National Geophysical and Solar-Terrestrial Data Center, Boulder, CO, February 1978, 55 pp, $1.00.

UAG-65 "The Information Explosion and Its Consequences for Data Acquisition, Documentation, Processing," by G.K. Hartmann, Max-Planck-Institut fur Aeronomie, Lindau, GFR, May 1978, 36 pp, $0.75.

UAG-66 "Synoptic Radio Maps of the Sun at 3.3 mm 1970-1973," by Earle B. Mayfield and Fred I. Shimabukuro, Aerospace Corp., El Segundo, CA, May 1978, 30 pp, $0.75.

UAG-67 "Ionospheric D-Region Profile Data Base, A Collection of Computer-Accessible Experimental Profiles of the D and Lower E Regions," by L.F. McNamara, Ionospheric Prediction Service, Sydney, Australia, August 1978, 30 pp, $0.88 (microfiche only).

UAG-68 "A Comparative Study of Methods of Electron Density Profile Analysis," by L.F. McNamara, Ionospheric Prediction Service, Sydney, Australia, August 1978, 30 pp, $0.88 (microfiche only).

UAG-69 "Selected Disturbed D-Region Electron Density Profiles. Their relation to the undisturbed D region," by L.F. McNamara, Ionospheric Prediction Service, Sydney, Australia, October 1978, 50 pp, $1.29 (microfiche only).

UAG-70 "Annotated Atlas of H-Alpha Synoptic Charts for Solar Cycle 20 (1964-1974) Carrington Solar Rotations 1487-1616," by Patrick S. McIntosh, NOAA Space Environment Laboratory, Boulder, CO, February 1979, 327 pp, $3.50.

UAG-71 "Magnetic Potential Plots over the Northern Hemisphere for 26-28 March 1976," A.D. Richmond, NOAA Space Environment Laboratory, Boulder, CO; H.W. Kroehl, National Geophysical and Solar-Terrestrial Data Center, Boulder, CO; M.A. Henning, Lockheed Missils and Space Co., Aurora, CO; and Y. Kamide, Kyoto Sangyo University, Kyoto, Japan, April 1979, 118 pp, $1.50.

UAG-72 "Energy Release in Solar Flares, Proceedings of the Workshop on Energy Release in Flares, 26 February - 1 March 1979, Cambridge, Massachusetts, U.S.A.," edited by David M. Rust, American Science and Engineering, Inc., Cambridge, MA, and A. Gordon Emslie, Harvard-Smithsonian Center for Astrophysics, Cambridge, MA, July 1979, 68 pp, $1.50 (microfiche only).

UAG-73 "Auroral Electrojet Magnetic Activity Indices AE(11-12) for January - June 1975," by Joe Haskell Allen, Carl C. Abston, J.E. Salazar and J.A. McKinnon, National Geophysical and Solar-Terrestrial Data Center, NOAA, Boulder, CO, August 1979, 114 pp, $1.75.

UAG-74 "ATS-6 Radio Beacon Electron Content Measurements at Ootacamund, India, October - July 1976," by S.D. Bouwer, K. Davies, R.F. Donnelly, R.N. Grubb, J.E. Jones and J.H. Taylor, NOAA Space Environment Laboratory, Boulder, CO, and R.G. Rastogi, M.R. Deshpande, H. Chandra and G. Sethia, Physical Research Laboratory, Ahmedabad, India, March 1980, 58 pp, $2.50.

UAG-75 "The Alaska IMS Meridian Chain: Magnetic Variations for 9 March - 27 April 1978," by H.W. Kroehl and G.P. Kosinski, National Geophysical and Solar-Terrestrial Data Center, Boulder, CO; S.-I Akasofu, G.J. Romick, C.E. Campbell and G.K. Corrick, University of Alaska, Fairbanks, AK; and C.E. Hornback and A.M. Gray, NOAA Space Environment Laboratory, Boulder, CO, June 1980, 107 pp, $3.00.

UAG-76 "Auroral Electrojet Magnetic Activity Indices AE(12) for July - December 1975," by Joe Haskell Allen, Carl C. Abston, J.E. Salazar and J.A. McKinnon, National Geophysical and Solar-Terrestrial Data Center, NOAA, Boulder, CO, August 1980, 116 pp, $2.50.

UAG-77 "Synoptic Solar Magnetic Field Maps for the Interval Including Carrington Rotations 1601-1680, May 5, 1973 - April 26, 1979," by J. Harvey, B. Gillespie, P. Miedaner and C. Slaughter, Kitt Peak National Observatory, Tucson, AZ, August 1980, 66 pp, $2.50.

UAG-78 "The Equatorial Latitude of Auroral Activity During 1972-1977," by N.R. Sheeley, Jr. and R.A. Howard, E. O. Hulbert Center for Space Research, U.S. Naval Research Laboratory, Washington, DC and B.S. Dandekar, Air Force Geophysics Laboratory, Hanscom AFB, MA, October 1980, 61 pp, $3.00.

UAG-79 "Solar Observations During Skylab, April 1973 - February 1974, I. Coronal X-Ray Structure, II. Solar Flare Activity," by J.M. Hanson, University of Michigan, Ann Arbor, MI; and E.C. Roelof and R.E. Gold, The Johns Hopkins University, Laurel, MD, December 1980, 43 pp, $2.50.

UAG-80 "Experimental Comprehensive Solar Flare Indices for 'Major' and Certain Lesser Flares, 1975-1979," compiled by Helen W. Dodson and E. Ruth Hedeman, The Johns Hopkins University, Laurel, MD, July 1981, 33 pp, $2.00.

UAG-81 "Evolutionary Charts of Solar Activity (Calcium Plages) as Functions of Heliographic Longitude and Time, 1964-1979," by E. Ruth Hedeman, Helen W. Dodson and Edmond C. Roelof, The Johns Hopkins University, Laurel, MD 20707, August 1981, 103 pp, $4.00.

UAG-82 "International Reference Ionosphere - IRI 79," edited by J. Virginia Lincoln and Raymond O. Conkright, National Geophysical and Solar-Terrestrial Data Center, NOAA, Boulder, CO, November 1981, 243 pp, $4.50.

UAG-83 "Solar-Geophysical Activity Reports for September 7-24, 1977 and November 22, 1977," Parts 1 and 2, compiled by John A. McKinnon and J. Virginia Lincoln, World Data Center A for Solar-Terrestrial Physics, NOAA, Boulder, CO, February 1982, 553 pp, $10.00.

UAG-84 "Catalog of Auroral Radio Absorption During 1976-1979 at Abisko, Sweden," by J.K. Hargreaves, C.M. Taylor and J.M. Penman, Environmental Sciences Department, University of Lancaster, Lancaster, UK, July 1982, 69 pp, $3.00.

UAG-85 "Catalog of Ionosphere Vertical Soundings Data," edited by Raymond O. Conkright and H. Irene Brophy, National Geophysical Data Center, NOAA, Boulder, CO, July 1982, 107 pp, $3.50.

UAG-86 "International Catalog of Geomagnetic Data," compiled by J.H. Allen and C.C. Abston, National Geophysical Data Center, NOAA, Boulder, CO; E.P. Kharin and N.E. Papitashvili, Academy of Sciences of the USSR, World Data Center B2, Moscow, USSR; and V.O. Papitashvili, IZMIRAN, Moscow Region, USSR, November 1982, 188 pp, $4.00.

UAG-87 "Changes in the Global Electric Fields and Currents for March 17-19, 1978, from Six IMS Meridian Chains of Magnetometers," by Y. Kamide, Kyoto Sangyo University, Kyoto, Japan; H.W. Kroehl, National Geophysical Data Center, NOAA, Boulder, CO; and A.D. Richmond, NOAA Space Environment Laboratory, Boulder, CO, November 1982, 102 pp, $3.50.